Title

Constructive Communications: Small Signaling Peptides Govern Stem Cell Homeostasis and Morphology in Plants

Author

Dao, Thai

Publication Date

2020

Peer reviewed|Thesis/dissertation

Constructive Communications:

Small Signaling Peptides Govern Stem Cell Homeostasis and Morphology in Plants

By

Thai Dao

A dissertation submitted in partial satisfaction of the

requirements for the degree of

Doctor of Philosophy

in

Plant Biology

in the

Graduate Division

of the

University of California, Berkeley

Committee in charge:

Professor Jennifer Fletcher, Chair

Professor Frank Harmon

Professor Kunxin Luo

Spring 2020

Abstract

Constructive Communications:

Small Signaling Peptides Govern Stem Cell Homeostasis and Morphology in Plants

by

Thai Dao

Doctor of Philosophy in Plant Biology

University of California, Berkeley

Professor Jennifer Fletcher, Chair

Each multicellular organism, much like the communities they belong to, is not a discrete biological unit, but an union of elements that require constant communication in order to sustain growth. In both animals and plants, small peptide hormones serve as one such means of intercellular correspondence, typically secreted into the apoplastic space to be perceived by receptors in neighbouring cells. These molecular messengers form intricate feedback pathways that allow connective tissue layers to coordinate their diverse roles and functions.

A large family of signaling molecules called CLAVATA3/EMBRYO SURROUNDING REGION-RELATED (CLE) is conserved throughout the evolution of the land plant lineage. Its members encode prepropeptides that are processed into small 12-13 amino acid ligands, whose functions are implicated in diverse developmental processes, including cell fate acquisition, cell proliferation, and cell division plane orientation. The founding member of the CLE family is CLAVATA3 (CLV3), which is expressed at the shoot apex of the mustard plant *Arabidopsis thaliana*, to mediate activity of the stem cell niche there, also called the shoot apical meristem (SAM). The CLV3 signal is perceived by multiple receptor complexes in the underlying tissue layers, triggering a pathway that targets the homeodomain transcription factor WUSCHEL (WUS). WUS is a mobile protein that promotes stem cell identity within its area of effect, while also directly activating *CLV3* expression. In turn, CLV3 signaling represses *WUS* expression and confines its domain to a few cells at the center of the SAM. The ensuing feedback loop between CLV3 and WUS thus maintains a small but stable stem cell population at the shoot tip, which proliferates to supply building materials for various growth processes aboveground, including vertical extension and generation of organs such as leaves, flowers, and axillary branches.

In this study, I characterized the biological functions of three genes related to *CLV3*, *CLE16*, *CLE17*, and *CLE27*, all of which are also expressed at the shoot apex of Arabidopsis. By themselves, *CLE16, CLE17,* and *CLE27* appear to have no significant impact on stem cell activity at the SAM and overall plant architecture. However, via analyzing higher order mutants, I demonstrated that in the loss of endogenous *CLV3* activity, the CLE16 and CLE17 peptides can

independently act in its place to restrict stem cell accumulation, starting at the embryonic stage and throughout the entirety of the life cycle, ending at flower production. In contrast, *CLE27* does not compensate for the loss of CLV3 signaling at least in the final stage of floral development. The ability of CLE16 and CLE17 to partially, but not fully, replace CLV3 function may stem from their binding affinity to a subset of CLV3's cognate receptors. In addition, while the CLE16 and CLE17 signaling pathways appear to target WUS in a similar manner to CLV3, I provided evidence that both may have WUS-independent functions that are specific to the development of axillary branches. Together, these observations describe a complex interrelation that both expand upon the known CLV-WUS module, and reveal novel aspects in the regulation of shoot stem cell activity by CLE peptides.

Finally, I characterized functions of two other *CLE* genes in Arabidopsis leaves, *CLE5* and *CLE6*. Both genes are expressed at the base of developing leaves, and appear to have a minor impact on overall leaf shape. Their expression levels are responsive to various transcription factors involved in leaf patterning, as well as the phytohormones auxin. This study provides the first instance of CLE peptides regulating leaf morphology, and thus opens up a new avenue for investigating the genetic regulation of leaf development in land plants.

DEDICATIONS

I got on a plane nine years ago, and flew across an ocean and two continents. The immensity, and perhaps inevitability of the ensuing journey is something I still struggle to comprehend. I feared it would be a difficult, and lonely experience. I was only right about half. To have got to know so many, to have been supported, surprised, and humbled by their love is a blessing I can barely begin to put into words.

I saw my first snow in Lancaster, Pennsylvania.

Thank you to the beautiful people at Franklin and Marshall. Thank you, Taylor, Minji, Gülce, and Cathryn for putting up with me, consuming massive amounts of TV, and being the most wonderful roommates one can ask for. You continue to hold me up through this whole journey. You ruined living with other people in the best possible ways. Thank you, Kelsey for walking with me to church on Sunday and being generally incredible. Thank you, Gabby and the VLSB crew for our late-night shenanigans. Thank you, Emily for showing me and the world how the coexistence of strength and vulnerability is everything worth fighting for. Thank you, my beloved Tammi, Jami, Lia, and furry Omar for embracing me as much as you did and letting me believe in my inner rhythm. Thank you, Xay, for our Costco trips and our community dinners, for teaching me that cooking is something that deserves celebration. When Berkeley feels tough and overwhelming, I think of my second home in Pennsylvania, I think of you.

Professor Pablo Jenik took this clueless and nervous international student into the lab, and walked them along a path they didn't know existed. You taught me how to be a scientist, gave me a seat at your Thanksgiving table, drove me to conferences, and encouraged me all the way through my application to graduate school. How can I ever express enough gratitude for all the things that you did? Thank you, Pablo, for seeing something worth nurturing in me, for helping me become who I am today.

I didn't start drinking coffee until I came to Berkeley.

I owe so much to my community at First Congregational Church of Berkeley. You welcomed me when I came to your door. You were there for me at the beginning and you're there for me at the end. You saw someone standing at the threshold and broke bread with them anyway. I have loved every moment of us singing together. Emma and Melani, look how far we've come!

And speaking of how far we've come, thank you, Gaby, for sticking with me in this apartment for the whole five years! I can't wait to see where you'll go next in your career.

Thank you to the folks at the USDA Albany, who continue to make all of our work possible. Lil and Rena, thank you for welcoming me, for being the bosses that you are, and keeping me on my toes. Thank you, Thelma, for the joy and warmth that you carry. Thank you, De and Tina, for your technical support with so many microscopes! Thank you, for being the willing subjects of my many baking experiments. I will always miss walking up and down and across the main building to bring you your muffins.

A special thank you to the Hake lab for letting me be a part of their social life. I feel absolutely no hesitation to call Sam and Annis my postdocs, even though we work in different groups. You taught me how to use the confocal. You commiserated with my every failed in situ. You gave me intellectual and emotional support. You made academia seems fun and doable even in the most maddening moments. Thank you, for being such fabulous role models.

Thank you, Jacob, for being my best friend and my anchor for so many years. I know it wasn't easy, yet you have grounded and centered me through such a whirlwind of a time. As I'm writing this in the middle of the quarantine, I'm missing all of our dinner dates, movie nights, city strolls, and hiking trips throughout the Bay. These little things have carried me through grad school, and I hold them in my heart to the finish line.

To Joe, whose kindness has brightened up my most stressful days. I'm forever grateful for the love you have showered me with, and the adventures that we have taken together.

To the people at Hillside house, Nanticha, Ahu, Greg, Caroline, Marlee, Sebastian, and Ellie, thank you, and I love you so very much. You continue to teach me what it means to be in a community. You put so much effort into creating a space to gather, experience, communicate, to carry one another, and to grow together. You are each so astounding in your own way. To share even just a part of your joy and your burden has been an honor that even just a year ago I could not have imagined to receive. Your labour is love and I have never tasted a wine so sweet.

When I first came to Professor Jennifer Fletcher lab, I had only just graduated from college two months ago. I held a fasciation for the growth and shaping of plants, and was eager to dive into the world of developmental genetics. She took that enthusiasm, and fostered it with intellectual rigor and thoughtful methodology. One project after another, she demanded nothing but the very best of myself, because she knew I was up for it. It is with her challenge, her guidance, her confidence, and her patience that this work was completed. This road, which has been filled with hurdles and

impossibilities, has been made possible, if not at times easy, because of you. Thank you, Jenn, for your infallible support, and for believing in me.

Thank you, to everyone who I have had the blessing to meet, whose names are too dear and too numerous to be invoked on these pages. Please never stop reminding me of the love I'm given and the love I'm meant to give back.

And finally,

Thank you,

To my family:

My brothers and sisters,

and their little ones,

for taking care of me in every possible way that they know. You are so annoying and so irritating. You have helped me every step of the way, you have come to my side every time I asked for, and I love you so so much.

To my parents, whose love languages are at times polar opposites.

To my dad,

To my mom,

whose love is embedded like ley lines in my veins. It is my hair, my eyes, my skin, the way I talk, and way I act, the way I touch. Without it I am not living, and by letting go of it I am growing.

I could not have done any of this without knowing, at the core of my being, that you love me.

And I love you.

TABLE OF CONTENTS

LIST OF FIGURES

LIST OF TABLES

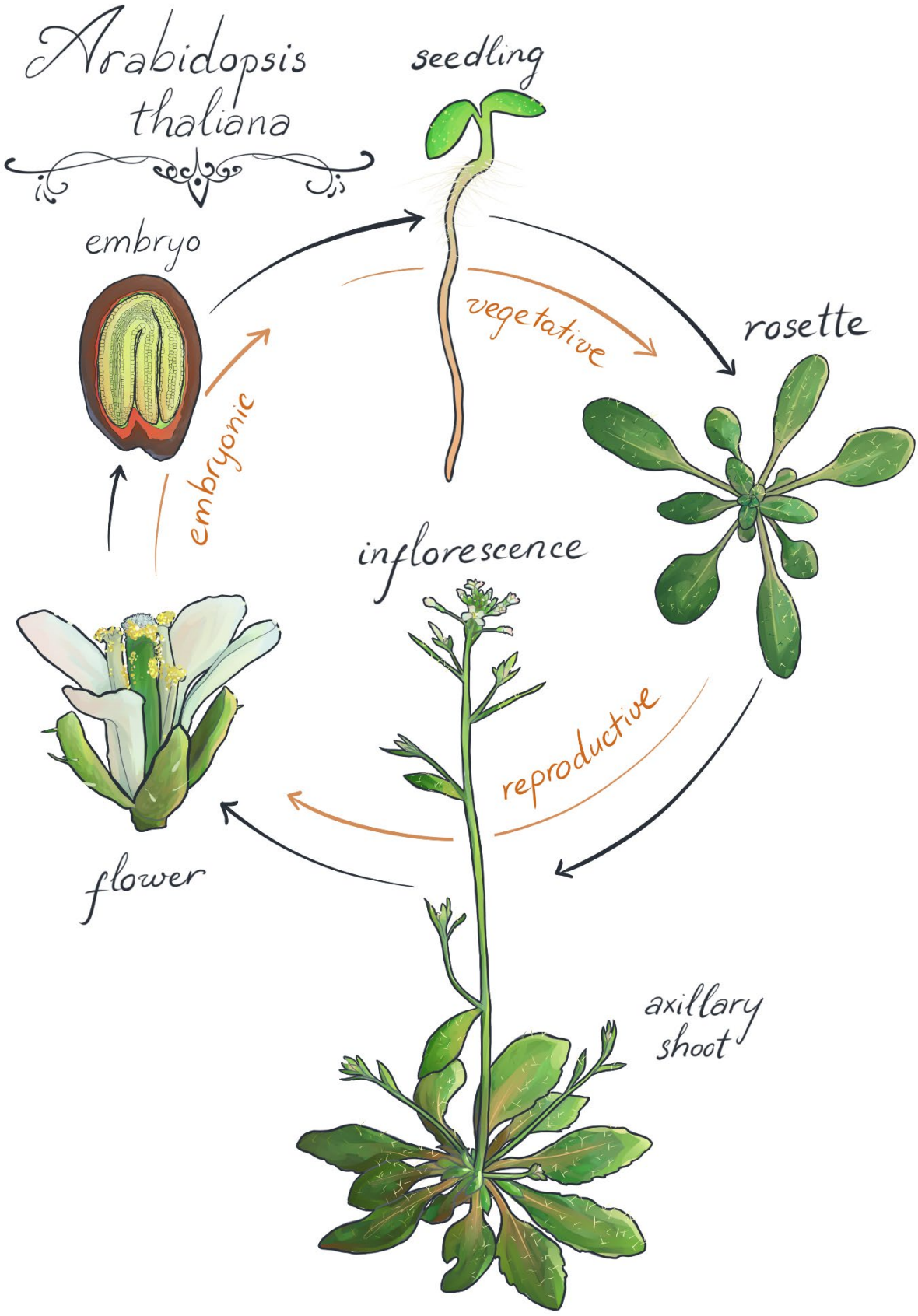

Figure 1.1. The life cycle of the mouse-ear cress *Arabidopsis thaliana*

CHAPTER I

INTRODUCTION

THE CONVERSATIONS THAT SHAPE A PLANT

The content of this chapter was adapted from the publication

Dao, T.Q. and Fletcher, J.C. (2017). CLE peptide-mediated signaling in shoot and vascular meristem development. Front. Biol. (Beijing). 12: 406–420.

The growth and development of multicellular organisms is heavily dependent on communication between groups of cells. Intercellular signaling pathways convey cell fate information, regulate cell division and differentiation processes, propagate and amplify specific signaling states, and coordinate tissue functions. Both plants and animals utilize systemic hormones as well as polypeptide signaling molecules to mediate cell-to-cell communication. In animals, polypeptides such as epidermal growth factor (EGF) and transforming growth factor-beta (TGF-b) act as extracellular ligands that are generated in certain cell types and perceived at the surface of neighboring cells, typically by transmembrane receptor kinases. Binding of the ligand to its receptor or receptors initiates a cascade of intracellular phosphorylation events that affects the activity of one or more nuclear transcription factors, resulting in the alteration of gene expression programs (Bergeron et al. 2016).

Although plants lack canonical EGF, TGF-b, Wingless and other peptide superfamilies found in animals, they also make extensive use of polypeptide signaling systems to mediate various biological processes (Matsubayashi, 2014; Tavormina et al.,2015). The genome of *Arabidopsis thaliana*, a member of the mustard family related to food plants such as broccoli and cauliflower (Fig. 1.1), encodes well over a thousand small proteins (<100 amino acids) that may function as peptide signaling molecules as well as more than 600 putative plasma membrane-bound receptor proteins (Shiu and Bleecker, 2001; Lease and Walker, 2006; Tavormina et al., 2015). The CLAVATA3/EMBRYO SURROUNDING REGION-RELATED (CLE) family represents one of the largest families of plant polypeptides identified to date, consisting of 32 members in Arabidopsis (Cock and McCormick, 2001) and as many as 84 members in other species (Hastwell et al., 2015). Members of the *CLE* gene family are present throughout the land plant lineage and in some plant parasitic nematodes, but have not been detected in green algae (Cock and McCormick, 2001; Wang et al., 2005).

The *CLE* genes encode polypeptides of less than 15 kDa in molecular mass that share several structural features. Each peptide consists of either an amino terminal signal peptide or a membrane anchor sequence, a 40- to 90-amino acid variable domain, and a highly conserved 14-amino acid motif near the carboxyl terminus called the CLE domain (Cock and McCormick, 2001). The signal peptide is sufficient to direct the CLE proteins through the secretory pathway (Rojo et al., 2002; Sharma et al., 2003) and is required for their *in vivo* function (Meng et al., 2010). Full length CLE pre-propeptides are processed (Casamitjana-Martinez et al., 2003; Ni and Clark, 2006) to produce biologically active 12-13 amino acid polypeptides consisting of the CLE domain (Kondo et al., 2006; Ohyama et al., 2009). The roles of the *CLE* genes are best understood in plant development and particularly in the meristems, which are small stem cell reservoirs that provide cells for continuous organ formation.

In a majority of known CLE signaling pathways, the key biologically relevant targets are transcription factors belonging to the plant-specific WUSCHEL-LIKE HOMEOBOX (WOX) family, named after the founding member WUSCHEL (WUS) in Arabidopsis. WOX transcription factors are distinguished by their conserved homeodomains, which directly bind DNA through a helix-turn-helix motif (HTH) superficially resembling those found in animal homeodomain proteins (Mayer et al., 1998). In addition, WOX proteins also contain a canonical WUS-box motif at the carboxyl-terminal side of the homeodomain. Some also possess a short acidic domain that may function in transcription activation, and an EAR domain that can mediate transcriptional repression at the C-terminus (Ohta et al., 2001). However, no clear nuclear localization signal

(NLS) has been predicted for these transcription factors. Thus, their subcellular localization might be mediated by cryptic signal sequences, or by partnering with other nuclear proteins.

Like the *CLE* gene family, *WOX* genes are present throughout the evolution of land plants, with 15 members encoded in the Arabidopsis genome and as many as 32 have been found in cotton (Haecker et al., 2004; He et al., 2019). Phylogenetic analysis divides the family into three major clades: the WUS clade, the intermediate clade, and the ancient clade. The WUS clade is represented by the prototypic member *AtWUS*, as well as *AtWOX1-7*, and is also the most recently derived clade, being restricted to seed plants. Members of the intermediate clade includes *AtWOX8/9/11/12*, along with sequences in the lycophyte *Selaginella moellendorfii*, and therefore was likely present in the last common ancestor of vascular plants. Lastly, *AtWOX10/13/14* belong to the ancient clade, which also occurs in unicellular green algae *Ostreococcus tauri* and *Ostreococcus lucimarinus* (Wu et al., 2019). Thus, the WOX family were present before the evolution of land plants, predating even the CLE genes. Their members are involved in various developmental processes, and functional divergence of the *WOX* gene family has been correlated with the evolution of increasing architectural complexities in planta (Nardmann et al., 2009; Dolsblasz et al., 2016; Segatto et al., 2016). Together, the two gene families, CLE and WOX are often found acting together to mediate many important developmental processes in various plant tissues, as will be described in the following sections.

I.1 Setting up the body plan

The development of each complex form from a single cell requires an immense amount of informational exchange within and between cells, as is in the case of zygotic embryogenesis. In Arabidopsis, after fertilization, the zygote passes through a transient symmetric state where the nucleus is situated at the center of the cell, evenly surrounded by vacuoles (Mansfield and Briarty, 1991). During this phase, the WRKY DNA-BINDING PROTEIN2 (WRKY2) directly activates transcription of the *WOX8* gene, as well as its close homologs *WOX9* in the zygotic cell (Ueda et al., 2011). WOX8 activity is required to initiate the repolarization of the zygote, shifting the nucleus towards the apical position and a large vacuole towards the basal position. An asymmetric division splits the zygote into the functionally distinct apical daughter cell, which will further divide to form the embryo, and basal daughter cell, which will become the extraembryonic suspensor. After the division, the expression domains of *WOX8/9* are shifted to the basal cell, and act non-cell autonomously to activate *WOX2* in the apical cell, where it regulates embryo development (Haecker et al., 2004; Breuninger et al., 2008). While it is still unclear how *WOX2* is excluded from the basal cell where *WOX8/9* is expressed, and vice versa, their complementary domains reinforce the boundary that separate the fates of the two cell lineages. Though not the focus of this work, it is worth mentioning two other pathways that are involved in setting up the apical-basal axis in the embryo, one being the YODA (YDA) MITOGEN-ACTIVATED PROTEIN KINASE (MAPK) pathway, and the other involving polar transport of the phytohormone auxin (Lukowitz et al., 2004; Friml et al., 2003; Robert et al. 2013).

After the initial cleavage, the basal cell undergoes a series of transverse division to form the suspensor that anchors the embryo to the ovule and facilitates nutrient supply from the maternal tissue into the developing embryo, analogous to the mammalian umbilical cord. The development of the suspensor continues to rely on information derived from the apical cell, and subsequently, the embryo proper. The CLE8 peptide presumably travels from the embryo proper to the upper cells of the suspensor, where it induces *WOX8* expression to regulate cell division and elongation

(Fiume and Fletcher, 2012). The hormone auxin is also transported downward from the embryo, as well as upward from the basal part of the suspensor to form an auxin maximum at the uppermost suspensor cell, called the hypophysis (Robert et al. 2013). A combination of auxin signaling and mobile transcription factors is required to specify identity of the hypophysis, which will be the only part of the suspensor that is incorporated into the embryo to become the precursor to the root stem cell niche (Scheres et al. 1994) (Fig. 1.2).

Meanwhile, the apical cell progresses through a combination of longitudinal and transverse divisions to form the 8-cell embryo proper, which is itself functionally separated along the apical-basal axis into two tiers, with the 4 upper-tier cells expressing *WOX2* and forming the shoot system, while the lower-tier cells do not express *WOX2* and will form the root (Haecker et al., 2004). Two sets of transcription factors are involved in this patterning event, the class III HOMEODOMAIN-LEUCINE ZIPPER (HD-ZIP III) family, which promotes apical identity, and the PLETHORA (PLT) family, which promotes basal identity (McConnell et al., 2001; Aida et al., 2004; Miyashima et al., 2013). Expression of the HD-ZIP III members in the upper tier is promoted by WOX2, and the HD-ZIP III and PLT factors antagonize each other, thus maintaining apical-basal polarity in the developing embryo (Smith and Long, 2010). Subsequently, each of these 8 cells undergo an oblique division to form a 16-cell embryo consisting of an outer protodermal layer (shown as green and yellow in Fig. 1.2), and an inner layer (blue and orange in Fig 1.2). Both WOX2 function and auxin signaling are crucial to this asymmetric division, although the specific mechanics are not clear (Breuninger et al., 2008; Yoshida et al., 2014). The lower-tier inner cells (orange) subsequently divide to generate ground tissues and vascular initials, while the upper tier cells (blue) form the shoot system, including the shoot stem cell niche and cotyledon leaves (Palovaara et al., 2016).

Initiation of the first stem cells begin after the 16-cell stage. At the base of the embryo, PLT activity induces expression of *WOX5* in the hypophysis, marking its transition into stem cell identity (Haecker et al., 2004; Shimotohno et al., 2018). The hypophysis then undergoes a transverse division to create an upper lens-shaped cell, which expresses WOX5 and becomes the quiescent center, and a larger basal cell, which does not express WOX5 and becomes the columella stem cell. Both are incorporated into the basal layers of the developing embryo proper to form the root stem cell niche, which is responsible for creating the entire root system of Arabidopsis (Scheres et al., 1994). However, the bulk of this work will focus on the signaling pathway that occurs in the shoot.

Figure 1.2. Arabidopsis embryogenesis. Embryonic development starts at the zygote stage and progresses through a series of cell divisions to set up the body axes of the plant – a process called embryo-morphogenesis. Key transcription factors mediating the establishment of these initial polarities of the embryo, as well as the first stem cell reservoirs are shown, along with the expression domains of shoot stem cell regulators: *CLV3*, *WUS*, and *STM*. By the transition from globular to heart stage, the shoot, root, ground tissues, and initial cotyledon leaf cells are largely determined. The embryo then switches into the maturation program, where nutrient accumulation occurs concurrently with further growth before the eventual onset of dormancy.

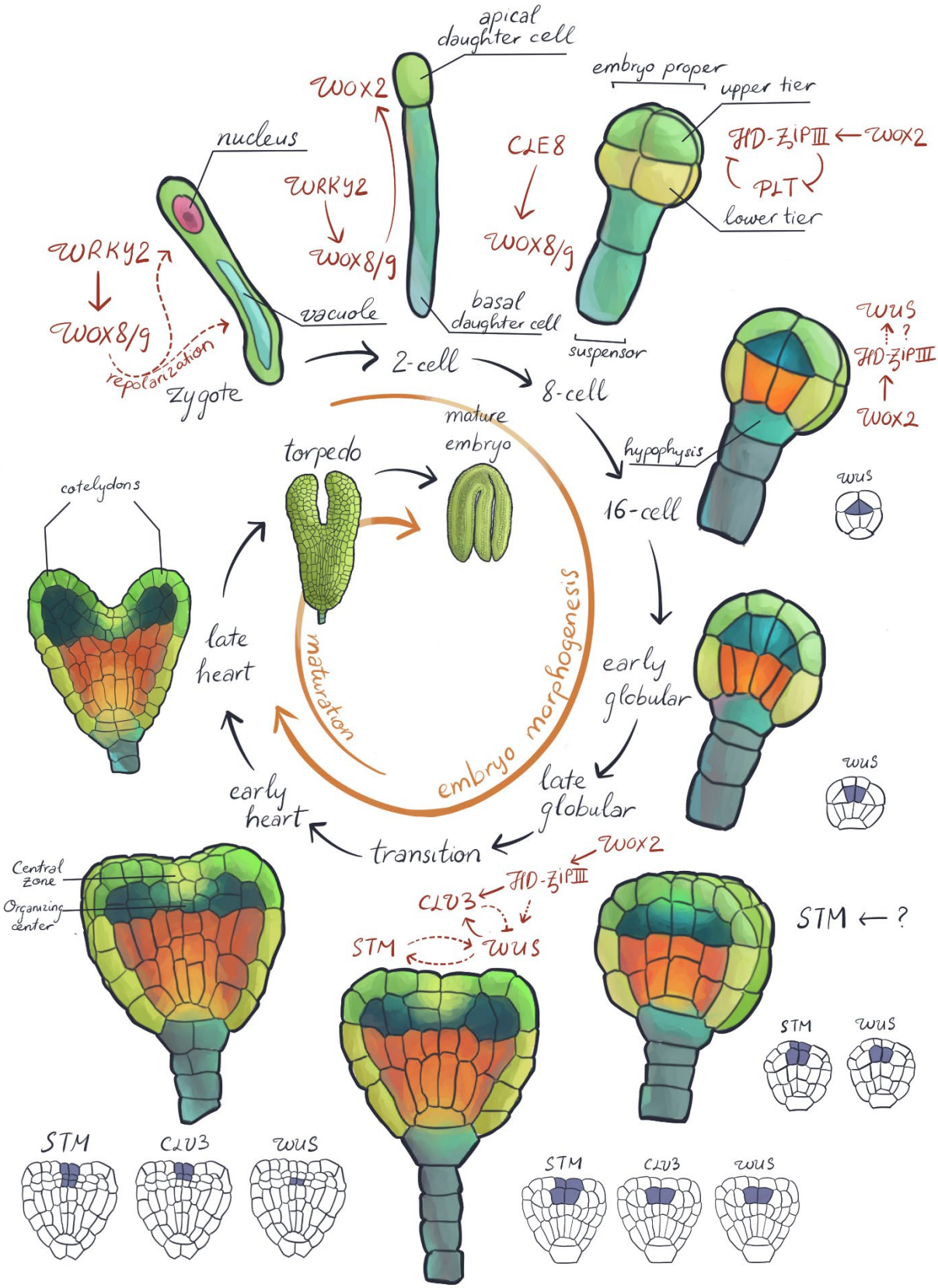
apical daughter cell
WOX2
embryo proper
upper tier
HD-ZIPIII ← WOX2
PLT
lower tier
nucleus
WRKY2
WOX8/9
CLE8
WOX8/9
vacuole
basal daughter cell
suspensor
WRKY2
WOX8/9
repolarization
Zygote
2-cell
8-cell
WUS
?
HD-ZIPIII
WOX2
hypophysis
mature embryo
torpedo
cotelydons
16-cell
WUS
late heart
maturation
embryo morphogenesis
early globular
late globular
WUS
early heart
transition
WOX2
HD-ZIPIII
Central zone
Organizing center
CLV3
STM
WUS
STM ← ?
STM
WUS
STM
CLV3
WUS
STM
CLV3
WUS

In the upper tier of the embryo, WOX2 plays a crucial role in the establishment of the shoot stem cell niche. WOX2 acts through a suite of downstream targets, including the HD-ZIP III transcription factors, to modulate the balance between auxin and cytokinin hormone signaling pathways and create a permissive microenvironment for stem cell establishment (Zhang et al., 2017). Another transcription factor related to WOX2 is encoded by *WUS*, whose expression domain begins at the 16-cell stage and overlaps with *WOX2*. While activation of WUS is dependent upon cytokinin response and HD-ZIP III transcription factors during somatic embryogenesis, or shoot regeneration, it's unclear whether the same process occurs during zygotic embryogenesis (Zhang et al., 2017). At the transition stage, through the HD-ZIP III factors, WOX2 activity also induces expression of *CLV3*, a prominent member of the CLE family, at a few central cells in the subepidermal apical layer. As CLV3 is considered a molecular marker for shoot stem cell identity, *CLV3* activation marks the initiation of the stem cell niche (Fletcher et al., 1999). While WUS is dispensable for the activation of CLV3 and initiation of the stem cell niche, its activity is required to maintain stem cell identity in the shoot. As embryonic development progresses, WUS and CLV3 are recruited into a negative feedback loop, in which WUS directly upregulates *CLV3* transcription, while CLV3 signaling represses *WUS* expression in a domain-specific manner (Brand et al., 2000; Schoof et al., 2000). Their interaction stabilizes stem cell proliferation at the shoot apex, with wide-ranging implications for post-embryonic shoot development and organ formation.

In an independent pathway of WOX2 and WUS, the *SHOOT MERISTEMLESS* (*STM*) gene encodes a class I KNOTTED1-LIKE HOMEOBOX (KNOX1) transcription factor, and is induced in the stem cell niche through a yet uncharacterized mechanism, at the late globular stage (Long et al., 1996). Unlike *CLV3* and *WUS*, which occupies discrete domains, STM is expressed broadly throughout the stem cell niche. STM act through both cytokinin-dependent and independent pathways to maintain stem cell competency by sustaining WUS expression, and prevent precocious recruitment of stem cells into the differentiation program (Endrizzi et al., 1996; Yanai et al., 2005; Scofield et al., 2013; Scofield et al., 2014). Cells on either side of the embryonic meristem, on the other hand, do not express STM and are available to differentiate and form the cotyledons, embryonic leaves that are responsible for the characteristic shape of the heart-stage and torpedo-stage embryos. Thus, following the establishment of shoot stem cell fate by WOX2, WUS and STM play complementary roles in sustaining the stem cell niche, which will continue to develop post germination as the shoot apical meristem (Gallois et al., 2002).

I.2 The Shoot Apical Meristem

The shoot apical meristem (SAM) of angiosperm plants is a small, highly organized structure at the growing shoot tip that provides all of the cells to generate the above ground architecture of the plant (Fig. 1.3). The SAM is established during embryogenesis and is maintained throughout the life of the plant. Its two major functions are to continuously initiate organs such as leaves and flowers and to sustain a stem cell reservoir for future organ formation. The organs arise as primordia on the flanks of the meristem, while at the apex the self-renewing stem cell reservoir replenishes the cells that have become incorporated into the organ primordia. To function as a site of ongoing organ formation, the SAM maintains a continuous balance between loss of stem cells through differentiation and their replacement through cell division.

The SAM is stratified into distinct cell layers called the tunica and corpus (Satina et al., 1940). In *Arabidopsis* and many other dicotyledonous plants, the tunica is comprised of an overlying L1 epidermal layer and a sub-epidermal L2 layer (Gifford, 1954). These layers are a single cell thick and remain clonally distinct from one another due to their specific cell division patterns (Poethig, 1987). The corpus, or L3, lies beneath the tunica and consists of cells that divide in all planes. Because cells in each layer participate in both SAM maintenance and organ formation (Poethig and Sussex, 1985a, b), these activities must be coordinated between all of the cell layers.

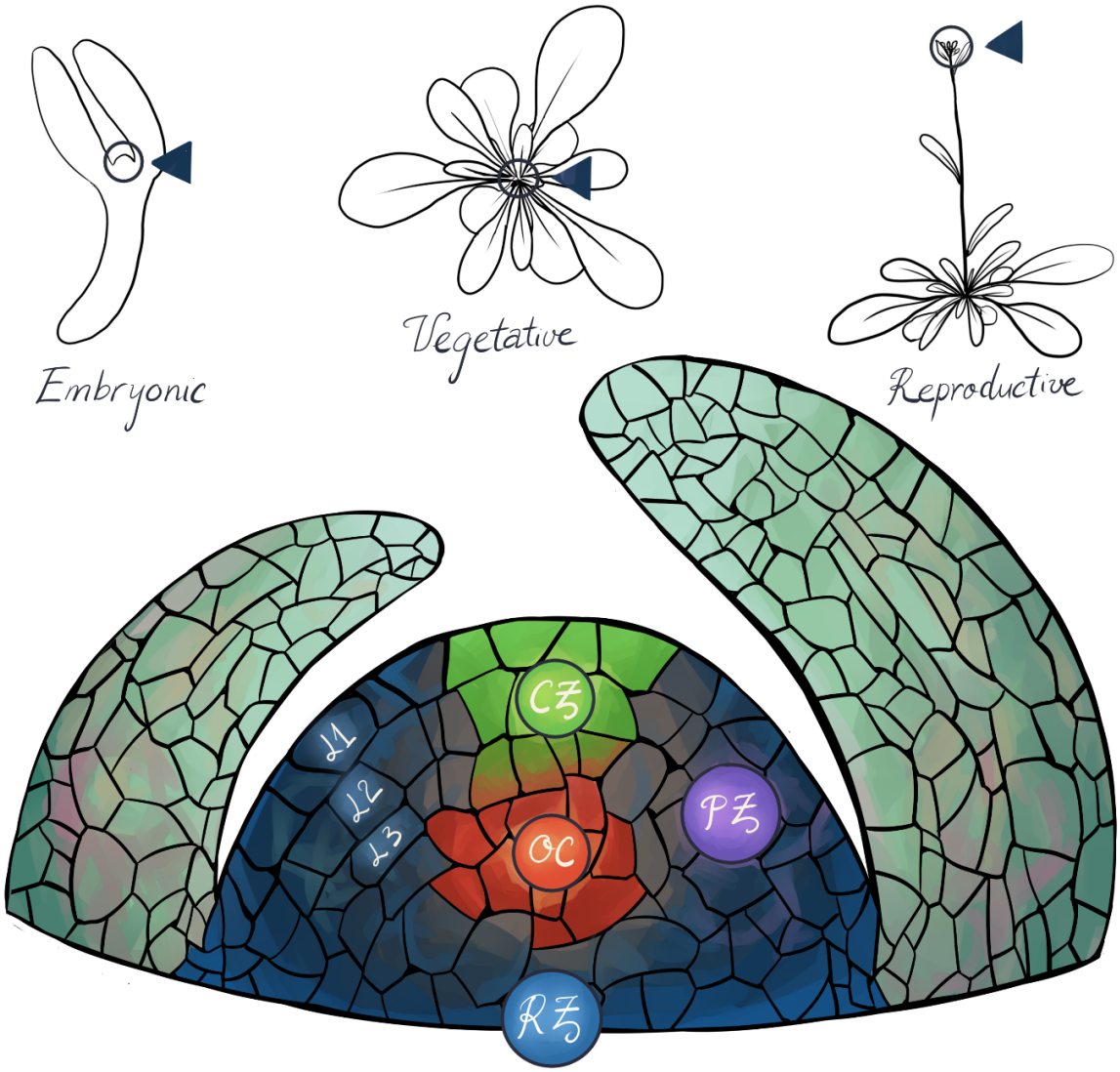

Figure 1.3. Organization of the *Arabidopsis thaliana* shoot apical meristem (SAM). The SAM is located at the growing shoot tip of the plant (blue circle and black arrowhead mark the location of the SAM in plants at three successive developmental stages). L1, L2, and L3 denote layers of distinct cell lineages. The central zone (CZ) is located at the apex and consists of stem cells that divide slowly into the surrounding peripheral zone (PZ) and the underlying rib zone (RZ). Cells in the PZ divide more rapidly and are recruited to form organ primordia or stem tissue. The organizing center (OC) at the top of the RZ functions as a niche that maintains stem cell identity in the CZ.

The SAM is also organized into three distinct functional domains. The central zone (CZ) at the very apex of the SAM consists of a reservoir of pluripotent stem cells with low mitotic activity (Steeves and Sussex, 1989). Divisions of stem cells in the CZ continuously displace their descendants outward into the surrounding peripheral zone (PZ) or downward into the interior rib zone (RZ). The PZ is a transitional region wherein more rapidly dividing stem cell descendants acquire more specified fates and become incorporated either into organ primordia or into regions of stem between the organs. The upper region of the RZ contains the organizing center (OC), which acts as a niche that sustains the overlying stem cell population. Cells in the RZ constitute the meristem pith and contribute to the bulk of the stem and vascular tissue (Steeves and Sussex, 1989). Classical experiments have demonstrated that the functional domains within the SAM exchange cell fate information (Sussex, 1954) and that the fate of each SAM cell is determined by positional information from the surrounding cells rather than from a lineage-specific heritage (Poethig et al., 1986; Furner and Pumfrey, 1992; Irish and Sussex, 1992). Thus SAM cells are in continuous communication with their neighbors in order to assess their relative positions in the meristem and behave accordingly.

A CLV3-mediated shoot apical meristem maintenance pathway

As mentioned above, the CLV-WUS pathway communicates cell fate decisions in the SAM and is essential for stem cell maintenance in higher plants (Somssich et al., 2016). The Arabidopsis *CLV3* gene is a founding member of the *CLE* gene family that is expressed exclusively within the stem cell reservoir of shoot apical and floral meristems (Fletcher et al., 1999). *CLV3* expression in the SAM initiates during the early heart stage of embryogenesis and continues throughout the life cycle. Loss-of-function mutations in *CLV3* cause an accumulation of supernumerary stem cells that leads to progressive SAM enlargement, resulting in the formation of strap-like fasciated stems that produce many more flowers than normal (Clark et al., 1995). Flowers arise from transient stem cell reservoirs in floral meristems (FM), which are also enlarged in *clv3* plants and produce extra floral organs. Thus, *CLV3* restricts above ground stem cell accumulation throughout the life of the plant. Live imaging experiments revealed that *CLV3* performs this function both by restricting stem cell fate to the CZ and also by non-cell autonomously limiting cell division rates in the PZ (Reddy and Meyerowitz, 2005).

CLV3 encodes a secreted signaling molecule that is localized to the extracellular space (Fletcher et al., 1999; Rojo et al., 2002). As with many animal polypeptides, the CLV3 ligand is generated from a larger pre-propeptide that undergoes proteolytic cleavage of the signal peptide and the pro-domain before displaying biological activity (Fig. 1.4A). Cleavage of CLV3 occurs between the Leu^{69} and Arg^{70} residues (Ni and Clark, 2006; Ni et al., 2011; Xu et al., 2013), and requires a recognition domain of five amino acids flanking the amino-terminus of the CLE domain (Xu et al., 2013). It has been suggested that CLV3 cleavage is catalyzed by a serine protease (Ni et al., 2011), but this remains to be confirmed experimentally.

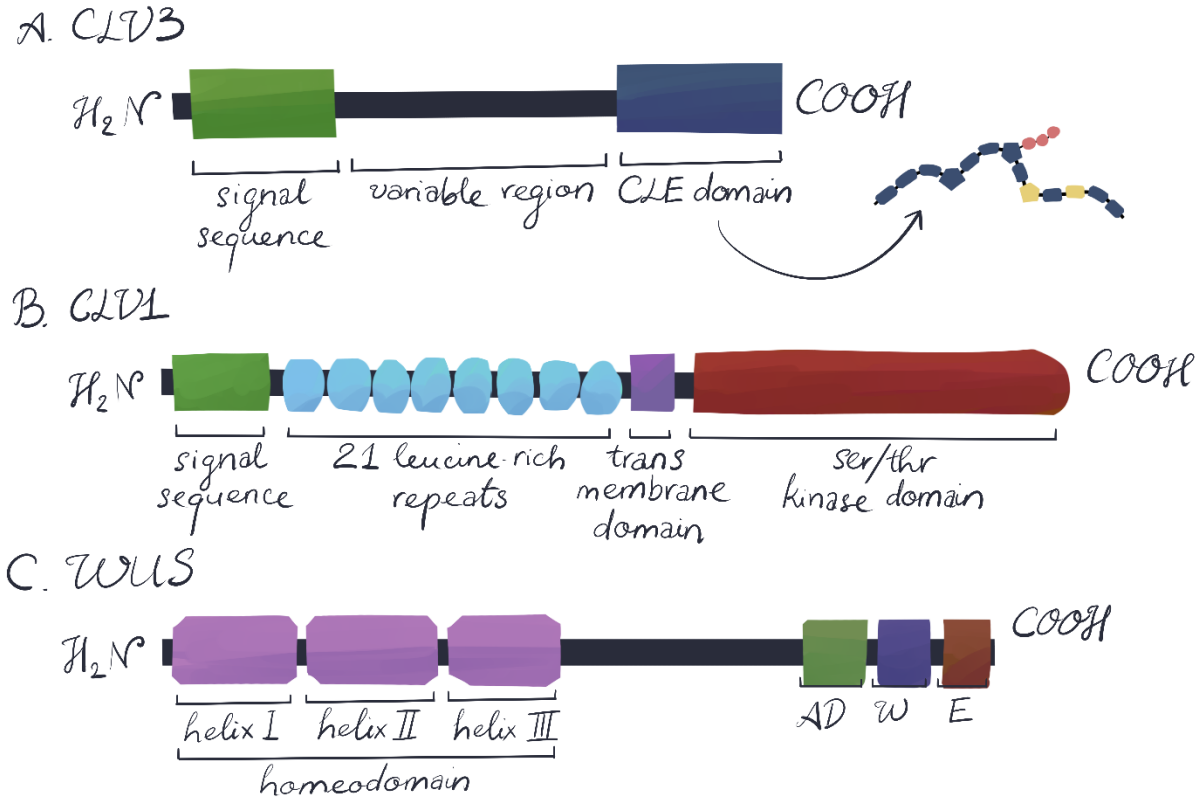

Figure 1.4. Functional domains of key SAM regulatory proteins. (A) The CLV3 pre-propeptide contains a signal sequence that directs it into the extracellular space, a variable region, and a CLE domain. The pre-propeptide is cleaved at the amino-terminus of the CLE domain (red arrowhead), and the released 12-13 amino-acid peptide is modified to generate a functional ligand. (B) The CLV1 protein is a receptor-like kinase (RLK) that consists of a signal sequence that directs it to the plasma membrane, 21 extracellular leucine-rich repeat domains, a transmembrane domain, and a cytosolic serine/threonine kinase domain. (C) The WUS protein is a transcription factor that contains an amino-terminal DNA-binding homeodomain consisting of three helices, as well as three conserved sequence motifs at the carboxyl-terminus: an acidic domain (AD), a WUS box (W), and an EAR domain (E). Molecules are not drawn to scale.

The active form of CLV3 was first identified as a 12 amino acid glycopeptide consisting of Arg^{70} to His^{81} of the CLE motif, in which the first two proline residues are modified to hydroxyproline (Kondo et al., 2006). When applied to Arabidopsis seedlings this synthetic MCLV3 peptide generates a SAM termination phenotype characteristic of *CLV3* gain-of-function plants, demonstrating its biological activity. Two studies have examined the contributions of individual residues within the CLV3 peptide to its function in restricting meristem cell accumulation. The transformation of constructs encoding Alanine-substituted CLV3 peptides into *clv3* null mutants revealed that, in order of importance, the Asp^{8}, His^{11}, Gly^{6}, Hyp^{4}, Arg^{1} and Pro^{9} residues are the most critical for CLV3 activity in the SAM (Song et al., 2012). However, the hydroxyproline residue at position 7 has a minimal impact on CLV3 function, as do the flanking sequences outside

the core CLE motif. A follow up study applying synthetic CLV3 peptides to cultured *clv3* null mutant seedlings demonstrated that the Pro^{9} and His^{11} residues of the CLV3 peptide (Fig. 1.5) are the most critical for restricting SAM size *in vitro* (Song et al., 2013). The presence of these two residues positively correlates with CLV3 protein stability *in vitro*, suggesting that CLV3 stability may be important for its role in SAM maintenance.

Sugar modification of the CLV3 peptide is also important for its activity in SAM maintenance. A 13 amino acid hydroxylated and arabinosylated secreted peptide was biochemically identified from Arabidopsis *CLV3* over-expressing plants (Ohyama et al., 2009), in which the Hyp^{7} residue of CLV3 is post-translationally modified with three L-arabinose residues (Fig. 1.5). This modification was shown to enhance CLV3 activity in the seedling SAM (Ohyama et al., 2009). NMR spectroscopy revealed that arabinosylation induces a conformational change in the carboxyl-terminal half of the CLV3 peptide and enhances receptor binding affinity (Shinohara and Matsubayashi, 2013). In tomato, three arabinosyltransferase genes, *FASCIATED INFLORESCENCE (FIN), REDUCED RESIDUAL ARABINOSE 3 (RRA3A)* and *FASCIATED AND BRANCHED2 (FAB2),* are implicated in the arabinosylation of CLV3 peptides (Xu et al., 2015). Mutations in any of these genes cause an increase in inflorescence branching and the formation of fasciated flowers with extra floral organs. *SlCLV3* null mutants generated using the CRISPR-Cas9 genome editing method display a fasciated SAM phenotype and closely resemble *fin* plants. Synthesized arabinosylated SlCLV3 peptides partially rescue the *fin* fasciated phenotype, confirming the importance of CLV3 arabinosylation *in vivo*. A similar effect was obtained using arabinosylated SlCLE9 peptides, implying a role for SlCLE9 in SAM signaling, although this is yet to be confirmed using mutational analysis. Together, the results indicate that the progressive addition of arabinose chains to CLV3, and potentially to related CLE peptides, by a cascade of arabinosyltransferases is required to fully maintain stem cell homeostasis in the SAM.

CLV3 orthologs are also present in a variety of other crop plants, which over the past ten thousand years have undergone intense selection by humans (Kuittinen and Aguade, 2000; Doebley et al., 2006) for yield traits such as larger and more numerous inflorescences, fruits, and seeds. The *CLV3* locus has been a target of selection during the domestication of several crop species to enhance agricultural yields (Somssich et al., 2016). A naturally occurring mutation in the mustard *(Brassica rapa) CLV3* gene *MULTILOCULAR4 (ML4)* leads to the formation of fruits with four chambers instead of two, which increases seed production (Fan et al., 2014). Likewise, the mild branching and fasciated flower and fruit phenotype of the classical tomato *fasciated (fas)* allele results from a regulatory mutation at the *SlCLV3* locus that reduces the size of the *CLV3* expression domain without affecting peptide function (Xu et al., 2015). These studies suggest that fine-tuning CLV signaling in the SAM by modulating *CLV3* mRNA expression levels and/or peptide activity may also be exploited in other crops to improve productivity.

CLV3 Signal Perception

Genetic analyses have uncovered a small suite of membrane-associated receptors that mediate CLV3 signaling in shoot and floral meristems (Fig. 1.5). However, the contributions of the various receptors to CLV3 signal transduction have remained unclear, as has the functional relationships between them and their relative effects on downstream signaling outputs. Several recent studies provide new insights into these questions.

The first receptor gene shown to play a role in SAM stem cell homeostasis was *CLV1*. Loss-of-function mutations in *CLV1* cause progressive shoot and floral meristem enlargement phenotypes that are similar to but weaker than *clv3* phenotypes, and the two genes act in the same genetic pathway (Clark et al., 1993, 1995; Dievart et al., 2003). CLV1 encodes a leucine-rich repeat (LRR) receptor serine/threonine kinase (Fig. 1.4B) that is produced in shoot and floral meristem cells interior to the *CLV3*-expressing stem cell domain (Clark et al., 1997). CLV1 is localized to the plasma membrane, where it forms homodimers (Bleckmann et al., 2009) and binds the CLV3 ligand (Ogawa et al., 2008). In contrast with other intercellular signaling pathways in plants, CLV3 appears to bind pre-formed receptor complexes at the plasma membrane (Somssich et al., 2015). Ligand binding triggers activation of the CLV1 kinase domain on the cytosolic surface of the cell, which is thought to lead to recruitment of accessory proteins and to result in CLV1 internalization and trafficking to the lytic vacuole for degradation (Nimchuk et al., 2011b). Signaling through the CLV3-CLV1 ligand-receptor pair limits SAM stem cell accumulation by negatively regulating the *WUS* expression domain in the underlying RZ cells (Brand et al., 2000). The CLV1 receptors are sequestered within plasma membrane microdomains following CLV3 perception, attenuating their signaling activity to prevent complete repression of *WUS* transcription and SAM termination (Somssich et al., 2015).

Genetic and biochemical studies also provide evidence for a second distinct receptor complex involved in CLV3-mediated stem cell signaling, consisting of the CLV2 and CORYNE (CRN) proteins (Guo et al., 2010; Durbak and Tax, 2011). *CLV2* encodes a receptor-like protein with extracellular LRRs, a transmembrane domain and a short cytoplasmic tail (Jeong et al., 1999a). Like *CLV3* and *CLV1*, *CLV2* restricts shoot and floral stem cell accumulation (Kayes and Clark, 1998), as does *FASCIATED EAR2 (FEA2)*, the maize ortholog of *CLV2* that maps to a quantitative trait locus (QTL) for kernel row number (Bommert et al., 2013). *CRN* encodes a membrane-associated protein with a cytoplasmic serine/threonine kinase domain, and *crn* mutants display *clv*-like enlarged SAM phenotypes (Muller et al., 2008). Unlike *CLV1*, both *CLV2* and *CRN* are widely expressed in many plant tissues and have broad effects on plant development (Jeong et al., 1999b; Muller et al., 2008).

CLV2 and CRN proteins localize to the plasma membrane and form heterodimers (Bleckmann et al., 2009; Zhu et al., 2010). However, CRN lacks kinase activity and is likely to be a pseudokinase that functions as a CLV2 co-receptor (Nimchuk et al., 2011a). Over-expression of *CLV3* in *clv2* plants fails to rescue the enlarged SAM phenotype, indicating that CLV2 is involved in CLV3 signal transduction (Brand et al., 2000). However, the observation that *clv1* phenotypes are enhanced by mutations in either *CLV2* or *CRN* shows that the CLV2-CRN complex functions independently of CLV1 in this process (Muller et al., 2008; Zhu et al., 2010). Whether the CLV2-CRN complex binds CLV3 peptide is unresolved, though, as immunoprecipitation experiments indicate that CLV2 generates a CLV3-binding activity in tobacco leaves (Guo et al., 2010), whereas photo affinity labeling experiments show that CLV2 does not directly bind to arabinosylated CLV3 peptide (Shinohara and Matsubayashi, 2015).

The transcriptional regulation of *CRN* is important for SAM maintenance (Yue et al., 2013). *CRN* transcription is directly repressed by SKB1/PRMT5, a member of the type II arginine methyltransferase family that in animals regulate chromatin remodeling, transcription and pre-mRNA splicing (Bedford and Clarke, 2009). SKB1 directs symmetric dimethylation of histone

H4R3 at the *CRN* locus, which leads to up-regulation of *CLV3* and *WUS* transcription in their native domains and maintenance of proper SAM size (Yue et al., 2013).

CLV1 forms a monophyletic group with three other LRR-RLK genes, *BARELY ANY MERISTEM1, 2* and *3 (BAM1-3)*, which are predominantly expressed on the flanks of the SAM (DeYoung et al., 2006). Plants carrying higher order combinations of *bam* alleles have reduced SAM size, indicating that the *BAM* genes redundantly promote stem cell maintenance (DeYoung et al., 2006). However, *clv1* null mutant phenotypes can be enhanced by mutations in *BAM1* or *BAM2* (DeYoung and Clark, 2008); thus BAM1 and BAM2 also function as redundant CLV3 receptors in the PZ. Indeed, both BAM1 and BAM2 bind CLV3 peptide (Guo et al., 2010; Shinohara and Matsubayashi, 2015). Because *clv1 bam1* plants are insensitive to exogenous arabinosylated CLV3 peptide treatment, CLV1 and BAM1 activity is sufficient to regulate CLV3-mediated stem cell homeostasis in the SAM (Shinohara and Matsubayashi, 2015). A recent study has clarified the relationship between *CLV1* and the *BAM* genes in SAM maintenance. CLV1 signaling was found to repress the expression of *BAM1* and *BAM3* in the RZ (Nimchuk et al., 2015). Thus, a dual-activity model suggests that under normal conditions, the BAM receptors prevent CLV3-CLV1 signaling at the flank of the SAM to maintain stem cell accumulation. However, in clv1 mutants, ectopic BAM expressions partially compensate for the loss of CLV1 activity by interacting with the CLV3 peptide. Interestingly, *clv1 bam123* quadruple mutants have stronger vegetative SAM phenotypes than *clv3* null mutants (Nimchuk et al., 2015), indicating that at least one other ligand that acts partially redundantly with CLV3 in SAM maintenance remains to be identified.

The BAM1 protein has been shown to physically associate with a LRR receptor-like kinase encoded by the *RECEPTOR-LIKE PROTEIN KINASE2 (RPK2)* gene (Kinoshita et al., 2010). Plants carrying *rpk2* mutations display slightly enlarged SAMs and are insensitive to CLV3 peptide treatment, indicating that RPK2 is involved in CLV3 ligand perception. *RPK2* is expressed uniformly throughout the SAM (Kinoshita et al., 2010), and forms homomers as well as interacting with BAM1. However, it neither associates with CLV1 or CLV2 (Kinoshita et al., 2010; Shimizu et al., 2015) nor binds directly to CLV3 peptide (Shinohara and Matsubayashi, 2015). RPK2 is therefore likely to regulate meristem maintenance by transmitting the CLV3 signal through the BAM1 pathway rather than the CLV1 or CLV2/CRN pathways.

The relationship between CLV1 and the other SAM receptors has been investigated using genetic analysis. Like *CLV1, CLV2* and *CRN* mediate stem cell regulation exclusively in the *WUS*-expressing cells of the RZ (Nimchuk, 2017). However, *CLV2, CRN* and *RPK2* are dispensable for the repression of the *BAM* receptor kinase genes by CLV3-CLV1 signaling. The CLV1-mediated repression of *WUS* transcription and consequent restriction of stem cell accumulation was determined to be genetically separable from its regulation of *BAM* gene expression. CLV1 therefore controls two distinct signaling outputs – the repression of *WUS* transcription and the repression of *BAM* transcription – in SAM stem cell niches in response to the CLV3 ligand independently of the other receptors.

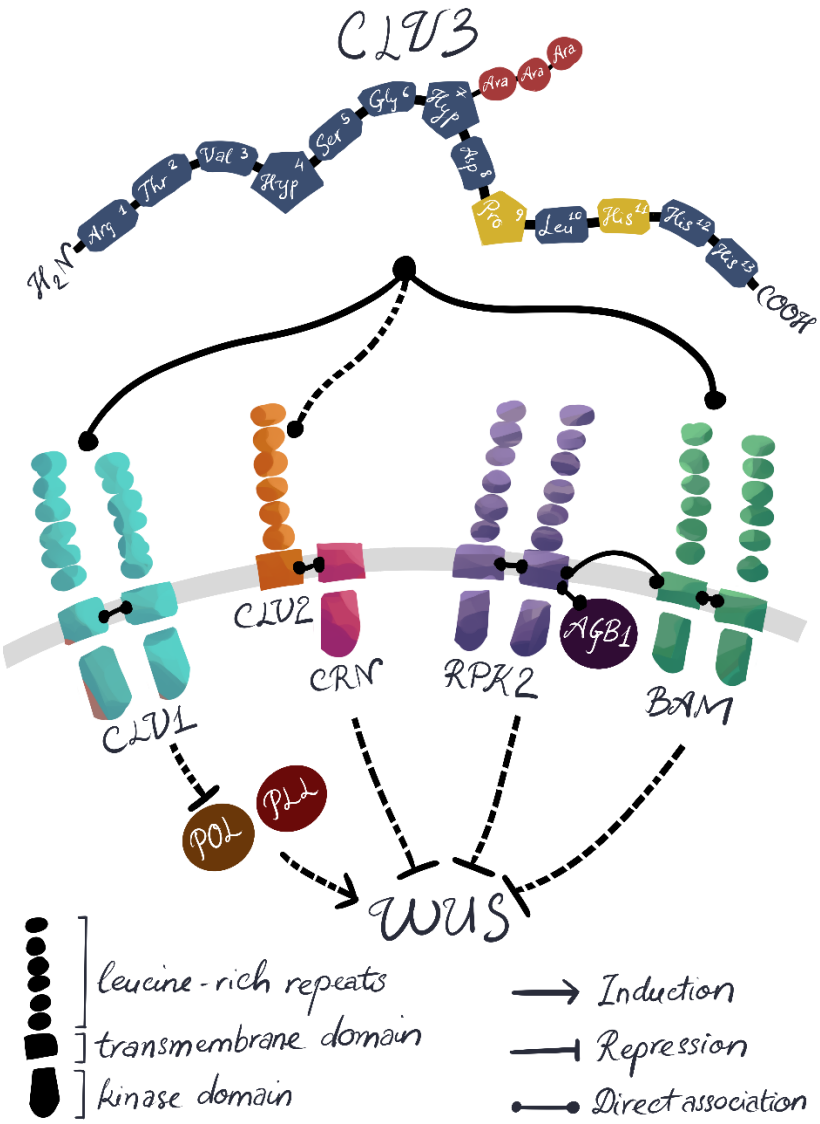

Figure 1.5 CLV3 signaling pathways. The mature CLV3 peptide forms a horseshoe-shaped kink around the Gly[6] and Hyp[7] residues that is likely recognized by its receptors. The Hyp[7] residue is post-translationally modified with three L-arabinose residues (red). The Pro[9] and His[11] residues (gold) are most critical for the ability of CLV3 to restrict SAM size *in vitro*. CLV3 signaling is mediated by a suite of receptors. The LRR-RLK CLV1 forms homodimers that bind to CLV3 peptide, and the protein phosphatases POL and PLL1 act downstream of CLV1 to promote *WUS* transcription. The LRR protein CLV2 and the pseudokinase CRN form a heterodimeric complex that is involved in CLV3 signal transduction, but whether it directly binds CLV3 is unclear. The LRR-RLK RLK2 forms homodimers that associate with the G protein subunit AGB1, but also does not bind directly to CLV3. RPK2 physically interacts with the CLV3-binding LRR-RLK BAM1 in the peripheral zone of the SAM, but not with CLV1 or CLV2. Molecules are not drawn to scale.

CLV3 Signal Transduction

Several classes of cytosolic components function in CLV3 signal transduction downstream of ligand binding (Fig. 1.5). In Arabidopsis, the kinase associated protein phosphatase KAPP and a Rho GTPase-related protein physically associate with the cytosolic CLV1 kinase domain (Williams et al., 1997; Trotochaud et al., 1999), while the related protein phosphatase 2C proteins POLTERGEIST (POL) and POL-LIKE1 (PLL1) act downstream of CLV1 to promote stem cell maintenance by regulating *WUS* expression (Song et al., 2006). A mitogen-activated protein kinase (MAPK) activity (Betsuyaku et al., 2011) and a E3 ubiquitin ligase called PLANT U-BOX4 (PUB4) (Kinoshita et al., 2015) have also been implicated in signaling downstream of the CLV receptors, although their roles in the signaling network remain to be precisely defined.

In maize, mutations in the *COMPACT PLANT2 (CT2)* gene, which encodes the alpha-subunit of a heterotrimeric GTP binding protein, cause *clv*-like SAM phenotypes (Bommert et al., 2013). Heterotrimeric GTP binding proteins, which are composed of alpha, beta and gamma subunits, are signaling molecules that link extracellular signals to intracellular readouts (Urano and Jones, 2014). The CT2 protein localizes to the plasma membrane and physically interacts with the FEA2 receptor protein *in vitro,* suggesting a molecular mechanism through which receptor-like proteins that lack a kinase domain can transmit information inside the cell (Bommert et al., 2013). Similarly, mutations in the Arabidopsis G protein beta-subunit1 gene *AGB1* produce enlarged SAMs similar to *clv* mutant SAMs and *AGB1* acts upstream of *WUS* in stem cell homeostasis (Ishida et al., 2014). AGB1 protein physically associates with RPK2 at the plasma membrane, although not with CLV1 or CLV2. In contrast to the situation in maize, Arabidopsis Ga activity does not affect SAM function, although Gg activity has a minor role in limiting SAM size (Ishida et al., 2014). Together these observations indicate a role for heterotrimeric GTP binding proteins in transducing CLV-dependent signals within the recipient cells.

CLV3-Independent Signaling Pathways in SAM Regulation

Members of the *ERECTA (ER)* receptor kinase gene family also influence stem cell homeostasis in the SAM. *ER, ERL1* and *ERL2* act redundantly to restrict vegetative SAM activity (Uchida et al., 2013). The promoters of all three genes are active in the SAM, and *er erl1 erl2* seedlings form enlarged SAMs in which the L1 and L2 cells are wider than normal (Chen et al., 2013). Hormone induction experiments suggest that ER family members regulate stem cell homeostasis in the SAM by buffering its responsiveness to cytokinin, which promotes cell proliferation and stem cell activity (Gordon et al., 2009). The ER pathway negatively regulates *WUS* transcription (Chen et al., 2013), although this occurs independently of the CLV pathway (Mandel et al., 2014). In fact, ER, CLV and a third pathway consisting of HD-ZIP III transcription factors (Prigge et al., 2005) act in parallel to regulate SAM size (Mandel et al., 2016). The three pathways seem to affect different aspects of SAM activity, as *CLV3* preferentially restricts SAM cell accumulation along the longitudinal axis whereas *ER* and the *HD-ZIP III* genes restrict its growth along distinct lateral orientations. RNA-seq analysis provides evidence that the CLV pathway limits the accumulation of stem cells in the CZ, whereas the ER pathway regulates mitotic activity in the PZ (Mandel et al., 2016). Thus the coordination of cell behaviors within the SAM appears to be orchestrated by distinct signaling pathways acting along discrete growth vectors.

A novel CLE ligand-receptor signal transduction pathway that regulates maize shoot apical meristem activity has been revealed by the study of the *FASCIATED EAR3 (FEA3)* gene (Je et al.,

2016). *FEA3* encodes a LRR receptor-like protein with 12 extracellular LRR motifs, a transmembrane domain and a short cytoplasmic tail. FEA3 functions to limit maize SAM size and suppresses *ZmWUS* expression in cells below the OC. However, FEA3 does not perceive a CLV3 signal. Rather it responds to a CLE peptide encoded by the *FON2-LIKE CLE PROTEIN 1 (ZmFCP1)* gene, which is orthologous to the rice *FCP1* gene. Mutations in *ZmFCP1* cause enlarged SAM phenotypes, and *ZmFCP1* and *FEA3* function in the same genetic pathway. Interestingly, *ZmFCP1* is not expressed in the SAM itself but in the initiating organ primordia on the SAM flanks. The authors propose that a ZmFCP1 signal originating from differentiating cells within organ primordia is perceived by FEA3 in the interior of the SAM where it acts to restrict stem cell proliferation by negatively regulating *ZmWUS* expression in the RZ cells beneath the OC. The Arabidopsis *FEA3* ortholog, *AtFEA3*, also appears to restrict SAM activity and *AtFEA3* RNAi lines are resistant to CLE27 peptide application, although *CLE27* is not the *ZmFCP1* ortholog. A more recent study revealed the role of yet another receptor kinase in the maize SAM encoded by the ZmFEA2 gene. Like ZmFEA3, ZmFEA2 perceives the ZmFCP1 ligand, but also another signal, ZmCLE7 (Je et al., 2017). Thus stem cell homeostasis in plants is mediated by multiple CLE peptides that originate from different cell types and associate with distinct transmembrane receptors.

WUS-CLV3 Stem Cell Homeostasis Feedback Loop

The key biologically relevant target of the CLV3 stem cell signaling pathway is the *WUSCHEL (WUS)* gene. WUS is the founding member of the WUSCHEL-LIKE HOMEOBOX (WOX) family of transcription factors that contain a homeodomain superficially resembling that found in animal homeodomain proteins (Mayer et al., 1998) (Fig. 1.6). In addition, the protein contains three conserved short sequence motifs at the carboxyl terminus: an acidic domain that may function in transcription activation, a canonical WUS box, and an EAR domain that can mediate transcriptional repression (Ohta et al., 2001). *WUS* expression is restricted to a small set of cells just beneath the stem cells (Mayer et al., 1998), which is called the organizing center (OC) based on its functional correspondence to animal stem cell niches (Fig. 1.3).

Although *WUS* is dispensable for the establishment of the Arabidopsis shoot stem cell reservoir (see below), it is required to sustain stem cell activity in shoot and floral meristems throughout the life of the plant (Laux et al., 1996). WUS promotes stem cell fate in a non-cell autonomous fashion, with the protein moving from the OC into the overlying stem cells where it accumulates at a lower level than in the OC cells themselves (Yadav et al., 2011). This movement occurs via cytoplasmic channels between neighboring cells called plasmodesmata and is essential for SAM maintenance (Daum et al., 2014). WUS protein accumulation in the CZ induces the expression of *CLV3* (Fig. 1.6), activating its own negative regulator in a dynamic feedback loop that regulates stem cell homeostasis in the SAM (Brand et al., 2000; Schoof et al., 2000).

The regulation of *CLV3* transcription by WUS occurs in a dosage-dependent manner. Lower concentrations of WUS protein activate *CLV3* transcription whereas higher concentrations repress *CLV3* transcription (Perales et al., 2016). WUS protein binds with different affinities to six *cis* elements in the regulatory region of the *CLV3* locus, five of which occur in a module in the 3' region, and these six elements mediate both the activation and repression of *CLV3* expression. WUS binds the *CLV3 cis* elements as monomers at lower concentrations, and as homodimers at higher concentrations (Perales et al., 2016). Structure-function analysis indicates that reduced WUS protein accumulation in the stem cell reservoir may occur through a combination of potent

nuclear export and weak nuclear retention of the protein within these cells, potentially due to a lower affinity for DNA and reduced dimerization activity (Rodriguez et al., 2016). In this manner, lower levels of WUS protein in the nucleus of the stem cells leads to *CLV3* activation, whereas higher levels of WUS protein in the nucleus of OC cells leads to *CLV3* repression (Perales et al., 2016).

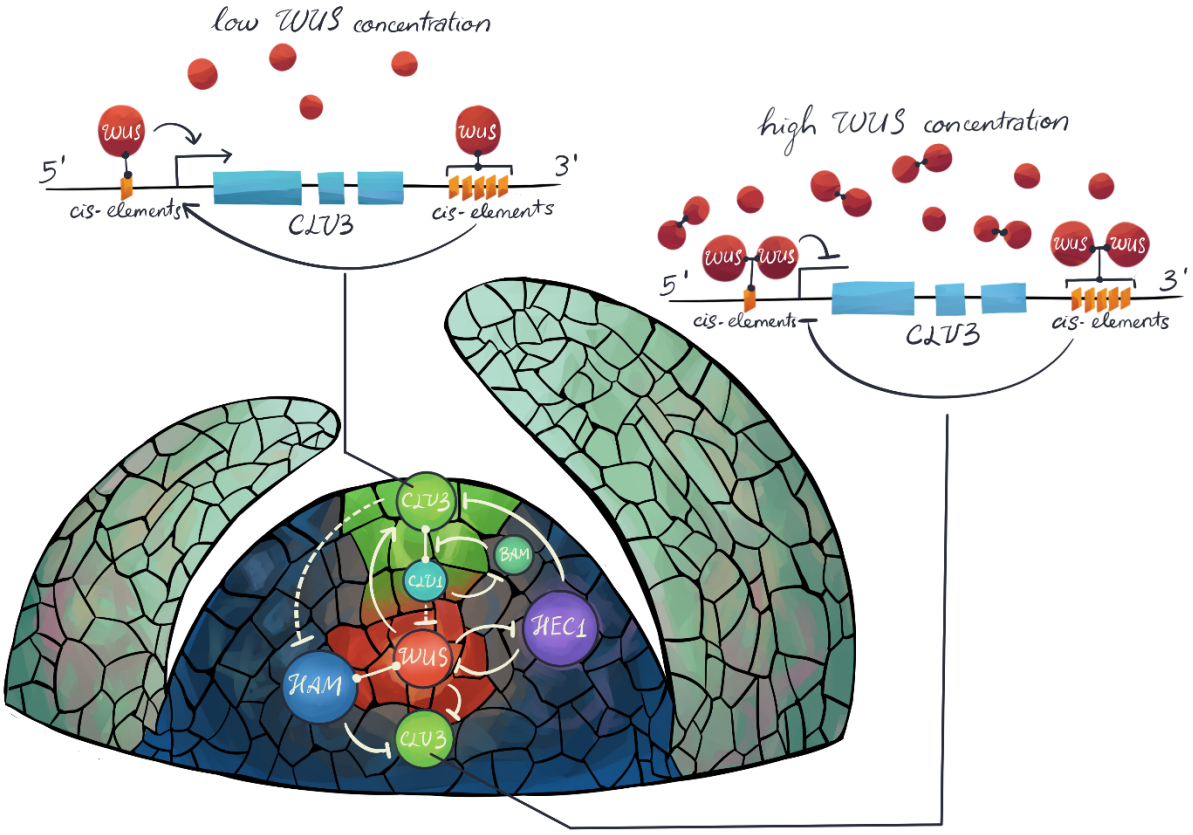

Figure 1.6. The CLV3-WUS stem cell homeostasis network. CLV3 ligand produced in the CZ diffuses into the underlying OC cells to associate with CLV1 and other receptors. CLV1 binding triggers signaling pathways that repress *BAM1* expression and limit the *WUS* expression domain to the OC. The *WUS* expression domain overlaps with that of the GRAS domain transcriptional regulatory gene *HAM1*, which is repressed by CLV3 signaling, and the WUS and HAM proteins act together as cofactors that share common target genes. WUS activity in the OC represses the expression of differentiation-promoting transcription factors (TFs) and the bHLH TF gene *HEC1*. WUS protein also moves into the adjacent CZ to promote stem cell fate and regulate *CLV3* transcription. WUS protein recognizes cis-elements both upstream and downstream of the *CLV3* coding region. In the CZ, where WUS protein concentration is low, WUS binds the cis elements as a monomer to activate *CLV3* transcription. In the OC, where WUS protein concentration is high, WUS binds the cis elements as a dimer to repress *CLV3* transcription. HEC1 activity in the PZ represses *CLV3* and *WUS* expression, and acts oppositely to WUS in the regulation of cytokinin signaling. Together this complex signaling network coordinates stem cell maintenance in the SAM.

WUS-Dependent Gene Regulatory Network

WUS is a bi-functional protein that can act as both an activator and a repressor of transcription (Ikeda et al., 2009), and regulates the expression of hundreds of genes in the shoot apical meristem. A genome-wide identification of WUS response genes using Arabidopsis ATH1 arrays yielded a total of 675 genes (Busch et al., 2010), including 4 hormone responsive type-A *ARABIDOPSIS RESPONSE REGULATOR (ARR)* genes previously described as WUS targets (Leibfried et al., 2005). Gene ontogeny analysis revealed an over-representation of WUS responsive genes in three categories: regulation of development, metabolic processes, and hormone signaling. The *CLV1* gene was found to be directly repressed by WUS despite their overlapping expression patterns in the interior of the SAM, suggesting that WUS acts to fine-tune *CLV1* transcription rather than acting as a binary switch. WUS also directly represses the transcription of *TPR1* and *TPR2*, members of the *TOPLESS/TOPLESS RELATED (TPL/TPR)* family of transcriptional co-repressor genes that play key roles in embryo patterning and auxin responses (Long et al., 2006; Szemenyei et al., 2008). WUS protein was shown to directly bind two distinct DNA motifs, one of which is a G-Box motif with striking similarity to binding sites for proteins involved in stem cell renewal in animals, the zinc-finger homeodomain transcription factor Zeb-1 (Grooteclaes and Frisch, 2000) and the bHLH-ZIP transcription factor MYC (Blackwell et al., 1990).

A second study using an inducible WUS system also identified over 600 WUS-responsive genes in SAM tissue, among which 49 up-regulated and 140 down-regulated genes are direct WUS targets (Yadav et al., 2013). The majority of WUS-activated genes are expressed in the CZ and OC of the SAM, whereas the majority of WUS-repressed genes are expressed in the PZ. Among the latter, WUS directly binds to the regulatory regions of key transcription factor genes such as *KANADI1 (KAN1), KAN2, ASYMMETRIC LEAVES2* and *YABBY3* that promote organ identity and cell differentiation. Thus WUS controls stem cell homeostasis in part by repressing the expression of differentiation-inducing transcription factor genes in the central regions of the SAM to prevent premature stem cell differentiation.

An important direct target of WUS repression in the OC is the bHLH transcription factor gene *HECATE1 (HEC1)* (Schuster et al., 2014). *HEC1* is expressed in the PZ of the SAM as well as in developing organ primordia, and functions redundantly with the related *HEC2* and *HEC3* genes to promote SAM cell accumulation. HEC1 activity represses *CLV3* and *WUS* expression while elevating the expression of cell-cycle regulatory genes to stimulate cell proliferation (Fig. 1.6). In addition, transcriptome analysis indicates that WUS and HEC1 oppositely regulate suites of metabolic and hormone signaling genes, including the type-A *ARR7* and *ARR15* genes. These *ARR* genes are involved in negative feedback regulation of cytokinin signaling (To et al., 2004) and can arrest SAM function when constitutively activated (Leibfried et al., 2005). Whereas WUS directly represses type-A *ARR* gene transcription to enhance cytokinin signaling in the SAM (Leibfried et al., 2005), HEC1 induces their expression and thereby acts as a negative regulator of downstream cytokinin signaling outputs (Schuster et al., 2014). The opposing activities of these two transcription factors in hormone regulation are thought to represent an important mechanism for coordinating a balance between cell proliferation and differentiation in distinct functional domains of the SAM.

WUS-Associated Factors

WUS does not regulate gene expression in isolation but physically associates with members of the HAIRY MERISTEM (HAM) family of GRAS domain transcriptional regulators (Zhou et al., 2015). Members of this family promote stem cell maintenance in Arabidopsis and petunia (Stuurman et al., 2002; Engstrom et al., 2011), and Arabidopsis *ham1234* plants arrest at early seedling stage with terminated SAMs (Zhou et al., 2015). The *HAM* gene expression patterns overlap with that of *WUS* in the SAM, with both *HAM1* and *HAM2* being expressed in the RM, including the OC cells. In addition *HAM1* expression, like *WUS* expression, is repressed by CLV3 signaling. Because a weak *wus-7* allele displays dose-dependent genetic interactions with *ham* null alleles, the strong *wus-1* mutant is epistatic to *ham123* null mutants, and the WUS and HAM proteins share some common downstream regulatory targets (Zhou et al., 2015), the HAM transcriptional regulators are proposed to act as conserved interacting cofactors with WUS in the OC of the SAM (Fig. 1.6). A recent study has shown that HAM activity also plays a role in constraining *CLV3* to the upper layers of the SAM, such that in the *ham123* mutant, *CLV3* expression migrates down to the center of the SAM and completely overlaps with *WUS* (Zhou et al., 2018).

WUS also physically associates with TPL and several TPR co-repressor proteins via the acidic domain, WUS box, and EAR motif in the carboxyl-terminal region of the WUS protein (Kieffer et al., 2006; Dolzblasz et al., 2016). The TPL and TPR proteins associate with HISTONE DEACETYLASE19 (HDA19) to form a transcription repression complex (Szemenyei et al., 2008), suggesting a mechanism through which WUS may repress the expression of differentiation-inducing genes within the OC by recruitment of histone modifying complexes. Whether members of either the HAM or TPL/TPR families act together with WUS to regulate *CLV3* transcription remains to be determined.

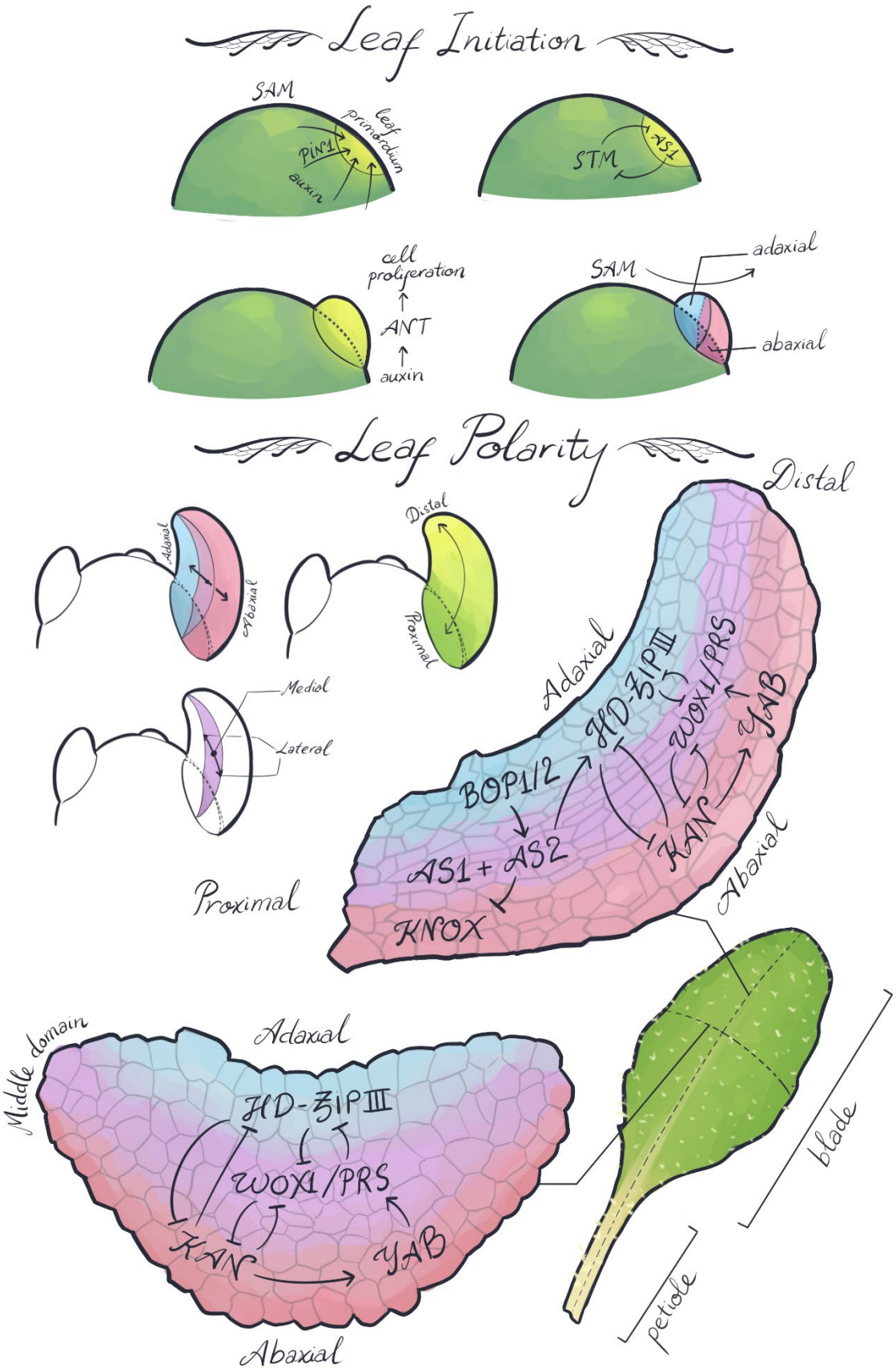
Leaf Initiation
SAM
leaf primordium
PIN1
auxin
STM
AS1
cell proliferation
ANT
auxin
SAM
adaxial
abaxial
Leaf Polarity
Distal
Adaxial
Abaxial
Distal
Proximal
Medial
Lateral
Proximal
Adaxial
HD-ZIPIII
WOX1/PRS
YAB
BOP1/2
AS1 + AS2
KNOX
KAN
Abaxial
Middle domain
Adaxial
HD-ZIPIII
WOX1/PRS
KAN
YAB
Abaxial
blade
petiole

Figure 1.7. Leaf development in Arabidopsis. An incipient leaf primordium is marked on the flank of the SAM by a local auxin maximum, mediated by the PIN1 auxin transporter. The boundary between pluripotent stem cells in the SAM and differentiated leaf cells is reinforced by mutual antagonistic interaction between STM and AS1. ANT is also upregulated in an auxin-dependent manner in the primordium to promote cell division and subsequent leaf outgrowth. Three major axes are specified during leaf development and contribute to its final shape: the adaxial-abaxial axis, proximal-distal axis, and medio-lateral axis. Important transcription factors in establishing and maintaining the adaxial-abaxial (ad: AS1/AS2 and HD-ZIP III, mid: WOX1/PRS, ab: KAN and YAB), and proximal-distal (BOP1/2, KNOX) axes are shown.

I.3. Organ formation at the SAM

Leaf and stomatal development

It does not come as any surprise that the first lateral organs that initiate from the SAM after germination are leaves, photosynthetic powerhouses that convert sunlight into nutrients. It is by these humble devices that some of the biggest organisms on earth are built. Their development begins with the recruitment of a few founder cells in the PZ into the differentiation program (Irish and Sussex, 1992; Barton et al., 2010). Specification of this incipient leaf primordium requires a local auxin maximum, which is mediated by the PINFORMED1 (PIN1) auxin transporter in Arabidopsis (Reinhardt et al., 2000; Reinhardt et al., 2003). Currently, the most prominent model of phyllotaxy involves the concept of an inhibitory field, where each incipient organ primordium alters the auxin concentration and auxin response pathway around it to prevent the formation of another primordium in its immediate vicinity (Vernoux et al., 2011; Galvan-Ampudia et al., 2016). As a result, leaves in wild-type Arabidopsis initiate in a relatively stable spiral pattern, each one separated from the last by approximately 135º - the Golden angle. In addition, expression of KNOX1 genes such as *STM*, *BREVIPEDICELLUS/KNOTTED-LIKE FROM ARABIDOPSIS THALIANA1* (*BP/KNAT1*) and *KNAT2*, which maintains stem cell competency, is excluded from the initiating primordium, while expression of the differentiation-promoting *ASYMMETRIC LEAF1* (*AS1*) transcription factor is induced (Byrne et al., 2000; Byrne et al., 2002; Guo et al., 2008). While the upstream mechanisms modulating their expressions is to be determined, once a polarity is set up, *KNOX1* genes and *AS1* will antagonize each other's expression, fortifying the boundary that separates stem cell from leaf cell identity (Fig. 1.7).

Once leaf identity has been acquired, the high concentration of auxin also induces expression of the plant-specific transcription factor *AINTEGUMENTA* (*ANT*), which in turn accelerates the cell cycle to promote outgrowth of the new primordium (Elliot et al., 1996; Mizukami and Fisher, 2000). Concurrently, within this growing but uniform mass of cells, a whole new set of body axes is set up to give leaves their distinctive shapes. The flatness of a leaf blade is contributed by an interplay between the adaxial domain (facing towards the meristem), and the abaxial domain (facing away from the meristem) (Waites and Hudson, 2001). The adaxial domain is marked by accumulation of the HD-ZIP III transcription factors PHABULOSA (PHB), PHAVOLUTA (PHV), and REVOLUTA (REV), which are induced by activity of the AS1/AS2 complex (McConnell and Barton, 1998; McConnell et al., 2001). On the other side, transcription factors encoded by the *KANADI* (*KAN*) genes *KAN1/2/3* as well as the *YABBY* (*YAB*) genes mark abaxial

identity (Siegfried et al., 1999; Kerstetter et al., 2001; Stahle et al., 2009). *HD-ZIP III* gene expression is induced by the AS1/AS2 complex, while KAN proteins repress *AS2* expression (Fu et al., 2007; Wu et al., 2008). *HD-ZIP III* and *KAN* genes also antagonize each other through opposing effects on components of the same pathways, such as auxin signaling (Huang et al., 2014). Mobile small interfering RNAs also contribute to confining HD-ZIP III and KAN expression to their relative domains (Emery et al., 2003; Husbands et al., 2015; Skopelitis et al., 2017). In addition, it was recognized by Ian Sussex in 1951 that a signal coming from the SAM is crucial to establish the adaxial-abaxial polarity in the developing leaf, as cutting off communication between the two organs via incision results in a radialized leaf with abaxial identity (Sussex, 1951). However, the identity of this signal is yet to be determined. Once established, the adaxial-abaxial polarity is further stabilized by a middle domain, marked by *WOX1/PRS* expression (Nakata et al., 2012). *WOX1/PRS* are positively regulated by YAB, but act in antagonistic manners with both the adaxial and abaxial cell fate determinants (Nakata et al., 2012; Zhang et al., 2014; Guan et al., 2017). WOX1 and PRS transcription factors redundantly promote cell proliferation in this middle domain, leading to the lateral outgrowth of the leaf blade.

Leaf blade expansion caused by WOX1/PRS leads to the establishment of another polarity, the medio-lateral axis. Specifically, cells at the margin of the leaf eventually adopt distinct fates from those towards the center, including the generation of long rectangular cells, and development of specialized structures called hydathodes. Leaf margin development depends both on the proper juxtaposition of the ad-ab axis, and the auxin signaling pathway, mediated by the *YUCCA* auxin-biosynthesis genes as well as the *CUP-SHAPED COTYLEDONS* (*CUC*) NAC-transcription factor genes (Bilsborough et al., 2011; Wang et al., 2011). At the same time, a proximal-distal axis is established as the developing leaf continues to extend outward. The *BLADE ON PETIOLE1* (*BOP1*) and *BOP2* genes are expressed at the base of the leaf primordium (Norberg et al., 2005). They encode redundant transcription factors that are involved in specifying the proximal domain. BOP1 and BOP2 directly induce expression of *AS2* at the proximal cells of the leaves (Ha et al., 2007; Jun et al., 2010). In turn, AS2 forms a complex with AS1 to repress class I *KNOX1* genes and prevent outgrowth at the base of the leaf, resulting in a typical leaf shape consisting of a narrow petiole at the base that connects the stem to a broad flat blade. Variations in the relative domains of these interacting factors thus provide an endless source of natural variants in leaf forms and functions.

Unlike in the SAM, however, there is yet any evidence of a CLE peptide signal contributing to leaf morphology. The only known role for CLE signaling during leaf development is restricted to the stomatal cell lineage. Stomata are specialized structures on the leaf epidermis, each consisting of a pair of guard cells that can respond to external and internal cues to facilitate gas exchange between the plant and its environment. Epidermal precursor cells on the surface of the leaf can either differentiate in pavement cells or become meristemoid mother cells (MMCs). Each MMC can then undergo an asymmetric cell division to form a pair of meristemoid and stomatal lineage ground cell (SLGC). The meristemoid can undergo further amplifying divisions before acquiring guard mother cell identity, which eventually form the pair of guard cells. Meanwhile, the SLGC can also differentiate into a pavement cell, or further divide to generate another pair of meristemoid and SLGC (Vatén et al., 2018). *CLE9* and *CLE10* genes encode the same peptide, and are expressed in the stomatal cell lineage starting at the MMC. The CLE9/10 peptide signals through the LRR receptor kinase HAESA-LIKE1 (HSL1) and its co-receptor SOMATIC EMBRYOGENESIS RECEPTOR KINASE1 (SERK1) to dampen activity of the transcription

factor SPEECHLESS (SPCH), which promotes asymmetric cell divisions (Qian et al., 2018). As a result, *CLE9/10* act both cell-autonomously to suppress division of the MMC where they are expressed, and non-cell autonomously to suppress division of the neighboring SLGCs (Fig. 1.8).

In addition, the opening and closing of guard cells are also under influence by CLE9/10 as a short range signal, and CLE25 as a long range signal. Unlike *CLE9/10*, *CLE25* is expressed in the root, from where it is presumably transported through the phloem to the leaves to interact with BAM1 and BAM3. Both peptides act through the abscisic acid (ABA) signaling pathway to induce stomatal closure in response to environmental conditions (Takahashi et al., 2018; Zhang et al., 2019).

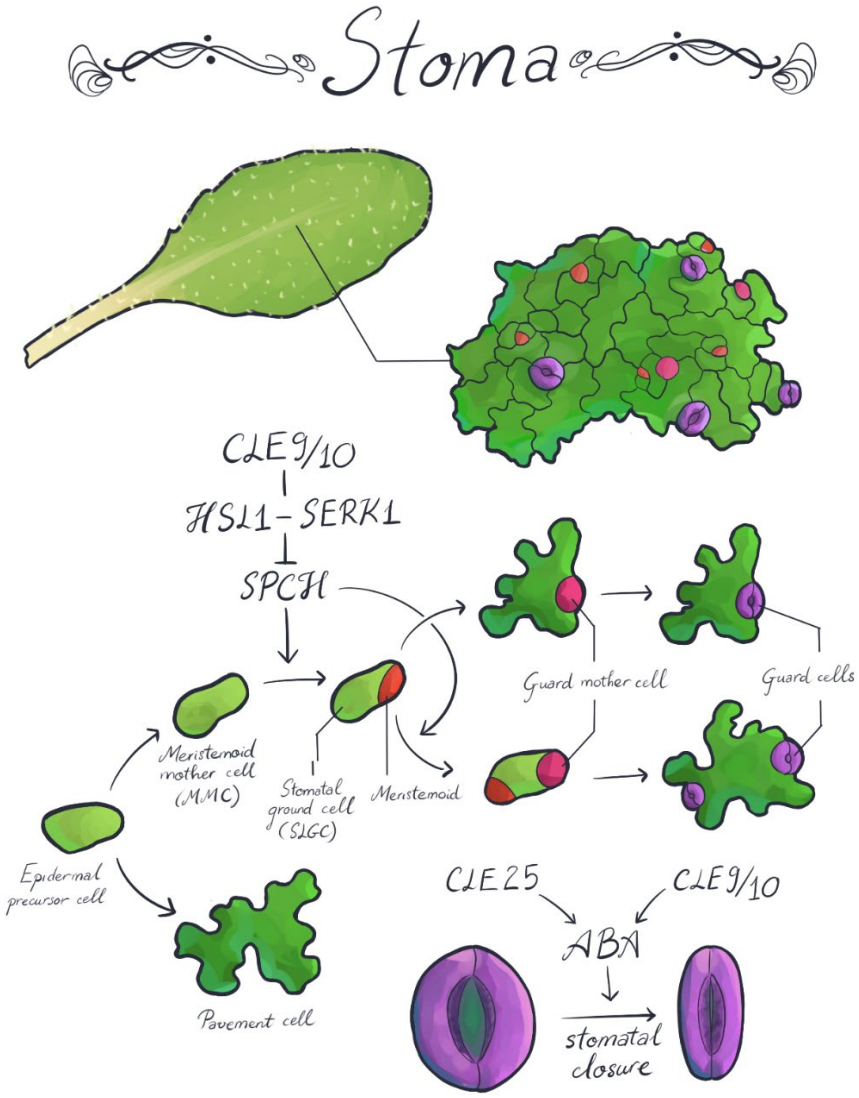

Figure 1.8. Stomatal development in Arabidopsis. Epidermal initial cells can undergo a series of asymmetric cell divisions to eventually form pavement cells, or guard cell pairs that make up stomata. The genetic pathway involving CLE9/10 peptide signal, HSL1 and SERK receptors, and SPCH transcription factor mediates these asymmetric cell divisions. Each stoma can open or close depending on internal signals to mediate gas exchange between the plant and the environment. CLE9/10 and CLE25 function in abscisic acid signaling pathway that mediates stomatal closure.

Axillary meristem

Unlike animals whose body plans remain relatively stable after embryogenesis, plants have the ability to continuously generate new body axes throughout their life cycle. This branching growth habit is exemplified by the production of lateral roots that form intricate water and nutrient-seeking networks underground, as well as the generation of axillary branches in the shoot.

Shoot branching occurs as a direct consequence of leaf development. As the leaf primordium grows, the junction between the adaxial side and the SAM is called the leaf axil. It is here that a new shoot stem cell population is initiated, hence the term axillary meristem (AM) (Hempel and Feldman, 1994; McConnell and Barton, 1998). Unlike SAM initiation during embryogenesis, where the early expression of *WOX* genes are required to establish the stem cell niche, AM initiation in the leaf axil requires activity of *STM* in Arabidopsis. While the *STM* transcript is excluded from the leaf primordia, a local auxin minimum at the boundary allows for continuous expression of *STM* at a low level to maintain meristematic competence (Long and Barton, 2000; Wang et al., 2014a,b). Right before AM initiation, STM is upregulated by a number of factors, including the HD-ZIP III transcription factor REV and its cofactors DORNROSCHEN (DRN), the GRAS family transcription factor LATERAL SUPPRESSOR (LAS), and the NAC domain proteins CUP-SHAPED COTYLEDON (CUC) (Otsuga et al., 2001; Greb et al., 2003; Hibara et al., 2006; Tian et al., 2014) (Fig. 1.9). The transcription factor ARABIDOPSIS THALIANA HOMEOBOX GENE1 (ATH1) also interacts with STM to form a self-activation loop and maintains *STM* expression in the incipient meristem (Cao et al., 2020).

High STM activity promotes cytokinin signaling, which in turn promotes *LAS* expression, creating a positive feedback loop that drives up cytokinin response in the incipient AM and inducing expression of *WUS* (Tian et al., 2014; Wang et al., 2017). WUS then induces *CLV3* expression in the developing stem cell population. At the same time, two epidermis-specific transcription factors, ARABIDOPSIS THALIANA MERISTEM LAYER1 (ATML1) and PROTODERMAL FACTOR2 (PDF2), suppress expression of *HAM* at the upper cell layers via the microRNAs MIR170/171, thus generating a gradient of HAM activity that is strongest at the inner region of the AM (Han et al., 2020). HAM activity represses *CLV3* in these inner layer cells, thus organizing the AM into functional domains mirroring that of the SAM (Zhou et al., 2018). Once formed, it is generally assumed that the AM behaves similarly to the SAM, although a combination of phytohormone balance and sugar demand may determine their dormancy and outgrowth.

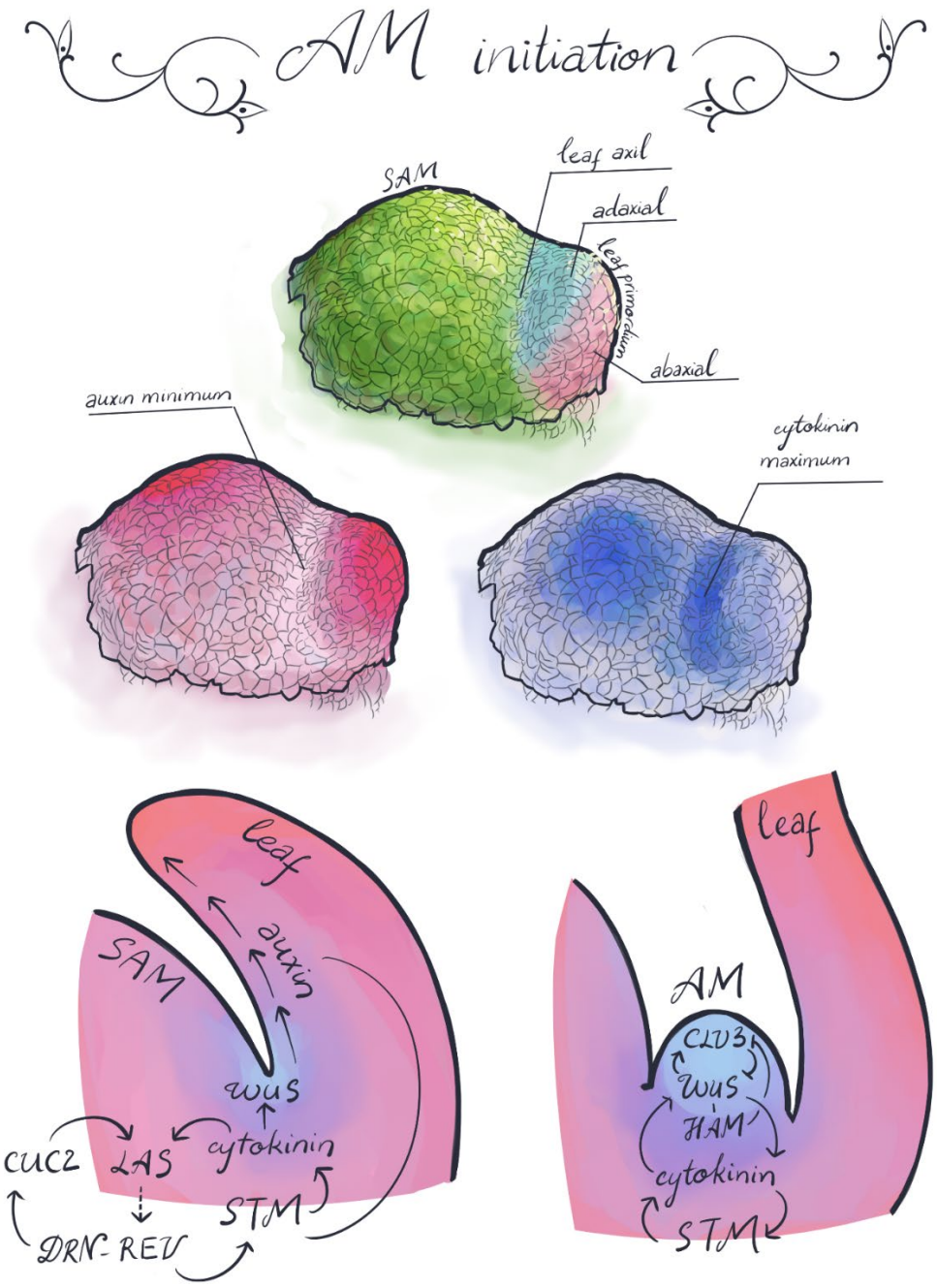

Figure 1.9. De novo axillary meristem formation. Axillary stem cells are specified at the leaf axil by a balance between auxin and cytokinin signaling. A combination of low auxin, high cytokinin level, and upregulation of STM is required to specify stem cell fate. The CLV3-WUS feedback loop is established later, with HAM transcription factors constraining CLV3 expression to the upper cell layers.

Inflorescence

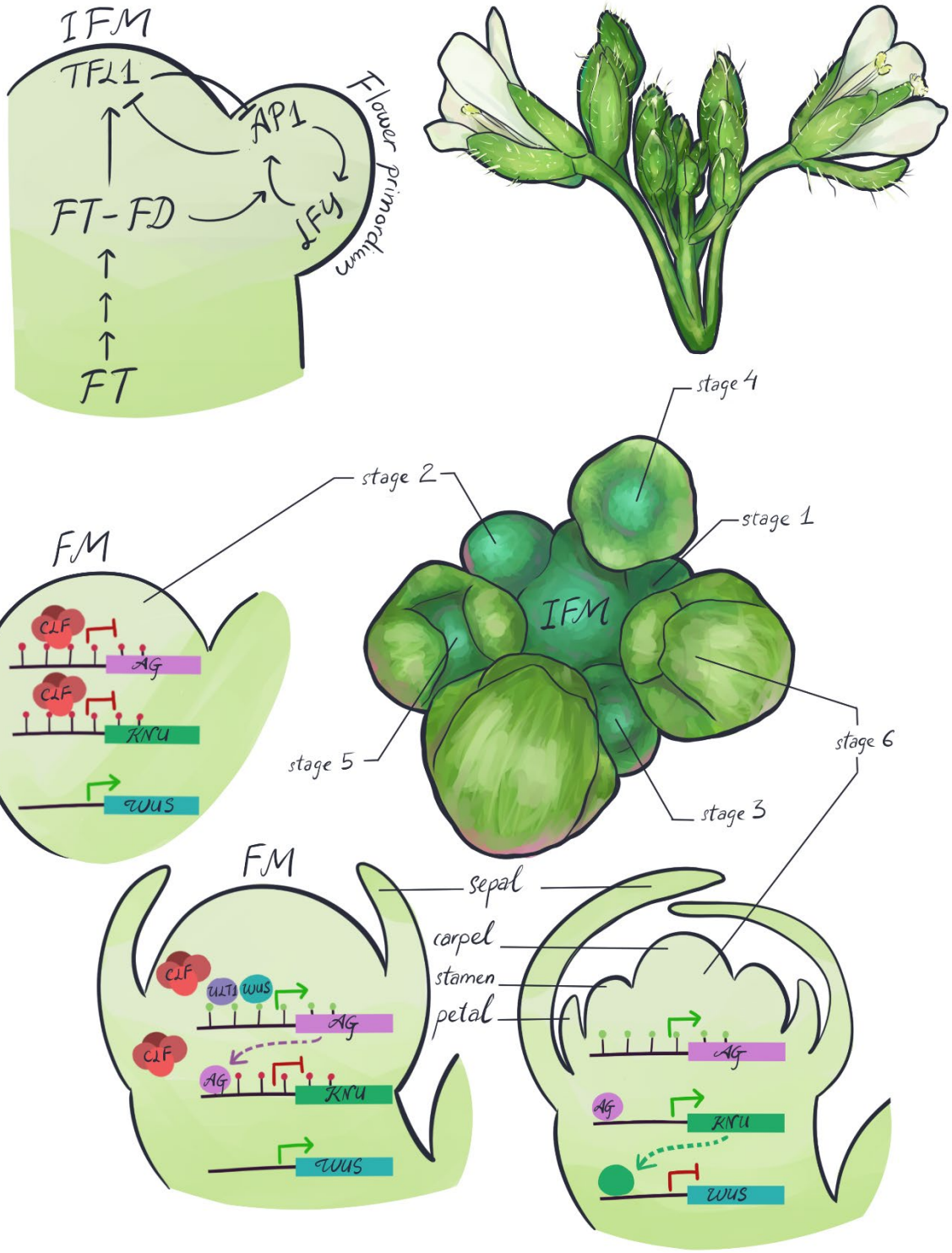

Figure 1.10. Development in the reproductive phase. Transition from vegetative to reproductive development is induced by the florigen factor FT-which is transported from leaves towards the shoot apex. Floral primordia are formed on the flank of the IFM, marked by the expression of transcription factor genes *AP1* and *LFY*, while the IFM itself expresses *TFL1* to maintain indeterminate growth. Each flower also harbors their own transient stem cell population, mediated by WUS. WUS activity induces its own repressors, *AG* and *KNU*, leading to the termination of the floral meristem after a delay.

Reproductive development – Inflorescence and flower

As the plant continues to progress through vegetative development, another biological program is set into motion, quietly integrating environmental cues with endogenous genetic circuitry, and slowly building up to a radical transition in plant form and function, from vegetative to reproductive development. One important pathway controlling the reproductive transition in Arabidopsis relies on the leaf-expressing *FLOWERING LOCUS T* (*FT*) gene, which is influenced by a number of external stimuli, including photoperiod and temperature, as well as internal programming, such as developmental age. *FT* encodes a small phospholipid binding protein that is transported from leaves to the shoot apex to physically associate with the transcription factor FLOWERING LOCUS D (FD) (Abe et al., 2005; Corbesier et al., 2007; Abe et al., 2019). The FT-FD complex affects expression of floral homeotic genes including *APETALA1* (*AP1*), *LEAFY* (*LFY*), and *SUPPRESSOR OF OVEREXPRESSION OF CO (SOC1* (Hempel et al., 1997; Michaels et al., 2005; Wigge et al., 2005; Lee et al., 2008) (Fig. 1.10). The sweeping change in transcriptional profiles that ensues converts the vegetative meristem into an inflorescence, and promotes the differentiation into floral fate of incipient primordia (Kaufmann et al., 2010; Winter et al., 2011). FT thus functions as a long-range molecular message from leaves to communicate that the right environmental conditions have been met for flowering to begin.

The SAM, which is now the inflorescence meristem (IFM), begins to initiate floral primordia on its flanks in a similar pattern as leaf primordia. Within each floral primordium, a new stem cell population arises, called the floral meristem (FM). The organization of the FM is similar to those of the SAM and AM, with a CZ expression *CLV3* and an OC expressing *WUS* (Schoof et al., 2000). Indeed, analysis of the molecular markers *STM* and *ANT* suggest that flowers are modified axillary shoots that form on the axils of subtending leaves, which are developmentally suppressed into cryptic bracts. Two important regulators of flower development are *AP1*, which encodes a MADS box transcription factor, and *LFY*, which encodes a novel type of plant-specific transcription factor. LFY is one of the earliest genes expressed in the incipient floral primordium, and acts synergistically with BOP1/2 to suppress bract formation (Norberg et al., 2005). LFY directly activates *AP1*, and both of which are incorporated in a positive feedback loop. Both AP1 and LFY also antagonize the shoot meristem-expressing *TERMINAL FLOWER1* (*TFL1*), and thus preventing the developing primordium from taking on shoot stem cell fate (Gustafson-Brown et al., 1994; Simon et al., 1996). As an interesting sidenote, while *LFY* is involved in FM specification in angiosperms, its origin precedes the evolution of flowers. In the moss *Physcomitrella patens*, *PpLFY* regulates cell division during sporophytic development, and in the fern *Ceratopteris richardii*, it functions in maintaining apical cell activity in a similar manner to WUS and STM

throughout the gametophyte and sporophyte stages (Tanahashi et al., 2005; Plackett et al., 2018). LFY was then recruited into the floral identity pathway later during the evolution of land plants.

Once initiated, the FM will begin to produce whorls of floral organs on its flanks, including sepals, petals, stamens, and carpels, all of which are modified leaves. The identity of each whorl is determined by a specific combination of MADS box transcription factors that are induced by LFY (Weigel et al., 1992). In Arabidopsis and most flowering plants, initiation of the forth and final whorl, the carpels, also consume the remaining stem cells of the FM to prevent another whorl from forming. Termination of the FM occurs by the timed suppression of *WUS*. At the beginning of flower development, the combined activity of WUS, LFY, and the SAND-domain protein ULTRAPETALA1 (ULT1) activate the transcription of *AGAMOUS* (*AG*) in the FM (Carles and Fletcher, 2009; Engelhorn et al., 2014). *AG* encodes a MADS box transcription factor that is involved in floral organ identity, but also directly induces expression of the DNA-binding protein *KNUCKLES* (*KNU*) by the beginning of carpel initiation (Fig. 1.10). In turn, KNU directly binds to the *WUS* sequence and dampens its transcription, thus superimposing on the CLV-WUS feedback loop and turning off *WUS* expression (Sun et al., 2009). Interestingly, ULT1 is also expressed in the SAM, and functions to limit stem cell accumulation by repressing *WUS*, although the pathway is not well defined (Monfared et al., 2013). Transcriptomic analysis has revealed a diverse role for ULT1 in many developmental processes as well biotic and abiotic stress response (Tyler et al., 2019).

I.4 Diverse CLE functions in Arabidopsis

Vascular development

Several *CLE* genes also play an important role in vascular development in shoot tissues. The wedge-shaped vascular bundles of the plant stem consist of two conducting tissues, the phloem and the xylem (Fig. 1.11). The phloem lies laterally and contains sieve tubes that transport sugars and amino acids, whereas the vessels and tracheids of the interior xylem transport water and ions absorbed from the soil. Between these two mature tissues lies a narrow strip of meristematic cells called the procambium or vascular cambium. Procambial cells divide parallel to the plane of the stem to generate phloem cells in one direction and xylem cells in the other direction. This secondary growth property of plant stems allows them to grow radially over long periods of time and is regulated by both systemic hormone signals and localized CLE peptide activity. TRACHEARY ELEMENT DIFFERENTIATION INHIBITORY FACTOR (TDIF) is an active peptide derived from the *CLE41* and *CLE44* coding sequences that has two related functions: to promote the proliferation of Arabidopsis procambial cells and to inhibit their differentiation into xylem (Ito et al., 2006). The effect of TDIF peptide application to procambial cell proliferation is enhanced by simultaneous treatment with CLE6 peptide (Whitford et al., 2008), although the biological significance of this is as yet unknown. The TDIF ligand is bound by the LRR receptor-like kinase PHLOEM INTERCALATED WITH XYLEM (PXY) (Hirakawa et al., 2008; Etchells and Turner, 2010), also known as TDIF RECEPTOR (TDF), which controls the rate and orientation of procambial cell division (Fisher and Turner, 2007; Etchells and Turner, 2010; Hirakawa et al., 2010). The CLE42 peptide, which differs from TDIF in one amino acid, also has partial TDIF activity (Hirakawa et al., 2008) and shows a weak interaction with the PXY extracellular domain in *in vitro* assays (Zhang et al., 2016). *PXY* also interacts genetically with the *ER* receptor kinase gene to regulate vascular organization, acting to prevent the intercalation of phloem and xylem in the inflorescence stem vascular bundles (Etchells et al., 2013).

Like its counterparts in the shoot apical meristem, the TDIF/PXY ligand-receptor duo appears to act as a short-range signaling module. Both *CLE41* and *CLE44* are both expressed in the phloem (Hirakawa et al., 2008; Etchells and Turner, 2010), and TDIF protein can be detected in the extracellular space around phloem precursor cells (Hirakawa et al., 2008). In contrast, *PXY* is specifically expressed in the adjacent vascular procambium (Fisher and Turner, 2007). Thus TDIF signals in a non-cell autonomous fashion from phloem cells to induce the proliferation and suppress the differentiation of the neighboring procambial cells. At the molecular level CLE41 signaling negatively regulates *PXY* expression in inflorescence stems (Etchells and Turner, 2010). Such ligand-mediated repression of receptor gene expression also occurs in animal systems to shape the gradient of ligand activity across tissues (Cadigan et al., 1998).

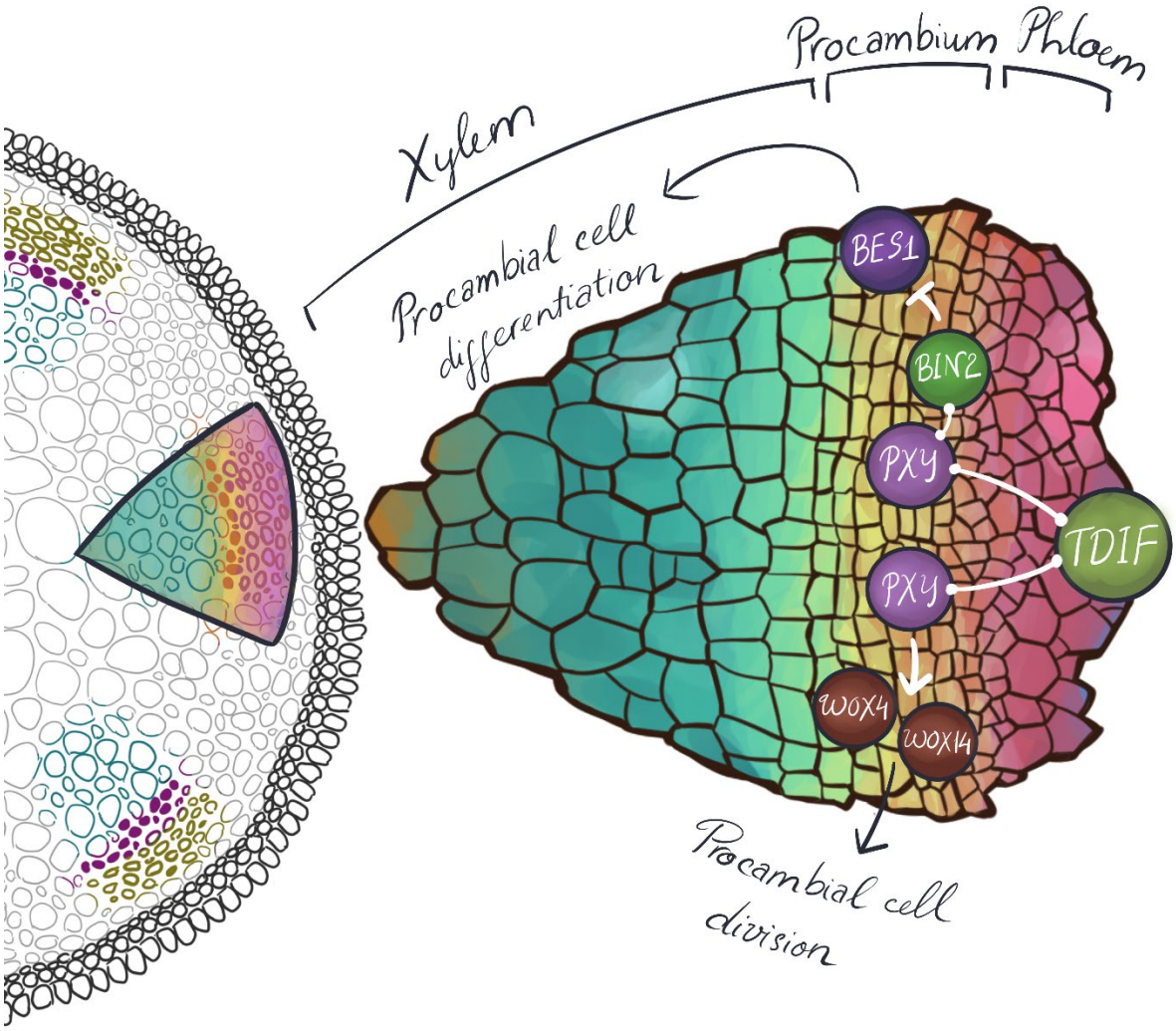

Figure 1.11 CLE regulation of vascular cambium activity. A wedge-shaped vascular bundle in the Arabidopsis stem containing meristematic procambial cells that divide to generate phloem and xylem cells is shown. *CLE41* and *CLE44*, both encoding the same peptide, are expressed in the phloem. The resulting ligand, called TDIF, is perceived by PXY, an LRR-RLK in the procambium. TDIF-PXY signaling induces *WOX4* and *WOX14* expression to promote procambial cell division.

In addition, PXY physically interacts with BIN2 to inhibit the transcription factor BES1, thus preventing procambial cell differentiation into xylem.
The dual functions of TDIF-PXY signaling in shoot vascular development are mediated by distinct downstream components. A key downstream target of TDIF-PXY signaling to direct procambial cell proliferation is *WOX4*, which is expressed in the vascular procambium and cambium (Hirakawa et al., 2010; Etchells et al., 2013). *WOX4* is rapidly induced by exogenous application of TDIF in a PXY-dependent fashion (Hirakawa et al., 2010), and promotes procambial cell division (Ji et al., 2010; Suer et al., 2011). The *WOX14* gene acts redundantly with *WOX4* to promote procambial cell division but not vascular organization (Etchells et al., 2013). This along with the data that the PXY-ER genetic interaction affects vascular organization but not vascular cell division indicates that these are genetically separable processes that may be regulated by CLE-WOX signaling modules with some shared and some unique constituents.

WOX4 is not required, however, for the suppression of xylem differentiation by TDIF (Hirakawa et al., 2010). Instead, at the plasma membrane of procambial cells, the PXY receptor kinase physically associates with and promotes the kinase activity of BRASSINOSTEROID-INSENSITIVE 2 (BIN2) and other members of the GLYCOGEN SYNTHASE KINASE 3 (GSK3) family of proteins in a TDIF-dependent manner (Kondo et al., 2014). The GSK3 proteins, which also function in brassinosteroid signaling, act redundantly to inhibit procambial cell differentiation into xylem by repressing the activity of the transcription factor BES1. Given that brassinosteroids also promote xylem cell differentiation (Cano-Delgado et al., 2004; Yamamoto et al., 2007), further studies should uncover the extent of crosstalk between the different signal transduction pathways.

Finally, the role of the TDIF/PXY pathway in shoot vascular development in trees, which produce wood via the differentiation of procambium cells into xylem, has been investigated by cloning *PtCLE41* and *PtPXY* from hybrid aspen (Etchells et al., 2015). Molecular complementation experiments showed that both *PtCLE41* and *PtPXY* are functional orthologs of the corresponding Arabidopsis genes. Tissue-specific over-expression of *PtCLE41* and *PtPXY* in hybrid aspen produced taller trees with a two-fold increase in the rate of wood formation and increased overall woody biomass, indicating that the CLE41 signaling pathway functions to regulate secondary growth in trees by controlling procambial activity. Such knowledge may be exploited to enhance secondary growth and wood formation in commercially grown tree species

Root development

CLE peptide signaling is not restricted to above-ground tissues, but is also involved in a broad range of developmental processes in the root. Indeed, the root apical meristem (RAM), much like the SAM, is also partitioned into many functional domains, whose constant communication is required to balance stem cell pluripotency with cell differentiation (Scheres et al., 1994; van den Berg et al., 1997). Furthermore, within the differentiated portions of the root, lateral root meristems are periodically formed de novo, reminiscent of axillary meristem initiation in the shoot (Péret et al., 2009). Many *CLE* genes are expressed in various parts of the root system, and application of certain CLE peptides to Arabidopsis seedlings can trigger RAM consumption and halt root development in a CLV2- and CRN-dependent manner (Fiers et al., 2005; Whitford et al., 2008). To briefly summarize the known functions of CLE signaling in the root, the CLE45 peptide signals through several receptor complexes, including CLV2-CRN, BAM3, and CLE-RESISTANT RECEPTOR KINASE (CLERK) to suppress protophloem cell differentiation (Depuydt et al., 2013; Hazak et al., 2017; Anne et al., 2018). Oppositely, CLE25 signals through the CLV2/CLERK complex to promote protophloem differentiation, although how the CLE25 and CLE45 pathways interact remains to be determined (Ren et al., 2019). The CLE9/10 peptide also functions in root vascular development, repressing division of the xylem precursor cell through the BAM receptors (Qian et al., 2018). *CLE14* is expressed in the root epidermis to mediate the acquisition of root hair cell fate by epidermal cells (Hayashi et al., 2018). CLE14 accumulation is also induced in the inner cell layers of the RAM under phosphate starvation, leading to RAM termination via CLV2/CRN and PEP1 RECEPTOR2 (PERP2) (Gutiérrez-Alanís et al., 2017). CLE14 thus acts as a molecular signal that helps tune root growth to nutrient availability in the soil.

Figure 1.12. Roles for CLE peptide signaling pathways in diverse Arabidopsis tissues. CLV3 mediates stem cell homeostasis in the shoot apical meristem. CLE41/44 regulates vascular cambium cell activity in the stem. CLE9/10 and CLE25 affect aspects of stomatal development and function and additionally act in root development, where CLE9/10 regulates xylem formation and CLE25 promotes protophloem cell differentiation. CLE45, in contrast, inhibits root protophloem cell differentiation. In response to low inorganic phosphate (-Pi) conditions, CLE14 induces terminal root apical meristem differentiation. Arrows depict positive regulatory relationships and bars depict negative regulatory relationships. Dashed lines indicate that a direct physical or regulatory association has not yet been demonstrated.

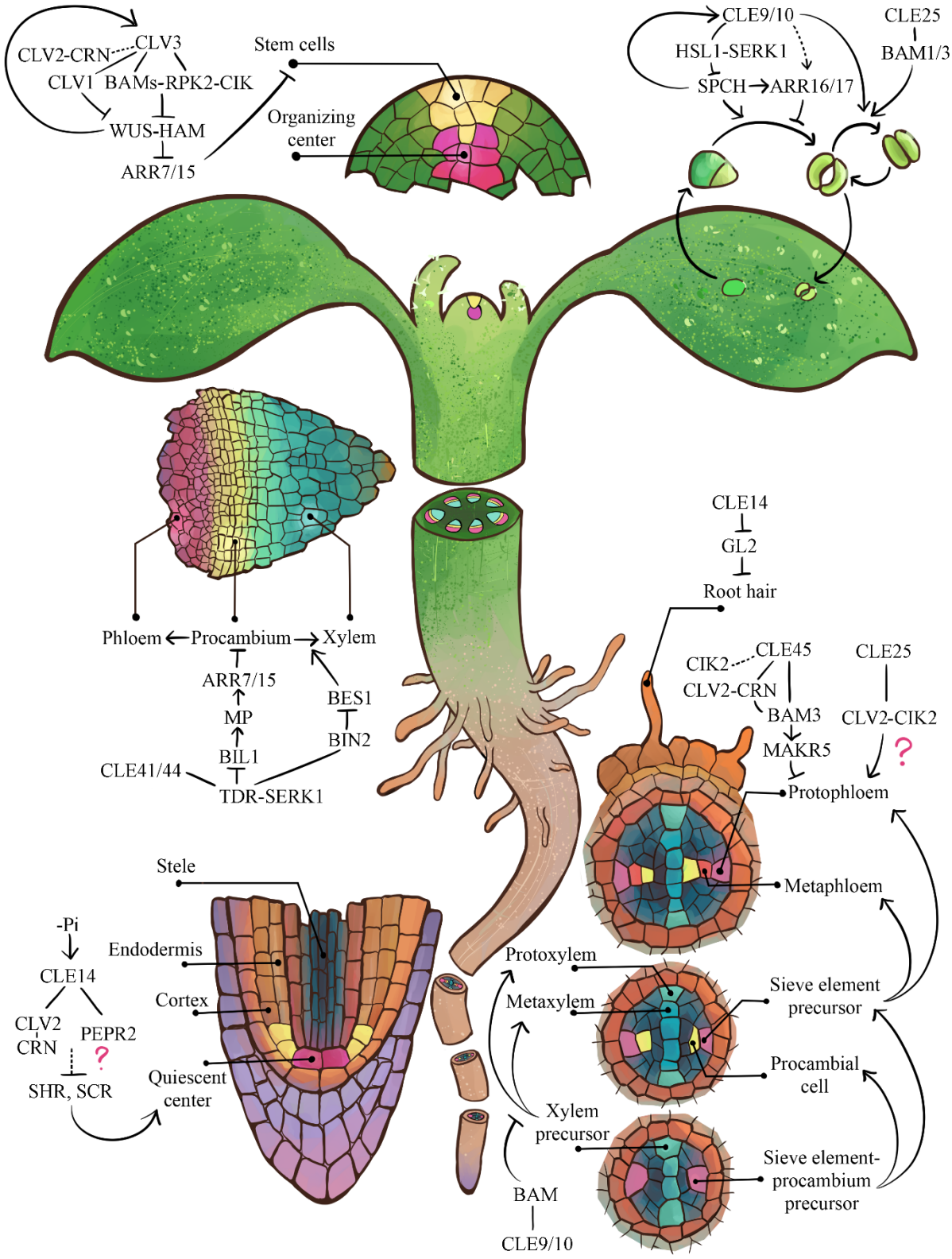
CLV2-CRN
CLV3
CLV1
BAMs-RPK2-CIK
WUS-HAM
ARR7/15
Stem cells
Organizing center
CLE9/10
CLE25
HSL1-SERK1
BAM1/3
SPCH→ARR16/17
Phloem←Procambium→Xylem
ARR7/15
MP
BIL1
CLE41/44
BES1
BIN2
TDR-SERK1
CLE14
GL2
Root hair
CIK2
CLE45
CLV2-CRN
BAM3
MAKR5
CLE25
CLV2-CIK2
Protophloem
Metaphloem
Stele
-Pi
Endodermis
CLE14
Cortex
CLV2
CRN
PEPR2
SHR, SCR
Quiescent center
Protoxylem
Metaxylem
Xylem precursor
BAM
CLE9/10
Sieve element precursor
Procambial cell
Sieve element-procambium precursor

CHAPTER II

CLE16, CLE17, AND CLE27 IN THE SAM

The following content was published as:

Gregory, E.F., Dao, T.Q., Alexander, M.A., Miller, M.J., and Fletcher, J.C. (2018). The signaling peptide-encoding genes CLE16, CLE17 and CLE27 are dispensable for Arabidopsis shoot apical meristem activity. PLoS One 13: 1–16.

In loving memory of Martin Alexander,

whose love language is the sweetest lemons.

In the last chapter, we described the informational feedback loop between CLV3 and WUS that maintains stem cell homeostasis in the SAM. However, *CLV3* is not the only *CLE* gene that is expressed at the shoot apex. Indeed, many *CLEs* exhibit promoter activity that can be detected by GUS assay within or around the SAM, including *CLE16*, *CLE17*, *CLE27*, and *CLE42*. During vegetative development, staining for pCLE16:GUS was observed in the organ primordia flanking the vegetative SAM, as well as at the base of developing leaves. pCLE17:GUS was detected throughout the entire SAM and surrounding leaves, with strongest activity at the outer layers. pCLE27:GUS staining was excluded from the SAM and incipient primordia, but present at the epidermal cells of rosette leaves. Promoter activity of *CLE42* was also detected broadly throughout the entire SAM, and its transcript level was found to be even higher than that of *CLV3*. Activities of *pCLE16*, *pCLE17*, and *pCLE27* were also detected at inflorescence and floral tissues, among many other *CLE* promoters. In addition, while binding affinity of CLV1, CLV2, and the BAM receptors have not been demonstrated with CLE16, 17, and 27, these receptors can physically interact with a number of other CLE peptides. Given that the *clv1 bam1/2/3* SAM overproliferation is more severe than that of *clv3* plants, it is possible that some of these shoot-expressing CLE genes might play a role in restricting stem cell accumulation as well.

The experiments in this chapter were performed in collaboration with E. Gregory, M. Alexander, M. Miller, and J. Fletcher in order to understand the biological function of other CLE peptides in the SAM. Using CRISPR/Cas-9 genome editing, we generated loss-of-function alleles for *CLE16*, *CLE17*, and *CLE27* and assayed for growth phenotypes in single homozygous mutant plants. However, we found that all single mutants were indistinguishable from wild-type regarding rosette leaf production, rosette morphology, axillary branch number, transition to flowering, IFM size, or floral development under normal growth condition. These results indicate a range of possible rationales, that *CLE16*, *CLE17*, and *CLE27* might not signal in the shoot meristem in the measured traits, that their activity might be suppressed by existing pathways, or that significant redundancy might exist among *CLE* genes such that the loss of a single *CLE* can be compensated by others, most likely *CLV3*. Further experimentation is needed to evaluate each of these possibilities, including phenotyping high-order allelic combinations, biochemical assays, and epistatic analysis with other components of the CLE signaling pathway.

Abstract

The shoot apical meristem produces all of the leaves, stems and flowers of a flowering plant from a reservoir of stem cells at its growing tip. In Arabidopsis, the small polypeptide signaling molecule CLAVATA3 (CLV3), a member of the CLV3/EMBRYO SURROUNDING REGION-RELATED (CLE*)* gene family, is a key component of a negative feedback loop that maintains stem cell activity in shoot and floral meristems throughout development. Because in some plant species multiple *CLE* genes are involved in regulating shoot apical meristem activity, we tested the hypothesis that *CLE* genes other than *CLV3* might function in stem cell homeostasis in Arabidopsis. We identified three Arabidopsis *CLE* genes expressed in the post-embryonic shoot apical meristem, generated loss-of-function alleles using genome editing, and analyzed the meristem phenotypes of the resulting mutant plants. We found that null mutations in *CLE16, CLE17* or *CLE27* affected neither vegetative nor reproductive shoot meristem activity under normal growth conditions. Our results indicate that the *CLE16, CLE17* and *CLE27* genes have largely redundant roles in the Arabidopsis shoot apical meristem and/or regulate meristem activity only under specific environmental conditions.

Introduction

Unlike animals, which develop their body plan predominantly during embryogenesis, the distinct architecture of plants is formed throughout the course of their lives. The growing tips of the plant, called the shoot and the root apical meristems, generate organs in a reiterative and continuous process. The shoot apical meristem (SAM) is organized during embryogenesis and produces all of the above ground elements of the plant (Steeves and Sussex, 1989). Following the germination of the seed, the seedling SAM produces leaves from its flanks during the vegetative phase of development. In response to environmental and endogenous cues the SAM of the mature seedling undergoes the transition to flowering, the reproductive phase in which the shoot meristem is transformed into an inflorescence meristem (IFM) that produces axillary meristems followed by floral meristems that generate the flowers. Fertilization then enables the formation of seeds that transmit the genes to the next generation.

The organization of the SAM provides the capacity for plants to perform lifelong organogenesis. The SAM consists of a small reservoir of stem cells at the apex that is surrounded by a peripheral zone of cells that transition to more differentiated fates within discrete organ primordia. Beneath the stem cell reservoir resides a central domain called the organizing center (OC), which acts as a niche that maintains the fate of the overlying stem cell population. The activity of the OC sustains a relatively constant number of stem cells at the apex of the SAM despite the continuous differentiation of their descendants into organ and stem tissue on the flanks. The spatial and temporal control of gene activity and cellular function within these various domains relies on elaborate networks of phytohormones, transcription factors and intercellular signals to communicate information throughout the shoot apical meristem (Barton, 2010; Gaillochet and Lohnmann, 2015; Soyars et al., 2016).

An intercellular signaling network known as the CLV-WUS pathway maintains stem cell homeostasis in Arabidopsis (Somssich et al., 2016). The *CLV3* gene is expressed in the stem cells and encodes a small, secreted polypeptide signaling molecule (Fletcher et al., 1999) that moves through the apoplast into the cells of the underlying OC, where it is perceived by several receptor kinases complexes (Clark et al., 1997; Kinoshita et al., 2010; Ogawa et al., 2008; Müller et al., 2008; Bleckmann et al., 2009). Signaling through the CLV pathway restricts the expression of the *WUSCHEL (WUS)* homeobox transcription factor gene to the cells of the OC (Brand et al., 2000). WUS protein, in turn, moves through the plasmodesmata into the apical domain (Yadav et al., 2011), where it sustains stem cell identity and directly induces *CLV3* expression (Daum et al., 2014; Schoof et al., 2000). WUS also integrates cytokinin signaling inputs in the interior of the SAM to stimulate cytokinin-mediated stem cell proliferation (Leibfried et al., 2005), while repressing the expression of genes that direct cell differentiation (Yadav et al., 2013).

CLV3 is a founding member of the *CLV3/EMBRYO SURROUNDING REGION-RELATED (CLE)* gene family, which is present throughout the plant lineage and in some plant parasitic nematodes (Cock et al., 2001; Wang et al., 2005). These genes encode polypeptides of less than 15 kDa in molecular mass that contain an amino-terminal signal peptide, a variable domain, and a conserved stretch of 14 amino acids near the carboxyl-terminus called the CLE domain that is processed to form the biologically active peptide (Ito et al., 2006; Ni and Clark, 2006; Kondo et al., 2006). Although the function of the vast majority of *CLE* genes is unknown, studies indicate that CLE peptides play key roles in stem cell homeostasis in Arabidopsis root and vascular meristems as well as in the SAM (Stahl et al., 2009; Etchells and Turner, 2010; Hirakawa et al., 2008). In some

plant species, multiple *CLE* genes appear to be involved in the regulation of stem cell maintenance in shoot and floral meristems (Galli and Gallavotti, 2016). In rice, the *CLV3*-related *FON2* and *FOS1* genes redundantly regulate stem cell activity within floral meristems (Suzaki et al, 2009), yet *FON2* also affects inflorescence and axillary meristem maintenance (Suzaki et al., 2006) whereas *FOS1* and a third rice *CLE* gene*, FCP1,* are likely to be involved in vegetative SAM maintenance Suzaki et al., 2006, Suzaki et al, 2009. In tomato, the SlCLV3 and SlCLE9 peptides both appear to affect vegetative meristem size (Xu et al., 2015), again illustrating potential redundancy within the CLE family. Thus, although they have not been identified in genetic screens, other members of the CLE gene family may likewise function as additional signaling pathway components in the Arabidopsis SAM.

In this study, we identified three Arabidopsis *CLE* genes that are expressed within the vegetative and/or reproductive SAM. We generated loss-of-function mutations in each of the three genes and analyzed their meristem phenotypes throughout development. We determined that null mutations in the *CLE16, CLE17* and *CLE27* genes caused no measurable vegetative, inflorescence or floral meristem phenotypes under normal growth conditions. Our data suggest that SAM-expressed *CLE* genes other than *CLV3* act largely redundantly in the Arabidopsis meristem and/or function to regulate SAM activity only under certain environmental conditions.

Materials and Methods

Plant materials and growth conditions

All Arabidopsis thaliana plants were in the Columbia-0 accession. The cle27-2 (SALK_077000) T-DNA insertion allele was generated by the SALK Institute (Alonso et al., 2003) and was obtained from the Arabidopsis Biological Resource Center (ABRC), sequenced to confirm the location of the insertion site, and backcrossed three times to Col-0 prior to analysis. Plants were grown on soil (1:1:1 mixture of perlite:vermiculite:topsoil) under continuous light (120 μmol·m-2·s-1) at 21ºC. Seeds were planted at a density of one seed per pot, except for the Col-0 and cle16 IFM histology experiment in which a density of two seeds per pot was used. Seeds were stratified at 4ºC for 5 days before exposure to light. Seedlings were watered every day with a 1:1500 dilution of Miracle-Gro 20-20-20 fertilizer prior to flowering and once a week with fertilizer thereafter. Homozygous mutant plants were confirmed by PCR-based genotyping prior to analysis (primers listed in Table S1).

Genome editing of CLE gene loci

CRISPR-Cas9 target gene sequences for CLE16 and CLE17 were identified using the CRISPR-P website (Lei et al., 2014). The target sequences were amplified and cloned into the sgRNA cassette of the Gateway-compatible pSGR_pGEMT entry vector, which also harbored a Cas9 expression cassette. The pSGR_pGEMT constructs containing the Cas9 cassette as well as the CLE16 or CLE17 genomic target sequences were transferred into the pEarleyGate 301 binary vector using the LR enzyme mix (ThermoFisher Scientific), and sequenced. The recombinant pEarleyGate 301 constructs were then transferred into Agrobacterium tumefaciens GV3101 and transformed into wild-type Col-0 plants using the floral dip method (Clough and Bent, 1998). The T1 seeds were sown and selected by spraying twice with 0.01% BASTA solution, 3-5 days apart. Resistant transformants were genotyped using the Cleaved Amplified Polymorphic Sequence (CAPS)

method with gene-specific primers (primers listed in Table S1). Heterozygous T1 mutant plants were self-fertilized and homozygous T2 individuals identified by genotyping, followed by sequencing to confirm the mutant allele.

Genotyping the CLE16 CRISPR alleles was performed by using forward and reverse primers (primers listed in Table S1) in a Polymerase Chain Reaction (PCR) to amplify a 995 bp product. Digesting the PCR product with MspI yielded 779 bp and 216 bp bands from wild-type tissue, whereas the product from mutant tissue remained undigested. Genotyping the CLE17 CRISPR alleles was performed by using forward and reverse primers in a PCR reaction to amplify a 1016 bp product. Digesting the PCR product with BslI yielded 770 bp, 233 bp and 13 bp bands from wild-type tissue, whereas the product from mutant tissue remained undigested. Genotyping to confirm the absence of the Cas9 cassette from cle16 and cle17 mutant plants was performed using Cas9 forward and reverse primers (primers listed in Table S1).

Phenotypic analysis

Whole seedlings, rosette leaves, inflorescences and flower specimens were imaged using Zeiss Stemi 2000-c and Zeiss Stemi SV11 microscopes, and images were acquired using a Canon D-40 digital camera. Inflorescence apices were prepared for scanning electron microscopy as described (Fiume et al., 2010) and visualized on a Hitachi S4700 scanning electron microscope. Inflorescence apices were prepared for histology as described (Carles et al., 2004), stained for 25 seconds in a 0.1% Toluidine blue 0 dye solution (Sigma), de-stained through an ethanol series, and sectioned at 4 m thickness. Sections were visualized using a Zeiss Axiovert 200M microscope. Floral organ counting was performed as described (Fiume et al., 2010).

Results

The starting point for our functional analysis was the identification of all *CLE* genes expressed in the SAM during vegetative or reproductive development. For the vegetative stage, we used promoter:GUS expression data gathered from the vegetative meristems of 10-day-old seedlings (Jun et al., 2010). These data indicated that, in addition to *CLV3*, the promoters of both *CLE16* and *CLE17* drove expression in the vegetative meristem as well as in the adjacent organ primordia, although the pCLE16:*GUS* signal was much weaker than the pCLE17:*GUS* signal in the SAM itself [35]. For the reproductive stage, we mined published transcriptome data generated from laser micro-dissected IFMs (Mantegazza et al., 2014) for *CLE* gene expression. The *CLV3* gene was used as a positive control and appeared with an expression value of 31.27 RPKM (Fig. S2.1). In addition, the *CLE17, CLE20, CLE27* and *CLE42* genes were all detected as being expressed in the IFMs transcriptome dataset (Fig. S2.1). Among these, we omitted *CLE20* from our analysis because our promoter:GUS data indicated that the promoter drove expression exclusively in the vasculature, including in the vascular strands directly beneath the SAM, but not within the SAM itself (Jun et al., 2010). We also excluded *CLE42* because a previous study reported that a loss-of-function *cle42* T-DNA insertion allele displayed no shoot phenotype (Yaginuma et al., 2011). Consequently we focused on the functional analysis of the *CLE16, CLE17* and *CLE27* genes during Arabidopsis shoot development.

Generation of *cle* loss-of-function alleles

Two independent loss-of-function alleles of each of the three *CLE* genes were identified for functional characterization. Although *CLE* gene loci represent small targets for mutagenesis, a single allele of both *CLE16* and *CLE17* had already been reported (Table 1). The *cle16-1* Ds transposon insertion in the *CLE16* coding region acts as a transcriptional null allele; however, the genetic background is the Nossen accession (Jun et al., 2010). The T-DNA insertion in the *cle17-1* Col-0 allele is located in the 3' untranslated region (UTR) downstream of the *CLE17* coding region, and behaves as a hypomorphic, partial loss-of-function allele rather than a null allele (Jun et al., 2010).

Because *CLE16* and *CLE17* null alleles in the Col-0 accession were unavailable for comparative analysis, we generated new loss-of-function alleles of the two genes using CRISPR-Cas9 genome engineering (Table 2.1 and Fig. 2.1). Transformation of wild-type Col-0 plants with an sgRNA targeted to the *CLE16* coding sequence yielded multiple independent transformants. We detected 21 mutant individuals among the 24 T1 plants analyzed, a remarkable 87.5% mutation rate. Mutations in the T1 individuals were made homozygous in the T2 generation and confirmed by sequencing, and two were chosen for further study. One line contained an insertion of a "C" nucleotide after position +59 downstream of the translation start site (Fig. 2.1A), and was designated *cle16-2.* A second line contained a deletion of a "G" nucleotide after position +59 and was designated *cle16-3*. Each of these mutations generates a frame shift in the *CLE16* coding sequence well upstream of the CLE domain, with the *cle16-2* mutation also introducing several premature stop codons.

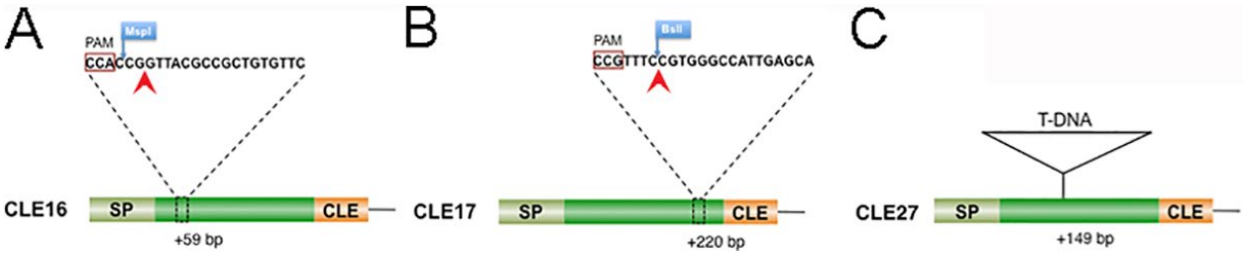

Fig 2.1. Graphic representation of mutations in the *CLE16*, *CLE17* and *CLE27* genes. (A) Location of the *cle16* CRISPR-Cas9 induced mutations (red arrowhead) relative to the sgRNA PAM site and MspI restriction site in the *CLE16* coding sequence. (B) Location of the *cle17* CRISPR-Cas9 induced mutations (red arrowhead) relative to the sgRNA PAM site and BslI restriction site in the *CLE17* coding sequence. (C) Location of the *cle27-2* T-DNA insertion in the *CLE27* coding sequence. SP, signal peptide sequence; CLE, CLE domain sequence.

Table 2.1. Alleles of *CLE* genes expressed in the shoot apical meristem.

CLE Gene	Mutant Allele	Type of Mutation	Source
CLE16	*cle16-1*	Ds transposon insertion at +37 bp	Jun et al 2010
CLE16	*cle16-2*	Insertion of "C" nucleotide at +59 bp	This work
CLE16	*cle16-3*	Deletion of "G" nucleotide at +59 bp	This work
CLE17	*cle17-1*	T-DNA insertion at +412 bp	Jun et al 2010
CLE17	*cle17-2*	Insertion of "A" nucleotide at +220 bp	This work
CLE17	*cle17-3*	Insertion of "T" nucleotide at +220 bp	This work
CLE27	*cle27-1*	T-DNA insertion at +149 bp	This work
CLE27	*cle27-cr1*	Insertion of "T" nucleotide at +173 bp	Yamaguchi et al 2017

https://doi.org/10.1371/journal.pone.0202595.t001

Transformation with an sgRNA targeted to the *CLE17* coding sequence also yielded multiple independent transformants. We detected 5 mutant individuals among the 24 T1 plants analyzed, a 20.1% mutation rate. Mutations in the T1 individuals were made homozygous in the T2 generation and confirmed by sequencing, and two were chosen for further study. One line contained an insertion of an "A" nucleotide after position +220 downstream of the translation start site (Fig. 2.1B), and was designated *cle17-2.* A second line contained an insertion of a "T" nucleotide after position +220, and was designated *cle17-3*. Each of these mutations generates a frame shift that introduces a premature stop codon in the *CLE17* coding sequence upstream of the CLE domain. Due to the frame shift mutations none of these *cle16* or *cle17* alleles produces a functional CLE polypeptide, and thus they represent loss-of-function alleles.

In addition we identified a *CLE27* T-DNA insertion allele in the Col-0 accession from the SALK collection [30], which to avoid confusion with the published CRISPR/Cas9 line described below we designate *cle27-2*. Sequencing indicated that *cle27-2* carries a T-DNA insertion +149 base pairs (bp) downstream of the translation start site (Fig. 2.1C), in the center of the *CLE27* coding region (Table 1). The insertion site is located upstream of the *CLE27* CLE domain, indicating that *cle27-2* represents a loss-of-function allele. A second, independent *CLE27* allele used was a CRISPR/Cas9-generated loss-of-function allele in the Col-0 accession designated *cle27-cr1* [38]. This allele generates a frame shift that introduces a premature stop codon in the *CLE27* coding sequence upstream of the CLE domain (Table 1), indicating that it is a null allele (Yamaguchi et al., 2017).

Analysis of SAM function during vegetative development

To determine whether the *CLE16, CLE17* or *CLE27* genes play a role in regulating shoot apical meristem activity during vegetative development, we analyzed the phenotypes of wild-type Col-0 as well as *cle16-2, cle16-3, cle17-2, cle17-3, cle27-cr1* and *cle27-2* seedlings from germination through the first four weeks of growth. We first measured the rate of rosette leaf initiation from the SAM beginning one day after germination (DAG), then again at 4 and 7 DAG, and weekly thereafter (Fig. 2.2A). We found that all of the wild type and *cle* mutant seedlings had produced two rosette leaves between 4 and 7 DAG, and that by 14 DAG plants of all genotypes had produced an average of 5-6 rosette leaves (Fig. 2.2A). The arrangement and morphology of the leaves was indistinguishable between the various genotypes at this stage of seedling development (Fig. 2.2B-

H). The rate of leaf initiation from the SAM was not significantly different between Col and *cle16, cle17* or *cle27* seedlings during the first 28 days of vegetative growth (Fig. 2.2A), after which time the plants began to undergo the transition to flowering. These results indicate that neither *CLE16, CLE17* nor *CLE27* individually functions in regulating SAM activity during the early stages of Arabidopsis vegetative development.

Next we quantified the rosette diameter of wild-type and *cle* mutant plants at the floral transition, when the mature seedlings ceased producing vegetative organs. Compared with wild-type Col-0 plants (Fig. 2.3A, B), the diameter of *cle17* rosettes (Fig. 2.3A, E-F) and *cle27* rosettes (Fig. 2.3A, G-H) was unaltered. The diameter of *cle16-3* rosettes was slightly but significantly larger than those of Col-0 and *cle16-2* rosettes (Fig. 2.3A, C, D); however, that of *cle16-2* plants was indistinguishable from the wild type (Fig. 2.3A, C). Because only one of the two *cle16* null alleles has this effect we conclude that neither *CLE16, CLE17* nor *CLE27* is likely to play an independent role in rosette growth.

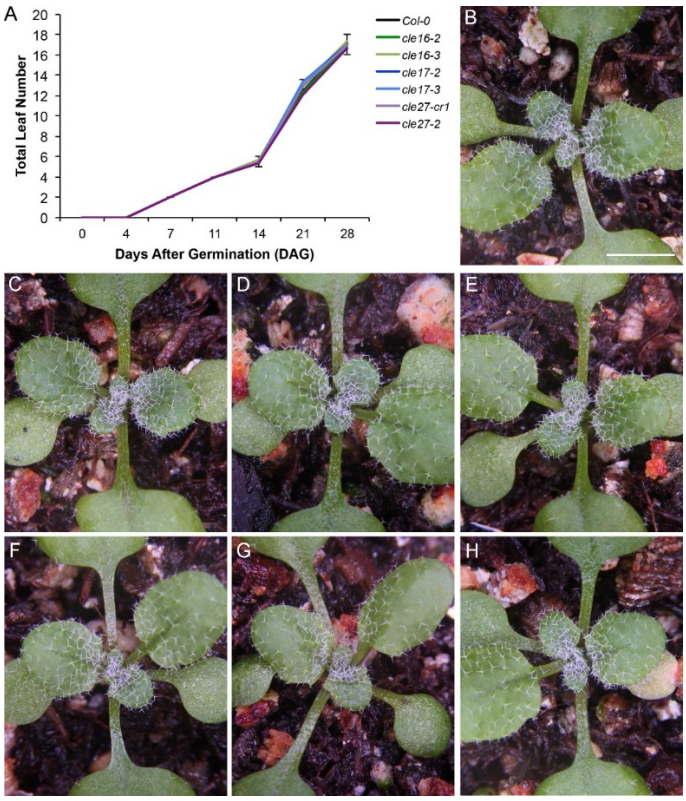

Fig 2.2. Mutations in *CLE16, CLE17* or *CLE27* have no effect on the leaf initiation rate of the shoot apical meristem. (A) Leaf initiation rate in wild-type and *cle* mutant plants from 1 to 28 days after germination (DAG). Values shown are mean ± standard deviation (S.D.). n = 12 individuals per genotype. (B) Wild-type Col-0 rosette at 14 DAG. (C) *cle16-2* rosette. (D) *cle16-3* rosette. (E) *cle17-2* rosette. (F) *cle17-3* rosette. (G) *cle27-cr1* rosette. (H) *cle27-2* rosette. Scale bar, 1 cm.

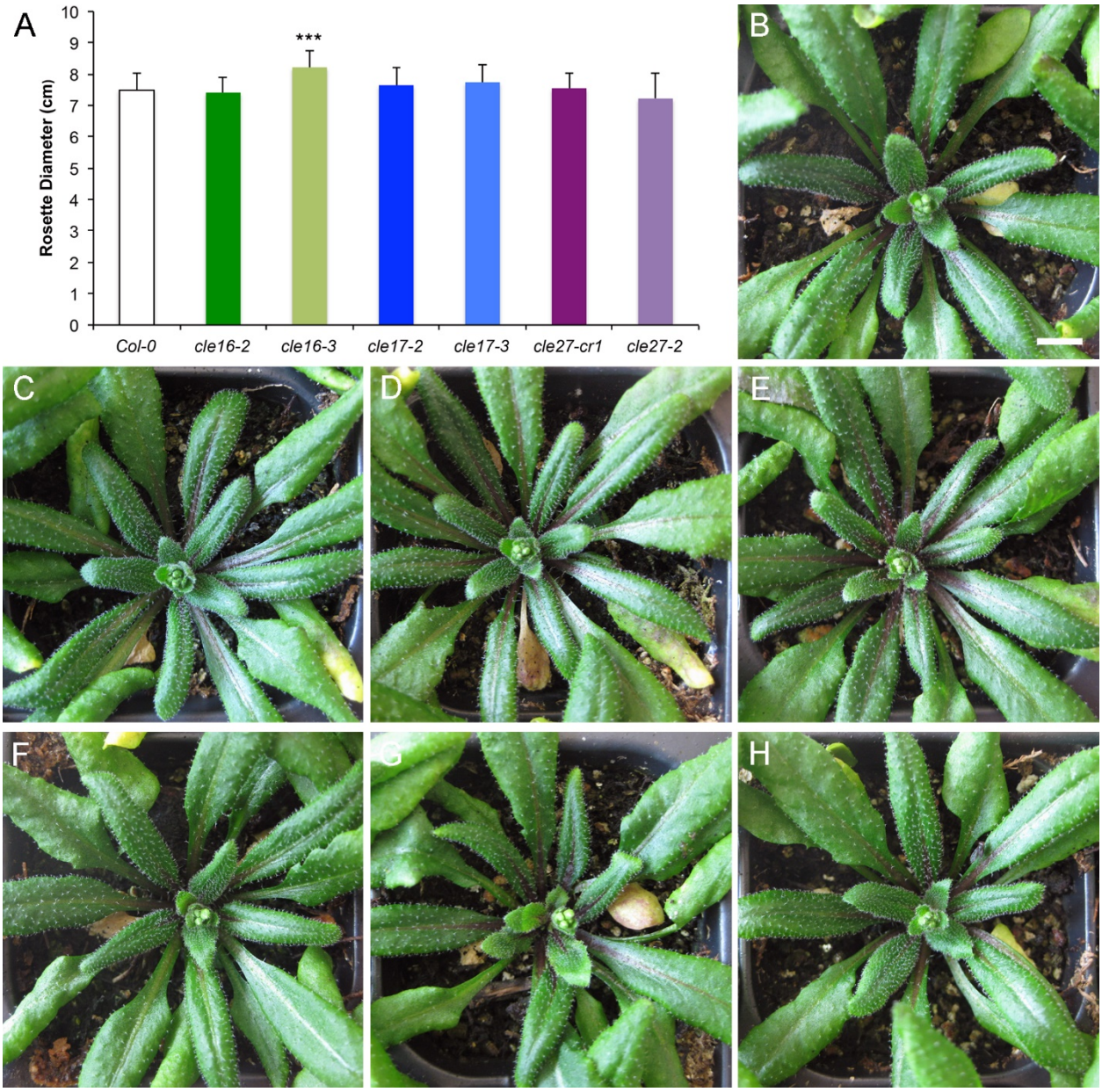

Fig 2.3. Mutations in *CLE16, CLE17* or *CLE27* have no effect on the rosette diameter of mature seedlings. (A) Rosette diameter of wild-type and *cle* mutant plants at the floral transition. Values shown are mean ± standard deviation (S.D.). Asterisks indicate a significant difference from wild-type at $p < 0.001$ (two-tailed Student's t test). n = 14-20 individuals per genotype. (B) Wild-type Col-0 rosette at the floral transition. (C) *cle16-2* rosette. (D) *cle16-3* rosette. (E) *cle17-2* rosette. (F) *cle17-3* rosette. (G) *cle27-cr1* rosette. (H) *cle27-2* rosette. Scale bar, 1 cm.

A major developmental event that alters the activity of the shoot apical meristem is the floral transition. This is when the SAM integrates endogenous signals as well as environmental signals from the leaves into broad transcriptional alterations that change the identity of the meristem from vegetative to reproductive. The reproductive, or inflorescence meristem, then initiates a number of axillary meristems followed by floral meristem primordia from its flanks. To determine whether the SAM-expressed *CLE* genes played any role in the transition of the meristem from vegetative to reproductive activity, we measured the number of days to bolting, total leaf number and axillary meristem number in wild-type and *cle* mutant plants.

We observed no difference in either mean days to bolting or total leaf number in *cle17* plants compared to wild-type Col-0 plants (Fig. 2.4A, B), indicating that *CLE17* activity does not affect the floral transition. We detected a small decrease in the number of days to bolting in plants homozygous for either *cle27* allele. Both *cle27-cr1* and *cle27-2* plants flowered an average of one day earlier than wild-type when grown under constant light conditions: 32.63±1.63 days for Col-0 compared to 31.2±2.29 for *cle27cr-1* and 31.39±1.79 days for *cle27-2* plants (Fig. 2.4A). However, the total number of leaves at flowering was unchanged in *cle27-cr1* and *cle27-2* plants (Fig. 2.4B), suggesting that *CLE27* may slightly modulate the plant growth rate over time rather than specifically affecting the floral transition (Koorneed et al,, 1991). Conversely, *cle16-2* and *cle16-3* plants both generated one to two more leaves than wild-type plants prior to flowering, and the *cle16-2* allele also slightly delayed the time to bolting (Fig. 2.4A, B). However, an independent experiment performed using identical growth conditions showed no significant difference between the two *cle16* alleles and wild-type Col-0 with respect to either days to bolting or total leaf number (Fig. S2.2). Thus these data indicate that *CLE16*, *CLE17* and *CLE27* have no significant effect on the transition to flowering under constant light conditions.

During the transition to flowering the Arabidopsis primary SAM produces a small number of axillary meristems from the axils of the cauline leaves. Under our growth conditions wild-type Col-0 plants generated an average of 5.2±0.66 axillary meristems per SAM (Fig. 2.4C). Neither *cle16* nor *cle27* plants displayed altered axillary meristem number (Fig. 2.4C). A very slight increase in axillary meristem number, to an average of 5.7±0.73, was detected in *cle17-2* plants (Fig. 2.4C). However, because such an increase was not observed in *cle17-3* plants we conclude that *CLE17* also has no significant effect on axillary meristem formation. These results indicate that neither *CLE16, CLE17* nor *CLE27* contributes to regulating the process of axillary meristem formation by the shoot apical meristem.

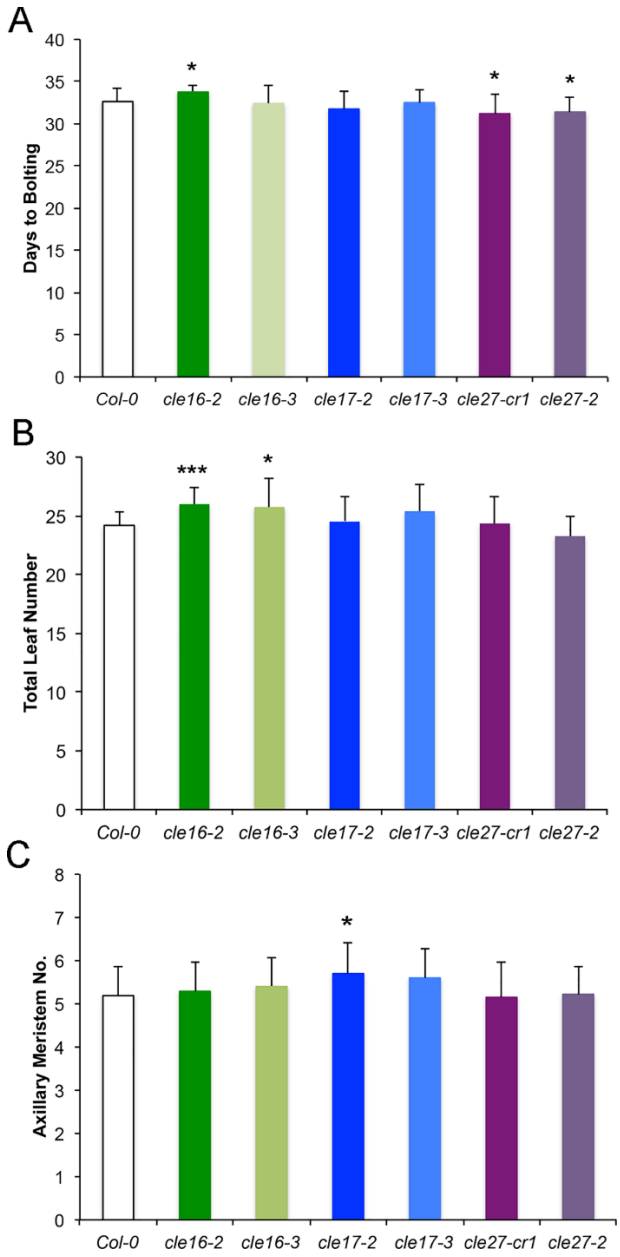

Fig 2.4. Mutations in *CLE16, CLE17* or *CLE27* have no significant effect on the floral transition. (A) Days to bolting of wild-type and *cle* mutant plants. (B) Total leaf number of wild-type and *cle* mutant plants at the transition to flowering. (C) Axillary meristem number in wild-type and *cle* mutant plants. Values shown in each graph are mean ± standard deviation (S.D.). Asterisks indicate a significant difference from wild-type at * $p < 0.05$; *** $p < 0.001$ (two-tailed Student's t test). n = 16-20 individuals per genotype.

Analysis of SAM function during reproductive development

Next we determined whether the *CLE16, CLE17* or *CLE27* genes functioned in regulating shoot apical meristem activity during reproductive development by comparing inflorescence and floral meristem activity between wild-type Col-0 and *cle16, cle17,* and *cle27* plants. It is known that *clv3*

plants form enlarged inflorescence meristems that produce many more flowers than wild-type plants in a random rather than a spiral phyllotaxy (Clark et al., 1995). Using scanning electron microscopy, we examined the tips of wild-type and *cle* mutant inflorescence meristems harvested when the length of the stem reached 1 cm. The morphology of the *cle16, cle17* and *cle27* IFMs was indistinguishable from that of wild-type Col-0 inflorescences, as was the rate of floral meristem initiation (Fig. 2.5). The phyllotaxy, or arrangement, of floral meristem formation from the IFM flanks was also unaffected, with successive floral primordia initiating in a spiral pattern in both wild-type and *cle* mutant plants (Fig. 2.5).

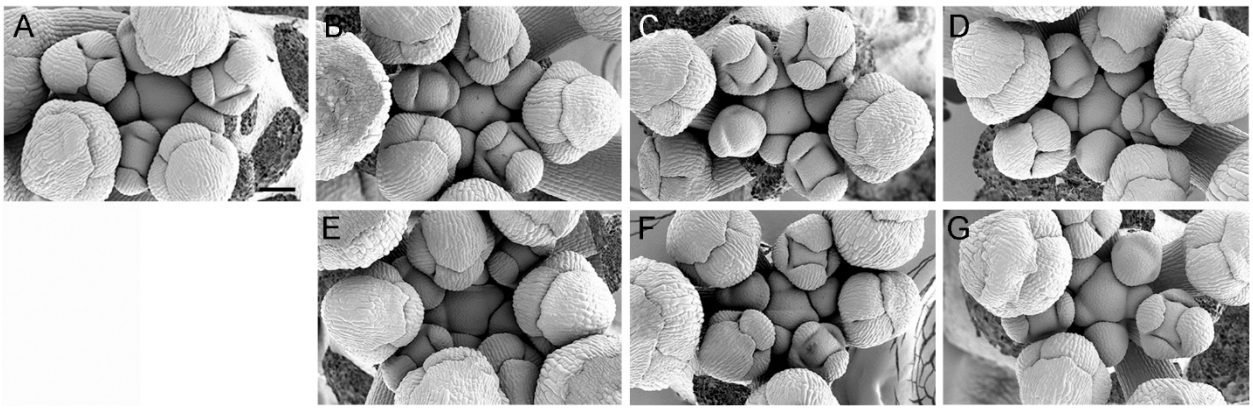

Fig 2.5. Mutations in *CLE16, CLE17* or *CLE27* have no effect on inflorescence meristem morphology or phyllotaxy. (A) Col-0 IFM. (B) *cle16-2* IFM. (C) *cle16-3* IFM. (D) *cle17-2* IFM. (E) *cle17-3* IFM. (F) *cle27-cr1* IFM. (F) *cle27-2* IFM. Scale bar, 50 mm.

We analyzed wild-type and *cle* inflorescence meristem morphology and size in greater detail by histological sectioning. The wild-type Col-0 inflorescence meristem is dome-shaped and is composed of three cell layers (Fig. 2.6A, D). The cells in the outermost two cell layers, L1 and L2, divide in a strictly anticlinal orientation and form the epidermal and sub-epidermal layers (Steeves and Sussex, 1989), respectively. The underlying L3 cells divide in all orientations and provide the girth of the IFM. The morphology of *cle16, cle17* and *cle27* IFMs was indistinguishable from that of wild-type IFMs, and the layering of the meristem was intact in all genotypes (Fig. 2.6B, C, E-H). *clv3* mutant inflorescence meristems contain many more cells and are both wider and taller than wild-type IFMs (Brand et al., 2000), so the diameter and height of Col-0, *cle16, cle17* and *cle27* IFMs was measured. Two experiments were performed, one comparing *cle16* homozygous IFMs to Col-0 and the other comparing *cle17* and *cle27* IFMs to Col-0. Although the mean Col-0 IFM size differed between the two experiments due to slightly different cultivation conditions (see Methods), the mean size of the *cle16, cle17* and *cle27* IFMs was not significantly different from that of the corresponding Col-0 IFMs (Fig. 2.6I, J). These observations show that, unlike *CLV3*, *CLE16, CLE17* and *CLE27* individually have no effect on inflorescence meristem activity under normal growth conditions.

Finally, we quantified the number of floral organs in wild-type and *cle* mutant flowers as a readout for potential alterations in floral meristem size. Compared to wild-type flowers, which consist of

four sepals in the first whorl, four petals in the second whorl, 5-6 stamens in the third whorl and two carpels in the fourth whorl (Fig. 2.7A, B), *clv3* flowers produce supernumerary organs in all four whorls, particularly the inner two, and can generate additional organs within the carpel whorl (Clark et al., 1995; Fletcher et al., 1999). The extra floral organs are a product of enlarged floral meristems and the extra whorls of organs result from reduced floral meristem determinacy (Clark et al., 1995). In contrast to *clv3* mutants, the mean number of sepals, petals and stamens produced by plants carrying null mutations in *CLE16, CLE17* or *CLE27* was indistinguishable from the wild type (Fig. 2.7A, C-H). Carpel number in all genotypes was invariant at two. These data indicate that individually *CLE16, CLE17* and *CLE27* are dispensable for regulating floral meristem activity.

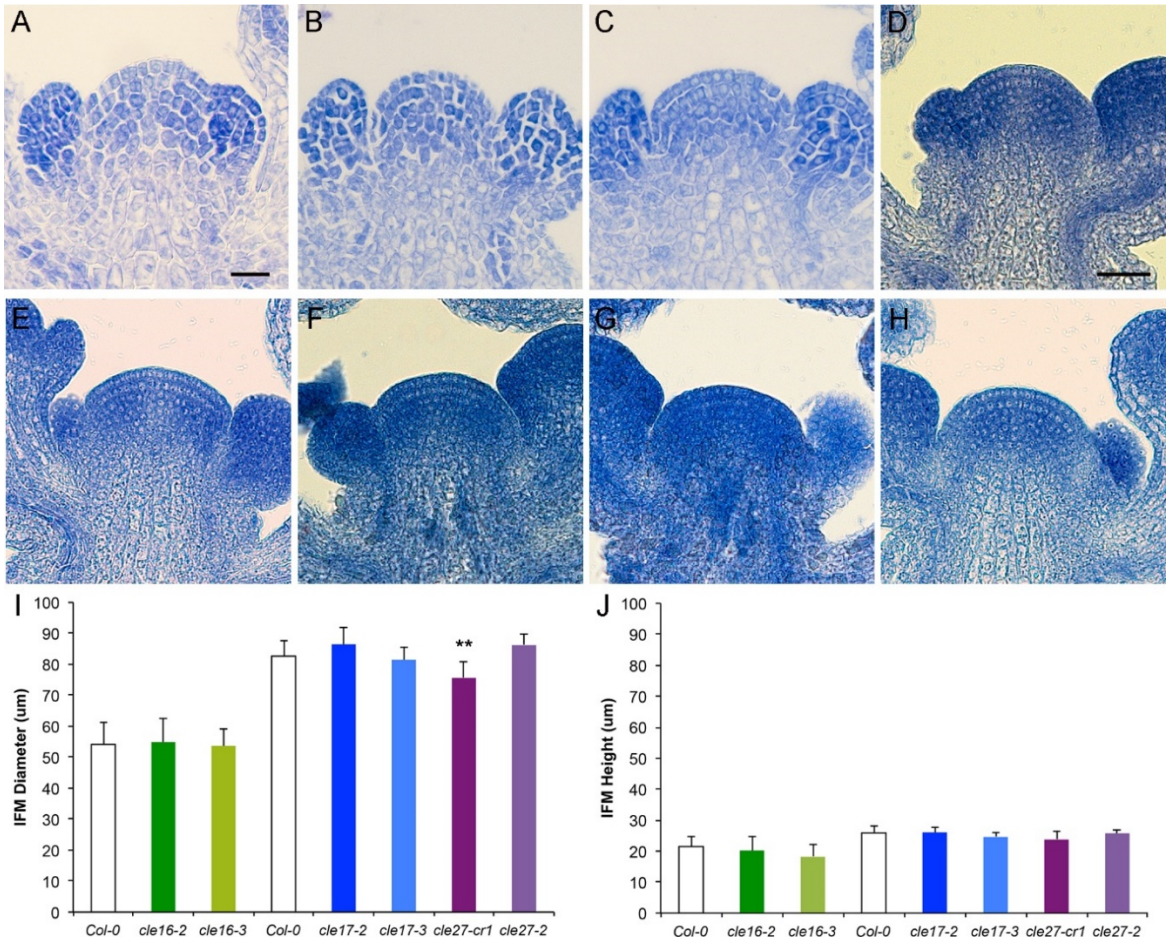

Fig 2.6. Mutations in *CLE16, CLE17* or *CLE27* have no effect on inflorescence meristem size.

(A-H) Longitudinal section through an (A) Col-0 IFM, (B) *cle16-2* IFM, (C) *cle16-3* IFM, (D) Col-0 IFM, (E) *cle17-2* IFM, (F) *cle17-3* IFM, (G) *cle27-cr1* IFM, (H) *cle27-2* IFM. (I, J) Inflorescence meristem diameter (I) and height (J) in wild-type and *cle* mutant plants. Values shown in each graph are mean ± standard deviation (S.D.). n = 10-17 individuals per genotype. Asterisks indicate a significant difference from wild-type at ** $p < 0.01$ (two-tailed Student's t test). Scale bar, 20 mm for A-C and 50 mm for D-H.

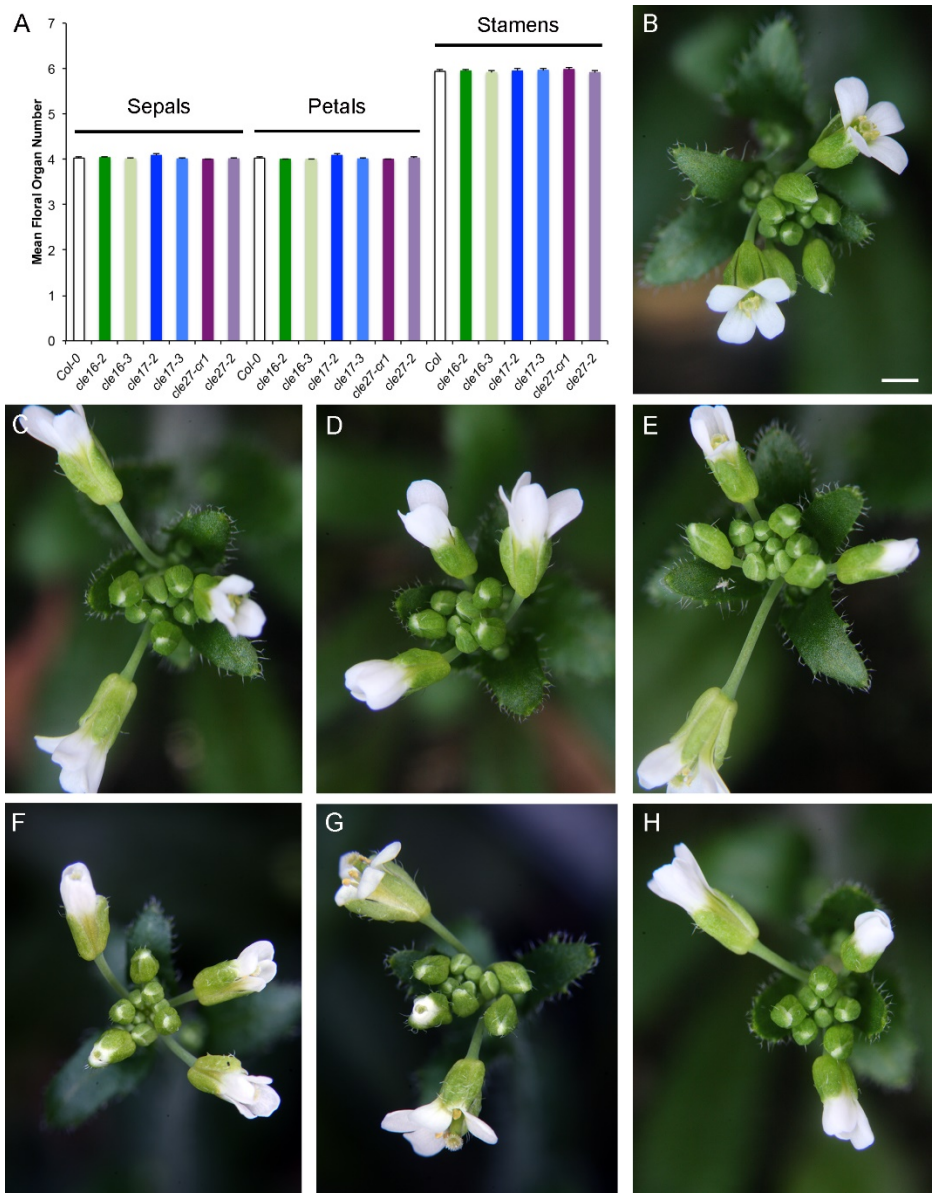

Fig 2.7. Mutations in *CLE16, CLE17* or *CLE27* do not affect floral organ number. (A) Floral organ number in wild-type and *cle* mutant plants. Values shown are mean ± standard error (S.E.). n = 80 flowers per genotype. (B) Col-0 buds and open flowers. (C) *cle16-2* buds and open flowers. (D) *cle16-3* buds and open flowers. (E) *cle17-2* buds and open flowers. (F) *cle17-3* buds and open flowers. (G) *cle27-cr1* buds and open flowers. (H) *cle27-2* buds and open flowers. Scale bar, 0.5 cm.

Discussion

The aim of our study was to identify additional members of the Arabidopsis *CLV3*-related *CLE* gene family that are expressed in above-ground meristems and to determine whether they played a role in regulating shoot apical meristem activity. We identified *CLE16* and *CLE17* as being expressed in both vegetative and inflorescence meristems, and *CLE27* as being expressed in inflorescence meristems. Our functional analysis indicates that loss-of-function mutations in *CLE16, CLE17* or *CLE27* have no significant effect on vegetative leaf initiation rate or rosette diameter, on inflorescence meristem morphology, phyllotaxy or size, or on floral organ number. Thus unlike *CLV3*, *CLE16, CLE17* and *CLE27* are dispensable for shoot apical meristem maintenance on their own. Consistent with this result, none of the three genes activates the *CLV3* signaling pathway when over-expressed in the SAM (Jun et al., 2010).

Comparison of the three CLE peptides with CLV3 reveals differences at key residues. The CLE16 and CLE17 peptides are identical except at position 2 (Jun et al., 2008), and both differ from the CLV3 peptide at several residues, including the C-terminal histidine residue that has an essential role in CLV3 peptide function and binding to the receptor kinase CLV1 (Kondo et al., 2009). The CLE27 peptide is also divergent, differing from CLV3 at the 2nd and 12th positions and also containing a cysteine residue in place of the highly conserved glycine residue at position 6 that when mutated in CLV3 causes a moderate stem cell accumulation phenotype (Fletcher et al., 1999). These observations suggest that the CLE16, CLE17 and CLE27 peptides are not perceived by the receptor kinase complexes that interact with CLV3, and instead may have functions within the SAM that are not related to maintaining stem cell homeostasis via the CLV-WUS pathway.

There may be several reasons why, unlike *CLV3*, the *CLE16, CLE17* and *CLE27* genes individually have no discernable developmental phenotypes under standard growth conditions. One possibility is that the three *CLE* genes have redundant functions in Arabidopsis meristems. The *CLE* gene family consists of 32 members in Arabidopsis (Cock and McCormick, 2001; Strabala et al., 2006), only a few of which exhibit single mutant phenotypes (Etchells and Turner, 2010; Jun et al., 2010; Yaginuma et al., 2011; Fiers et al., 2004). In addition, most Arabidopsis tissues express multiple *CLE* genes in overlapping patterns (Jun et al., 2010), and many CLE peptides act interchangeably when ectopically expressed in roots or shoots (Ito et al., 2006; Strabala et al., 2006; Fiers et al., 2006; Meng et al., 2010). These observations suggest that *CLE* gene functional redundancy may be widespread. Consistent with this notion, we have observed no meristem-related phenotypes among *cle16 cle17, cle16 cle27,* or *cle17 cle27* double mutant plants. Therefore generating even higher order mutant combinations among SAM-expressed *CLE* genes may be required to uncover meristem-related phenotypes.

A second, and non-exclusive, explanation for the absence of phenotypes is that the three *CLE* genes regulate SAM activity only under specific environmental conditions. To date only a handful of studies describing the effect of different environmental states on Arabidopsis *CLE* gene activity have been published. In roots, induction of *CLE14* expression under phosphorus limiting conditions causes terminal differentiation of the root apical meristem (Gutiérrez-Alanís et al., 2017), while a CLE-CLV1 signaling module is proposed to prevent the expansion of the lateral root system in nitrogen-poor environments (Araya et al., 2014). Above ground, *CLE45* has been shown to play a role in prolonging pollen tube growth only at high temperatures (Endo et al., 2013). With the recent availability of null alleles for all Arabidopsis *CLE* genes generated using

genome-editing technology [38], we are rapidly developing the tools needed to determine the significance of these small but important signaling molecules for Arabidopsis biology.

Acknowledgements

We thank Dr. Jian Kang Zhu for providing vectors, Dr. Takashi Ishida and the Arabidopsis Biological Resource Center for providing seeds, Dr. Etienne Grienenberger for genome editing advice, and Tina Williams for microscopy assistance.

Supporting Information

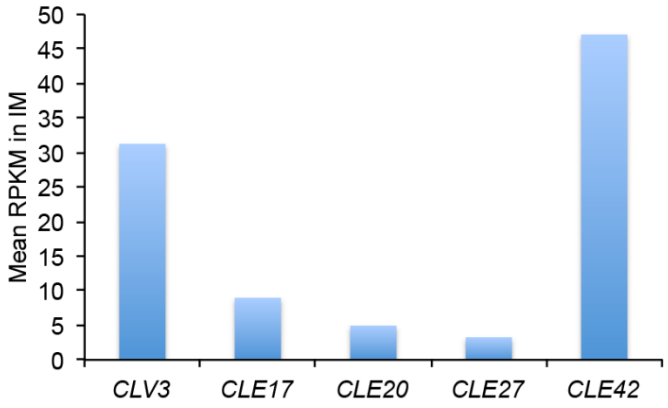

Fig. S2.1. Mean *CLE* gene expression levels in inflorescence meristems (IM).

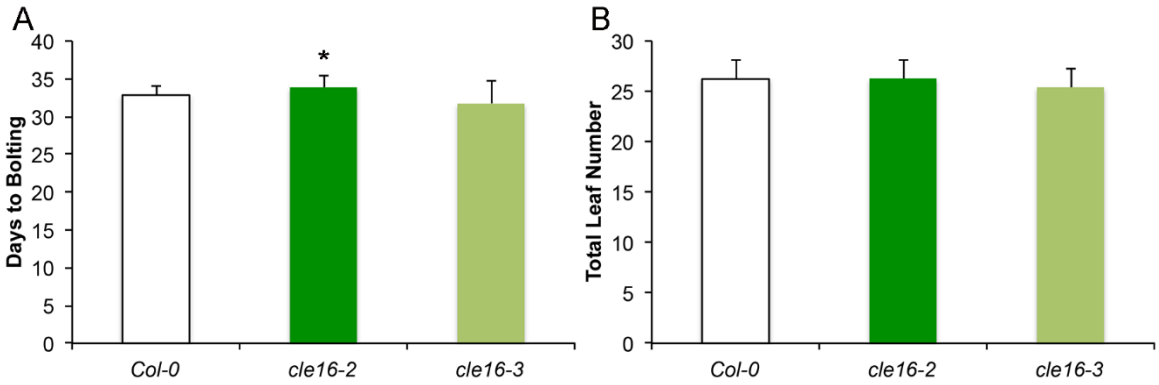

Fig. S2.2. Mutations in *CLE16* have no significant effect on the floral transition.

Table S2.1. Primer sequences used in the study.

Name	Sequence
Cloning	
CLE16guideF	5’-GATTGAACACAGCGGCGTAACCGG-3’
CLE16guideR	5’-AAACCCGGTTACGCCGCTGTGTTC-3’
CLE17guideF	5’-GATTGCTGCTCAATGGCCCACGAAA-3’
CLE17guideR	5’-AAACTTTCGTGGGCCATTGAGCAGC-3’
Genotyping	
CLE16CF	5’-GAATCCAAAACCTGCTCTGC-3’
CLE16CR	5’-CGAAGGAGCAGTCAACACCT-3’
CLE17CF	5’-ACTCCTCCGGAACAAGGTTT-3’
CLE17CR	5’-CTTCTGCACGCACTTTCTCA-3’
cle27LP	5’-ATGACTCATGCTCGAGAATG-3’
cle27RP	5’-CTAGTTATGCAAAGGATCCG-3’
cle27-2RP	5’-TGACGAGTACCAAGAAGAAACG-3’
SALK LBb1.3	5’-ATTTTGCCGATTTCGGAAC-3’
sgRNA_FW	5’-AGAAGAGAAGCAGGCCCATT-3’
sgRNA_RV	5’-TTCCCAAGGTCCAAAGACAC-3’

CHAPTER III

INTERACTIVE CLV3, CLE16, AND CLE17 SIGNALING AT THE SHOOT APEX

In the previous chapter, we performed phenotypic analysis for *cle16*, *cle17*, and *cle27* loss-of-function mutants, and found that they were indistinguishable from wild-type plants. However, given that many *CLE* genes are expressed at the Arabidopsis shoot apex, including *CLV3*, and that their mature peptide sequences are highly similar, it's likely that significant redundancy exists among these CLE peptides. I put this hypothesis to the test by analyzing higher-order allelic combinations of *clv3*, *cle16*, and *cle17*. Indeed, while *CLE16* and *CLE17* does not seem to have an effect on SAM activity by themselves, each can independently and partially buffer the loss of *CLV3* function to restrict stem cell accumulation at the shoot apex.

Using chemical genetics, I demonstrated that endogenous CLV3 activity can prevent the CLE16 and CLE17 peptide from restricting SAM stem cell proliferation. I also provided evidence that while the receptor-like kinase CLV1 serves as a specific binding partner for CLV3, BAM1/2/3 are generic receptors for all three peptides, thus supporting a hierarchy of CLE signaling within the SAM where CLV3 is the dominant factor in maintaining stem cell homeostasis, and CLE16/17 ready to step in only when necessary.

In collaboration with N. Weksler and H. Liu, we generated mutant combinations of *clv3*, *cle16*, and *cle17* with loss-of-function *wus* and *stm* alleles in order to understand the downstream signaling targets of CLE16 and CLE17. My phenotypic analysis of these mutants suggest that WUS and not STM is the main downstream target of CLE16 and CLE17 signaling in the SAM, much like CLV3. Furthermore, I also uncovered a potential novel role for CLE16/17 in controlling axillary meristem development that is independent of CLV3, WUS, and STM. While it is assumed that once established, the biological mechanisms regulating AM are the same as that in the SAM, very little is known about the role of CLE peptides and their cognate receptor-like kinases during de novo AM formation. This, the work described in this chapter opens up a host of new possibilities for investigating CLE signaling in shoot branching and crop improvement.

Abstract

The ability of plants to grow and form organs throughout their lifetime is dependent upon their sustained stem cell activity. These stem cell populations are maintained by intricate networks of intercellular signaling pathways. In *Arabidopsis thaliana*, the small secreted peptide CLAVATA3 (CLV3) controls shoot apical meristem (SAM) maintenance by activating a signal transduction pathway that modulates the expression of the homeodomain transcription factor WUSCHEL (WUS). Here, we demonstrate that two CLV3-related peptides, CLE16 and CLE17, restrict stem cell accumulation in the absence of CLV3 by signaling upstream of WUS. CLE16 and CLE17 contribute independently to SAM maintenance and organ production in *clv3* null mutant plants at all stages of development. Using chemical genetics, we demonstrate that CLE16 and CLE17 signal through a subset of CLV3 receptors, the BARELY ANY MERISTEM (BAM) receptor kinases. Our study also reveals a novel pathway for CLE signaling to control axillary meristem initiation independently of WUS, expanding the potential targets for enhancing yield traits in crop species.

Introduction

In both animals and plants, pluripotent stem cell populations persist and continuously divide to supply building materials for growth and regeneration. Despite their lack of mobility, plants have been successfully colonizing almost every ecological niche on land. Their ability to continuously establish new body axes in the form of branches, leaves, flowers, and lateral roots, in response to internal and external stimuli lie at the crux of their adaptive fitness. Such dynamic de novo organ formation requires robust stem cell activity. These stem cells are supported within special micro-environments called the stem cell niches that are maintained by intricate networks of intercellular communication (Aichinger et al., 2012, Heidstra and Sabatini, 2014).

Primary aboveground growth in plants is mediated by the shoot apical meristem (SAM) (Steeves and Sussex, 1989). The center-most region at the apex of the SAM is called the central zone (CZ), and is occupied by the stem cell niche. Descendents of these cells that are pushed into the periphery undergo rapid divisions before differentiating to form leaf and flower primordia, the latter of which also harbors their own stem cell reservoir to produce floral organs before terminating. Stem cell identity at the CZ is maintained by molecular factors originating from directly underlying cells, collectively called the organizing center (OC) (Barton, 2010; Gaillochet and Lohnmann, 2015; Soyars et al., 2016). In the model plant *Arabidopsis thaliana*, one of the master regulators of stem cell identity in the SAM is WUSCHEL (WUS). *WUS* is expressed in the OC, and encodes a homeodomain transcription factor that diffuses through the plasmodesmata to promote stem cell identity and suppress differentiation in neighboring cells (Mayer et al., 1998; Yadav et al., 2011). The WUS protein also moves into the CZ to directly activate transcription of *CLAVATA3* (*CLV3*), which encodes a prepropeptide that is secreted to the extracellular space, and is proteolytically processed into a small 12-13 amino acid peptide hormone (Fletcher et al., 1999; Ito et al., 2006; Ohyama et al. 2008; Ni et al., 2011; Xu et al., 2013). This mature peptide interacts with receptors in the underlying layers, where it functions to limit stem cell accumulation by restricting the *WUS* expression domain to the OC. CLV3-WUS thus forms a core negative feedback loop that maintains stem cell homeostasis in the SAM, and also in the transient floral meristem (Somssich et al., 2016; Dao and Fletcher, 2017). As a result, loss-of-function *clv3* mutants have enlarged shoot meristems that produce flowers with extra organs, while *CLV3* overexpression is sufficient to consume the

stem cell population in the SAM, leading to growth arrest at the vegetative or reproductive stage (Strabala et al., 2006).

Several complexes of leucine-rich repeat receptor-like kinases function to transduce the CLV3 signal. CLAVATA1 (CLV1) forms homodimers that localize to the interior cells directly below the *CLV3* expression domain and physically interact with CLV3 peptide (Clark et al., 1997; Ogawa et al., 2008). CLAVATA2 (CLV2) and its co-receptor CORYNE (CRN) form heterodimers throughout the SAM and transduce CLV3 signal independently of CLV1, although it is unclear whether CLV2/CRN directly binds CLV3 (Müller et al., 2008; Bleckmann et al., 2009; Guo et al., 2010). The BARELY ANY MERISTEM (BAM) receptors are close homologs of CLV1, and localize to the periphery of the SAM in a complementary manner to CLV1 (DeYoung et al., 2006; DeYoung et al., 2008; Nimchuk et al., 2015). BAM1 is able to bind CLV3 in vivo, and expression of *BAM1* and *BAM3* is excluded from the SAM interior by CLV1 activity (Shinohara and Matsubayashi, 2014). While *bam1/2/3* triple mutants show a reduction in SAM size, *clv1 bam1/2/3* plants display a dramatic enhancement of stem cell accumulation beyond that of *clv3* plants. Thus, a dual-activity model suggests that under normal conditions, the BAM receptors prevent CLV3-CLV1 signaling at the flank of the SAM to maintain stem cell accumulation. However, when CLV1 is absent, *BAM* gene expression extends into the SAM center, which allows the receptors to partially compensate for the absence of CLV1 by interacting with CLV3 peptides (Nimchuk, 2017).

CLV3 is the founding member of a large family of polypeptides called CLAVATA3/EMBRYO SURROUNDING REGION-RELATED (CLE) peptides. *CLE* genes are conserved throughout the land plant lineage, and their origination is associated with the evolution of three-dimensional growth in plants (Goad et al., 2016; Whitewoods et al., 2018). The Arabidopsis genome contains 32 *CLE* sequences encoding 27 distinct peptides (Jun et al., 2008). Only a handful of *CLE* genes have been functionally characterized, all of which are involved in diverse developmental processes (Wang et al., 2016). However, the majority of *cle* single mutants lack a phenotype, likely due to the high degree of redundancy typical of large gene families. Indeed, recent studies have revealed combinatory actions of multiple CLE peptides in regulating SAM stem cell accumulation in other species. In maize, the CLE peptides FON2-LIKE CLE PROTEIN1 (ZmFCP1) and ZmCLE7 signal through separate pathways to restrict meristem size (Je et al., 2016; Je et al., 2017). In tomato, both SlCLV3 and SlCLE9 restrict SAM size by signaling through SlCLV1, and loss-of-function *Slclv3* is actively compensated by the upregulation of *SlCLE9* expression (Rodriguez-Leal et al., 2019).

Evidence suggests that multiple CLE peptides may also function in the *Arabidopsis* SAM. A previous comprehensive reporter assay revealed the promoter activity of several *CLE* genes in or around the shoot meristem (Jun et al., 2010). That *clv1 bam1/2/3* plants have more severe phenotype than *clv3* plants indicates that peptides other than CLV3 may also signal through the CLV1/BAM receptor kinases to restrict stem cell accumulation (Nimchuk et al., 2015). Finally, an *Arabidopsis dodeca-cle* mutant in which *CLV3* and 11 other *CLE* genes were knocked out using genome editing showed a stronger meristem phenotype than *clv3* plants, demonstrating that at least some of these 11 CLE peptides can partially compensate for CLV3 activity (Rodriguez-Leal et al., 2019). However, it is still unknown exactly which *CLE* genes are responsible for this compensation activity, or the signaling pathway(s) through which they function.

Previously, we used genome editing to generate lines containing null alleles of *CLE16* and *CLE17*, which displayed no phenotypes under normal growth conditions despite their reported promoter

activity in the SAM (Gregory et al., 2019). In this study, we address the biological function of these CLE peptides in *clv3* null mutant backgrounds, and reveal a partial compensation of CLV3 activity by CLE16 and CLE17 beginning at the embryonic stage and continuing throughout the rest of development. Using synthetic peptide application, we demonstrate that while CLV1 appears to bind CLV3 specifically, BAM1, BAM2 and BAM3 act as receptors for all three CLE peptides. Finally, we show that CLE16 and CLE17 signal upstream of WUSCHEL in a manner similar to CLV3. Together, these results suggest that CLE16 and CLE17 partially compensate for CLV3 to maintain stem cell homeostasis by interacting with a different suite of receptors at the shoot apex.

Materials and methods

Plant materials and growth conditions

All *Arabidopsis thaliana* plants were in the Columbia-0 (Col-0) accession. Plants were grown on a mixture of 1:1:1 mixture of perlite:vermiculite:top soil under long day condition (16-hour light/8-hour dark, light intensity ~ 120 μmol/m^2/s) at 21˚C. Seeds were planted at a density of one seed per pot. Seeds were stratified at 4˚C for 5 days before exposure to light. Seedlings were watered every day with a 1:1500 dilution of Miracle-Gro 20-20-20 fertilizer prior to flowering and once a week with fertilizer thereafter. Homozygous plants were confirmed by PCR-based genotyping and restriction digestion (primers and restriction enzymes are listed in Table S1).

In situ hybridization

In situ hybridization was carried out as described in Jun et al. 2010a, with a few modifications in the fixation process. Samples were fixed in a neutral buffered formalin solution (Sigma) overnight at 4˚C, washed in methanol at least three times for 15 min each, washed in ethanol twice for 10 min, then transferred to a Leica TP1020 tissue processor for automated tissue infiltration into McCormick Paraplast X-tra. Samples were sectioned at 8 μm and transferred to microscopy slides. After proteinase K digestion, samples were hybridized overnight at 55°C with sense and antisense RNA probes labeled with Digoxegenin (Roche) in a hybridization mix of 50% (deionized) formamide, 6X SSC, 3% SDS, 0.5 mg/mL tRNA. After washing with 2× SCC and 0.2× SSC, 0.2% SDS at 55-60°C, probes were detected by incubation with anti-Digoxegenin antibody linked to Alkaline Phosphatase (Roche) for 60 min to overnight. Visualization was carried out by incubation with nitro blue tetrazolium chloride – 5-bromo-4-chloro-3-indolyl-phosphate (NBT-BCIP, Roche) for 4-48 hours after washing. Tissue sections were imaged using a Leica DM4000 B light microscope.

Peptide assays

For peptide treatment of seedlings, Murashige and Skoog (MS) growing medium, 0.7% agar, pH 5.7 was prepared and autoclaved. Before pouring, either water (Mock) or a 3 mM solution of either synthetic scrambled peptide, CLV3, CLE16, or CLE17 (Genscript, purity ≥ 90%, no residue modification) in water was added to the MS medium to a final concentration of 30 μM. Arabidopsis seeds were sterilized in 70% ethanol, followed by 10% bleach with 0.2% SDS, and then plated on mock-treated or peptide-treated MS plates. Plates were stratified at 4˚C for 5 days, then germinated under long day conditions as described above. The shoot portions of the seedlings were harvested at 5 days after germination for confocal microscopy.

Confocal laser scanning microscopy

Propidium iodide (PI) staining of tissues was carried out as described in Truernit *et al.* 2008. Briefly, whole seedlings or plant organs were fixed in 50% methanol and 10% acetic acid, boiled in 80% ethanol at 80°C for 1-5 min, then transferred back into fresh fixative for at least 1 hour. Tissues were then incubated in 1% periodic acid at room temperature for 40 min, and transferred into pseudo-Schiff reagent (100 mM sodium metabisulfite and 0.15 N HCl) with PI freshly added to 100 μg/mL for 1 to 2 h. To observe embryonic meristems, Arabidopsis seeds were imbibed in water at 4˚C overnight, and embryos were dissected from the seed coat for PI staining. For imaging, embryos and vegetative tissues were cleared in methyl salicylate, whereas inflorescences were partially embedded in 1% agarose in an upright position and submerged in water, before mounting on depression slides. Samples were visualized using a Leica TCS-SP8 spectral confocal laser scanning microscope (Leica Microsystems). The excitation wavelength for PI–stained samples was 488 nm, and emission was collected at 600 to 650 nm wavelength.

Phenotypic analysis

Shoot meristem measurements were performed using the Fiji software. Parameters for each meristem were determined by defining three sets of coordinates: one for the apical point, and two for the notches where the meristematic zone ends and organ primordia begins. Meristem height and diameter were calculated as the height and base, respectively of the resulting triangle. Z-stacks of inflorescence meristems were projected into 2-D images for surface area measurement, and reconstructed in Fiji's Volume Viewer for height measurement. Floral organ counting was performed as described.

Results

CLE16 and *CLE17* are expressed in the SAM

The *CLE16* and *CLE17* genes encode prepropeptides with near-identical CLE domains, which only differ in their second residue (Fig. 3.1i). Both CLE peptides also share significant sequence similarity with the CLV3 peptide, retaining most of the biologically important residues. In a previous comprehensive expression assay using promoter:GUS/GFP transgenic lines, CLE16 and CLE17 were identified to have promoter activity at the shoot apex (Jun et al., 2010). During vegetative development, staining for pCLE16:GUS was observed in the organ primordia flanking the vegetative SAM, as well as at the base of developing leaves. pCLE17:GUS was detected throughout the entire SAM and surrounding leaves, with strongest activity at the outer layers. Activities of pCLE16 and pCLE17 were also detected in the embryo, as well as at inflorescence and floral tissues (Jun et al., 2010; Fiume et al., 2011). We took a closer look at *pCLE16:GUS/GFP* and *pCLE17:GUS/GFP* expression in the inflorescence using fluorescent confocal microscopy, and found that both were localized to the flanks of the shoot meristem, while absent from the center of the SAM (Fig. S3.1 a, b).

To confirm their expression dynamics, we performed mRNA in situ hybridization (ISH) for *CLE16* transcripts in wild-type and *clv3* SAMs. While staining for *CLE16* was not detectable in 7 days after germination (DAG) Col-0 vegetative SAM, we observed a broad signal in the *clv3* VM, with strongest staining in the outer cell layers, as well as at the organ primordia (Fig. 3.1a -d). We also performed ISH for *CLV3* and *WUS* transcripts as positive controls, both of which were readily

detected in their relative specific domains in both wild-type and *clv3* VM (Fig. 3.1e-h). At the moment, we continue to work on the detection for *CLE17* transcript in the VM, as well as during other stages of plant development, namely in the embryonic and inflorescence meristem. Regardless, our current result suggests that at least *CLE16* is upregulated in *clv3* mutant VM, albeit not as strongly as *CLV3* (Fig 3.1a, b, e, f).

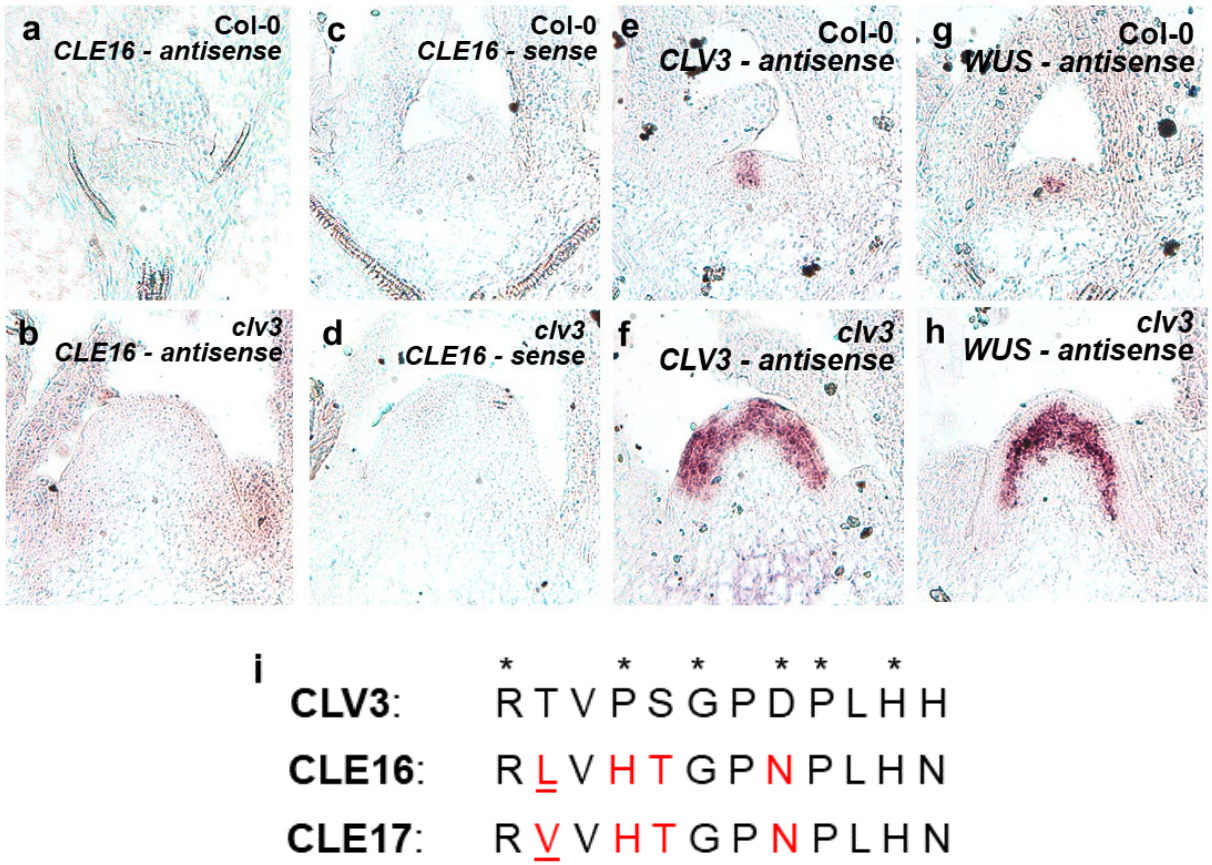

Figure 3.1. *CLE16* mRNA expression patterns in wild-type and *clv3* vegetative meristems. RNA *in situ* hybridization of *CLE16* antisense probe (a and b), negative control *CLE16* sense probe (c and d), *CLV3* antisense (e and f), and *WUS* (g and h) antisense probes to 7 DAG wild-type (a, c, e, and g) and *clv3-15* (b, d, f, and h) SAMs. g, Alignment of the CLV3, CLE16, and CLE17 CLE domains. Asterisks denote amino acids in CLV3 that are important for receptor binding. Black text denotes amino acids that are conserved between all three proteins. Red text denotes sequence differences between CLV3 and CLE16/17. Underlined text at position #2 denotes difference between CLE16 and CLE17.

CLE16 and *CLE17* compensate for loss of *CLV3* activity to restrict stem cell accumulation

Our previous study showed that unlike the *clv3* alleles, *cle16-2* and *cle17-5* null alleles do not affect shoot apical meristem phenotypes in the Col-0 background under normal growth conditions (Gregory et al., 2018). However, because both genes have broad, overlapping expression patterns in the SAM, we hypothesized that CLE16 and CLE17 function redundantly either with each other or with CLV3 peptide. We tested this by generating *cle16-2 cle17-5*, *clv3-15 cle16-2*, *clv3-15*

cle17-5, and *clv3-15 cle16-2 cle17-5* mutants (alleles in Table 3.1), and assayed stem cell accumulation by measuring SAM height and diameter across the embryonic, vegetative, and reproductive developmental stages.

Table 3.1. List of CLE alleles used in this study

Gene	Allele	Type of Mutation	Effect on protein	Source
CLV3	*clv3-15*	Deletion of 78 bp and insertion of 8 bp at +547	Deletion of half of CLE domain at aa75	Forner *et al.* 2015
CLE16	*cle16-2*	Insertion of C at +59	Premature stop codon at aa 45	Gregory *et al.* 2018
CLE17	*cle17-5*	Insertion of A at +220	Premature stop codon at aa 80	Gregory *et al.* 2018

The CLV-WUS signaling pathway functions to limit shoot apical meristem cell accumulation as early as the mature embryo stage (Schoof et al., 2000). Using confocal laser scanning microscopy (CLSM), we visualized the SAMs of mature embryos carrying the above allelic combinations. We found that the dimensions of *cle16 cle17* embryo SAMs were indistinguishable from those of wild type Col-0 SAMs (Fig. 3.2a, b, s), revealing that removing both *CLE16* and *CLE17* activity has no effect on embryo SAM size. In contrast, the diameter and height of *clv3* embryo SAMs was significantly increased compared to wild-type SAMs (Fig. 3.2a, c, s). Neither *clv3 cle16* nor *clv3 cle17* embryos displayed significant changes in SAM size relative to *clv3* embryos, although *clv3 cle16* embryos showed a small increase in SAM diameter ($P = 0.03$, Fig. 3.2c, d, s). In contrast, *clv3 cle16 cle17* embryos formed SAMs that were significantly taller and broader than those of the double mutants (height: $P < 10^{-5}$, diameter: $P = 0.002$; Fig. 3.2d-f, s). These results indicate that both *CLE16* and *CLE17* can restrict stem cell accumulation in the absence of *CLV3* beginning during embryogenesis. In addition, they suggest that either *CLE16* and *CLE17* act redundantly with one another, or their individual contributions are too subtle to measure at the embryonic stage under our experimental conditions.

At 7 DAG, the vegetative meristems (VMs) of *cle16 cle17* plants remained indistinguishable from those of the wild type, while *clv3* plants showed an even greater enhancement of VM size (Fig. 3.2g, h, t). At this stage *clv3 cle16* plants formed VMs that were significantly larger in both height and diameter than *clv3* plants (height: $P = 0.001$, diameter: $P < 10^{-3}$; Fig. 3.2i, j, t). Although *clv3 cle17* VMs were not significantly taller than those of *clv3*, their diameter was significantly increased (height: $P = 0.11$, diameter: $P < 10^{-4}$; 3.2i, k, t). *clv3 cle16 cle17* seedlings produced VMs that were significantly larger in all dimensions than those of *clv3*, but were indistinguishable from either of the double mutants (Fig. 3.2i-l, t). These results suggest that *CLE16* and *CLE17* independently restrict stem cell accumulation in *clv3* seedlings at the vegetative stage.

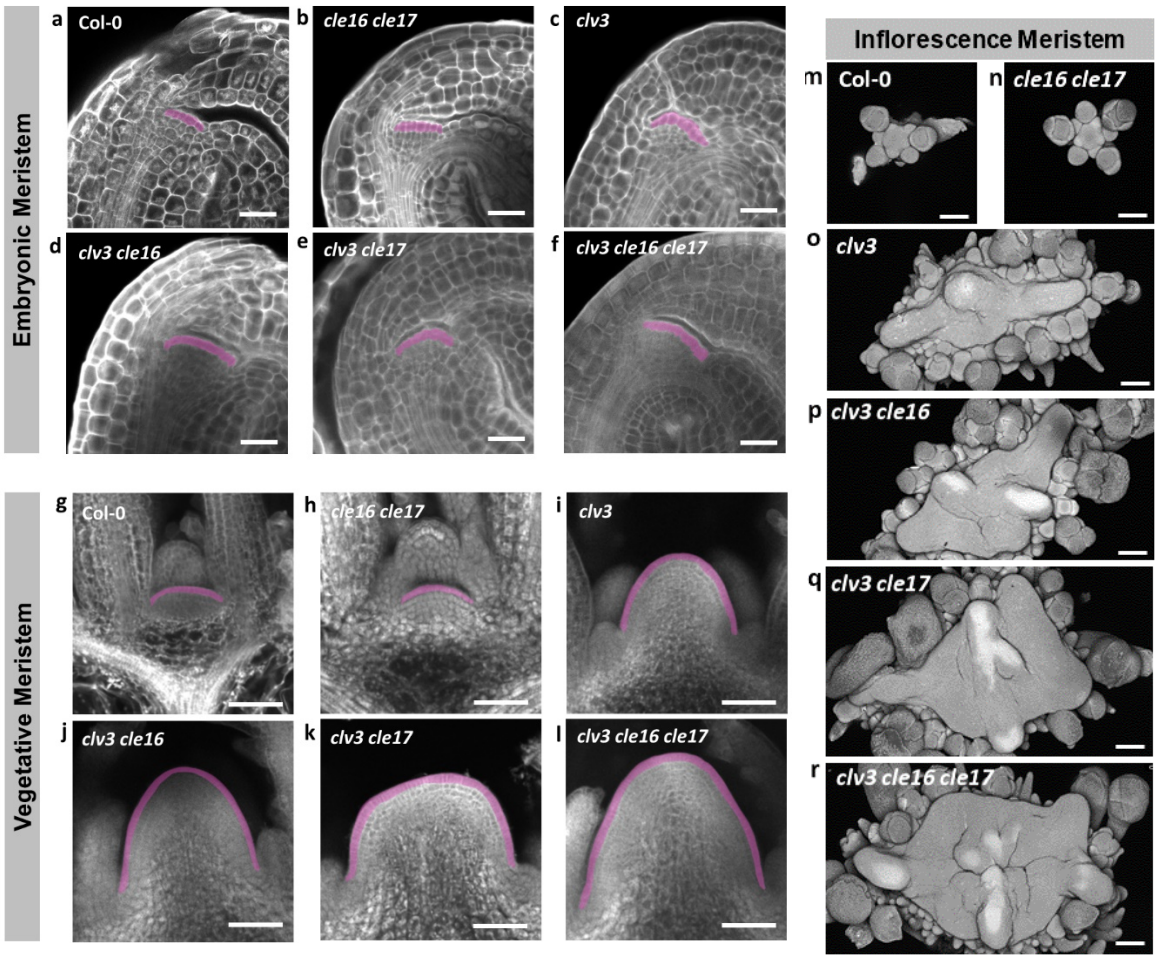
Embryonic Meristem
Vegetative Meristem
Inflorescence Meristem
a Col-0
b cle16 cle17
c clv3
d clv3 cle16
e clv3 cle17
f clv3 cle16 cle17
g Col-0
h cle16 cle17
i clv3
j clv3 cle16
k clv3 cle17
l clv3 cle16 cle17
m Col-0
n cle16 cle17
o clv3
p clv3 cle16
q clv3 cle17
r clv3 cle16 cle17

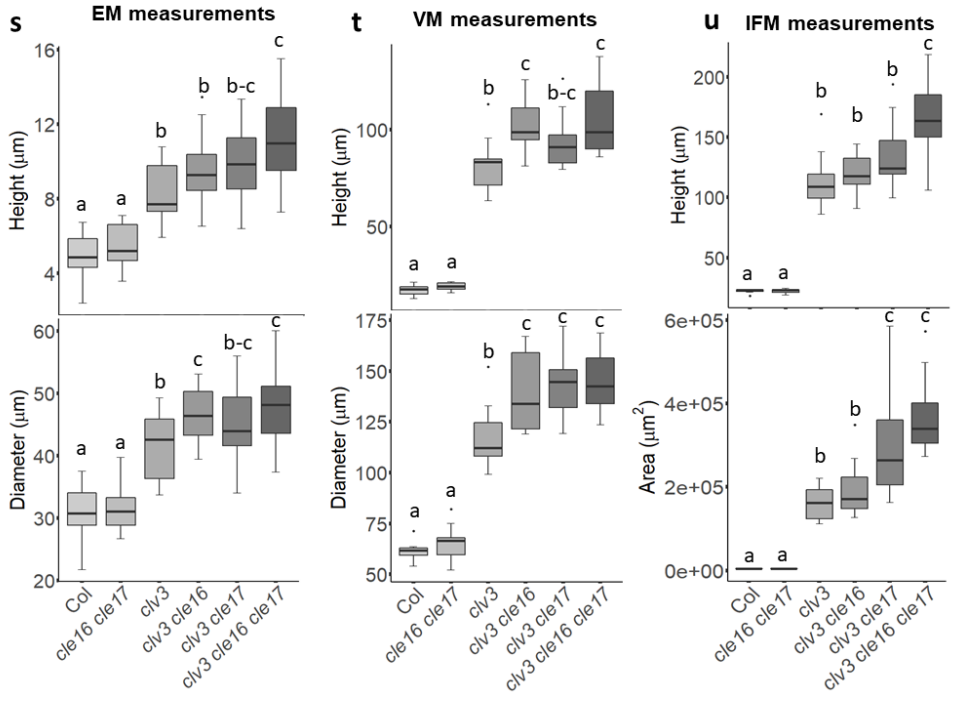
s EM measurements
t VM measurements
u IFM measurements
Height (µm)
Diameter (µm)
Area (µm²)
Col
cle16 cle17
clv3
clv3 cle16
clv3 cle17
clv3 cle16 cle17

Figure 3.2. *CLE16* and *CLE17* restrict stem cell accumulation in the SAM in the absence of *CLV3* activity. a-q, Confocal micrographs of Arabidopsis SAMs at the embryonic stage (a-f), vegetative stage (g-l), and reproductive stage (m-r) from wild-type (a, g, and m), *cle16 cle17* (b, h, and n), *clv3* (c, i, and o), *clv3 cle16* (d, j, and p), *clv3 cle17* (e, k, and q), and *clv3 cle16 cle17* (k, l, and r) plants. Cells in the L1 layer of the meristem were false colored pink. d-f, Meristem size measurements at the embryonic stage (s), vegetative stage t), and reproductive stage (u) from wild-type, *cle16 cle17*, *clv3*, *clv3 cle16*, *clv3 cle17*, and *clv3 cle16 cle17* plants. Sample size: (d) n = 16 to 22, (e) n = 11 to 15, (f) n = 8 to 16. For the box plots, the bottom and top of the boxes represent the twenty-fifth and seventy-fifth percentile, respectively; the whiskers represent the minimum and maximum values; and the middle line is the median. Statistical analysis was performed using one-way ANOVA and Tukey test; letters represent different significance groups at $P < 0.05$ and joint-letters indicate a group that shares $P < 0.05$ with two other groups. Scale bars: 25 μm in (a), 50 μm in (b), 100 μm in (c).

Inflorescence meristems (IFMs) were analyzed by harvesting the shoot apices when the stem reached 1 cm in length and visualizing the tissues in Z-stacks using CLSM. Subsequent 3-D reconstruction allowed us to measure the height of the whole IFM. However, due to the irregular shape of the IFMs we measured the projected surface area from the top-down view of the whole IFM by maximal 2D projection instead of meristem diameter. Our analysis revealed no differences in projected surface area and height of *cle16 cle17* IFMs compared to those of wild-type IFMs (Fig. 3.2m, n, u). In contrast, *clv3* plants formed fasciated IFMs that were significantly larger in both surface area and height than those of wild type IFMs (Fig. 3.2m, o, u). Although *clv3 cle16* plants did not exhibit increased IFM height or projected area compared to those of *clv3*, *clv3 cle17* plants showed significantly increased IFM projected area ($P < 10^{-4}$, Fig. 3.2o-q, u). The *clv3 cle16 cle17* triple mutants formed the largest IFMs on average, with both height and projected surface area significantly larger than those of *clv3* IFMs (height: $P < 10^{-6}$, area: $P < 10^{-8}$; Fig. 3.2o, r, u). Compared to *clv3 cle17*, the triple mutant IFMs are also greater in height, but not in projected surface area on average (height: $P = 0.008$, area: $P = 0.34$; Fig. 3.2q, r, u). However, it should be noted that the extreme fasciation resulting from stem cell over-proliferation likely led to more distinct differences in total volume among these genotypes that was not measured under our methodology. Both *CLE16* and *CLE17* therefore appeared to limit IFM activity in the absence of *CLV3* activity during reproductive development, with *CLE17* contributing more to stem cell restriction at this stage than *CLE16*.

Because the CLV-WUS signaling pathway is also active in the floral meristem (FM), we tested whether CLE16 and/or CLE17 could compensate for CLV3 activity during flower development. We used carpel number as a readout for FM size, because larger FMs produce more organs, and the carpels are the final whorl of organs to form before the floral meristem undergoes termination. We found that whereas wild-type and *cle16 cle17* plants invariably made two carpels per flower, *clv3* plants made an average of one additional carpel (3.3 ± 0.08, S.E.M.) (Fig. 3.3 a-c, g). The mean number of carpels per flower was significantly enhanced in *clv3 cle16* (3.85 ± 0.08) and *clv3 cle17* (4.59 ± 0.10) flowers compared to *clv3* flowers, whereas *clv3 cle16 cle17* (5.92 ± 0.09) flowers generated significantly more carpels than either of the double mutants (Fig. 3.3 c-f, g). These results suggest that CLE16 and CLE17 also compensate for CLV3 signaling to restrict floral meristem size. It's also interesting to note that *clv3 cle17* plants appeared to produce larger IFMs and more carpels than *clv3 cle16* plants, but embryonic and vegetative meristem sizes are similar

between the two genotypes, indicating that *CLE17* might play a greater role in restricting stem cell accumulation than *CLE16* specifically during reproductive development.

Taken together, our results indicate that *CLE16* and *CLE17* each play a role in controlling stem cell accumulation in shoot and floral meristems throughout development, but only in the absence of endogenous *CLV3* activity. *CLE16* and *CLE17* appear to act independently of one another during vegetative and floral development but synergistically during the inflorescence phase. Furthermore, *CLE17* may play a more prominent role than *CLE16* in controlling shoot and floral meristem activity during the reproductive stage, as indicated by greater IFM size and carpel number in *clv3 cle17* plants compared to *clv3 cle16* plants.

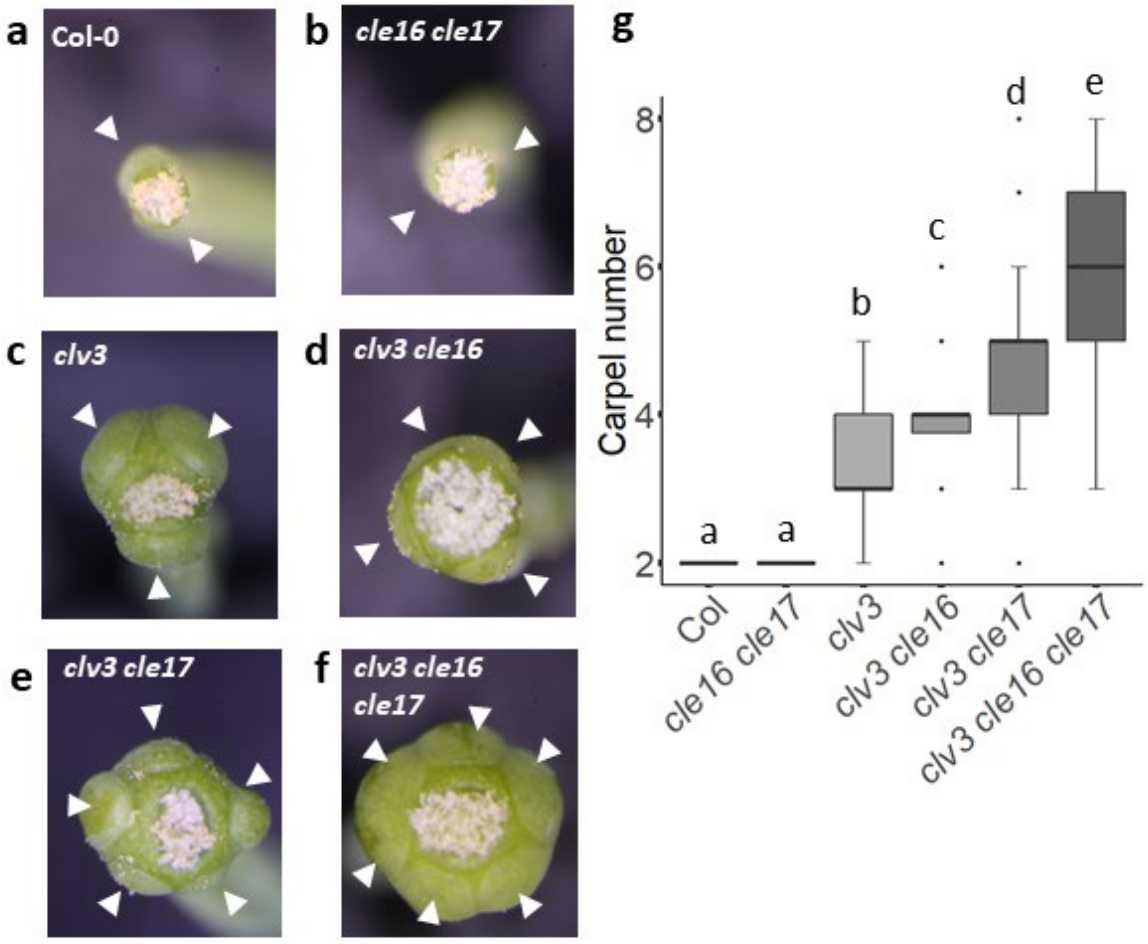

Figure 3.3. Multiple *CLE* genes control floral organ production in the absence of *CLV3*. a, b, Top-down view of siliques from (a) and quantification of carpel number in (b) wild-type, *cle16 cle17*, *clv3*, *clv3 cle16*, *clv3 cle17*, and *clv3 cle16 cle17* flowers (n = 100 per genotype). White arrowhead, carpel. For the box plots, the bottom and top of the boxes represent the twenty-fifth and seventy-fifth percentile, respectively; the whiskers represent the minimum and maximum values; and the middle line is the median. Statistical analysis was performed using one-way ANOVA and Tukey test; letters represent different significance groups at $P < 0.05$ and joint-letters indicate a group that shares $P < 0.05$ with two other groups.

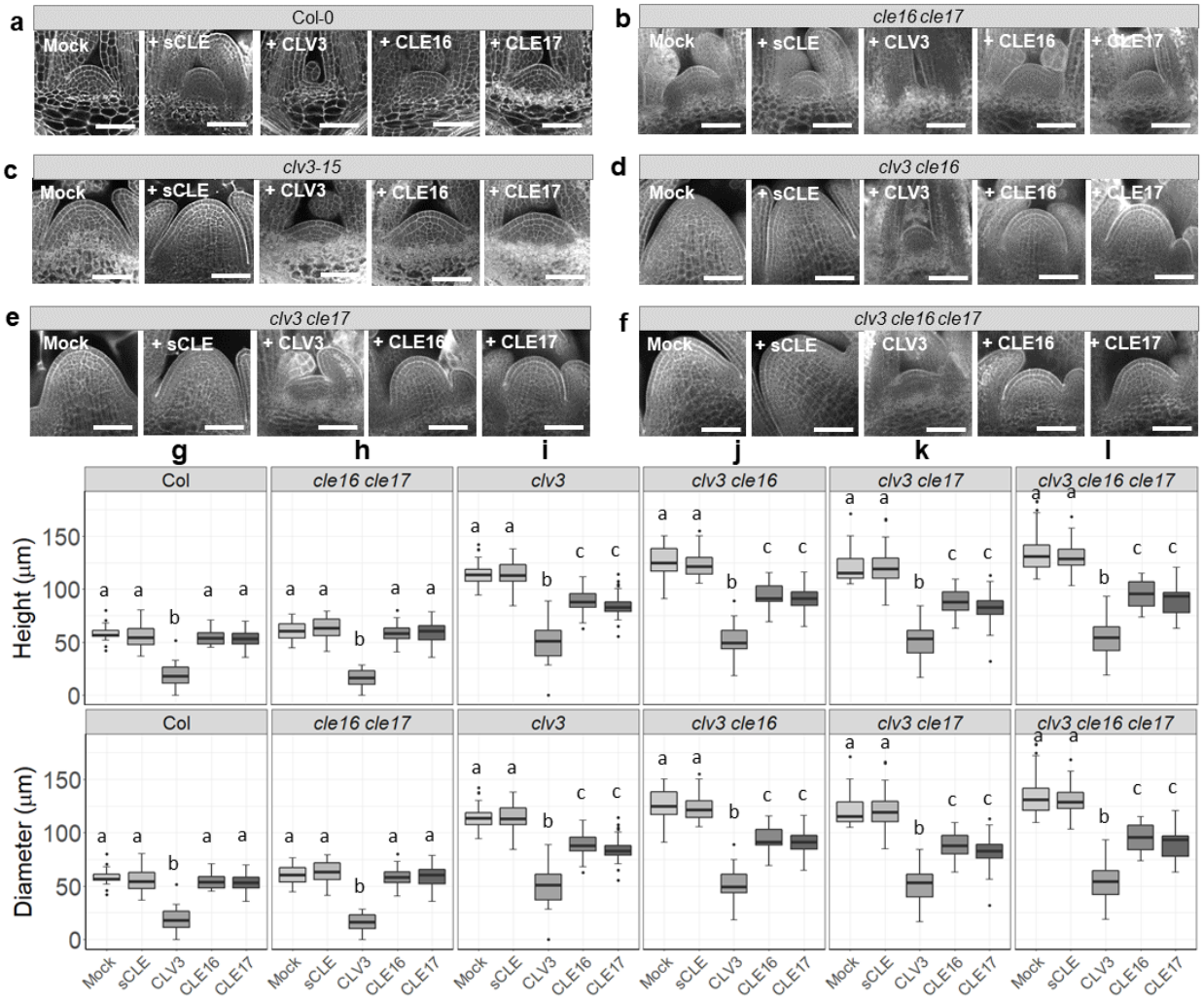

Figure 3.4. CLE16 and CLE17 synthetic peptide treatments affect stem cell accumulation in the SAM in the absence of CLV3 activity. Confocal micrographs (a-f) and vegetative meristem size measurements (g-l) of 7 DAG wild-type (a and g), *cle16 cle17* (b and h), *clv3* (c and i), *clv3 cle16* (d and j), *clv3 cle17* (e and k), and *clv3 cle16 cle17* (f and l) plants grown on MS plates containing a mock solution or 30 µM of synthetic sCLE, CLV3, CLE16, or CLE17 peptide (n = 17 to 36). For the box plots, the bottom and top of the boxes represent the twenty-fifth and seventy-fifth percentile, respectively; the whiskers represent the minimum and maximum values; and the middle line is the median. Statistical analysis was performed using one-way ANOVA and Tukey test; letters represent different significance groups at $P < 0.05$. Scale bars: 50 µm.

Exogenous application of CLE16 and CLE17 peptide only affects clv3 mutants

Two scenarios can be invoked to explain how the loss of CLE16 and/or CLE17 peptide function results in observable phenotypes in *clv3* but not wild type plants. One is that endogenous CLE16 and CLE17 normally signal to restrict stem cell activity in wild-type shoot and floral meristems, but loss of their function is fully complemented by CLV3 activity. The other is that CLV3 signaling

actively precludes the biological activity of CLE16 and CLE17, either by repressing *CLE16/17* gene expression, or by preventing CLE16/17 ligand-receptor interaction. In order to differentiate between the two hypotheses, we artificially induced CLE signaling in the SAM by germinating Arabidopsis seedlings on agar plates containing 30 μM of synthetic CLV3, CLE16 or CLE17 peptides (Table 2). We used the unmodified 12-amino acid CLE sequences of the three peptides, as this portion of the CLV3 peptide was demonstrated to be of comparable biological potency as the mature arabinosylated peptide at the concentration used. We also used both a blank water treatment and a scrambled CLV3 amino acid sequence (referred to as sCLE) as negative controls.

Table 3.2. Synthetic peptide sequences used in this study.

Peptide	Sequences
sCLE	PPTRGLSHHPVD
CLV3	RTVPSGPDPLHH
CLE16	RLVHTGPNPLHN
CLE17	RVVHTGPNPLHN

We germinated *Col-0*, *cle16 cle17*, *clv3*, *clv3 cle16*, *clv3 cle17*, and *clv3 cle16 cle17* seeds on the peptide plates and measured vegetative SAM size in 7 DAG seedlings using CLSM (Fig. 3.4). We found that seedling SAM size of any given genotype was indistinguishable when grown on mock-treated or on sCLE plates, indicating that the control scrambled peptide indeed had no biological function. In contrast, treatment with CLV3 peptide strongly reduced the SAM size of all genotypes, suggesting that the synthetic CLE peptides in the growth media were effectively transported to the shoot apical meristem. In contrast, treatment with either CLE16 or CLE17 peptides did not affect the meristem size of wild type or *cle16 cle17* seedlings, indicating that neither CLE16 nor CLE17 synthetic peptides are functional in the vegetative SAM of these genotypes (Fig. 3.4a, b, g, h). However, application of either CLE16 or CLE17 peptides significantly reduced SAM size in *clv3* plants compared to mock or sCLE treatments, albeit not to the same efficacy as CLV3 peptide treatment (Fig. 3.4c, i). Similarly, CLE16 and CLE17 application significantly restricted stem cell accumulation in *clv3 cle16*, *clv3 cle17*, and *clv3 cle16 cle17* plants, again to a lesser degree than CLV3 (Fig. 3.4d-f, j-l). These results suggest that endogenous CLV3 signaling prevents the biological activity of CLE16 and CLE17 peptides in the SAM, whether through suppression of *CLE16/CLE17* transcription or through receptor occupancy by CLV3 peptide. In addition, CLE16 and CLE17 peptides appear to regulate shoot stem cell activity to a lesser extent than CLV3 peptides, indicating possible differences in downstream signaling mechanics among the different peptides.

Receptor mutants confer resistance to different CLE peptides

CLV3 signal at the shoot apex is transduced by a suite of receptor-like kinase complexes, which include CLV1, BAMs, and potentially CLV2-CRN. To begin to understand how CLE16 and CLE17 affect stem cell signal transduction at the SAM, we determined whether CLE16/17 could interact with the same receptors that CLV3 does by performing peptide treatment assays as described above using the *clv1-11*, *clv2-3*, and *bam1-4 bam2-4 bam3-2* loss-of-function receptor mutants. Because synthetic CLE16 and CLE17 peptides only effectively restricted stem cell activity in the absence of endogenous CLV3, we also included *clv1 clv3*, *clv2 clv3*, and *bam1/2/3 clv3* plants in the analysis, alongside Col-0 and *clv3* plants as controls.

Our quantification of 5 DAG seedlings grown on peptide plates showed that treatment with synthetic CLV3 significantly reduced the shoot meristem size of *clv1* plants compared to those grown on mock-treated plates. In contrast CLE16 and CLE17 treatment had no effect on *clv1* SAMs, most likely due to endogenous CLV3 activity (Fig. 3.5a, i). On the other hand, *clv1 clv3* SAMs were effectively restricted when grown on either CLV3, CLE16, or CLE17-treated agar compared to the mock treatment, indicating that all three peptides were still able to restrict stem cell accumulation without CLV1. For the most part, *clv1 clv3* SAMs grown on CLE16 or CLE17 plates were not significantly different from those grown on CLV3 plates (height: CLE16-CLV3 P = 0.07, CLE17-CLV3 P = 1.00, diameter: CLE16-CLV3 P = 0.01, CLE17-CLV3 P = 0.67, Fig. 3.5b, j), suggesting that CLV1 receptor activity is responsible for most of the observed gap in biological efficacy between CLV3 and CLE16/17.

Similarly to *clv1* SAMs, *bam1/2/3* SAMs were also restricted by exogenous CLV3 application, but were resistant to CLE16 and CLE17 application (Fig. 3.5c, m). CLV3 treatment was also able to significantly reduce SAM size of *bam1/2/3 clv3* quadruple mutants. In contrast, *bam1/2/3 clv3* SAMs were unaffected when grown on CLE16 and CLE17 peptide plates (height: CLE16-Mock P = 0.34, CLE17-Mock P= 0.97; diameter: CLE16-Mock P = 0.95, CLE17-Mock P= 0.84; Fig. 3.5f, n). These results suggest that while the BAM receptors are dispensable for CLV3 signaling, they are required to transmit CLE16 and CLE17 signals.

Interestingly, *clv2* SAMs were minimally affected by CLV3 peptide treatment (height: P = 0.18, diameter: P = 0.01, Fig. 3.5c, k), suggesting that either CLV2 is required to sense the synthetic CLV3 peptide, or CLV2 controls stem cell accumulation independently of CLV3 signaling. However, *clv2 clv3* SAMs were clearly susceptible to the meristem-restricting effect of synthetic CLV3, CLE16 and CLE17 peptides (Fig. 3.5d, l). CLV2 therefore appears to be dispensable for the full signal transduction of the CLV3, CLE16, CLE17 peptides. In addition, whereas *clv1 clv3* SAMs were very similar in size to those of *clv3* SAMs (height: P = 0.99; diameter: P = 0.02, Fig. 3.5h, j), *clv2 clv3* SAM size was significantly enhanced compared to *clv3* SAM size (height: $P < 10^{-4}$, diameter: $P < 10^{-4}$, Fig. 3.5h, l). This observation indicates that CLV2 can control meristem size independently of CLV3 signaling. Unlike the other genotypes examined, all of which exhibited a similar response to CLE16 and CLE17 peptide treatments, *clv2 clv3* SAMs were more effectively restricted by CLE17 compared to CLE16 (height: P = 0.05, diameter: $P < 10^{-8}$, Fig. 3.5d, l). Indeed, CLE17 was as effective as CLV3 in reducing SAM size in *clv2 clv3* plants (height: P = 0.17, diameter: P = 0.75, Fig. 3.5d, l) Thus, CLV2 might play a role in monitoring stem cell response towards these two CLE peptides during vegetative development, either by increasing sensitivity towards CLE16, or more likely, by dampening sensitivity towards CLE17.

Figure 3.5. Receptor kinase genes respond differentially to CLE16, CLE17 and CLV3 synthetic peptide treatments. Confocal micrographs (a-f) and vegetative meristem size measurements (g-n) of 5 DAG Col-0 (g), *clv3* (h), *clv1* (a and i), *clv1 clv3* (b and j), *clv2* (c and k), *clv2 clv3* (d and l), *bam1 bam2 bam3* (e and m), *bam1 bam2 bam3 clv3* (f and n) plants grown on MS plates containing a mock solution or 30 μM of synthetic CLV3, CLE16, or CLE17 peptide (n = 14 to 29). For the box plots, the bottom and top of the boxes represent the twenty-fifth and

seventy-fifth percentile, respectively; the whiskers represent the minimum and maximum values; and the middle line is the median. Statistical analysis was performed using one-way ANOVA and Tukey test; letters represent different significance groups at $P < 0.05$ and joint-letters indicate a group that shares $P < 0.05$ with two other groups. Scale bars: 25 µm.

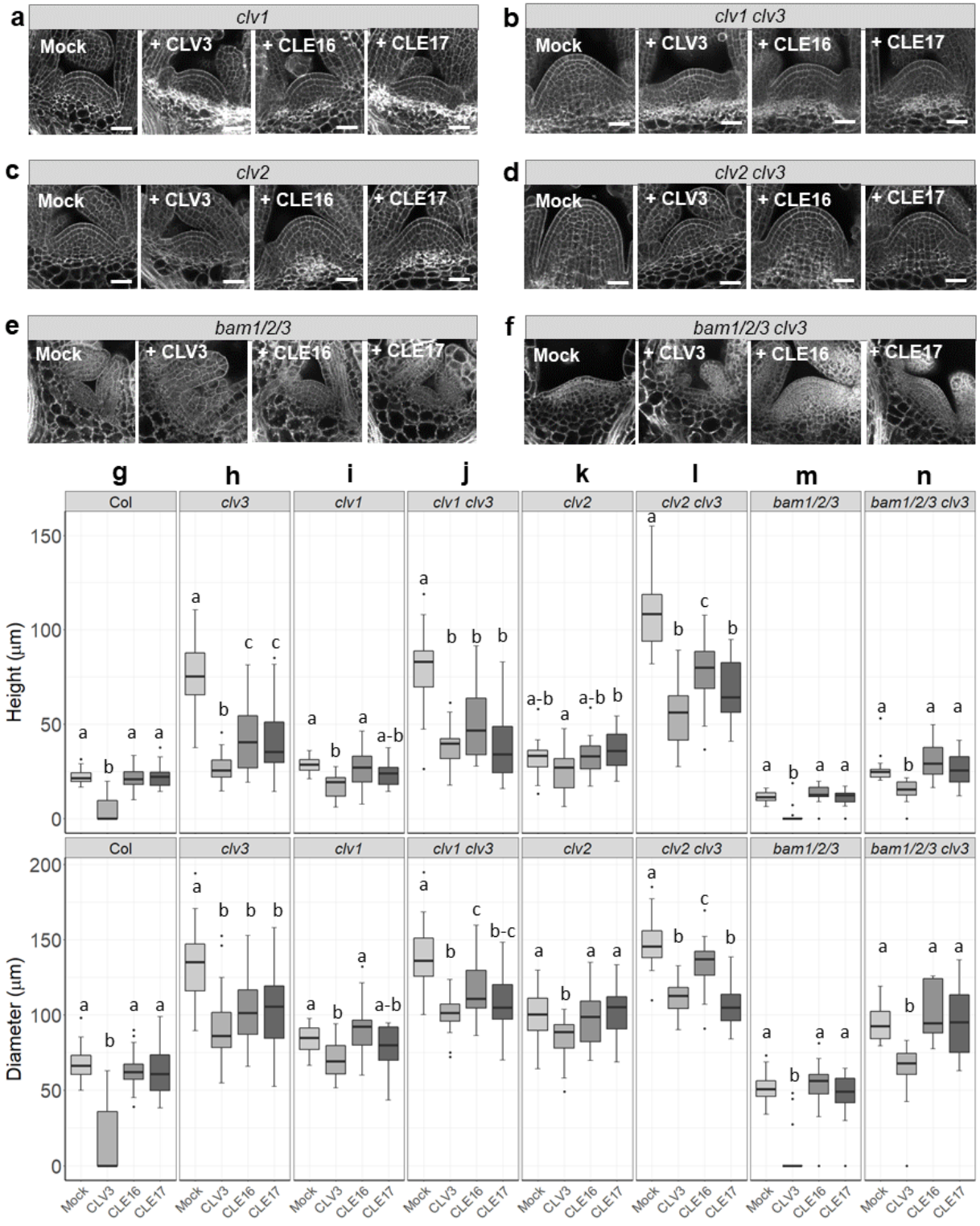

CLE16 and CLE17 signal upstream of WUS as well as a novel pathway

While there might be differences in the suite of receptors that CLV3, CLE16 and CLE17 interact with, our current understanding of CLV1 and BAMs suggest that these receptors mainly target the WUS transcription factor in the SAM. Therefore, we ask whether CLE16 and CLE17 also signal upstream of WUS, or in a different genetic pathway, by crossing our *cle16 cle17*, *clv3*, *clv3 cle16*, *clv3 cle17*, and *clv3 cle16 cle17* plants into the null *wus-1* mutant in the Col-0 background. The loss of WUS function leads to a deficiency in shoot meristem maintenance but not initiation. As a result, homozygous *wus* SAMs typically produce a few rosette leaves during vegetative growth and then prematurely arrest. In some cases, axillary meristems (AMs) arise from the existing rosette leaves and are sustained long enough to undergo the transition to flowering, producing a limited number of floral meristems before prematurely terminating (Fig. 3.6a) (Laux et al., 1996). We therefore used the frequency of AM bolting as a proxy for meristem activity and maintenance in *wus* plants. All mutant populations segregating for the *wus-1* allele displayed a 3:1 ratio of wild type to meristem-deficient phenotypes, with reduced rosette leaf numbers, and SAM termination. Among individuals that displayed initial meristem defects, 17-44% of *wus* and *wus cle16 cle17* lines produced one or two AMs at 42 days after germination (DAG). *wus cle16 cle17* plants were phenotypically indistinguishable from *wus*, indicating that CLV3 was still fully redundant to CLE16 and CLE17 in this context (Fig. 3.6a, b, Fig. S3.4a, b). It's important to note that the genetic background of *wus-1* plants used for crossing contained an *erecta* (*er*) mutation that was retained in the *wus cle16 cle17* line but was lost in the other crosses. The ER pathway controls SAM size independently of WUS, and *er* plants show greater SAM cell accumulation than wild type plants. As a result, it is likely that the *er* allele contributed to increased meristem activity in our *wus* and *wus cle16 cle17* backgrounds, but not in the other lines.

At 42 DAG, *wus clv3, wus clv3 cle16*, *wus clv3 cle17,* and *wus clv3 cle16 cle17* plants all lacked a primary shoot, demonstrating early developmental arrest of the vegetative SAM (Fig. 3.6c-f, Fig. S3.4c-f). Thus, WUS functions downstream of both CLE16 and CLE17 in SAM maintenance. However, we observed a difference in AM development among these phenotypes. Among homozygous *wus clv3* plants, axillary branches formed in only 1 out of 15 individuals in the first growth trial, and none out of 17 in the second trial. Therefore, consistent with previous studies, the null *wus* allele is fully epistatic to *clv3* under our growth conditions. *wus clv3 cle16* plants exhibited a similar phenotype to *wus clv3* plants, and never produced observable axillary stems in either trial. However, an increase in AM initiation frequency was observed in *wus clv3 cle17* individuals, with 40% of the homozygotes forming up to three AMs per plant in the first biological replicate and 8% in the second replicate. *CLE17* thus appears to be able to regulate stem cell activity in the absence of both CLV3 and WUS function. A more stable enhancement of stem cell activity was observed in *wus clv3 cle16 cle17* plants, approximately 25% of which were able to produce axillary branches in both biological replicates. In addition, around half of the rescued plants produced more than three axillary shoots per individual, more so than *wus clv3 cle17* ($P = 0.007$, Fig. 3.6e, f, g, Fig. S3.4e, f). The increased meristem activity in *wus clv3 cle16 cle17* plants suggests a novel role for CLV3, CLE16, and CLE17 in regulating stem cell activity at the AM that is independent of WUS. The lack of visible axillary shoots in *wus clv3* and *wus clv3 cle16* plants indicates a different level of redundancy among these CLE peptides from what was previously observed. In the SAM, *CLE16* and *CLE17* each partially compensates for the loss of *CLV3* activity. Whereas in the AM, *CLV3* and *CLE17* might be fully redundant to each other, and CLE16 can only compensate in the loss of both.

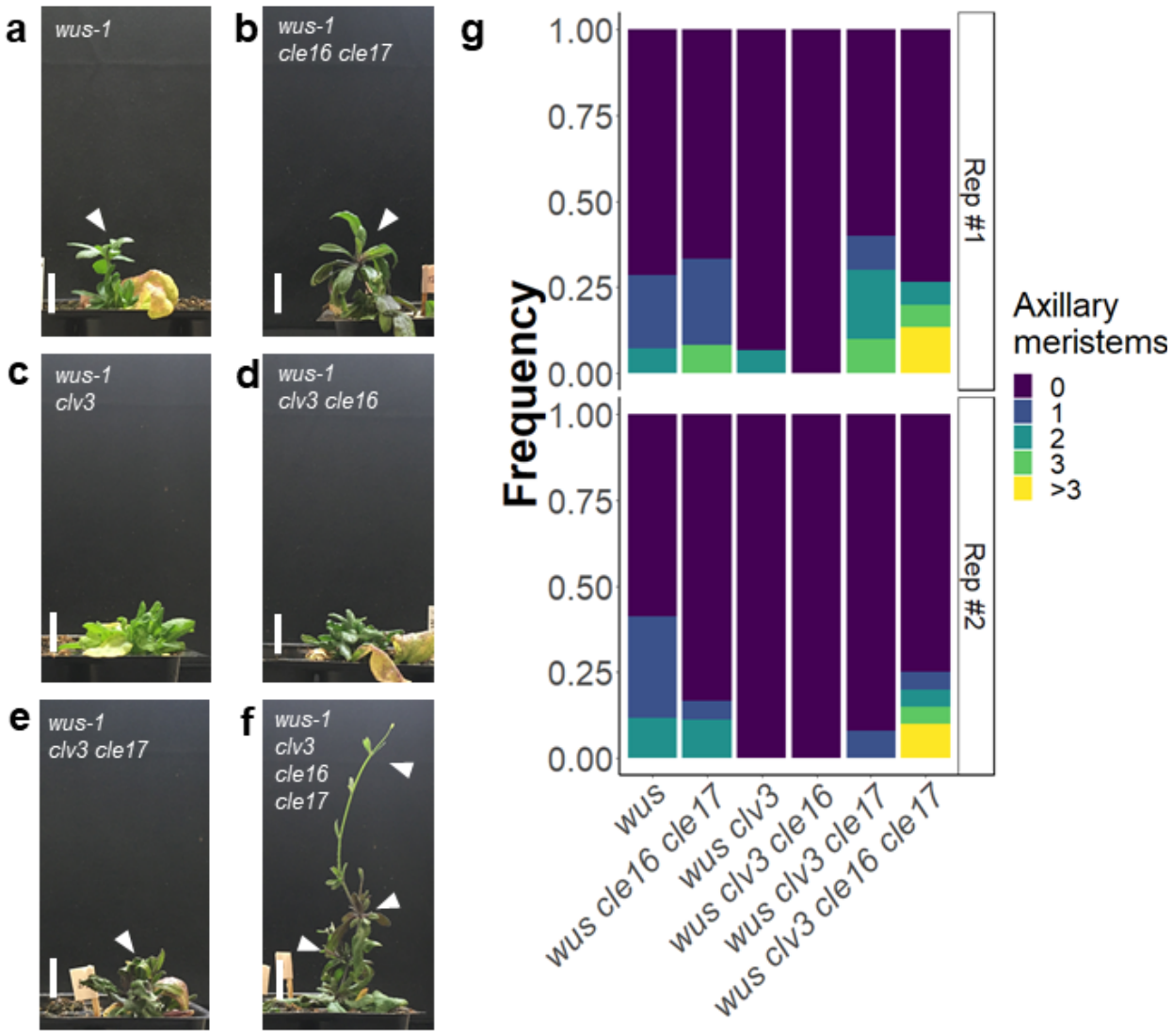

Figure 3.6. Genetic interactions between *CLE16* and *CLE17* signaling pathways and the *WUS* stem cell promoting gene. a-f, Side view of *wus-1* (a), *wus cle16 cle17* (b), *wus clv3* (c), *wus clv3 cle16* (d), *wus clv3 cle17* (e), and *wus clv3 cle16 cle17* (f) plants. White arrowhead, axillary meristem. (g) Quantification of meristematic activity as the frequency of individuals with 0, 1, 2, 3, or more axillary meristems, in 42 DAG *wus-1*, *wus cle16 cle17, wus clv3, wus clv3 cle16, wus clv3 cle17,* and *wus clv3 cle16 cle17* plants in two biological replicates (Rep #1: n = 12 to 20; Rep #2: n = 14 to 25). Scale bar: 2 cm.

An alternative explanation is that the increase in axillary shoot numbers in higher order mutants is tied to the increased size or maintenance of the transient SAM. In this case, the stem cell enhancement effect from either the *clv3* or *clv3 cle16* allelic combination is not sufficient to maintain the SAM long enough to initiate AMs at the flank. This is consistent with our previous observation that *clv3 cle17* IFMs are bigger than those of *clv3* or *clv3 cle16*.

To further dissect the role of *CLE16* and *CLE17* signaling in AM formation versus SAM maintenance, we examined their interaction with the *SHOOT MERISTEMLESS* (*STM*) gene, which

encodes a homeodomain transcription factor of the KNOTTED class (Long et al., 1996). STM functions to maintain stem cell competency and suppress differentiation at the shoot apex independently of WUS (Clark et al., 1996; Lenhard et al., 2002). *stm* mutant phenotypes range from a complete loss of shoot meristem and failure to produce true leaves in seedlings, to growth arrest after initial vegetative shoot development. Plants that lack both functional *WUS* and *STM* are completely embryo lethal. Despite functioning in separable genetic pathways, *WU*S and *STM* can indirectly reinforce each other through the phytohormone cytokinin, and are necessary to sustain each other's expression in seedling (Lenhard et al., 2002; Scofield et al., 2014). During AM development, *STM* is upregulated at the leaf axil to induce cytokinin signaling, and thus indirectly activates WUS expression to establish the AM stem cell niche. As the CLV3 peptide does not signal through STM, *clv3* alleles act antagonistically towards *stm* alleles, partially but not completely restoring shoot and floral meristem activity to *stm* plants (Clark et al., 1996). To investigate whether CLE16 and/or CLE17 signal through STM, we combined our *clv3, cle16* and *cle17* alleles with the loss-of-function *stm-11* allele, and analyzed AM development phenotype as described above.

We observed that all lines segregating for the *stm-11* allele displayed a 3:1 ratio of phenotypically wild-type to shoot meristem deficient mutants, indicating that none of the *cle* alleles are epistatic to *stm* (Fig. 3.6, Fig. S3.5). We followed up our analysis by further examining plants that were homozygous for *stm-11*. Under our growth conditions, 31-44% *stm* plants produced one or two visible AMs across two trials at 42 DAG. The frequency of AM development was increased in *stm cle16 cle17* plants, where 62-72% of individuals produced up to four shoots (Fig. 3.7a, b, g, Fig. S3.5a, b). The enhancement of shoot meristem initiation in *stm cle16 cle17* compared to *stm* plants provided the only instance where the *cle16* and *cle17* alleles produced a phenotype even in the presence of endogenous CLV3 activity. Given our previous observation that *cle16 cle17* SAMs are indistinguishable from those of the WT (Fig. 2), the increased AM activity in *stm cle16 cle17* plants likely arises from a specific role of CLE16 and CLE17 in AM development and not SAM maintenance. It is important to note that the loss of apical dominance in *stm* mutants can stimulate axillary bud outgrowth, and our assay method did not distinguish between *de novo* AM formation and extended development of existing AMs. Nevertheless, our observations suggest a role for CLE16 and CLE17 in controlling stem cell activity in AMs that is independent of both CLV3 and STM.

Meristem activity was also enhanced in *stm clv3, stm clv3 cle16,* and *stm clv3 cle17* plants, all of which developed AM outgrowths that are able to produce flowers (Fig. 3.7c-g, Fig. S3.5c-f). Flowers of these plants however exhibit a premature termination phenotype, often forming no recognizable carpels (data not shown). Thus, while loss of CLV3, CLE16, and CLE17 signaling enhance stem cell accumulation via increased *WUS* expression, *STM* is still required to properly maintain stem cell fate. It should be noted that our experimental setup did not allow for distinguishing stem cell activity at the SAM from that at the AM, due to WUS function being intact. On the one hand, increased WUS activity in the loss of CLE signaling can enhance the cytokinin response that allows for more AM initiation on the flank of an enlarged SAM. On the other, the apical dominant effect from a hyperactive SAM can inhibit AM outgrowth, making estimation of AM activity from the quantification of visible axillary shoots alone unreliable. This is evident in the stm clv3 cle16 cle17, which produced massive fasciated shoots that could not be accurately counted (Fig. 6c-vi, d, Fig. S8). Nevertheless, our data indicates that, like CLV3, CLE16 and CLE17 signal through a genetic pathway that is independent of STM.

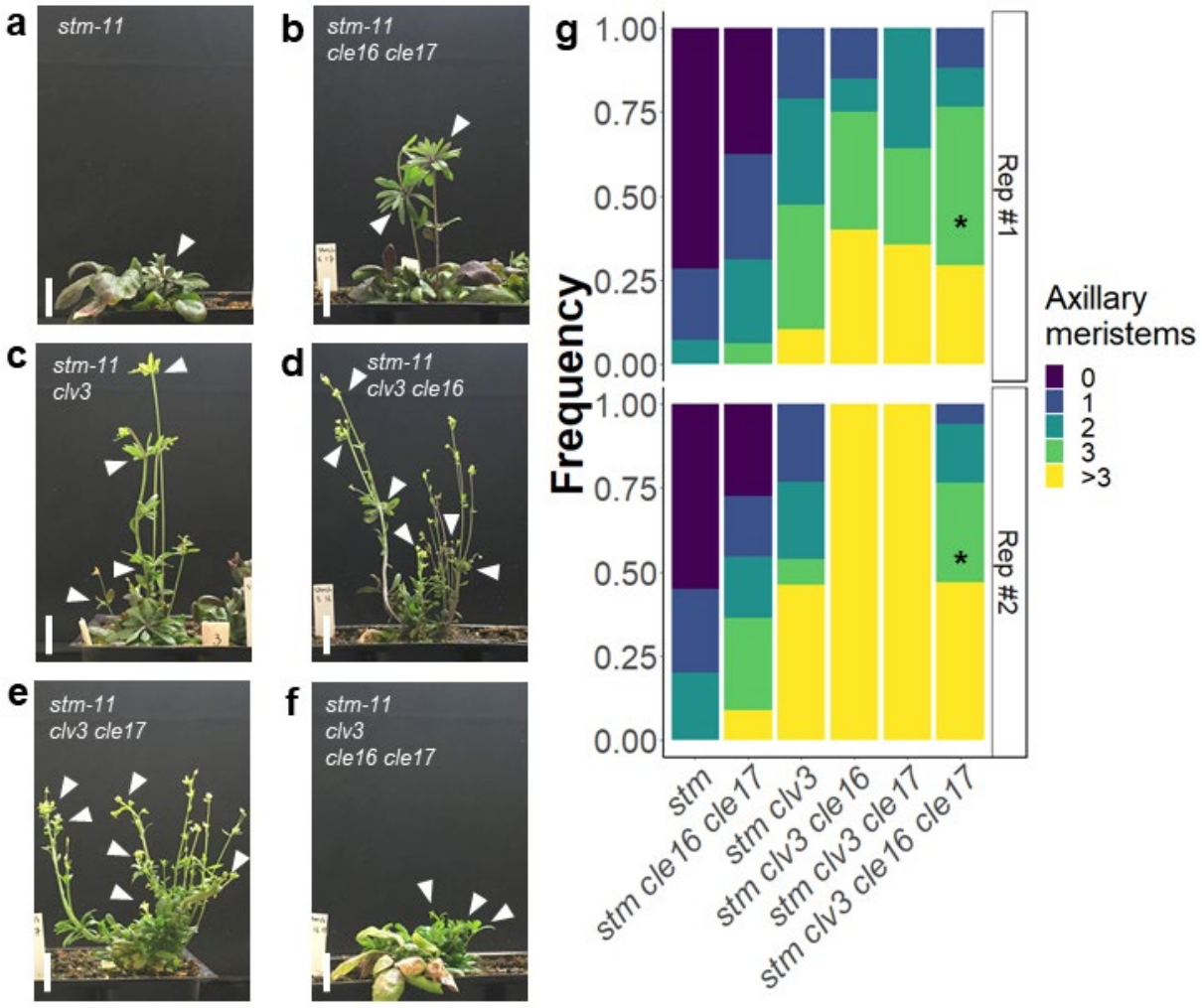

Figure 3.7. Genetic interactions between *CLE16* and *CLE17* signaling pathways and the *STM* stem cell promoting gene. (a-f) Side view of *stm-11* (a)*, stm cle16 cle17* (b)*, stm clv3* (c), *stm clv3 cle16* (d), *stm clv3 cle17* (e), *stm clv3 cle16 cle17* (f) plants. White arrowhead, axillary meristem. (d) Quantification of meristematic activity as the frequency of individuals with 0, 1, 2, 3, or more axillary meristems, in 42 DAG *stm-11, stm cle16 cle17, stm clv3, stm clv3 cle16, stm clv3 cle17,* and *stm clv3 cle16 cle17* plants in two biological replicates (Rep #1: n = 14 to 20; Rep #2: n = 14 to 22). Asterisk denotes lack of accuracy in determining the number of axillary meristems in *stm clv3 cle16 cle17* plants due to the high degree of stem fasciation. Scale bar: 2 cm.

Discussion

Each plant stem cell niche requires molecular signals from neighboring cells in order to maintain homeostasis and continuously supply new cells for growth and organogenesis. CLE peptide signaling plays an integral role in controlling shoot stem cell accumulation in multiple model species such as maize and tomato, with direct consequences for plant development and productivity (Fletcher et al., 1999; Je et al., 2017; Rodriguez-Leal et al., 2019). In this study, we

identified the role of two CLE peptides, CLE16 and CLE17, in buffering stem cell homeostasis at the shoot apex in the absence of CLV3 signaling activity. Following up, we dissected the downstream signaling pathway of CLE16 and CLE17 to examine their interactions with known receptors in the SAM, as well as their target transcription factor targets that regulate stem cell activity in the SAM and AM.

Both CLE16 and CLE17 are expressed in the shoot apex, making them likely candidates for SAM regulation (Jun et al., 2010). Whereas CLE16 and CLE17 were previously reported to be dispensable for maintaining SAM function on their own (Gregory et al., 2018), our analysis reveals that in null *clv3* mutants, both peptides play an important role in limiting shoot stem cell accumulation beginning at the embryonic stage and continuing throughout the entire life cycle. In addition, the *cle16* and *cle17* null alleles appear to have cumulative effects on the *clv3* mutant background, suggesting CLE16 and CLE17 signal independently of each other in vegetative, inflorescence, and floral meristems.

Chemical genetic analysis reveals that CLE16/17 signaling in the SAM is blocked at the post-translational level by endogenous CLV3 activity, as treatment with synthetic CLE16 or CLE17 peptides did not alter shoot meristem activity in wild type or *cle16 cle17* plants, yet effectively restricted stem cell accumulation in *clv3* mutants. One possible explanation is that neither CLE16 nor CLE17 can compete with the binding of CLV3 to receptor kinases that are present in the shoot apical meristem. Another possibility is that CLV3 signaling prevents the biological activity of CLE16/17's cognate receptors in the SAM. Reciprocal feedback among receptor kinases at the shoot apex has been previously reported. For example, CLV3-CLV1 interaction limits the expression domains of the BAM1/2/3 receptors to the flank of the SAM (Nimchuk et al., 2017). The BAM proteins, in turn, prevent CLV3 signaling in the peripheral zone through an unknown mechanism, thus maintaining the appropriate expression domain for *WUS* (DeYoung et al., 2008). Our peptide assay indicates that the BAM receptors, but not CLV1, are required to transmit CLE16/17 signal in the SAM. Previous ligand competition assays have demonstrated a higher degree of specificity in CLE binding by CLV1 and CLV2 compared to BAMs (Guo et al., 2011).

Together, our results support a model in which CLV1 is a specific receptor for CLV3, while the BAM proteins act as receptors for CLV3, CLE16 and CLE17 (Fig 3.8). In the presence of endogenous CLV3 peptide, downstream signaling via CLV1 prevents the interactions among the BAM receptors and their cognate ligands from affecting stem cell activity in the SAM. In the absence of CLV3 signal, the expression domains of the *BAM* genes extend into the central zone of the shoot apex, where both CLV1 and the BAM receptors are able to interact with other CLE ligands (Fig. 3.8). This model might explain our observation that CLV3 synthetic peptide is more effective than either CLE16 or CLE17 peptide at restricting stem cell accumulation in *clv3* plants, as CLV3 is able to interact with both CLV1 and the BAM proteins, while CLE16 and CLE17 can only signal through the BAM receptors. A similar CLE signaling module has been observed in maize SAM, where the transmembrane protein FASCIATED EAR3 (ZmFEA3) serves as receptor for the CLE peptide encoded by *FON2-LIKE CLE PROTEIN1* (*ZmFCP1*), whereas ZmFEA2, an ortholog of CLV2, can respond to both ZmFCP1 and ZmCLE7 (Je et al., 2018). In tomato, the CLE peptides SlCLV3 and SlCLE9 buffer stem cell homeostasis by signaling through the SlCLV1 receptor kinase, and likely other receptors as well (Rodriguez-Leal et al., 2019). Observations in the moss *Physcomitrella patens* also suggest that multiple CLE peptides may control apical cell activity in leafy shoots via the partially redundant receptors PpCLV1a/b and PpRPK2

(Whitewoods et al., 2018). Redundancy and compensation among CLE peptides and their cognate receptors therefore appears to be a common feature throughout the land plant lineage.

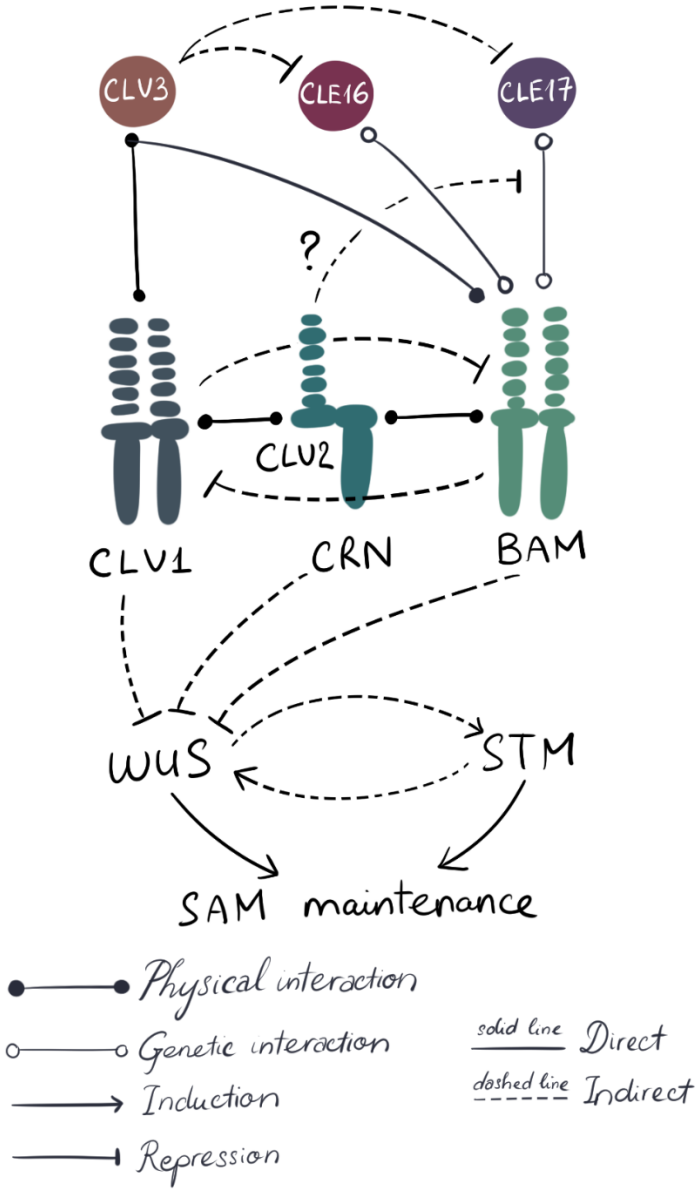

Figure 3.8. Model of CLV3, CLE16, and CLE17 signaling in the SAM. CLV3 can physically interact with the CLV1 and BAM receptor kinases. CLV3 signaling through CLV1 excludes *BAM* gene expression from the central region of the SAM, whereas BAM receptor kinase activity blocks CLV3-CLV1 signaling from the peripheral region. The CLV2-CRN complex can interact with CLV1 and the BAM proteins to fine-tune their activity. CLE16 and CLE17 can physically interact with the BAMs, but are blocked by CLV3 activity. CLE signaling through CLV1 and/or BAMs restrict the *WUS* expression domain to regulate stem cell homeostasis in the SAM. CLE16 and CLE17 also signal through an undefined pathway to affect AM initiation and/or AM maintenance.

Further experimentation will be required to test this model. For instance, peptide binding assays are needed to verify any differences in binding specificity of the CLV1, CLV2, and BAM receptors towards the CLE16 and CLE17 peptides. The amino acid sequences of the mature CLE16 and CLE17 peptides each differ in four residues from that of CLV3 (Fig. 3.1), and two of these residues were previously demonstrated to be important for CLV3 activity *in planta* (Song et al., 2012; Song et al., 2013). It will be interesting to see whether substituting any of these residues in CLE16 and CLE17 is sufficient to allow them to acquire the same biological function and binding affinity as CLV3. It is also tempting to speculate that the binding of CLE16 and CLE17 to the BAM receptors prevents CLV3 signaling in the peripheral zone. However, this hypothesis remains to be examined, as *cle16 cle17* plants are indistinguishable from the wild type. It's likely that yet other CLE peptides function redundantly with CLE16 and CLE17 to bind BAMs and regulate shoot stem cell activity. Furthermore, a domain swapping experiment, where *CLE16/17* coding sequence is expressed under native *CLV3* promoter and vice versa, can determine whether the spatiotemporal expression pattern of these genes contribute to their differential ability to regulate SAM stem cells.

CLV2 is implicated in various developmental processes in *planta*, and its function in the SAM requires interaction with other signaling components including CRN, CLV1, and the BAM receptors (Bleckmann et al., 2010; Zhu et al., 2010). Although CLV2 has not been shown to bind the arabinosylated 13-amino-acid CLV3 peptide, it is capable of binding the non-arabinosylated 12-amino-acid CLV3 peptide form, as well as other CLE peptides with varying affinities (Guo et al., 2010; Shinohara and Matsubayashi, 2014). However, our phenotypic analysis shows that clv2 clv3 mutant SAMs can still be restricted by treatment with the 12-amino-acid CLV3, CLE16, or CLE17 peptide. Thus, CLV2 does not seem to be required for the full sensing of these peptides during vegetative development. Instead, we speculate that CLV2 plays a part in fine-tuning the meristem response to different CLE peptides in the absence of CLV3 activity. Specifically, CLV2 may dampen the stem cell restricting effect of CLE17 but not CLE16, perhaps by forming complexes with the BAM receptors and preventing them from binding to CLE17. Indeed, we observed a difference in biological activity between CLE16 and CLE17 during the reproductive phase, as both IFM size and carpel production phenotypes were stronger in *clv3 cle17* than in *clv3 cle16* plants. CLE17 thus may make a greater contribution to stem cell regulation than CLE16 during reproductive development, possibly due to differences in their respective downstream signal transduction pathways. CLV2 is involved in both CLE14, CLE25 and CLE45 signaling in the root, and whether it is also involved in the perception of other CLE peptides than CLV3, CLE16, and CLE17 in the SAM remains to be determined (Gutiérrez-Alanís et al., 2017; Hazak et al., 2017; Ren et al., 2019). Given the ability of CLV2 to form multimeric complexes with other receptor kinases in the SAM, it could be an important factor in determining with which particular suite of CLE ligands a given complex can interact.

Aside from CLV3 and CLE16/17, it is highly likely that other CLE signals are perceived by CLV1, CLV2, and/or the BAM receptors. *CLE16* and *CLE17* were not among the genes knocked out in the *dodeca-cle* background, and both our *clv3 cle16 cle17* plants and the *dodeca-cle* lines seem to display weaker meristem phenotypes than those of *clv1 bam1/2/3* plants, which showed severe defects in shoot architecture and flower development (Rodriguez-Leal et al., 2019). Similarly, other receptor-like kinases, such as RECEPTOR-LIKE PROTEIN KINASE2 (RPK2), and CLE-RESISTANT RECEPTOR KINASE (CLERK), are also active within the SAM but remain to be studied with respect to CLE16 and CLE17 signaling. Both RPK2 and CLERK play a role in transmitting CLE peptide signal in the roots, although their roles in the shoot are less clear

(Kinoshita et al., 2010; Shimizu et al., 2015; Anne et al., 2018). It will therefore be informative to define a complete list of biologically relevant CLE peptides in the SAM and their interacting partners for further biochemical analysis.

The major downstream target of the CLV signaling pathway at the shoot apex is the mobile transcription factor WUS, which promotes stem cell identity and suppresses differentiation at the central region of the SAM (Mayer et al., 1998). WUS travels from the OC to the CZ where it directly activates *CLV3* transcription, and CLV3 signaling in turn excludes *WUS* expression from the CZ (Daum et al., 2014). As a result, the CLV-WUS feedback loop maintains a small but stable stem cell niche at the shoot apex (Brand et al., 2000; Schoof et al., 2000). Our examination of the *wus* mutant lines indicates that WUS is the main target of CLE16 and CLE17 in the SAM, similar to CLV3. However, WUS activity alone is not sufficient for normal shoot development. Function of the KNOTTED class transcription factor *STM* suppresses the differentiation program in a separate pathway from *WUS*, and is necessary for proper SAM maintenance, as well as initiation of axillary stem cell populations at the flank of the SAM (Lenhard et al., 2002). In particular, de novo formation of the AM requires an upregulation of *STM*, which leads to an increase in cytokinin level, and subsequent activation of *WUS* expression (Shi et al., 2016; Wang et al., 2017).

Our phenotypic analysis indicates that CLE16/17 function upstream of WUS to mediate SAM stem cell accumulation in a similar manner to CLV3, as *wus clv3 cle16 cle17* plants could not sustain primary SAM growth. If CLE16 and CLE17 fulfill the same role as CLV3 in the SAM, it is likely that they do not signal upstream of STM, though more detailed analysis of SAM activity is needed to test this hypothesis. Furthermore, we discovered a novel aspect of CLE signaling, in which CLE16 and CLE17 are involved in AM development independently of both WUS and STM activity. Loss of CLV3, CLE16, and CLE17 signaling was sufficient to increase axillary shoot numbers in *wus* and *stm* mutants. Unlike their activity in the SAM, the role of CLE16 and CLE17 in AM development might be independent of CLV3 signaling, as *stm cle16 cle17* plants also formed more axillary branches than *stm* plants. One possibility is that CLE16 and CLE17 expression might precede the formation of the CLV3-WUS module during de novo AM formation. It will therefore be of interest to compare *CLE16* and *CLE17* expression dynamics to those of *CLV3*, *WUS*, *STM* and other AM markers such as *ARR1* during AM initiation.

Aside from STM, several other factors are involved in patterning at the incipient AM, such as members of the HAIRY MERISTEM family of GRAS-domain transcription factors, which act as a co-factors of WUS and are required to confine CLV3 to the apical region of the SAM and AM (Zhou et al., 2018). HAM proteins themselves are patterned in a gradient from the epidermis towards the inner layers of the incipient AM by activity of the epidermal factor ARABIDOPSIS THALIANA MERISTEM LAYER 1 (ATML1) (Han et al., 2020). A recent study also uncovered the role of the TALE-class transcription factor ARABIDOPSIS THALIANA HOMEOBOX GENE1 (ATH1) in inducing high STM transcript level leading up to AM formation (Cao et al., 2020). Thus the HAM proteins or ATH1 might serve as potential downstream elements that can receive input from a variety of CLE signals. Since AM development also depends on the balance between auxin and cytokinin response, it will be interesting to see how CLE16/17 interact with the phytohormone signaling elements. In the moss *Physcomitrella patens*, disruption of the PpCLV1a/b or PpRPK2 receptor function impairs the transition from 2-D protonemal growth to 3-D gametophore development (Whitewoods et al., 2018). Thus, the involvement of CLE16 and CLE17 in AM development at least superficially resemble the ancestral role of CLE signaling in de novo organogenesis and shoot branching. Recent efforts to edit the tomato genome using

CRISPR/Cas9 has revealed the potential of modifying the cis-regulatory elements of SlCLV3 to create a continuum of quantitative traits. Understanding the signaling pathway of CLE16 and CLE17, how they contribute to shoot stem cell activity and inflorescence architecture, and how analogous systems might be present in other plant models can exponentially expands our repertoire of candidate targets for crop improvements.

Supporting Information

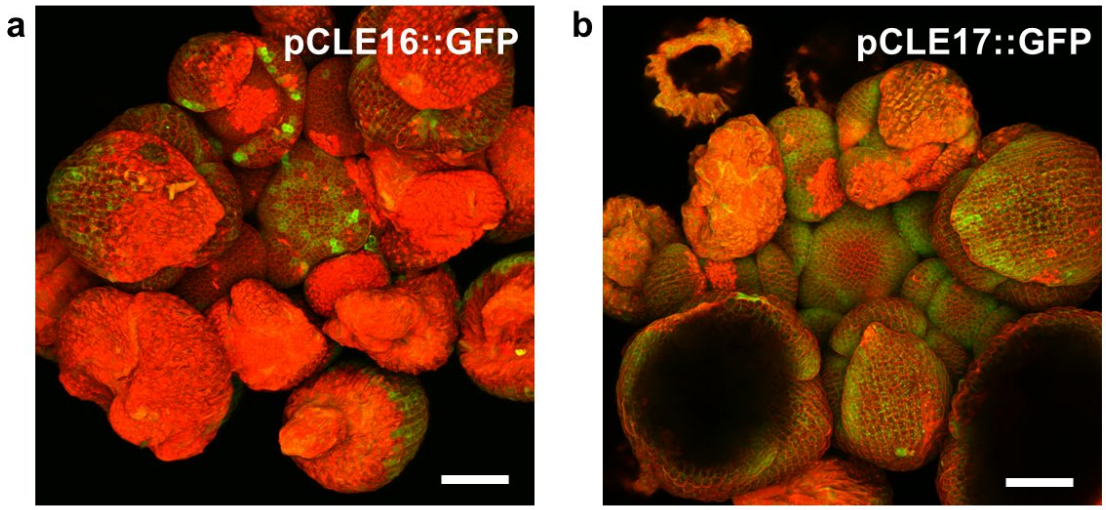

Supplemental Figure S3.1. CLE16 and CLE17 exhibit promoter activity in the SAM. g-h, Expression of pCLE16::*GUS-eGFP* (g) and pCLE17::*GUS-eGFP* (h) reporters in Col-0 inflorescence and floral meristems. Live meristems were stained with propidium iodide (red) to visualize cell walls, and eGFP fluorescence was false colored green. Scale bars: 100 μm in g, h.

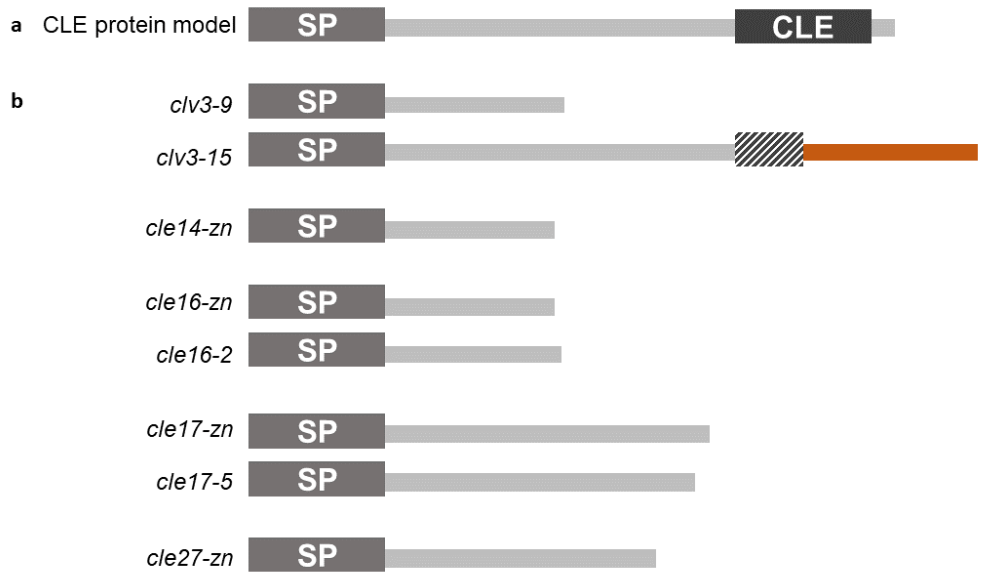

Figure S3.2. Graphical representations of mutant CLE proteins. a, Schematic of a generic CLE protein with an amino terminal signal peptide (SP), followed by a variable region and a 13 amino acid CLE domain. b, Schematics of mutant CLE pre-pro-peptides generated by the alleles used in this study. The *clv3-9* allele was generated using ethylmethanesulfonate (EMS), the *clv3-15* allele using TALEN, and the other alleles using CRISPR-Cas9 genome editing. All alleles except for *clv3-15* introduce a premature stop codon that eliminates the CLE domain. The *clv3-15* allele leads to deletion of half of the critical CLE domain and its replacement with 36 random amino acids.

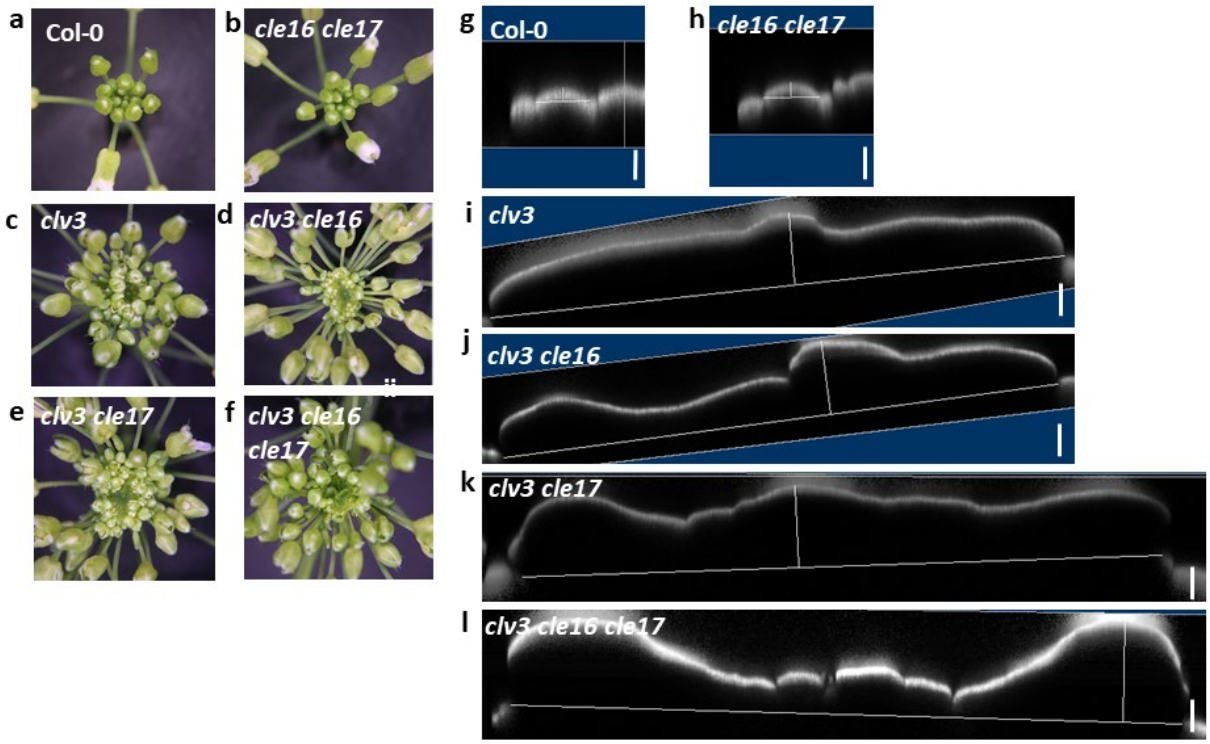

Supplemental Figure S3.3. *CLE16* and *CLE17* restrict stem cell accumulation in the inflorescence meristem in the absence of CLV3 activity. Representative top-down view of inflorescence (a-f), and a reconstructed longitudinal section of inflorescence meristem from confocal stacks (g-l) from wild-type (a), *cle16 cle17* (b), *clv3* (c), *clv3 cle16* (d), *clv3 cle17* (e), and *clv3 cle16 cle17* (e) plants (n = 8 to 16). Scale bars: 300 μm.

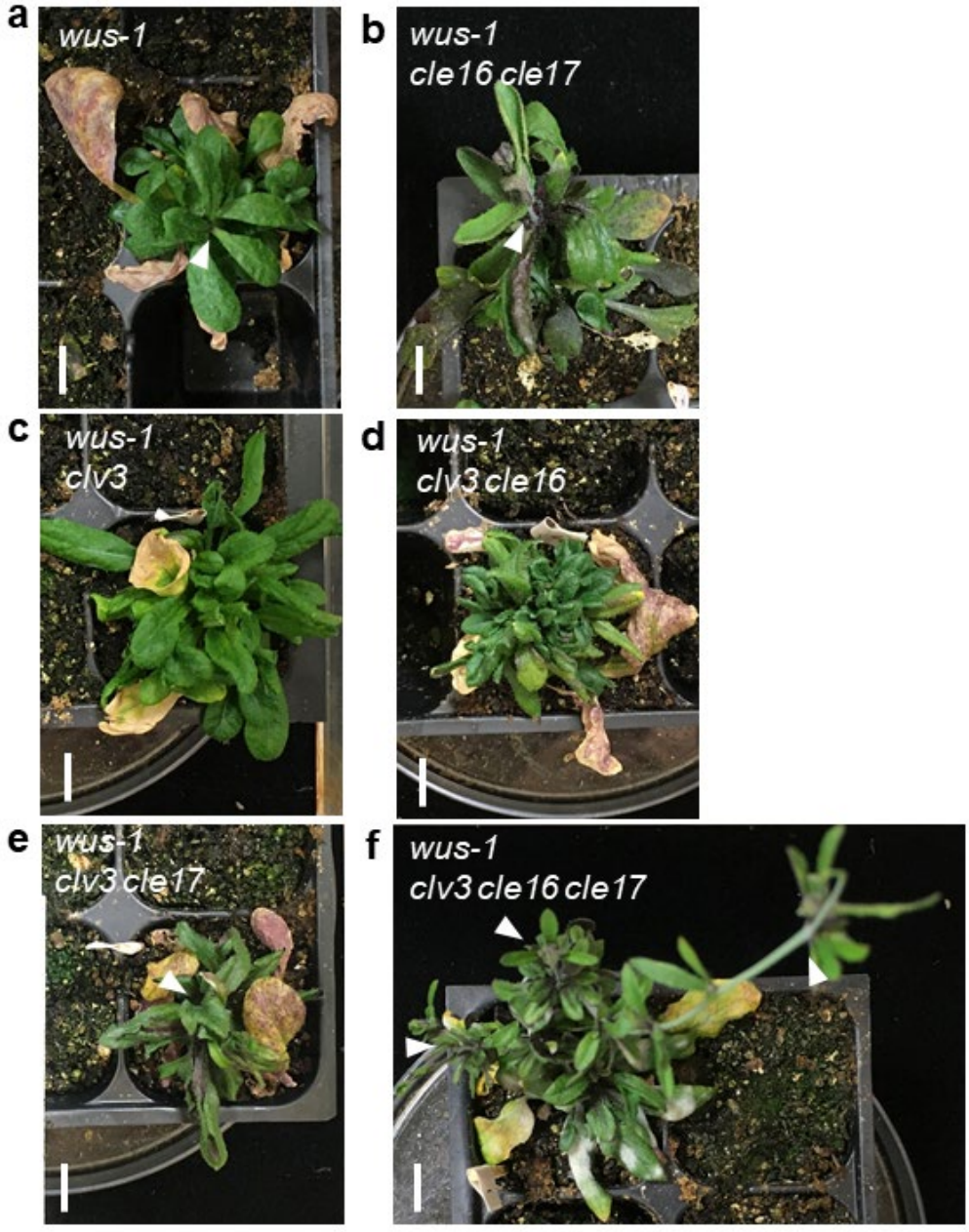

Supplemental Figure S3.4. *WUS* genetically interact with the *CLV3*, *CLE16*, and *CLE17* signaling pathways. Top-down view of 42 DAG *wus-1* (a), *wus cle16 cle17* (a), *wus clv3* (b), *wus clv3 cle16* (c), *wus clv3 cle17* (d), and *wus clv3 cle16 cle17* (e) plants. White arrowhead, axillary meristem. Scale bar: 1 cm.

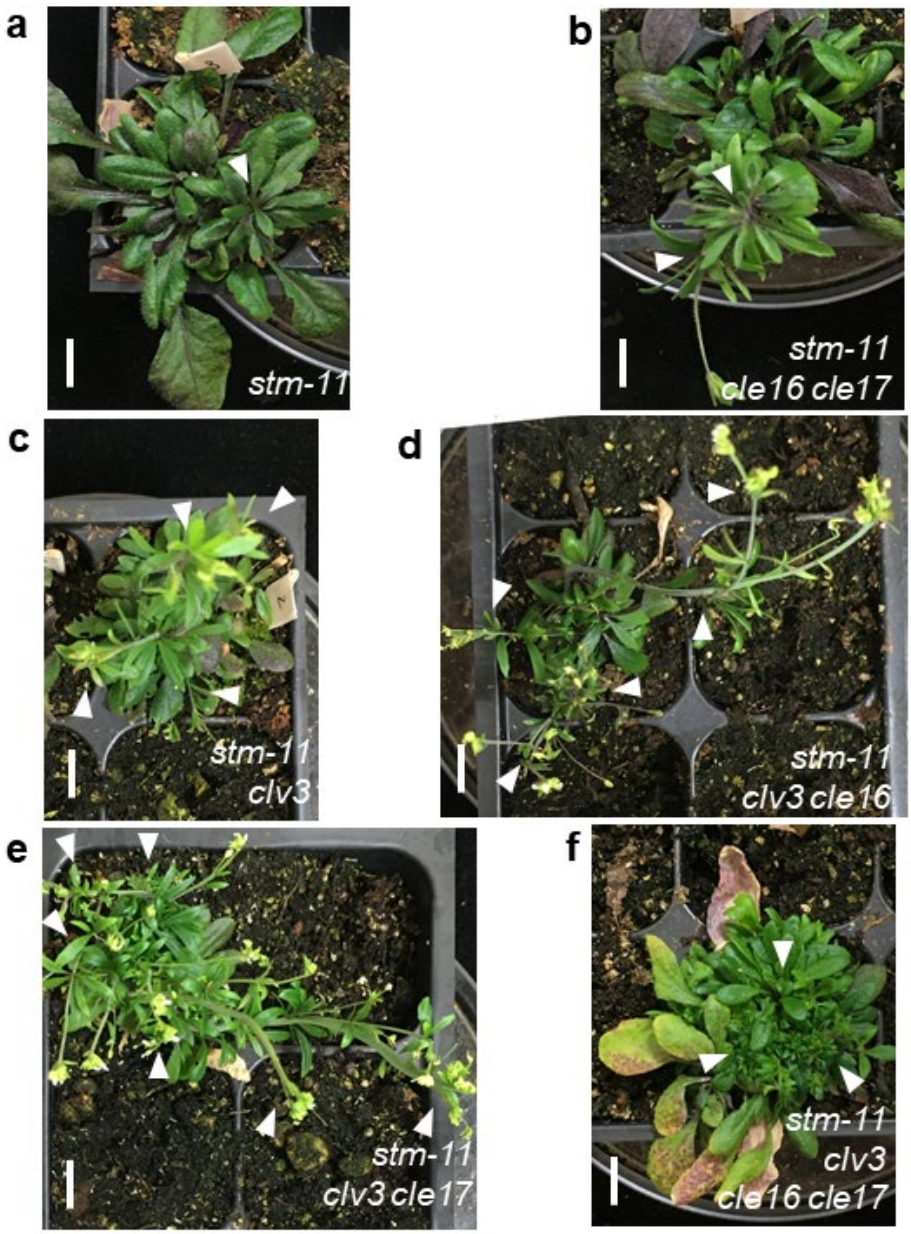

Supplemental Figure S3.5. *STM* genetically interact with the *CLV3*, *CLE16*, and *CLE17* signaling pathways. Top-down view of 42 DAG *stm-11* (a), *stm cle16 cle17* (a), *stm clv3* (b), *stm clv3 cle16* (c), *stm clv3 cle17* (d), and *stm clv3 cle16 cle17* (e) plants. White arrowhead, axillary meristem. Scale bar: 1 cm.

Table S3.1. List of primers used in this study.

Primer name	Sequence	Restriction enzyme
CLV3-F	ATGGATTCGAAGAGTTTTCTGCT	
CLV3-R	GACTCCCGAAATGGTAAAACCG	
CLE14-ZN-F	CATTCCTCTTCCGCCGGCCGCAAGCTCCCTAGTATGCCGA	BslI
CLE14-ZN-R	GGCGACAAAATGTAACTATAATAG	
CLE16-2-F	GAATCCAAAACCTGCTCTGC	MspI
CLE16-2-R	CGAAGGAGCAGTCAACACCT	
CLE16-ZN-F	CAAATCAAACAGCCATGGAAGCTTGTTCCAGAACCAGA	BslI
CLE16-ZN-R	CTTGGAGAGAGACCAGACAC	
CLE17-5-F	ACTCCTCCGGAACAAGGTTT	BslI
CLE17-5-R	CTTCTGCACGCACTTTCTCA	
CLE17-ZN-F	CGTGTTGGTACGAAGACAGGGACAAGGAAAGACCAGA	BslI
CLE17-ZN-R	CATCTCTGCTCAATGGCGCACGAAACGGTGC	
CLE27-ZN-F	ATGACTCATGCTCGAGAATGGAGAAG	ScaI
CLE27-ZN-R	CTAGTTATGCAAAGGATCCGGACAAC	

CHAPTER IV
CLE5 AND CLE6 SIGNALING IN LEAF DEVELOPMENT

The following content was published as:

Digennaro, P., Grienenberger, E., Dao, T.Q., Jun, J.H., and Fletcher, J.C. (2018). Peptide signaling molecules CLE5 and CLE6 affect Arabidopsis leaf shape downstream of leaf patterning transcription factors and auxin. Plant Direct:1-14

The enormous diversity in leaf morphology across the plant kingdom has served as an inexhaustible source of fascination and inspiration for botanists and artists alike. While we have established a view into the basic genetic elements that interact to set up the body plan of a leaf, much remains to be learned about how these elements are modulated to fine-tune diverse leaf shapes within and across species. Given the multi-faceted functions of CLE peptides in plant tissues, it stands to reason that they might also play a role in some of the key cell fate determinant processes during leaf development.

Of the shoot-expressing CLE genes in Arabidopsis, *CLE5* and *CLE6* encode for the same polypeptide and likely arose from a gene duplication event. Both exhibit very specific promoter activity at the base of rosette leaves and in the hydathode region at the leaf margin, and thus might play a role in coordinating leaf development. In a collaboration with P. Digennaro, E. Grienenberger, and J. Jun, we used *promoter:GUS* expression and mRNA in situ hybridization to take a closer look at their expression pattern in vegetative leaves. We found that despite their sequence similarity, these two *CLE* genes are expressed in distinct but overlapping manners at the proximal region of the leaf. *CLE6* transcript is specifically located on the adaxial side, with strongest expression in the medial domain, and *CLE5* is detected on both adaxial and abaxial side towards the margin. Using CRISPR/Cas9 gene editing, we generated loss-of-function alleles for both genes. While no major changes in gross morphology was detected in either single or double mutant plants, careful analysis of shape parameters showed subtle deviations from wild-type leaf petiole width and curvature. The former parameter was most affected in *cle5* and *cle5 cle6* plants, while the later was most affected in *cle6* mutants. We also demonstrated using qRT-PCR analysis, combined with inducible genetic constructs and phytohormone applications, that *CLE5* and *CLE6* transcript levels are under influence by the leaf identity-regulating transcription factors AS1, BOP1/2, and WOX1/PRS, as well as the hormones auxin and gibberellic acid. Interestingly, we observed subtle disparities between *CLE5* and *CLE6* in how each gene responds to transcription factor induction and hormone treatment, which might underlie their distinct expression patterns, and potential differences in their signaling and functions.

Together, our results provide evidence for a novel CLE peptide signaling pathway that regulates leaf morphology, particularly in the petiole at the base of the leaf. It is likely that their larger roles in leaf development are compensated by yet other CLE signals, similar to the redundancy between CLV3 and CLE16/17 in the SAM. Indeed, a large number of *CLE* genes exhibit broad promoter activity in Arabidopsis leaves, including *CLE16*, *CLE17*, and *CLE27* among many others. Thus their true biological significance might not be revealed without the right allelic combinations. In addition, subtle differences in how *CLE5* and *CLE6* affect leaf phenotype, and in how these two near-identical sequences are regulated at the transcriptional level hint at a larger genetic circuitry that fine-tunes leaf morphogenesis. Our understanding of receptor-like kinase activity in the leaf is currently limited. However, loss of *CLV2*, *RPK2*, and *BAMs* functions all produce pleiotropic phenotypes that include leaf deformities. Therefore, it will be interesting to see whether CLE5/6 signals through any of these receptors, or through a different set of receptor complexes in the leaf.

SUMMARY

Intercellular signaling mediated by small peptides is critical to coordinate organ formation in animals, but whether extracellular polypeptides play similar roles in plants is unknown. Here we describe a role in Arabidopsis leaf development for two members of the CLAVATA3/ESR-RELATED peptide family, CLE5 and CLE6, which lie adjacent to each other on chromosome 2. Uniquely among the *CLE* genes, *CLE5* and *CLE6* are expressed specifically at the base of developing leaves and floral organs, adjacent to the boundary with the shoot apical meristem. During vegetative development *CLE5* and *CLE6* transcription is regulated by the leaf patterning transcription factors BLADE-ON-PETIOLE1 (BOP1) and ASYMMETRIC LEAVES2 (AS2), as well as by the WUSCHEL-RELATED HOMEOBOX (WOX) transcription factors WOX1 and PRESSED FLOWER (PRS). Moreover, *CLE5* and *CLE6* transcript levels are differentially regulated in various genetic backgrounds by the phytohormone auxin. Analysis of loss-of-function mutations generated by genome engineering reveals that *CLE5* and *CLE6* independently and together have subtle effects on rosette leaf shape. Our study indicates that the CLE5 and CLE6 peptides function downstream of leaf patterning factors and phytohormones to modulate the final leaf morphology.

SIGNIFICANCE STATEMENT

The coordination of organ formation by plants is dependent on communication between cells, but the role of peptide signaling molecules in this process is poorly understood. We report that the closely related *CLE5* and *CLE6* peptide-encoding genes are differentially regulated by BOP, AS2 and WOX transcription factors as well as by auxin, and function downstream of these leaf patterning factors and hormones to direct formation of the final leaf shape.

INTRODUCTION

Plants are unique in their ability to generate new organs and tissues throughout their life span, producing intricate structures such as flowers and leaves via complex molecular regulatory mechanisms (Tsukaya, 2013; Bar and Ori, 2014). During vegetative development, leaves initiate as small, regularly spaced primordia on the flanks of the shoot apical meristem. Following leaf initiation, individual primordia develop along three axes of polarity: the adaxial-abaxial, proximal-distal, and medial-lateral axes. Early polarization along these three axes serves to specify the unique cell types within the emergent leaf. In simple-leaved species, such as Arabidopsis, subsequent cell growth and differentiation then results in a mature three-dimensional structure with a narrow petiole and a broad lamina, or blade (Kalve et al., 2014). The blade tissue contains an epidermal layer of jigsaw-shaped pavement cells bounded by several narrow layers of elongated cells at the margin, and is specialized for light capture. Yet despite the importance of leaves as the main sites for photosynthesis, as well as carbon fixation and gas exchange in plants (Tsukaya, 2013), much remains to be understood about the genetic mechanisms that control leaf formation, shape and function.

The coordination of complex developmental activities such as leaf formation by growing plants is critically dependent on the communication of information between cells. Long-range intercellular signaling is mediated by phytohormones such as cytokinin, auxin, gibberellin (GA), abscisic acid (ABA) and brassinosteroids (BL). Among these hormones, auxin, GA and BL have well-characterized roles in orchestrating leaf development (Kalve et al., 2014). In addition to setting the positions of newly arising leaf primordia, auxin contributes to the establishment of leaf adaxial-abaxial polarity as well as the coordinated transition from cell proliferation to cell expansion. GA and also BL regulate cell division and expansion during the leaf maturation process. These phytohormone-mediated effects on leaf morphogenesis can occur via changes in hormone biosynthesis, as in the case of GA and BL, and/or in hormone transport or response, as in the case of auxin (Tsukaya, 2013; Kalve et al., 2014).

In addition to phytohormone signaling pathways, families of secreted signaling peptides are involved in regulating plant developmental events (Matsubayashi, 2014; Grienenberger and Fletcher, 2015). The CLAVATA3/EMBRYO SURROUNDING REGION-related (CLE) family is one of the largest and best-studied secreted signaling peptide families in plants. CLE family members are found throughout the plant kingdom as well as in some plant-parasitic nematodes (Miyawaki et al., 2013). The Arabidopsis genome encodes 32 *CLE* gene family members, which are expressed in a wide variety of tissues and developmental stages (Jun et al., 2010b). The genes encode secreted 12- to 13-amino-acid mature polypeptides, derived from a conserved C-terminal CLE domain, which undergo various post-translational modifications (Matsubayashi, 2014).

Although intercellular signaling molecules are crucial for orchestrating plant growth and development, determining their biological activities has proven challenging. To date only a handful of Arabidopsis CLE family members have defined functions. The founding CLE family member CLAVATA3 (CLV3) acts in a negative feedback loop that regulates stem cell homeostasis in the shoot apical meristem (Brand et al., 2000; Schoof et al., 2000). In addition CLE40 plays a role in root stem cell homeostasis, and CLE41 and CLE44 function in vascular development and lateral root formation (Matsubayashi, 2014; Wang et al., 2016). Although a comprehensive library of *CLE* loss-of-function alleles now exists (Yamaguchi et al., 2017), plants

carrying most single *cle* null alleles show no obvious developmental or physiological phenotypes (Jun et al., 2010b). One possible explanation is that due to a high degree of sequence homology, many *CLE* genes play largely redundant roles in plant biology (Strabala et al., 2006).

Key components of CLE-mediated signaling pathways are members of the WUSCHEL-RELATED HOMEOBOX (WOX) family of homeodomain-containing transcription factors (Haecker et al., 2004). Expression of the founding Arabidopsis *WOX* gene family member, *WUSCHEL (WUS)*, is limited by CLV3 signaling to the most central region of the shoot apical meristem (Laux et al., 1996), where it functions in a non-cell-autonomous manner to maintain stem cell activity in the overlying cells (Schoof et al., 2000; Brand et al., 2002; Yadav et al., 2011). In roots, CLE40 likewise restricts the expression domain of *WOX5* (Stahl et al., 2009), which acts non-cell-autonomously to promote columella stem cell maintenance (Sarkar et al., 2007). The identical CLE41 and CLE44 peptides induce *WOX4* and *WOX14* expression to promote vascular cell division (Hirakawa et al., 2010; Etchells et al., 2013). These examples suggest that the use of CLE-WOX signaling modules during plant development is widespread.

Evidence is accumulating that CLE polypeptide signaling pathways intersect with classical phytohormone signaling pathways to direct various plant developmental processes (Wang et al., 2016). For example, the CLV3 pathway target WUS maintains shoot and floral meristem activity by directly regulating components of cytokinin response pathways (Leibfried et al., 2005). CLE40 controls the expression of auxin, cytokinin and ABA signaling genes to inhibit cell differentiation in the root apical meristem (Pallakies and Simon, 2014). CLE6 and CLE41/44 peptide-stimulated vascular cell proliferation is positively regulated by auxin, and exogenous CLE6 peptide application induces the expression of auxin signaling-related promoters such as *proPIN1*:GUS in the hypocotyl stele (Whitford et al., 2008). In addition, GA promotes *CLE6* expression in the root stele, and *CLE6* over-expression can partly suppress the phenotypes of GA-deficient plants (Bidadi et al., 2014). Based on such observations it has been proposed that CLE peptides may play general roles in controlling stem cell fate via their communication with plant hormone-regulated signaling networks (Whitford et al., 2008).

Yet although there is increasing evidence that CLE peptide and phytohormone signaling pathways connect to regulate Arabidopsis growth and development, most studies to date have been conducted using root or vascular tissues (Wang et al., 2016). In contrast, beyond the role of *CLV3* in shoot apical meristem maintenance, very little is known about the regulation or activity of *CLE* genes in shoot or shoot-derived tissues. However, a good deal of work has focused on the regulation of leaf development, including the adaxial side adjacent to the SAM boundary as well as at the base of the developing floral organs (Ha et al., 2004; Hepworth et al., 2005; Norberg et al., 2005). Two closely related genes that encode transcriptional regulatory proteins, *BLADE-ON-PETIOLE1* (*BOP1)* and *BOP2,* are expressed at the base of developing rosette leaves and have largely redundant functions in developing lateral organs, including suppressing ectopic blade outgrowth from the leaf petiole (Ha et al., 2003; Ha et al., 2007). The BOP proteins activate the transcription of *ASYMMETRIC LEAVES2 (AS2)* in the proximal region of developing leaf primordia. *AS2* encodes a member of the LATERAL ORGAN BOUNDARIES (LOB) family of leucine-zipper proteins (Iwakawa et al., 2002; Lin et al., 2003; Xu et al., 2003) that physically interacts with the ARP domain transcription factor AS1 (Xu et al., 2003) to promote lateral organ identity and adaxial leaf polarity (Machida et al., 2015). *AS2* transcription occurs in developing

leaf and floral primordia in a broad domain (Byrne et al., 2000; Iwakawa et al., 2007) that overlaps with those of *BOP1* and *BOP2*.

Here we investigate the expression and function of the closely related *CLE5* and *CLE6* genes, which lie adjacent to one another on chromosome 2 and encode identical CLE polypeptides (Cock and McCormick, 2001). We show that *CLE5* and *CLE6* have highly specific, overlapping expression patterns at the base of lateral organ primordia. We find that, despite having a high degree of overall sequence similarity, they are differentially regulated during vegetative development by the *BOP* and *AS2* genes, the WOX transcription factors PRS and WOX1, and by auxin. Using null alleles of *CLE5* and *CLE6* generated by genome editing, we demonstrate that although neither single nor double mutations in *CLE5* and *CLE6* have a detectable impact on Arabidopsis organ initiation or patterning, they have subtle effects on overall leaf shape. Our studies indicate that *CLE5* and *CLE6* act downstream of leaf patterning factors and phytohormones to direct formation of the final leaf morphology.

EXPERIMENTAL PROCEDURES

Plant Material and Growth Conditions

Seeds were imbibed at 4°C for 5 days before sowing and plants were grown in Percival growth chambers at 21°C under long day conditions (16 hours light, 8 hours dark) with a light fluence rate of approximately 110 $mmol/m^{-2}\times sec^{-1}$. Transgenic plants carrying the pCLE5:*GUS* or pCLE6:*GUS* constructs were generated as described (Jun et al., 2010b), using 2570 bp upstream of the *CLE5* translation start site or 1713 bp upstream of the *CLE6* translation start site. Promoter alignments were performed using the EMBOSS Needle program for pairwise sequence alignment (Rice et al., 2000). For the generation of the pBOP1:*CLE6 bop1-4 bop2-11* lines, a 5797 bp *BOP1* promoter fragment was PCR-amplified using the primers pBOP1(-5797) FW and pBOP1 RV (primers listed in **Table S1**). The *CLE6* coding sequence was PCR-amplified using the primers pBOP1:CLE6 FW and CLE6_CDS+Stop RV (**Table S1**). Both PCR products were gel-purified and used as a template for a third PCR with the primers pBOP1(-5797) FW and CLE6_CDS+Stop RV to generate a pBOP1:*CLE6* product. The product was subcloned into the TOPO pCR8-GW vector (ThermoFisher) and recombined using Gateway technology into the pEarley Gate 300 destination vector. The recombined vector was used for floral dip transformation with Agrobacterium tumefasciens GV3101. T1 transgenic plants were analyzed for *CLE6* expression. All lines were in the *Arabidopsis* Columbia-0 (Col-0) background unless otherwise stated.

Histochemical Assays

GUS staining of 10 to 14-day-old seedlings was performed as described (Jun et al., 2010b). For Dex treatments, seedlings were transferred into half strength liquid Murashige and Skoog (MS) media and then either mock-treated with 70% ethanol (as a solvent for Dex) or treated with Dex at a final concentration of 10μM for 4 hours. RNA *in situ* hybridization was performed on 7-day-old seedlings as described (Jun et al., 2010a). Non-radioactively labeled probes were generated from the full cDNA sequences of *CLE5* and *CLE6* transcripts using primers listed in **Table S1.**

p35S:*BOP1-GR* and p35S:*AS2-GR* Activation Assays

Eleven-day-old p35S:*BOP1-GR bop1-1* or p35S:*AS2-GR as2-1* seedlings were transferred into half strength liquid MS media. Seedlings were then mock-treated with 70% ethanol or treated with Dex at a final concentration of 10μM, incubated under slight agitation, and harvested between 30 minutes and 4 hours for RT-qPCR analysis. For the hormone assays, a final concentration of 10μM IAA, 10μM NAA, 20-30μM GA_4, or 2μM BL was added to the wild-type and p35S:*BOP1-GR bop1-1* seedlings at the same time as the Dex.

RT-qPCR Analyses

For RT-qPCR studies, total RNA was extracted using TriReagent (Sigma-Aldrich), treated with DNase I and purified with the RNeasy Mini Kit (Quiagen). Four to five μg of total RNA were used for reverse transcription with SuperScript III and oligo(dT_{15}) (ThermoFisher Scientific). Quantitative real-time Polymerase Chain Reaction (PCR) was performed using the iTaq Universal Sybr Green Supermix (Biorad) with the primers listed in **Table S1**. PCR reactions were run and analyzed using a MyiQTM Single-Color real-time PCR detection system (Bio-Rad). Two-step PCR conditions were as follows: initial denaturation at 95°C for 3 minutes, followed by 40 cycles of 95°C for 10 seconds and 60°C for 30 seconds. Quantification of relative gene expression was performed using the ΔΔCt method (Livak and Schmittgen, 2001), and calculated based on at least three biological replicates with three technical replicates each. Expression values were normalized to *TUBULIN2 (TUB2)* or *MON1* (Czechowski et al., 2005).

ChIP-qPCR Analyses

ChIP was performed as described (Yamaguchi et al., 2014) using an anti-GR antibody (SC-1004, Santa Cruz Biotechnology). Seedlings were mock-treated in 70% ethanol or Dex-treated for 4 hours. Quantification of immunoprecipitated DNA was performed by semi-quantitative PCR using the primers listed in **Table S1**.

CRISPR/Cas9 Cloning and Analysis

The Cas9 and sgRNA cassettes were PCR-amplified from the At-psgR-Cas9 vectors (obtained from Dr. Jian-Kang Zhu, Purdue University) using M13 FW and M13 RV primers and subcloned into the pCR8/GW/TOPO vector (ThermoFisher Scientific) to add the attL1 and attL2 Gateway sequences. The CRISPR/Cas9 Gateway-compatible cassette was then PCR-amplified using primers T7_promoter and pCR8_FW (**Table S1**) and cloned into the pGEMT vector (Promega) for subsequent experiments (named thereafter At-psgR/GW). The genomic target sequences for *CLE5* and *CLE6* were 5'-AGTTCCGACAGGGTTTCACCCGG-3' and 5'-TACATATCGCCCCACAACCATGG-3' respectively. The At-psgR/GW plasmid was digested with *BbsI* restriction enzyme and used for ligation with the annealed primers CLE5 P1 and P2 or CLE6 P1 and P2 (**Table S1**). At-psgR/GW plasmids containing the *CLE5* or *CLE6* genomic target sequences were transferred into the pEarleyGate 301 vector using the LR enzyme mix (ThermoFisher Scientific). The recombinant pEarleyGate 301 constructs were transferred into *Agrobacterium tumefaciens* GV3101 and transformed into Arabidopsis Col-0 using the floral dip method (Clough and Bent, 1998).

Genotyping the *CLE5* CRISPR alleles was performed by using the primers CLE5CR_FW and CLE5CR_RV (**Table S1**) in a PCR reaction to amplify a 727 base pair (bp) product. Digesting the PCR product with *HphI* yielded 384 bp and 343 bp bands from wild-type tissue, whereas the

product from mutant tissue remained undigested. Genotyping the *CLE6* CRISPR alleles was performed by using the primers CLE6CR_FW and CLE6CR_RV (**Table S1**) in a PCR reaction to amplify an 882 bp product. Digesting the PCR product with *MslI* yielded 545 bp and 337 bp bands from wild-type tissue, whereas the product from mutant tissue remained undigested. T2 mutant plants lacking the Cas9 cassette were identified by PCR using primers sgRNA_FW and sgRNA_RV specific to the Cas9 sequence.

Phenotypic Analysis

Leaf morphometrics experiments were conducted using LeafAnalyser software as described (Weight et al., 2008), using 50 landmarks per leaf sample and >50 leaf samples per genotype. Principal component analyses were also conducted using LeafAnalyser by calculating eigenvectors (principal components) and eigenvalues (variances) from the covariance matrix generated by LeafAnalyser of each landmark from each leaf (see Weight et al., 2008; Appendix S2). Histological analysis was performed as described (Ha et al., 2003). Scanning electron microscopy was performed as described (Fiume et al., 2010) and samples visualized on a Hitachi S4700 scanning electron microscope.

RESULTS

CLE5 and *CLE6* have distinct yet overlapping expression patterns

To investigate *CLE5* and *CLE6* transcription patterns in detail throughout the Arabidopsis life cycle, we performed promoter:GUS and *in situ* hybridization analysis of the two genes in aerial tissues. In wild-type Col-0 plants pCLE6:*GUS* specific promoter activity was detected at the base of young rosette leaves (Fig. 4.1**a**) and at the base of the floral organs (Fig 4.1b). Similarly, specific pCLE5:*GUS* activity was detected at the base of young rosette leaves (Fig. 4.1c), at the base of the cotyledons in mature embryos (Fig. 4.1d), and at the base of the cauline leaves (Fig. 4.1e). pCLE6:*GUS* promoter activity was also found at the base of the cotyledons. Previously reported pCLE6:*GUS* expression included the base of the cauline leaves at the primary branching point on the inflorescence stem and pCLE5:*GUS* expression in floral organs (Jun et al., 2010b). Overall, activity of the *CLE5* and *CLE6* promoters was restricted to the most proximal region of lateral organ primordia, adjacent to the boundary with the shoot meristem.

Transverse sections through wild-type vegetative shoot apices revealed further region-specific expression of *CLE5* and *CLE6*. pCLE6:*GUS* promoter activity in the developing rosette leaves was confined to the adaxial domain (Fig. 4.1f), and this expression pattern was confirmed using RNA *in situ* hybridization (Fig. 4.1g). In contrast, *CLE5* expression occurred in both the adaxial and abaxial domains (Fig. 4.1h, i). Furthermore, *CLE5* and *CLE6* displayed reciprocal expression patterns along the medio-lateral axis of developing rosette leaf primordia. *CLE6* was transcribed predominantly within the medial domain above the midvein (Fig. 4.1a, f, g) whereas *CLE5* transcription was restricted to the lateral domain at the very edges of the primordia (Fig. 4.1c, h, i). Thus, although the promoter activity patterns of *CLE5* and *CLE6* overlap extensively, the two genes display distinct expression patterns along the adaxial-abaxial and medial-lateral polarity axes within the developing leaf primordia.

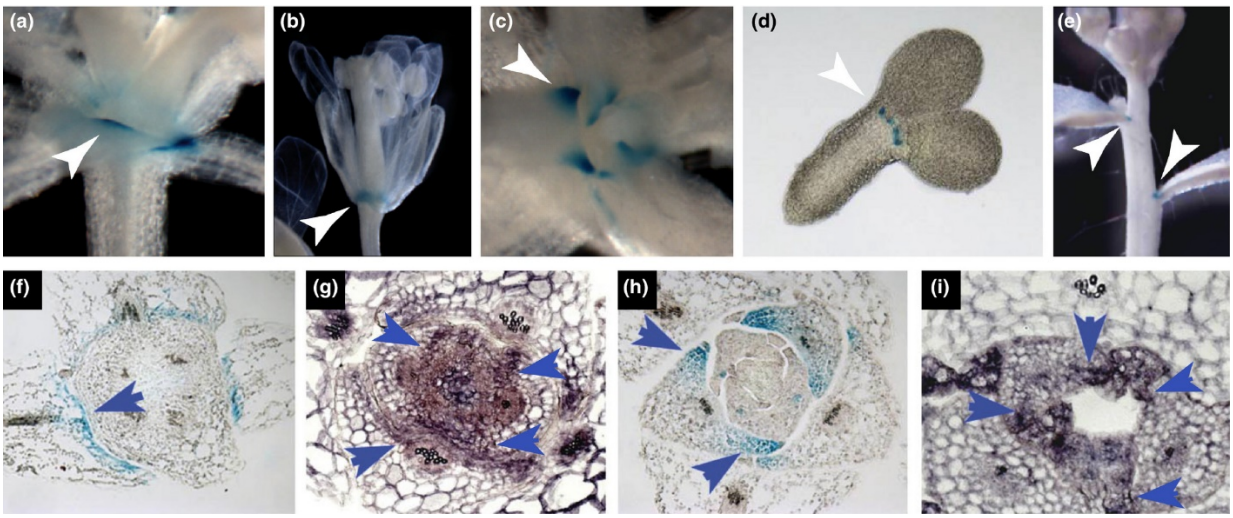

Figure 4.1. ***CLE5* and *CLE6* expression in wild-type Arabidopsis plants.**
(a-b) pCLE6:*GUS* promoter activity at the base of wild-type Col-0 (a) rosette leaves and (b) floral organs. (c-e) pCLE5:*GUS* promoter activity at the base of Col-0 (c) rosette leaves, (d) embryo cotyledons, and (e) cauline leaves. (f-g) *CLE6* mRNA expression in transverse sections of leaves from 7-day-old wild-type plants. (h-i) *CLE5* mRNA expression in transverse sections of leaves from 7-day-old wild-type plants. Arrowheads indicate gene expression at the base of the organ.

Known leaf patterning transcriptional factors regulate *CLE5* and *CLE6* expression

The *CLE5* and *CLE6* expression patterns at the base of developing lateral organs were very similar to those reported for the *BOP1* and *BOP2* leaf patterning genes (Ha et al., 2004; Hepworth et al., 2005; Norberg et al., 2005), as well as for their downstream target *AS2* (Byrne et al., 2000; Iwakawa et al., 2007) Given the overlap in expression patterns between these genes, we examined whether *CLE5* and/or *CLE6* transcription was regulated by *BOP* or *AS2* gene activity in developing rosette leaf primordia using RT-qPCR. Compared to wild-type 10-day-old Col-0 seedlings, *CLE5* and *CLE6* expression was reduced by 25-50% in *bop1-4 bop2-11* (*b1b2*) null mutant seedlings (Fig. 4.2a), indicating that BOP1 and BOP2 are positive regulators of *CLE5* and *CLE6* transcription. Conversely, in *as2-1* seedlings, *CLE5* and *CLE6* expression levels were elevated compared to wild-type (Fig. 4.2a), indicating that AS2 negatively regulates *CLE5* and *CLE6* transcription. Taken together, these results indicate that *CLE5* and *CLE6* function downstream of BOP1/2 and AS2 transcriptional regulation as direct or indirect targets of these key leaf patterning factors.

The BOP1/2 and AS2 proteins could regulate *CLE5* and *CLE6* transcription by affecting their mRNA levels, their expression domains within developing leaves, or both. To determine which, we performed *in situ* hybridization experiments using 10-day-old Col-0, *b1b2* and *as2-1* seedling tissues. Compared to the sense probe, which showed no specific *CLE6* expression in wild-type Col-0 leaves (Fig. 4.2b), the antisense probe detected strong *CLE6* expression across the adaxial domain of young Col-0 leaf primordia and the marginal region (tips) of older primordia (Fig. 4.2c). This expression pattern was unchanged in *b1b2* leaf primordia (Fig. 4.2d), indicating that BOP1 and BOP2 induce *CLE6* mRNA expression levels without altering its expression domain.

Similarly, we detected no difference in the *CLE6* expression domain between developing Col-0 and *as2-1* leaves (Fig. 4.2e), showing that the elevation in *CLE6* mRNA levels in *as2* leaves does not result from an enlarged expression domain. These data indicate that neither BOP1/2 nor AS2 affect the *CLE6* expression pattern but that a combination of activators and repressors is required to restrict *CLE5* and *CLE6* transcription to the appropriate levels in developing rosette leaves.

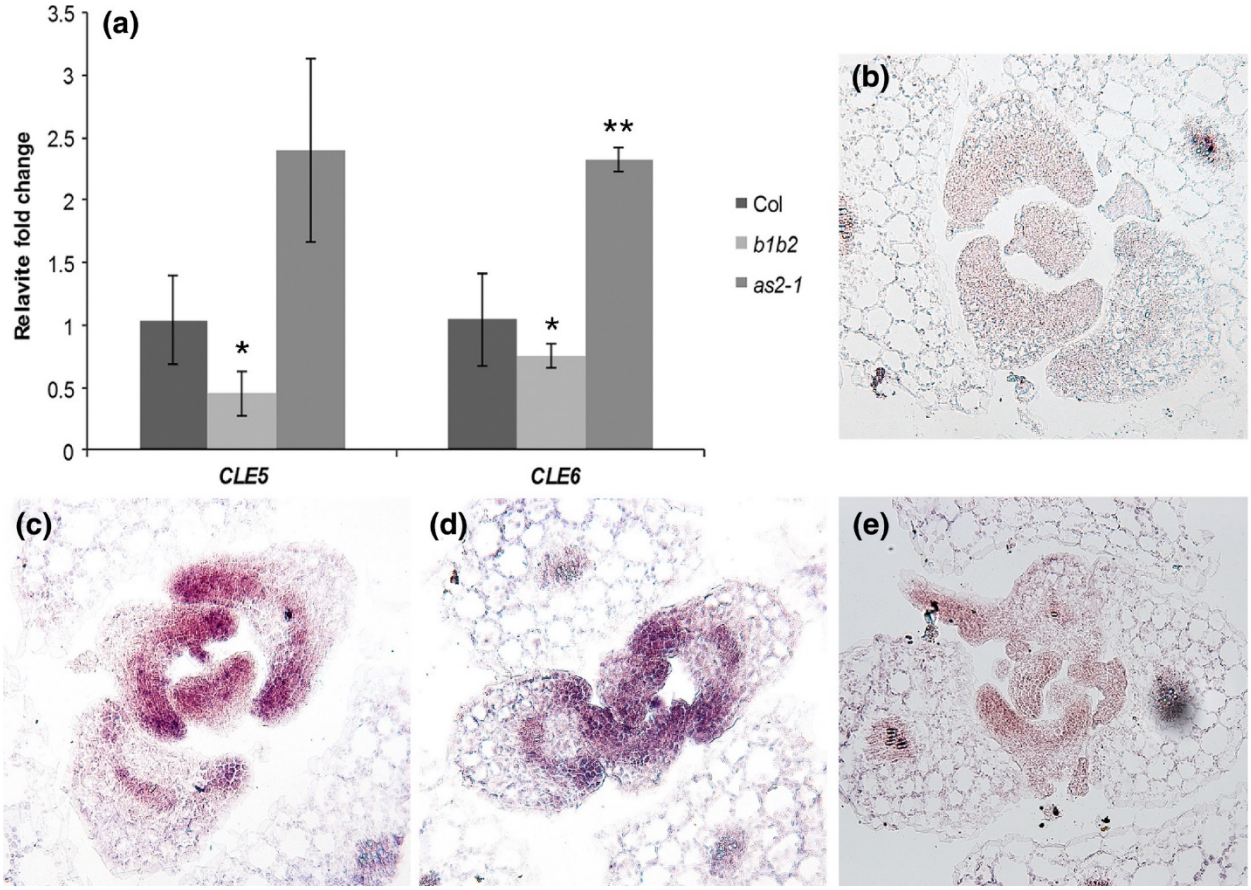

Figure 4.2. ***CLE5* and *CLE6* expression in leaf patterning mutants.**
(a) Relative fold change in *CLE5* and *CLE6* transcript levels in 10-day-old Col-0, *bop1-4 bop2-11 (b1b2)*, and *as2-1* seedlings. Expression values (mean ± S.D.) were normalized to *MON1* and asterisks indicate a significant difference from the wild-type mean (* = $p<0.05$; ** = $p<0.01$) using Student's t test. (b) Transverse section of a Col-0 seedling hybridized with a *CLE6* sense probe. (c) Transverse section of a Col-0 seedling hybridized with a *CLE6* antisense probe. (d) Transverse section of a *b1b2* seedling hybridized with a *CLE6* antisense probe. (e) Transverse section of an *as2-1* seedling hybridized with a *CLE6* antisense probe.

Next, we investigated whether the regulation of the two *CLE* genes by BOP1 was direct or indirect by conducting a time course of *CLE5* and *CLE6* transcription in p35S:*BOP1-GR bop1-1* transgenic plants. In this system, application of the hormone dexamethasone (Dex) translocates the ectopically produced BOP1 transcriptional regulatory protein into the nucleus, rescuing the dominant negative *bop1-1* ectopic leaf outgrowth phenotype (Jun et al., 2010a) that phenocopies

the *b1b2* null mutant phenotype (Ha et al., 2004). We first examined *AS2* transcription over the 4-hour time course as a positive control. Consistent with previous data (Jun et al., 2010a), we found that *AS2* transcription was induced by BOP1-GR after 30 minutes of 10 μM Dex application and continued to be induced over the full 4 hours of Dex treatment (Fig. 4.3a). *CLE6* transcription was significantly up-regulated by BOP1 after 1 hour of Dex treatment, and its expression levels continued to increase to >2 fold after 4 hours (Fig. 4.3a). Thus BOP1 is sufficient to induce *CLE6* transcription, although only to moderate levels. The rapid activation of *CLE6* transcription after 1 hour of Dex application suggests that *CLE6* could be an immediate target of BOP1 induction. In contrast, *CLE5* expression was slightly down-regulated after 30 minutes of Dex treatment and remained steady thereafter (Fig. 4.3a), indicating that BOP1 is insufficient to induce *CLE5* transcription on its own.

As a control for the Dex treatment itself we applied 10 μM Dex for 4 hours to Col-0 and *bop1-1* plants and quantified *AS2, CLE5* and *CLE6* mRNA levels. We found that Dex application to wild-type plants had no effect on *AS2, CLE5* or *CLE6* transcript abundance (Fig. 4.3b), although we observed considerable variability in the transcript levels within each genotype because only a very small number of cells within the total leaf tissue assayed express *CLE5* or *CLE6*. Dex application to *bop1-1* plants lacking the p35S:*BOP1-GR* transgene also did not affect *AS2* or *CLE6* mRNA levels; however, *CLE5* mRNA levels were reduced by approximately 40% compared to mock-treated *bop1-1* plants. Thus the slight reduction in *CLE5* mRNA levels during the time course can be attributed to a repressive effect of Dex application to *bop1-1* plants rather than of BOP1-GR activity.

Both *CLE5* and *CLE6* are expressed in root tissues as well as in shoot tissues (Jun et al., 2010b), so we determined whether the effect of BOP1 on *CLE5* and/or *CLE6* expression was limited to one of the two tissue types. We treated p35S:*BOP1-GR bop1-1* plants with 10 μM Dex for 4 hours, isolated shoot and root tissues, and measured *CLE5* and *CLE6* mRNA levels using RT-qPCR. We found that although *CLE5* expression levels were unaltered in shoot versus root tissues, BOP1 induction of *CLE6* expression occurred in the shoot tissues but not in the root tissues (**Fig.**). Thus, the regulation of *CLE6* transcription by BOP1 is restricted to above-ground shoot tissues that contain the leaf primordia.

To determine if *CLE6* induction by BOP1 was due to direct transcriptional regulation, we tested whether BOP1 protein directly associated with *CLE6* regulatory sequences. We performed chromatin immunoprecipitation (ChIP-qPCR) assays with Dex-treated p35S:*BOP1-GR bop1-1* seedlings using primer sets spanning 3.2 kb upstream of the *CLE5* coding region, the intergenic region between *CLE5* and *CLE6,* and 1 kb downstream of the *CLE6* coding region. No BOP1 binding to these *CLE5* and *CLE6* regulatory regions was detected (Fig. S4.1), although BOP1 binding was detected as expected to regulatory sites within the *AS2* promoter (Jun et al., 2010a). Therefore the regulation of *CLE6* by BOP1 appears to occur indirectly through an intermediary factor. We also attempted to rescue the *bop1-4 bop2-11* ectopic blade outgrowth phenotype (Ha et al., 2007) by directing *CLE6* expression within the BOP domain under the control of 6.0 kb of *BOP1* promoter sequence. This promoter region is sufficient to drive *BOP1* transcription in its native domain (Jun et al., 2010a). However, none of the pBOP1:*CLE6 bop1-4 bop2-11* lines exhibited rescue of the ectopic blade outgrowth phenotype, indicating that *CLE6* expression in the *BOP1* domain alone is not sufficient to restore wild-type petiole identity. Thus it is likely that

rescue of the *bop* phenotype requires *CLE6* expression beyond the *BOP* expression domain and/or other factors in addition to *CLE6*.

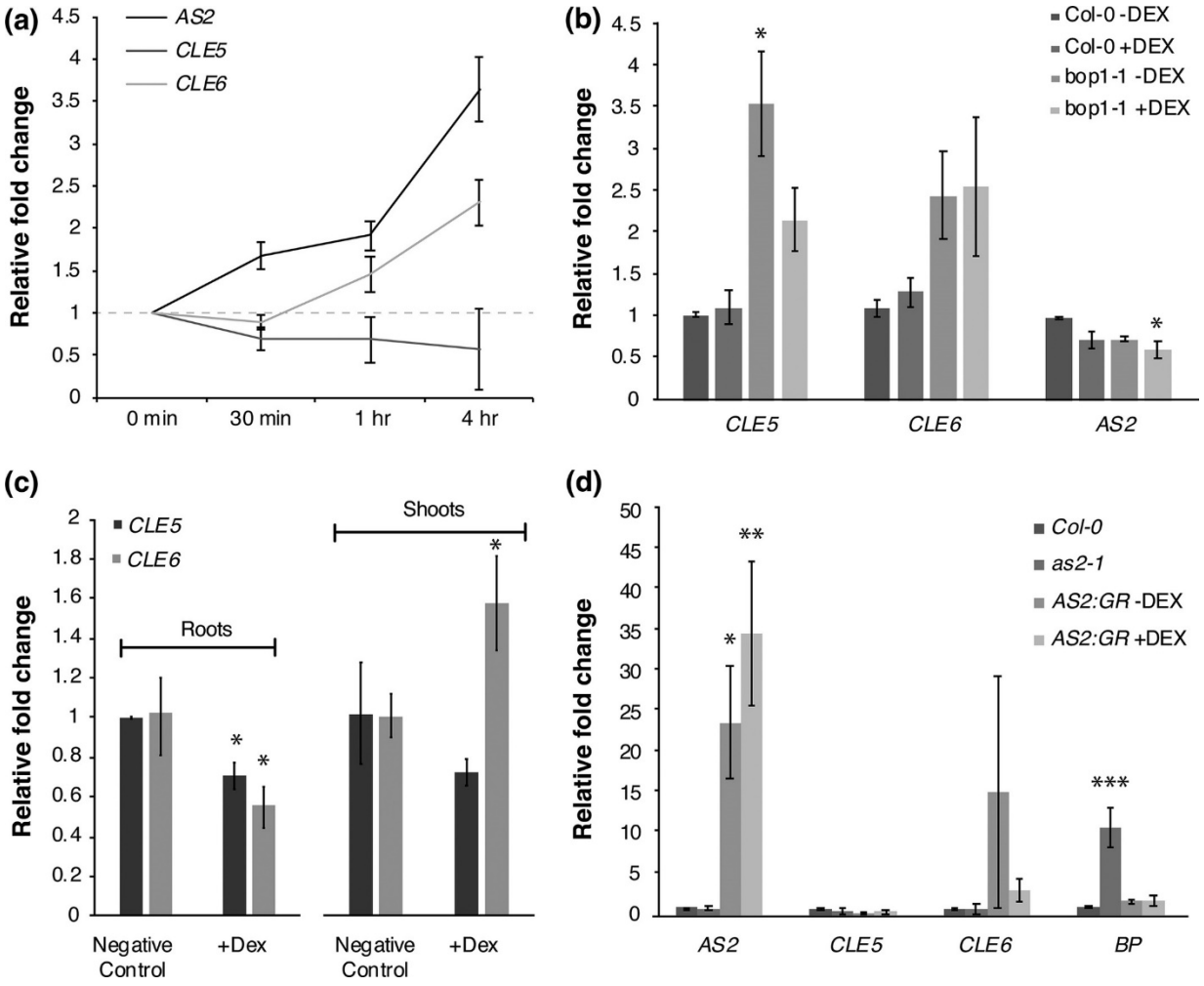

Figure 4.3. *CLE5* and *CLE6* expression in response to BOP1 or AS2 induction.
(a) Time course of *AS2*, *CLE5* and *CLE6* transcript levels in p35S:*BOP1-GR bop1-1* seedlings treated with Dex for 0 to 4 hours. (b) Relative fold change in *AS2, CLE5* and *CLE6* transcript levels in Col-0 and *bop1-1* seedlings treated with Dex for 4 hours. (c) Relative fold change in *CLE5* and *CLE6* transcript levels in root or shoot tissues from p35S:*BOP1-GR bop1-1* seedlings treated with Dex for 4 hours. (d) Relative fold change in *AS2, CLE5, CLE6* and *BP* transcript levels in shoot tissues from *as2-1* and p35S:*AS2-GR as2-1* seedlings treated with Dex for 2 or 4 hours. Expression values (mean ± S.D.) were normalized to *TUB2* or *MON1* and asterisks indicate a significant difference from the wild-type mean (* = $p<0.05$; ** = $p<0.01$; *** = $p<0.001$).

The observation that BOP1 was not a direct regulator of *CLE5* or *CLE6* transcription suggested that role would fall to a downstream component of the BOP1 regulatory pathway. Our time course showed that *AS2* induction by BOP1-GR occurred prior to *CLE6* induction, so we tested whether the AS2 transcription factor might directly regulate *CLE5* and/or *CLE6* transcription. We analyzed *CLE5* and *CLE6* mRNA levels in shoots of 11-day-old p35S:*AS2-GR as2-1* seedlings after 2 and

4 hours of Dex induction using RT-qPCR. At both time points we observed a slight decrease in *CLE5* mRNA levels compared to mock-treated seedlings (Fig. 4.3d); however, this decline was not statistically significant. We also detected no significant change in *CLE6* mRNA levels at either time point (Fig. 4.3d). These data show that AS2 alone is not sufficient to affect *CLE5* and/or *CLE6* transcription, either because the *CLE* genes are not direct AS2 regulatory targets or because the amount of its partner protein AS1 becomes rate-limiting when AS2 is over-expressed.

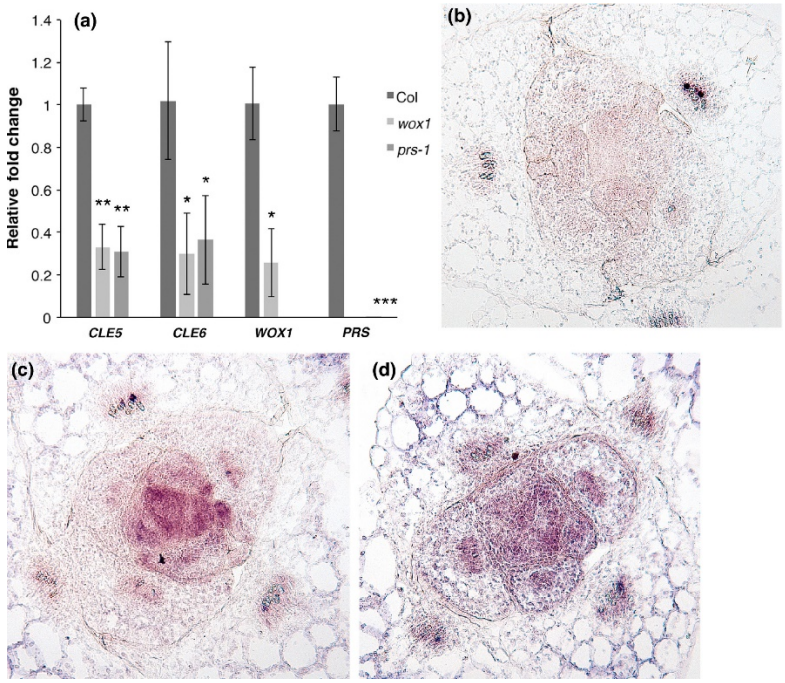

Figure 4.4. *CLE5* and *CLE6* expression in *prs wox1* mutants.

(a) *CLE5* and *CLE6* transcript levels in 10-day-old Col-0 and *prs-1 wox1-1* seedlings. Expression values (mean ± S.D.) were normalized to *MON1* and asterisks indicate a significant difference from the wild-type mean (* = $p<0.05$; ** = $p<0.01$; *** = $p<0.001$). (b) Transverse section of a Col-0 seedling hybridized with a *CLE6* sense probe. (c) Transverse section of a Col-0 seedling hybridized with a *CLE6* antisense probe. (d) Transverse section of a *prs-1 wox1-1* seedling hybridized with a *CLE6* antisense probe.

Other well-characterized players in *CLE* gene regulation are members of the WOX family of transcription factors. Among these, *WOX1* and *PRESSED FLOWER (PRS)*, also known as *WOX3*, have described roles in early leaf development (Nakata et al., 2012), and act in blade outgrowth and leaf margin formation. To assess whether these WOX transcription factors regulated *CLE5* and *CLE6* transcription, we measured *CLE5* and *CLE6* mRNA levels in the shoots of 10-day-old *wox1-1* and *prs-1* null mutant seedlings. Expression of *CLE5* and *CLE6* was reduced by about 50% in both *prs* and *wox1* seedlings compared to wild-type Col-0 (Fig. 4.4a), indicating that WOX1 and PRS are each positive regulators of *CLE5* and *CLE6* transcription. In situ hybridization showed no alteration in the *CLE6* expression domain in 10-day-old *prs wox1* seedlings compared to Col-0 (Fig. 4.4c, d), indicating that PRS and WOX1 do not affect the *CLE6* spatial domain. We also noted that *WOX1* transcripts were absent from *prs-1* seedlings and *PRS* transcripts were absent

from *wox-1* seedlings (Fig. 4.4a). Thus *PRS* and *WOX1* are required for one another's expression in developing leaf primordia.

CLE5 and *CLE6* transcription is regulated by plant hormones

Because hormones have long been implicated in regulation of leaf development and architecture, we sought to define the effect of various hormones on *CLE5* and *CLE6* expression in developing Arabidopsis rosette leaves. First, we treated 11-day-old wild-type seedlings with 30μM gibberellin (GA_4), 2μM brassinolide (BL), or 10μM indole-3-acetic acid (IAA), a naturally occurring auxin, for 4 hours and quantified *CLE5* and *CLE6* transcription levels using RT-qPCR. We found that the mRNA levels of both genes were slightly elevated in after application of both GA_4 and BL (Fig. 4.5a), indicating that the two *CLE* genes respond to hormones that regulate leaf formation. Interestingly, IAA treatment led to a much higher up-regulation of *CLE5* and *CLE6* expression (Fig. 4.5a), with *CLE6* transcription showing a ~24-fold induction. Thus both the *CLE5* and especially the *CLE6* gene appear to be auxin responsive.

Next we examined whether phytohormones played a role in BOP1-mediated regulation of *CLE5* and *CLE6* expression. We treated 11-day-old p35S:BOP1-GR *bop1-1* seedlings with 10 μM Dex alone or together with 20μM GA_4, 2μM BL, or 10μM IAA for 4 hours and quantified *CLE5* and *CLE6* transcription levels using RT-qPCR. No significant change in *CLE5* or *CLE6* mRNA expression levels was observed following application of both +Dex and +GA, or of both +Dex and +BL (Fig. 4.5b). This indicates that neither GA nor BL affects the BOP1-mediated regulation of *CLE5* or *CLE6* transcription, nor vice versa. In contrast, the application of both +Dex and +IAA resulted in differential effects on *CLE5* and *CLE6* expression. For *CLE5*, BOP1-GR induction by 4 hours of Dex treatment led to a moderate reduction in *CLE5* transcript levels, as did 4 hours application of 10μM IAA (Fig. 4.5c). Simultaneous treatment with both Dex and IAA for 4 hours did not further reduce *CLE5* mRNA levels, indicating that the two treatments did not have cumulative effects. Our data indicate that in a *bop1-1* background *CLE5* is repressed by Dex application, as shown earlier (Fig. 4.3b), as well as by exogenous auxin. In the case of *CLE6*, BOP1-GR induction by Dex treatment alone led to no significant change in *CLE6* transcript levels, whereas IAA treatment resulted in a slight reduction in *CLE6* mRNA levels (Fig. 4.5c). *CLE6* transcript levels were much more mildly affected by IAA treatment in *bop1-1* plants (Fig. 4.5c) than in Col plants (Fig. 4.5a). Upon simultaneous treatment with both Dex and IAA for 4 hours, *CLE6* transcription was elevated beyond the levels detected upon BOP1-GR induction alone (Fig. 4.5c). These results suggest that *CLE6* transcript levels are independently regulated by BOP1 and auxin. Thus the *CLE5* and *CLE6* genes show differential regulation by BOP1 and phytohormones in developing leaves.

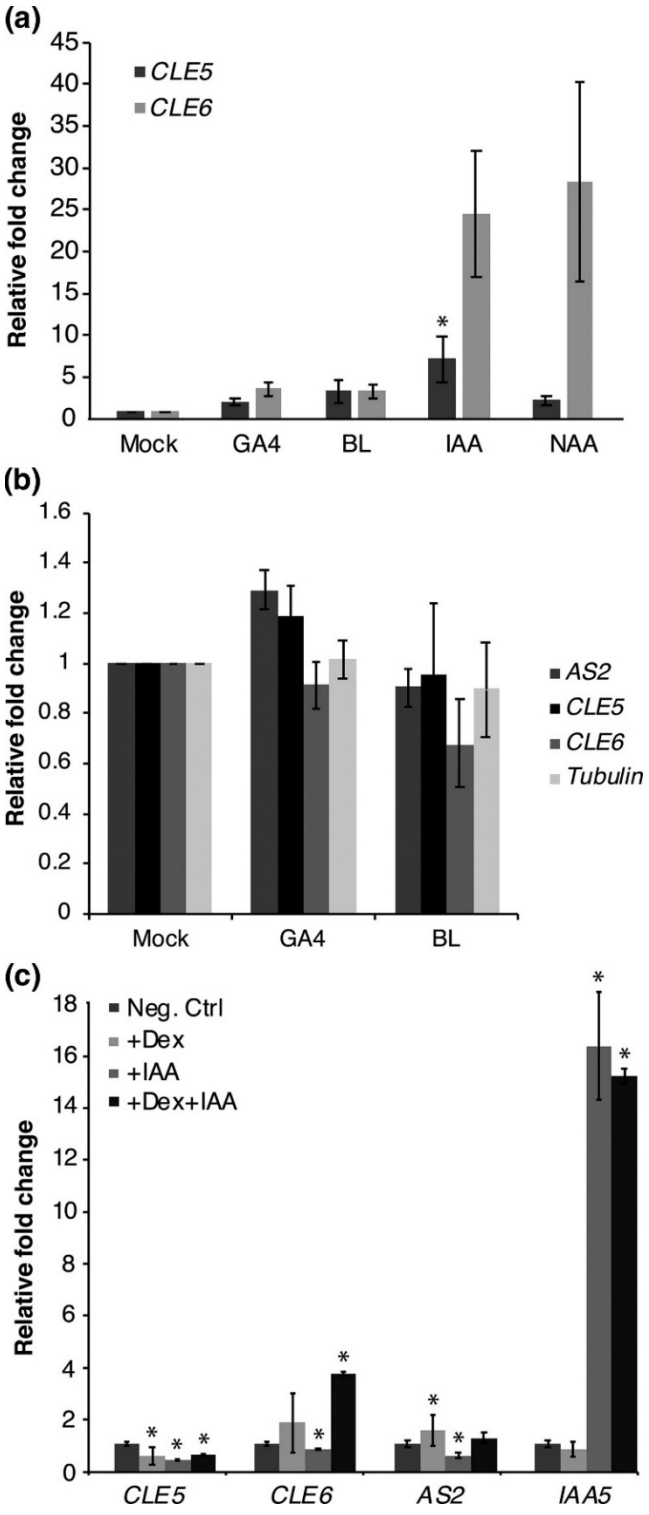

Figure 4.5. *CLE5* and *CLE6* expression in response to BOP1 induction in the absence or presence of hormones.
(a) Relative fold change in *CLE5* and *CLE6* transcript levels in 11-day-old Col-0 seedlings treated with gibberellin (GA_4), brassinolide (BL), or auxin (IAA or NAA) for 4 hours. (b) Relative fold change in *AS2, CLE5* and *CLE6* transcript levels 11-day-old p35S:*BOP1-GR bop1-1* seedlings treated with Dex plus either GA_4 or BL for 4 hours. (c) Relative fold change in *CLE5, CLE6, AS2,* and *IAA5* transcript levels of 11-day old p35S:*BOP1-GR bop1-1* seedlings treated with Dex and/or IAA for 4 hours. Expression values (mean ± S.D.) were normalized to *MON1* and asterisks indicate a significant difference from the wild-type mean at $p<0.05$.

CLE5 and *CLE6* have mild effects on overall leaf shape

In order to determine the function of *CLE5* and *CLE6* during Arabidopsis development we generated null alleles of the two genes using the CRISPR/Cas9 genome engineering technology (Feng et al., 2013; Nekrasov et al., 2013). Transformation of wild-type Col-0 plants with a single guide RNA (sgRNA) construct targeted to the *CLE5* or *CLE6* coding sequences yielded multiple independent transformants. Independent T1 plants were self-fertilized and homozygous individuals were identified in the T2 or T3 generations by restriction enzyme digestion and sequencing.

Two independent *CLE5* and two independent *CLE6* homozygous lines were chosen for further study (Fig. 4.6a). One *cle5* allele consisted of an insertion of an "A" nucleotide at position +215 downstream of the translation start site, and was designated *cle5-1.* A second allele contained a deletion of a five nucleotides starting at position +210 and was designated *cle5-2*. The *cle5-1* mutation introduces a frameshift that alters the amino acid sequence of the CLE domain beginning at the third residue, while the *cle5-2* mutation deletes the first three residues of the CLE domain and also introduces a frameshift. The first *cle6* allele consisted of an insertion of an "A" nucleotide at position +106 downstream of the translation start site, and was designated *cle6-1.* A second allele contained a deletion of four nucleotides starting at position +102 and was designated *cle6-2*. Each of these mutations generates a frameshift in the *CLE6* coding sequence upstream of the CLE domain. Due to the nature of the mutations none of these *cle5* or *cle6* alleles produces a functional CLE polypeptide, and thus they represent loss-of-function alleles.

Because *CLE5* and *CLE6* loci are located approximately 1.7 kilobases (kb) apart in a head-to-tail arrangement on chromosome 2, their proximity makes it improbable to produce double mutants by conventional genetic crosses. Therefore we took advantage of genome engineering to target both *CLE5* and *CLE6* for simultaneous mutation by transforming wild-type Col-0 plants with a construct that contain both of the sgRNAs used in the previous experiments, the one targeted to the *CLE5* coding sequence and the one targeted to the *CLE6* coding sequence. Three doubly homozygous mutants were obtained, one of which contained an insertion of an "A" nucleotide at position +215 downstream of the *CLE5* translation start site as well as an insertion of an "A" nucleotide at position +106 downstream of the *CLE6* translation start site. Because each mutation generates a frameshift in the respective *CLE5* or *CLE6* coding sequence upstream of the CLE domain, no functional polypeptides are generated and this *cle5-3 cle6-3* double mutant represents a knockout of both genes.

We next performed a large-scale morphological analysis of Col-0, *cle5-1, cle6-1* and *cle5-3 cle6-3* plants from germination through the vegetative phase of development. We observed no significant differences in leaf initiation rate, total rosette leaf number, mature rosette leaf size, rosette diameter, or flowering time under different photoperiods between Col-0 and *cle5, cle6* or *cle5 cle6* plants. We also analyzed the size, number, composition and morphology of wild-type and mutant rosette leaf cells using scanning electron microscopy (SEM) and histological analysis but detected no differences between the genotypes. WOX1 and PRS promote leaf margin cell file formation (Nakata et al., 2012), with *prs wox1* rosette leaves having fewer and p35S:*PRS* leaves having more margin cell files than wild-type rosette leaves (Fig. S4.2). Because *wox1-1* and *prs-1* plants display reduced *CLE5* and *CLE6* expression, we used SEM to assess whether mutations in *CLE5* and/or *CLE6* caused leaf margin cell file defects. However, we found no reproducible

differences in margin cell file number, morphology or fate between Col-0, *cle5, cle6* and *cle5 cle6* rosette leaves (Fig. S4.2). Thus *CLE5* and *CLE6* separately or together have no macroscopic effects on vegetative development under normal growth conditions.

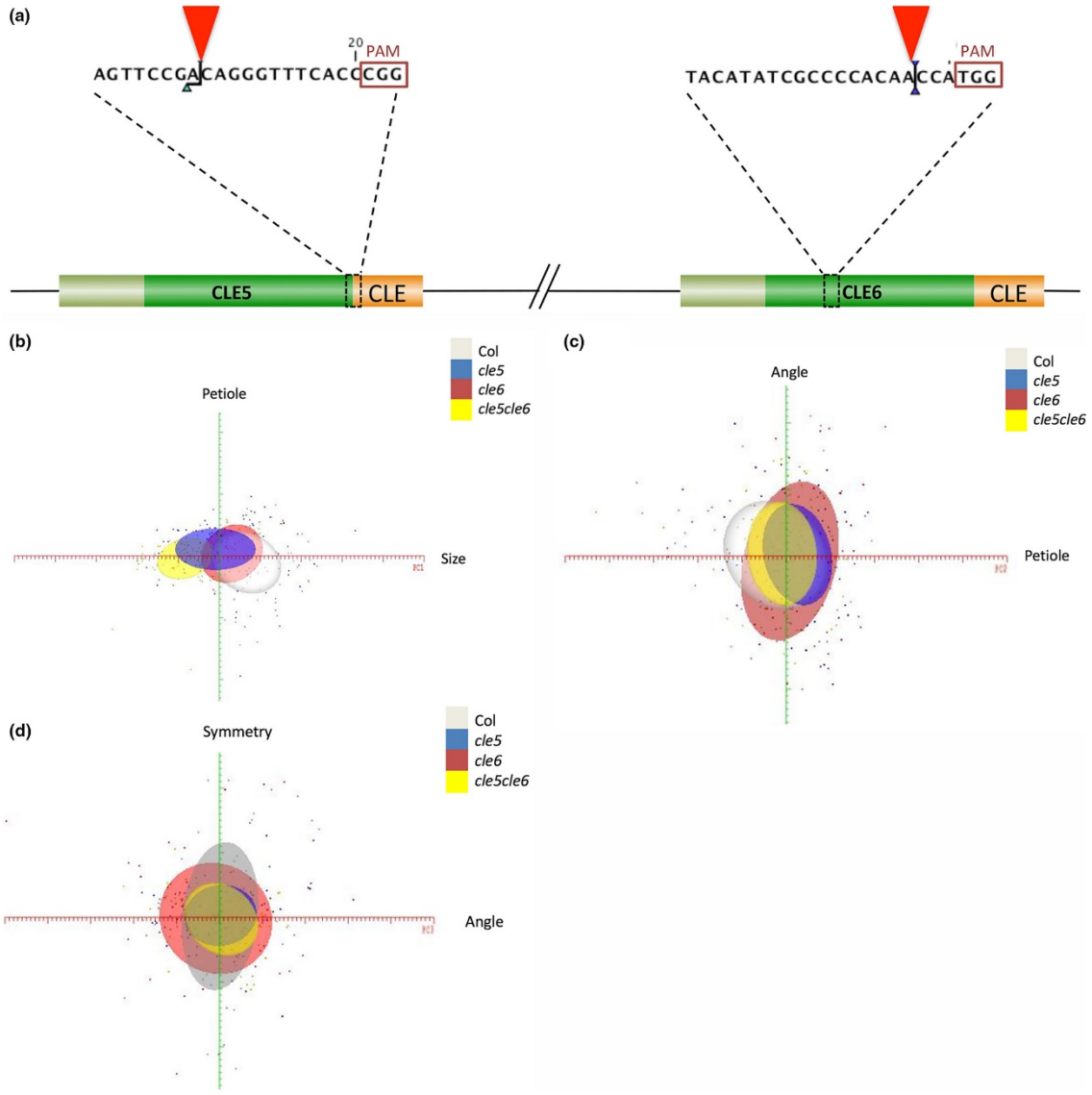

Figure 4.6. *CLE5* and *CLE6* loss-of-function allele generation and role in leaf formation. (a) Locations of the *cle5* and *cle6* CRISPR-Cas9 induced mutations (red arrowheads) upstream of the PAM site (red box) within the sgRNA for the *CLE5* and *CLE6* coding sequences. The coding sequences of the signal peptides are represented in olive, the variable domains in green, and the CLE domains in orange. (b-d) Two-dimensional PC maps generated using ≥5 standard deviations from the mean leaf along the X-axis PC (red) and ≥2.5 standard deviations along the Y-axis PC (green). Each standard deviation is represented by a major tick on the axis, and each leaf measured is represented by a single colored point. (b) Variation along PC1 and PC2 for Col-0 (white oval), *cle5* (blue oval), *cle6* (red oval), and *cle5 cle6* (yellow oval) leaves. (c) Variation along PC2 and PC3 for each genotype. (d) Variation along PC3 and PC4 for each genotype.

Finally, we conducted a leaf morphometric study to identify any subtle phenotypes attributable to the loss of *CLE5* or *CLE6* activity. The LeafAnalyser image processing program (Weight et al., 2008) was used to quantify the shape of Col-0, *cle5-1, cle6-1,* and *cle5-3 cle6-3* first through fourth rosette leaves by performing a principal component (PC) analysis of distinct aspects of overall rosette leaf shape among the different genotypes. LeafAnalyser parsed the major sources of variation in leaf shape into four principal components – leaf size, width, petiole angle, and tip-to-base asymmetry – that together account for 95% of the total Arabidopsis leaf shape variation. Using the LeafAnalyser software we measured each of the four PCs for at least 50 leaves per genotype, and then generated two-dimensional PC maps by plotting the values for each genotype for two of the PCs (leaf size versus width, width versus petiole angle, etc.). Each oval represented one standard deviation from the mean leaf for one genotype, such that the extent of overlap between ovals showed the relative similarity in phenotype.

This morphological analysis revealed modest effects of *CLE5* and *CLE6* on leaf shape (Fig. 4.6b-d). The first component, which accounted for almost 66% of the variation, was overall leaf size and was likely due to leaf age, independent of genotype. The second component was variation in leaf width that accounted for 12% of the variability and was most apparent in the *cle5* and *cle5 cle6* genotypes (Fig. 4.6b). The third component was leaf curvature due to petiole angle and accounted for almost 10% of the total leaf shape variability. This variance was most evident in *cle6* leaves (Fig. 4.6c). The fourth component, leaf symmetry, accounted for 7% of the variability and was detected in both single and double mutants (Fig. 4.6d). While these effects are subtle, they do distinguish possible distinct roles for *CLE5* and *CLE6* in regulating leaf shape during development.

DISCUSSION

Vegetative development is a highly coordinated series of events that starts with a primordium initiated from the shoot apical meristem. This primordium undergoes pattern formation along three polarized axes, the establishment of the basic cell types of the petiole, lamina and marginal structures, and a maturation process that involves cell differentiation and expansion to achieve the mature leaf shape (Bar and Ori, 2014). Long-range hormonal signals such as auxin, GA, and BR are well-characterized players in leaf development; however, their relative ubiquity and omnipresence due to diffusion and active transport likely limit their ability to regulate the highly coordinated and precise events required in organ development alone. While small peptides are known integral signals in plant root and vasculature cell development, we pose a model of CLE signaling that plays a role in regulating shoot organ formation in plants.

Analyses of *CLE* gene expression reveal *CLE5* and *CLE6* promoter activity in the aerial tissues of wild-type Arabidopsis seedlings was uniquely confined to the area around the shoot apex, the base of the lateral organs, and the leaf hydathodes (Jun et al., 2010b). We investigated the expression of *CLE5* and *CLE6* at higher resolution in aerial tissues of wild-type Arabidopsis plants using promoter:*GUS* and *in situ* hybridization (Fig. 4.1). Interestingly, the two closely related genes displayed distinct expression patterns. *CLE6* was expressed exclusively within the adaxial domain of developing rosette leaf primordia, while *CLE5* transcription was restricted to the lateral regions of the primordia but was detected in both the adaxial and abaxial domains. Thus, the upper, outer

periphery of the developing leaves express both *CLE5* and *CLE6*, whereas the underside of the leaf margins expresses only *CLE5* and the midvein region expresses only *CLE6*. Our data show subtle but distinct differences between the *CLE5* and *CLE6* expression patterns despite the high degree of similarity between the two transcription units. The *CLE5* and *CLE6* genes encode precursor proteins with 77% identity and 84% similarity (Sharma et al., 2003), and produce predicted mature CLE peptides with identical amino acid sequences (Cock and McCormick, 2001). The two genes, along with *CLE4* and *CLE7*, lie within a 16.5 kb region on chromosome 2. Within this gene cluster, the *CLE5, CLE6* and *CLE7* coding regions are more similar to one another than to other members of the family, suggesting they may have arisen by local gene duplication events (Cock and McCormick, 2001). Nonetheless, analysis of 1.7 kb of upstream promoter sequence, corresponding to the distance between the *CLE5* stop codon and the *CLE6* start codon, between these three genes shows only 49.6% similarity between the *CLE5* and *CLE6* promoters. This is comparable to the 45.2% similarity between the *CLE5* and *CLE7* promoters, despite *CLE7* expression being restricted to the root (Jun et al., 2010b). Therefore the divergence of the upstream regulatory regions between the *CLE5* and *CLE6* genes may account for the differences in their expression patterns. Still, determining how highly similar peptides are differentially regulated in space and time is crucial to understanding the roles of such signaling molecules in the larger context of plant development.

Our study reveals that *CLE5* and *CLE6* are downstream targets of two transcriptional regulators that affect leaf patterning, BOP1/2 and AS2. Both *CLE5* and *CLE6* are down regulated in *bop1 bop2* seedlings, showing that BOP1 and BOP2 are positive regulators of *CLE5* and *CLE6* transcription (Fig. 4.2). Conversely, an increase in *CLE5/6* transcript levels in *as2-1* seedlings indicates that AS2 negatively regulates *CLE5* and *CLE6* transcription. *AS2* transcripts are present throughout the adaxial leaf domain (Byrne et al., 2000; Iwakawa et al., 2007), whereas *BOP1* and *BOP2* expression is confined to the most proximal end of the adaxial domain (Ha et al., 2004; Norberg et al., 2005). This suggested that BOP1/2 might induce *CLE5/6* transcription at the base of the petiole and AS2 might repress it in more distal positions along the petiole and in the blade. However, *in situ* hybridization experiments indicated that the absence of neither BOP1/2 nor AS2 altered the *CLE6* expression domain (Fig. 4.2), indicating that BOP1/2 and AS2 affect *CLE5* and *CLE6* transcript levels within their native domain rather than establishing the boundaries of their spatial expression domains.

Additional experiments showed that *CLE5* and *CLE6* are differentially regulated by BOP1/2 and AS2. *CLE6* transcription was up-regulated in shoot tissues within 1 hour in response to BOP1-GR translocation (Fig. 4.3), suggesting that *CLE6,* like *AS2*, might be a direct target of BOP1 activation. However, using ChIP-qPCR we detected no BOP1 binding to the *CLE6* (or the *CLE5)* regulatory region (Fig. S4.1). Thus, either the regulation of *CLE6* transcription by the BOP proteins is indirect or additional rate-limiting factors are required for BOP1 binding to the *CLE6* locus. Our data also show that the inductive effect of BOP1 on *CLE6* transcription overcomes the repressive effect of AS2 we observed in the *as2-1* background (Fig. 4.2). This oppositional effect of AS2 and BOP1/2 on *CLE6* expression indicates that a combination of activators and repressors likely controls *CLE* gene transcription in developing leaves.

In contrast to *CLE6, CLE5* expression was not up-regulated upon BOP1-GR translocation (Fig. 4.3), which indicates that BOP1 is sufficient to induce *CLE6* but not *CLE5* transcription in leaves. Based on control experiments (Fig. 4.3), the slight reduction observed in *CLE5* transcript levels is

more likely to be a result of Dex application itself, as has been noted elsewhere (Kang et al., 1999), than of targeted transcriptional regulation by BOP1. Finally, we detected no significant effect on either *CLE5* or *CLE6* transcription in the AS2-GR system (Fig. 4.3**)**. One possible explanation is that over-expression of AS2 alters the expression or activity of its partner AS1. Alternatively, the amount of endogenous AS1 may be a rate-limiting factor for the activity of the complex, rendering the excess AS2 protein unable to affect target gene transcription.

WOX transcription factors are known key components of CLE signaling pathways, and *WOX* transcription factor genes have been linked to the promotion of leaf blade outgrowth in several plant species. These include *LAM1* in *Nicotiana sylvestris* (Lin et al., 2013), *STF* in *Medicago truncatula* (Tadege et al., 2011), *narrow sheath1* and *2* in maize (Nardmann et al., 2004), and *narrow leaf2* and *3* in rice (Ishiwata et al., 2013). In Arabidopsis, the closely related *WOX1* and *PRS* (aka *WOX3*) genes have described roles in leaf development (Nakata et al., 2012), during which their expression is induced by auxin (Caggiano et al., 2017). *prs wox1* leaves display reduced blade outgrowth and fewer margin cell files (Nakata et al., 2012) while *PRS* over-expressor lines show an increase in leaf margin cell file number (Fig. S4.2), indicating that *PRS* and *WOX1* promote blade outgrowth and margin cell file formation. Our expression analysis reveals that both WOX1 and PRS are positive regulators of *CLE5* and *CLE6* transcription (Fig. 4.4). This is consistent with a role for a WOX-CLE signaling module in leaf development and provides further evidence that multiple factors regulate *CLE* gene expression and organize leaf development. Based on the subtle leaf shape defects in *cle5 cle6* seedlings we propose that *CLE5* and *CLE6* may act downstream of *PRS* and *WOX1* in regulating lamina outgrowth. In contrast, no obvious leaf margin cell file phenotype was observed in *cle5* or *cle6* single or double mutant plants (Fig. S4.2), either because *CLE5* and *CLE6* are not required for margin cell development or because their loss is compensated by other *CLE* genes.

In addition to transcriptional regulators, several long-range hormones have well-established roles in plant organ development. GA acts subsequent to initial patterning events to regulate the rate of cell proliferation and expansion during leaf outgrowth (Achard et al., 2009). In addition, auxin, ABA and BL all play roles in regulating the transition from leaf growth by cell division to growth by cell expansion (Kalve et al., 2014). GA is known to promote *CLE6* transcription in the root stele, and ectopic expression of *CLE6* has been shown to partially compensate for GA-deficiency during vegetative growth as well (Bidadi et al., 2014). Our work shows that *CLE5* and *CLE6* are indeed responsive to GA in shoot tissues, as well as to BL and IAA (Fig. 4.5). *CLE5* and *CLE6* expression is slightly induced by GA (Fig. 4.5), which promotes leaf differentiation, and thus the *CLE* genes may act downstream of GA (and/or other hormones) during the later stages of leaf differentiation to achieve the mature leaf morphology.

The transcription of both *CLE5* and *CLE6* is also auxin responsive, with *CLE6* responding more strongly to IAA application than *CLE5* (Fig. 4.5). Interestingly, simultaneous BOP1-GR induction and auxin application resulted in differential effects on *CLE5* and *CLE6* transcription. Whereas *CLE5* mRNA expression levels were slightly reduced, *CLE6* transcription levels were elevated in the presence of both BOP1 and auxin (Fig. 4.5). These data reveal that *CLE5* and *CLE6* undergo differential regulation by BOP1 and phytohormones, again indicating that a combination of activators and repressors are required to control *CLE* gene expression in developing leaves.

Although gross morphological phenotypes were not visible in *cle5/6* single or double mutant plants, more sensitive morphometric analysis showed that the two genes affect the final shape of the rosette leaves. Specifically, variation in leaf petiole width (PC2) accounted for 12% of the variability in leaf shape and was most apparent in the *cle5* and *cle5 cle6* genotypes (Fig. 4.6**)**. This subtle effect on petiole width is reminiscent of the blade-on-petiole phenotype of *bop* leaves, where formation of ectopic blade tissue along the petiole results in a wider than normal leaf base (Ha et al., 2003; Ha et al., 2007). Thus, the regulation of *CLE5* and *CLE6* expression by the BOP proteins appears to be important for fine-tuning leaf formation by limiting the lateral growth of the petiole. Collectively, our data are consistent with a scenario in which BOP1/2, AS2, PRS/WOX1 and phytohormones act combinatorially to modulate *CLE5* and *CLE6* transcription at the leaf base to levels appropriate to produce the final leaf shape, although additional experiments will be necessary to fully clarify the relationships between these various factors. A role for *CLE5* and *CLE6* in regulating the activity of differentiating cells during the later stages of leaf development contrasts with that of most other *CLE* genes functionally characterized to date, which predominantly affect undifferentiated, meristematic cells (Fletcher et al., 1999; Hirakawa et al., 2008; Whitford et al., 2008; Stahl et al., 2009; Gutierrez-Alanis et al., 2017).

The fact that two genes that encode identical CLE peptides are expressed in overlapping but not identical patterns and are differentially regulated by upstream hormones and transcription factors may be an evolutionary artifact or may have functional significance. To date we have not observed a unique function for either *CLE5* or *CLE6* in organ development. However, overlapping domains of genes expressing secreted peptides may contribute to dose-dependent signaling events that functional analysis at the level of single cells may be required to uncover. Such multiple independent yet cross-talking regulatory mechanisms may provide the range of distinct signaling events required for the highly coordinated development of an organ with three polar axes and multiple specific cell types.

Supporting Information

Additional Supporting Information may be found in the online version of this article.

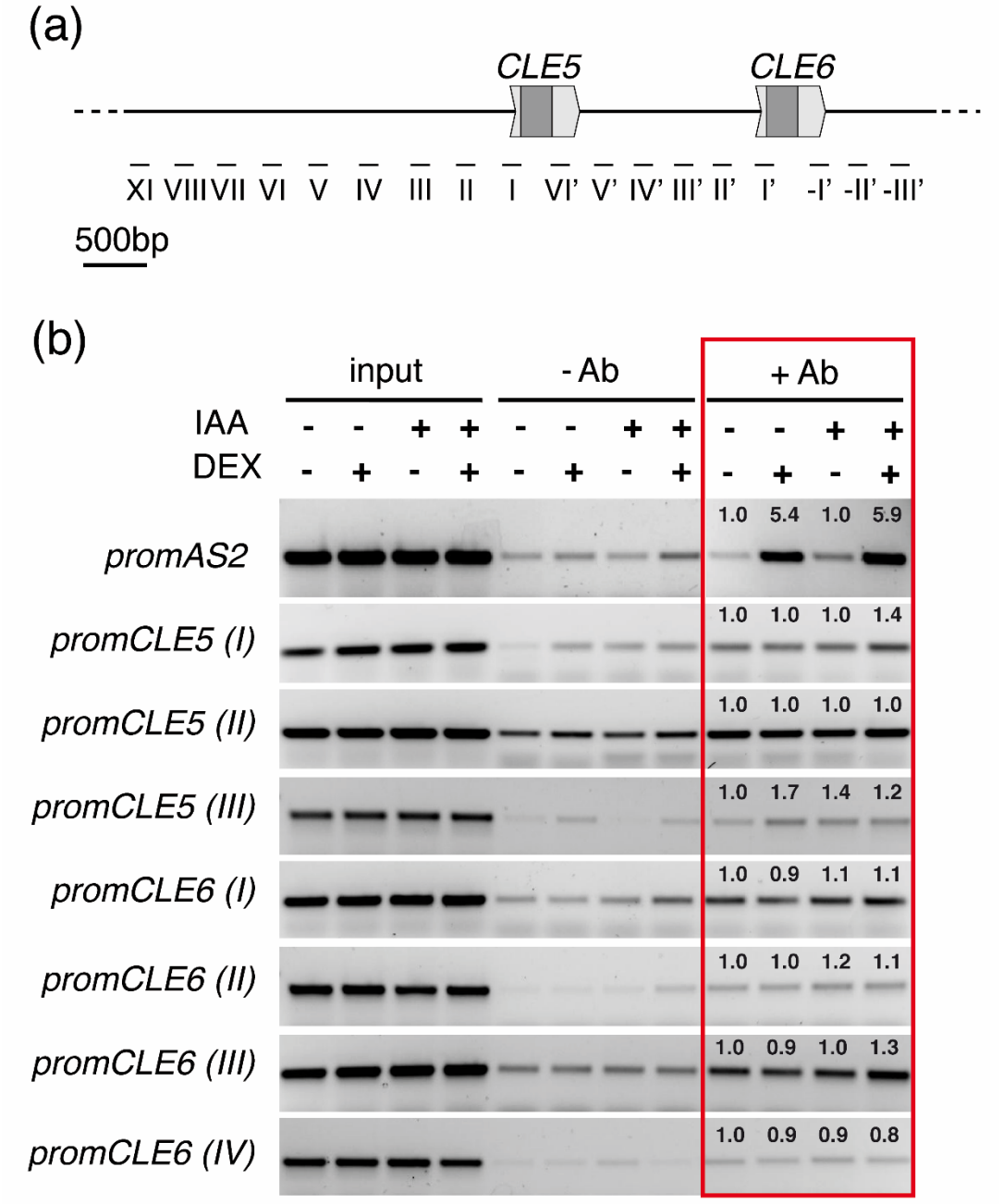

Figure S4.1. Absence of BOP1-GR protein binding to *CLE5* or *CLE6* regulatory regions.

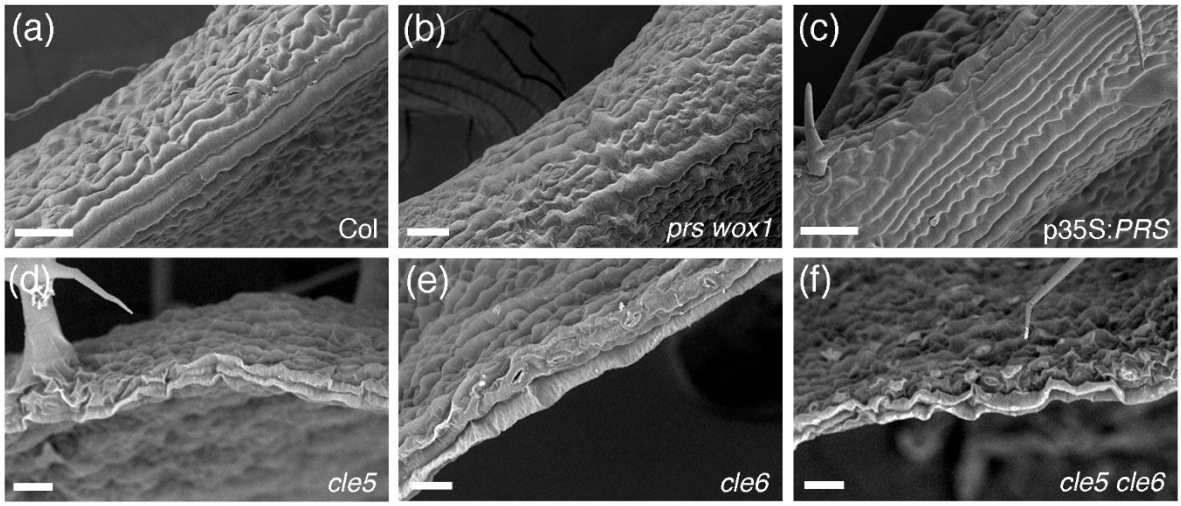

Figure S4.2. Margin cell layer files in wild-type and mutant rosette leaves.

Table S4.1. Primer sequences used in the study.

Name	Sequence
Cloning	
pBOP1(-5797) FW	5'- TGGGAAGCGGAGTGTAATTC
pBOP1 RV	5'- CATAGCTCCTTTGTTGATTTCTTTGATAC
pBOP1:CLE6 FW	5'- CAAAGAAATCAACAAAGGAGCTATGGCGAATTTGATCCTTAAGC
CLE6_CDS+Stop RV	5'- TCAATGGTGTTGTGGATCAG
T7_promoter	5'- TAATACGACTCACTATAG
pCR8_FW	5'- GTTTTCCCAGTCACGACGTT
CLE5 P1	5'- GATTGACACGGCACGATATGAACGG
CLE5 P2	5'- AAACCCGTTCATATCGTGCCGTGTC
CLE6 P1	5'- GATTGCCCCACAACCATGGGCGATA
CLE6 P2	5'- AAACTATCGCCCATGGTTGTGGGGC
RT-qPCR	
CLE5 FW	5'- GCTCGAATCCTCCGTTCATA
CLE5 RV	5'- TCGCCTCTCGTTATGACCTT
CLE6 FW	5'- CGTGAACTCGGGATTGATCT
CLE6 RV	5'- CAATGGTGTTGTGGATCAGG
PRS FW	5'- ACGGAGAATGAGTCCTGTGG
PRS RV	5'- TGTTGTATCTGCACCGCATT
WOX1 FW	5'- TTCCTCCAACATGTCCAACA
WOX1 RV	5'- TGTGTTCGTTGCTTCTCTCG
IAA5 FW	5'- TCACCGAACTACGGCTAGGT
IAA5 RV	5'- ACACATTCACTTTCCTTCAACG
MON1 FW	5'- AACTCTATGCAGCATTTGATCCACT
MON1 RV	5'- TGATTGCATATCTTTATCGCCATC
AtBT (tubulin) FW	5'- TGGGAACTCTGCTCATATCT
AtBT (tubulin) RV	5'- GAAAGGAATGAGGTTCACTG
ChIP-qPCR	
pAS2 FW	5'- AATGCAATATGCAACCACGA
pAS2 RV	5'- CTAACGAAGAAGCGTGCAAA
pCLE5 I FW	5'- CCCACTCATGACCCAAACTT
pCLE5 I RV	5'- GGGTGGGAGTTGAGAGAGAG
pCLE5 II FW	5'- TCCTAGTGAACCTTATGTCAAGCA
pCLE5 II RV	5'- AACGCTCGGAATTCTCATCA
pCLE5 III FW	5'- CAAACCTGAAAATCATCAGAATG
pCLE5 III RV	5'- TGGACGAAAACAATTGTACCTG
pCLE5 IV FW	5'- GAGCTTTCCAAAGCCAAAAA
pCLE5 IV RV	5'- CGGTAAAATGTTTTGGTCCAT
pCLE5 V FW	5'- CGGTCCCCTAAAACATAATACG
pCLE5 V RV	5'- TGTGTTTCTTTTTGTAGAAACATTG
pCLE5 VI FW	5'- TGCTTGGTTTATTTGGTTTCA
pCLE5 VI RV	5'- TGTTGCAAATGCCACTTTCT

pCLE5 VII FW	5’- AAGCAGAAGAATGGTTTGACA
pCLE5 VII RV	5’- GGGAGACGAAGAAGCAGTTG
pCLE5 VIII FW	5’- ATTCGCAGTTGAATCGCATA
pCLE5 VIII RV	5’- AATAGTTCAGCGCGTCATCA
pCLE5 IX FW	5’- TGTGGGCATGTTTTCATTTC
pCLE5 IX RV	5’- CTCAACGGCGAGAAACAAAT
pCLE5 X FW	5’- CAACCGAATAAAAGTGAGAATGG
pCLE5 X RV	5’- TGCCACTCAACAACCACATT
pCLE5 XI FW	5’- CCGACGACGACTAACTGTCA
pCLE5 XI RV	5’- TGCTCTTTGATTCGGTTTGA
pCLE6 I’ FW	5’- TCCTTAACCTGTTCCCGTTTT
pCLE6 I’ RV	5’- TCGCCATTAAAGGTGATTAAGAA
pCLE6 II’ FW	5’- TTTCGATCGTTAAGGGTCAACT
pCLE6 II’ RV	5’- GCCGAATCCTACGCATATTT
pCLE6 III’ FW	5’- ACCGCAAAAGAAATCCATGA
pCLE6 III’ RV	5’- TCGAAATTCTCAGGTGGAAA
pCLE6 IV’ FW	5’- TTGATCGGCTATCCTCAGAA
pCLE6 IV’ RV	5’- GCAATGGAGTCATCTTTGTAGG
pCLE6 V’ FW	5’- GATTGGACGTCTTAGCACTTCA
pCLE6 V’ RV	5’- TTCGAATTAACCCTCTAAAACCTC
pCLE6 VI’ FW	5’- CCGAAGATCCAAGCACAAAT
pCLE6 VI’ RV	5’- TGTGGTACAAGGATACCAAAACC
pCLE6 –I’ FW	5’- AGTGGATTCCGAAAGGGTTT
pCLE6 –I’ RV	5’- TGACTTGCATGGATCAGTCAC
pCLE6 –II’ FW	5’- TTGGCTATTTCCCCTGTCTTT
pCLE6 –II’ RV	5’- ATCAGCTGAAAAGCATGCAA
pCLE6 –III’ FW	5’- TCTGCCACCAGTTGAAAAGA
pCLE6 –III’ RV	5’- TCCTGTTGCCATGAAAAGAA

Genotyping	
CLE5CR_FW	5’- AACGATTAAAACCGGGGAAC
CLE5CR_RV	5’- AACGATTAAAACCGGGGAAC
CLE6CR_FW	5’- TTTCGATCGTTAAGGGTCAACT
CLE6CR_RV	5’- GCCAATCGCTGTTACAAAAA
sgRNA_FW	5’- AGAAGAGAAGCAGGCCCATT
sgRNA_RV	5’- TTCCCAAGGTCCAAAGACAC

CHAPTER V

CONCLUDING THOUGHTS AND OUTLOOK

In the previous chapters, I discussed the importance of intercellular communications in determining cell fate and tissue organization in planta, and introduced the CLE peptides, an important family of small signaling polypeptides that contributes to various developmental processes that shape plant form and function. I then followed up with a series of experiments that demonstrated the expression and function of several *CLE* genes during shoot development of the mustard plant Arabidopsis thaliana. Specifically, *CLE16*, *CLE17*, and *CLE27* are expressed at the shoot apex. Without any obvious biological activity by themselves, *CLE16* and *CLE17* work together with *CLV3* to control stem cell fate and proliferation. Their cooperation directly affects multiple aspects of plant architecture, including fruit production and branching. I then switched the view from the shoot apex to the leaf, where *CLE5* and *CLE6* are expressed and exert subtle control on leaf morphology under the influence of transcription factors and phytohormones. As a whole, this work sheds light on a complex network of interacting factors, whose identity are yet to be fully revealed, and whose interdependency buffers stem cell homeostasis and determines overall plant architecture.

Much remains to be done to comprehensively identify suites of CLE ligands acting in any given tissue and how their signals are transduced by their cognate receptors. For example, it is likely that a combination of binding affinity, spatiotemporal co-expression pattern, and cross-regulation among downstream signaling pathways determine how a given receptor kinase can interact with a particular set of CLE peptides but not others. Biochemical analyses have recently begun to shed light on the relationship between peptide sequences, binding affinity, and bioactivity of CLE ligands. For example, modifications in the CLV3 peptide sequence led to the generation of a bifunctional peptide that can interact with both CLV1 and TDR, and exhibits both the SAM-restricting characteristic of CLV3, and the vascular-promoting effect of TDIF/CLE41/CLE44 (Hirakawa et al., 2017). Our detailed functional dissection of multiple CLE peptides in the shoot will serve as an important resource to understand how the substitution of a few important amino acids can lead to fine-tuned divergence in their signaling pathway and biological significance.

While *Arabidopsis thaliana* remains an essential model in studying gene functions in land plants, emphasis must be placed on the evolution and diversification of any given gene family. Functional analysis of CLE peptide ligands across a wide range of model organisms will become increasingly important as systematic genome-wide analyses continue to identify *CLE* gene families in agriculturally valuable crop species. Recently, 84 *CLE* peptide-encoding genes were identified in soybean CLE45n *(Glycine max)* and 44 in common bean *(Phaseolus vulgaris)* (Hastwell et al., 2015). Phylogenetic analyses of the soybean, common bean and Arabidopsis pre-propeptide sequences yielded seven distinct groups based on their CLE domain sequence and predicted function, enabling the distinguishing of soybean and common bean orthologs of the Arabidopsis CLV3, CLE40 and the TDIF peptides. In poplar *(Populus trichocarpa),* genome-wide analysis identified a total of 50 *CLE* genes (Han et al., 2016), adding 24 genes to those found in a previous study (Oelkers et al., 2008). The first systematic analysis of *CLE* genes in gymnosperms identified 93 *CLE* genes among eight conifer species (Strabala et al., 2014). In this case, only the TDIF peptide sequence was completely conserved between gymnosperms and angiosperms. Two TDIF

orthologs from *Pinus radiata* were shown to be expressed in the root and in the phloem of the inflorescence stem, suggesting a possible conserved role for TDIF peptides in regulating vascular cambium development between dicots and conifers whose ancestors diverged over 270 million years ago (Bowe et al., 2000).

In addition, a phenetic method was used to identify 1628 *CLE* genes from 57 different plant genomes (Goad et al., 2016). This study found two additional *CLE* genes in soybean, two in poplar, and 19 more in maize *(Zea mays)* than previously reported (Je et al., 2016). Up to nine *CLE* genes were identified in mosses and lycophytes, but none were detected in green algae. Clustering analysis based on the full pre-propeptide sequences generated 12 groups of CLE proteins sequences, with CLE peptides known to be involved in meristem activity, vascular development or nodulation clustering together.

Despite more than two decades of research, our current understanding of CLE signaling in planta can only be said to be in its nascence. Already we are seeing both conservation and variation of the CLE ligand-receptor pathway in disparate plant lineages. In maize, the CLE peptide ZmFCP1 signals through the receptor-kinases FEA2 and FEA3 to control shoot meristem size (Je et al., 2016) (Fig. A.1). However, while both *ZmFEA2* and *ZmFEA3* are expressed within the domains of the SAM, *ZmFCP1* is expressed only in the flanking organ primordia. Thus, a CLE signal is able to travel from nearby differentiated tissues towards the SAM to regulate stem cell identity there. There is already a host of evidence indicating feedback from lateral organs play an important role in modulating SAM activity, either via mobile transcription factors or phytohormone pathways (Corbesier et al., 2007; Shi et al., 2018). What significance this CLE-mediated communication might have with regards to tuning plant growth to environmental context remains to be seen. Furthermore, a recent study indicates that in addition to ZmFCP1, ZmFEA2 responds to another CLE peptide, ZmCLE7. Signal transduction of ZmFCP1 and ZmCLE7 depends upon separate cofactors of ZmFEA2, with the former occurring through the pseudokinase ZmCRN, and the later through the heterotrimeric G protein alpha subunit COMPACT PLANT2 (ZmCT2) (Je et al., 2017). The maize *TD1* gene is expressed in lateral organ primordia, and encodes an ortholog of AtCLV1 that is also involved in controlling IFM size, although which CLE peptide(s) it responds to remain to be discovered (Bommert et al., 2005). Multiple CLE signaling is also observed in the tomato SAM, where both SlCLV3 and SlCLE9 are both perceived by SlCLV1 to restrict stem cell accumulation (Rodriguez-Leal et al., 2019) (Fig. A.2). The relationship between these two peptides in tomato is similar to that between Arabidopsis CLV3 and CLE16/17, where SlCLV3 is the dominant signal, and SlCLE9 buffers for the loss of SlCLV3 activity.

The advent of genome engineering through the CRISPR-Cas9 system (Feng et al., 2013; Nekrasov et al., 2013) has the potential to dramatically accelerate our understanding of *CLE* gene function in plants. Unlike other methods such as TILLING (McCallum et al., 2000) or transposon mutagenesis, the small size of the *CLE* coding sequences is not an impediment to generating null mutations using the CRISPR-Cas9 system. Moreover, multiple *CLE* genes that show tight genetic linkage and/or strongly overlapping expression patterns can be targeted simultaneously, helping to surmount the widespread functional redundancy that occurs among *CLE* family members (Jun et al., 2010). The application of genome editing to *CLE* genes in both model plants and crop systems will provide valuable new insights into the mechanisms of cell-to-cell communication in plants as well as an expanded toolkit for augmenting crop plant growth and resilience in response to global climate change.

Practically speaking, due to the ability of each receptor to perceive many different signals, their mutations can lead to extreme phenotypes such as the stunted development and sterility of *bam1/2/3* plants (DeYoung et al., 2006). In contrast, the *CLE* genes serve as more amenable targets that can be modulated to generate subtler enhancements in yield traits. Recently, several mutant lines were generated using CRISPR-Cas9 gene editing with variations in the cis-regulatory sequence of SlCLV3, resulting in a wide continuum of quantitative phenotypes, including inflorescence branching and fruit size. (Rodriguez-Leal et al., 2017). Multiplex CRISPR/Cas9 gene editing can be used to quickly generate high-order *cle* mutants, as in the instance of the *dodeca-cle* mutant in Arabidopsis (Rodriguez-Leal et al., 2019). However, care must be taken in considering which genes to target for maximal efficiency. To this end, a scheme combining synthetic peptide treatments on varied genetic backgrounds such as one used in this work can be utilized not just for peptide function validation, but also to narrow down candidate ligands that have biological roles in a given tissue type. Thus, functional characterization of different CLE peptides within a given tissue, such as those presented in this work, exponentially increases the repertoire of targets that can be modified to improve quantitative traits of interest.

In addition to functional characterization in higher plants, recent efforts have elucidated the ancestral role of CLE signaling in the moss *Physcomitrella patens* and the liverwort *Marchantia polymorpha*, two representative members of the Bryophyta, a paraphyletic group consisting of the earliest diverging lineages of land plants. The Marchantia genome encodes two CLE homologs, *MpCLE1* and *MpCLE2*, with the former being an ortholog of Arabidopsis *TDIF/CLE41/CLE44*. *MpCLE1* has recently been demonstrated to signal through the MpTDR receptor to affect the proliferation and division plane of the apical notch stem cells, as well as the morphology of reproductive structures, suggesting that the role of CLE peptides in regulating meristematic activity is conserved in land plants (Hirakawa et al., 2019) (Fig. A.3).

Nine CLE sequences are present in Physcomitrella genome, *PpCLE1-9*, along with three CLE receptor-encoding genes, *PpCLV1a*, *PpCLV1b*, and *PpRPK2*. Their functions are implicated in the transition between two modes of growth, from one in which protonemal filaments spread in a 2-D manner, into the other in which 3-D leafy structures called gametophores are initiated from the filaments (Fig. A.4). This transition from 2-D to 3-D growth is an important evolutionary feature that allows for the adaptation of plants to terrestrial life. Mutants with disrupted CLE signaling exhibit defects in the early division plane orientation required for gametophore development, as well as the regulation of apical cell identity in this leafy shoot (Whitewoods et al., 2017). Given that functional CLE sequences have not been identified in the more basal aquatic algae, which grow strictly in 2-D, CLE signaling is hypothesized to be one of the essential elements in the evolution of 3-D growth in land plants. Interestingly, the moss genomes also contain three WOX homologs, *PpWOX13La*, *b*, and *c*. Functional studies of *PpWOX13La/b* place them outside of the CLE signaling pathway, while the role *PpWOX13Lc* is not yet known (Sakakibara et al., 2014). The only proteins known to transduce CLV signal are the *Arabidopsis* POL and PLL1 protein phosphatases (Song et al., 2006). The HAM proteins are also emerging as conserved co-factors of WOX proteins, and play an important role in stem cell specification (Zhou et al., 2015). *POL* and *HAM* each has one homolog in *Physcomitrella* genome, but their biological functions are unknown (Rensing et al., 2008; Engstrom, 2011). Further research should be done to address their potential to be ancestral downstream elements of CLE signal transduction before the WOX proteins are integrated into the pathway. Thus, beyond its agricultural and commercial implications, systematic

identification and functional characterization of CLE peptides and their targets provide us with a powerful tool to investigate the architectural evolution in land plants.

The diversity of forms is inseparable from the conservation and divergence of gene families. The signals, the receptors, and the regulators, all constantly mutating, yet invariably intertwined in a dynamic pattern in every lifeform. Beneath their appearances, a humble mustard plant is every bit as intricate as a majestic sequoia, both resulting from millennia of evolutions, and both relying on the same principles to grow and thrive in their own ecological niche. Along with the continual expansion of genomic data that allows us to investigate new model organisms, functional studies will bring us ever closer to understanding the fundamental, molecular conversation that continues to shape and sustain life on Earth.

REFERENCES

Aichinger, E., Kornet, N., Friedrich, T., and Laux, T. (2012). Plant Stem Cell Niches. Annu. Rev. Plant Biol. **63**: 615–36.

Abe, M., Kobayashi, Y., Yamamoto, S., Daimon, Y., Yamaguchi, A., Ikeda, Y., Ichinoki, H., Notaguchi, M., Goto, K., and Araki, T. (2005). FD, a bZIP protein mediating signals from the floral pathway integrator FT at the shoot apex. Science (80-.). **309**: 1052–1056.

Abe, M., Kosaka, S., Shibuta, M., Nagata, K., Uemura, T., Nakano, A., and Kaya, H. (2019). Transient activity of the florigen complex during the floral transition in arabidopsis thaliana. Dev. **146**: dev171504.

Aida, M., Beis, D., Heidstra, R., Willemsen, V., Blilou, I., Galinha, C., Nussaume, L., Noh, Y.S., Amasino, R., and Scheres, B. (2004). The PLETHORA genes mediate patterning of the Arabidopsis root stem cell niche. Cell **119**: 109–120.

Alonso, J.M. et al. (2003). Genome-wide insertional mutagenesis of Arabidopsis thaliana. Science (80-.). **301**: 653–657.

Anne, P., Amiguet-Vercher, A., Brandt, B., Kalmbach, L., Geldner, N., Hothorn, M., and Hardtke, C.S. (2018). CLERK is a novel receptor kinase required for sensing of root-active CLE peptides in arabidopsis. Dev. **145**.

Araya, T., Miyamoto, M., Wibowo, J., Suzuki, A., Kojima, S., Tsuchiya, Y.N., Sawa, S., Fukuda, H., Von Wirén, N., and Takahashi, H. (2014). CLE-CLAVATA1 peptide-receptor signaling module regulates the expansion of plant root systems in a nitrogen-dependent manner. Proc. Natl. Acad. Sci. U. S. A. **111**: 2029–2034.

Achard, P., Gusti, A., Cheminant, S., Alioua, M., Dhondt, S., Coppens, F., Beemster, G.T.S., and Genschik, P. (2009). Gibberellin Signaling Controls Cell Proliferation Rate in Arabidopsis. Curr. Biol. **19**: 1188–1193.

Bar, M. and Ori, N. (2014). Leaf development and morphogenesis. Dev. **141**: 4219–4230.

Barton, M.K. (2010). Twenty years on : The inner workings of the shoot apical meristem, a developmental dynamo. Dev. Biol. **341**: 95–113.

Bedford, M.T. and Clarke, S.G. (2009). Protein Arginine Methylation in Mammals: Who, What, and Why. Mol. Cell **33**: 1–13.

Bergeron, J.J.M., Di Guglielmo, G.M., Dahan, S., Dominguez, M., and Posner, B.I. (2016). Spatial and Temporal Regulation of Receptor Tyrosine Kinase Activation and Intracellular Signal Transduction. Annu. Rev. Biochem. **85**: 573–597.

Betsuyaku, S., Takahashi, F., Kinoshita, A., Miwa, H., Shinozaki, K., Fukuda, H., and Sawa, S. (2011). Mitogen-activated protein kinase regulated by the CLAVATA receptors contributes to shoot apical meristem homeostasis. Plant Cell Physiol. **52**: 14–29.

Bidadi, H., Matsuoka, K., Sage-Ono, K., Fukushima, J., Pitaksaringkarn, W., Asahina, M., Yamaguchi, S., Sawa, S., Fukuda, H., Matsubayashi, Y., Ono, M., and Satoh, S. (2014). CLE6 expression recovers gibberellin deficiency to promote shoot growth in Arabidopsis. Plant J. **78**: 241–252.

Bilsborough, G.D., Runions, A., Barkoulas, M., Jenkins, H.W., Hasson, A., and Galinha, C. (2011). Model for the regulation of Arabidopsis thaliana leaf margin development. Proc. Natl. Acad. Sci. **108**: 3424–3429.

Blackwell T.K., Kretzner L., Blackwood E.M., Eisenman R.N., Weintraub H. (1990). Sequence-specific DNA binding by the c-Myc protein. Science. **250**: 1149–1151.

Bleckmann, A., Weidtkamp-Peters, S., Seidel, C. a M., and Simon, R. (2010). Stem cell signaling in Arabidopsis requires CRN to localize CLV2 to the plasma membrane. Plant Physiol. **152**: 166–76.

Bommert, P., Je, B. Il, Goldshmidt, A., and Jackson, D. (2013). The maize Gα gene COMPACT PLANT2 functions in CLAVATA signalling to control shoot meristem size. Nature **502**: 555–8.

Bommert, P., Lunde, C., Nardmann, J., Vollbrecht, E., Running, M., Jackson, D., Hake, S., and Werr, W. (2005). thick tassel dwarf1 encodes a putative maize ortholog of the Arabidopsis CLAVATA1 leucine-rich repeat receptor-like kinase. Development **132**: 1235–1245.

Bowe, L.M., Coat, G., and DePamphilis, C.W. (2000). Phylogeny of seed plants based on all three genomic compartments: Extant gymnosperms are monophyletic and Gnetales' closest relatives are conifers. Proc. Natl. Acad. Sci. U. S. A. **97**: 4092–4097.

Brand, U., Fletcher, J.C., Hobe, M., and Meyerowitz, E.M. (2000). Dependence of Stem Cell Fate in Arabidopsis on a Feedback Loop Regulated by CLV3 Activity. Science (80-.). **289**: 617–619.

Brand, U., Gru, M., and Hobe, M. (2002). Regulation of CLV3 Expression by Two Homeobox Genes in Arabidopsis. Plant Physiol. **129**: 565–575.

Breuninger, H., Rikirsch, E., Hermann, M., Ueda, M., and Laux, T. (2008). Differential Expression of WOX Genes Mediates Apical-Basal Axis Formation in the Arabidopsis Embryo. Dev. Cell **14**: 867–876.

Busch, W. et al. (2010). Transcriptional control of a plant stem cell niche. Dev. Cell **18**: 841–853.

Byrne, M.E., Barley, R., Curtis, M., Arroyo, J.M., Dunham, M., Hudson, a, and Martienssen, R. a (2000). Asymmetric leaves1 mediates leaf patterning and stem cell function in Arabidopsis. Nature **408**: 967–971.

Byrne, M.E., Simorowski, J., and Martienssen, R. a (2002). ASYMMETRIC LEAVES1 reveals knox gene redundancy in Arabidopsis. Development **129**: 1957–1965.

Cadigan, K.M., Fish, M.P., Rulifson, E.J., and Nusse, R. (1998). Wingless repression of Drosophila frizzled 2 expression SHAPES THE wingless morphogen gradient in the wing. Cell **93**: 767–777.

Caggiano, M.P., Yu, X., Bhatia, N., Larsson, A., Ram, H., Ohno, C.K., Sappl, P., Meyerowitz, E.M., Jönsson, H., and Heisler, M.G. (2017). Cell type boundaries organize plant development. Elife **6**: e27421.

Caño-Delgado, A., Yin, Y., Yu, C., Vefeados, D., Mora-García, S., Cheng, J.C., Nam, K.H., Li, J., and Chory, J. (2004). BRL1 and BRL3 are novel brassinosteroid receptors that function in vascular defferentiation in Arabidopsis. Development **131**: 5341–5351.

Cao, X., Wang, J., Xiong, Y., Yang, H., Yang, M., Ye, P., Bencivenga, S., Sablowski, R., Jiao, Y. (2020). A self-activation loop maintains meristematic cell fate for branching. Curr. Biol. **30**:1-12.

Carles, C.C. and Fletcher, J.C. (2009). The SAND domain protein ULTRAPETALA1 acts as a trithorax group factor to regulate cell fate in plants. Genes Dev. **23**: 2723–2728.

Carles, C.C., Lertpiriyapong, K., Reville, K., and Fletcher, J.C. (2004). The ULTRAPETALA1 gene functions early in Arabidopsis development to restrict shoot apical meristem activity and acts through WUSCHEL to regulate floral meristem determinacy. Genetics **167**: 1893–1903.

Casamitjana-Martínez, E., Hofhuis, H.F., Xu, J., Liu, C.-M., Heidstra, R., and Scheres, B. (2003). Root-Specific CLE19 Overexpression and the sol1/2 Suppressors Implicate a CLV-like Pathway in the Control of Arabidopsis Root Meristem Maintenance. Curr. Biol. **13**: 1435–1441.

Chen, M., Wilson, R.L., Palme, K., Ditengou, F.A., and Shpak, E.D. (2013). ERECTA Family Genes Regulate Auxin Transport in the Shoot Apical Meristem and Forming. **162**: 1978–1991.

Clark, S.E., Jacobsen, S.E., Levin, J.Z., and Meyerowitz, E.M. (1996). The CLAVATA and SHOOT MERISTEMLESS loci competitively regulate meristem activity in Arabidopsis. Development **122**: 1567–1575.

Clark, S.E., Running, M.P., and Meyerowitz, E.M. (1993). CLAVATA1 , a regulator of meristem and flower development in Arabidopsis. **418**: 397–418.

Clark, S., Running, M., and Meyerowitz, E. (1995). *CLAVATA3* is a specific regulator of shoot and floral meristem development affecting the same processes as *CLAVATA1*. Development **121**: 2057–2067.

Clark, S.E., Williams, R.W., and Meyerowitz, E.M. (1997). The CLAVATA1 gene encodes a putative receptor kinase that controls shoot and floral meristem size in Arabidopsis. Cell **89**: 575–585.

Clough, S.J. and Bent, A.F. (1998). Floral dip: A simplified method for Agrobacterium-mediated transformation of Arabidopsis thaliana. Plant J. **16**: 735–743.

Cock, J.M. and McCormick, S. (2001). A large family of genes that share homology with CLAVATA3. Plant Physiol. **126**: 939–942.

Corbesier, L., Vincent, C., Jang, S., Fornara, F., Fan, Q., Searle, I., Giakountis, A., Farrona, S., Gissot, L., Turnbull, C., and Coupland, G. (2007). FT protein movement contributes to long-distance signaling in floral induction of Arabidopsis. Science (80-.). **316**: 1030–1033.

Czechowski, T., Stitt, M., Altmann, T., Udvardi, M.K., and Scheible, W.-R. (2005). Genome-Wide Identification and Testing of Superior Reference Genes for Transcript Normalization in Arabidopsis. Plant Physiol. **139**: 5–17.

Daum, G., Medzihradszky, A., Suzaki, T., and Lohmann, J.U. (2014). A mechanistic framework for noncell autonomous stem cell induction in Arabidopsis. Proc. Natl. Acad. Sci. U. S. A. **111**: 14619–14624.

Depuydt, S., Rodriguez-Villalon, A., Santuari, L., Wyser-Rmili, C., Ragni, L., and Hardtke, C.S. (2013). Suppression of Arabidopsis protophloem differentiation and root meristem growth by CLE45 requires the receptor-like kinase BAM3. Proc. Natl. Acad. Sci. U. S. A. **110**: 7074–9.

DeYoung, B.J., Bickle, K.L., Schrage, K.J., Muskett, P., Patel, K., and Clark, S.E. (2006). The CLAVATA1-related BAM1, BAM2 and BAM3 receptor kinase-like proteins are required for meristem function in Arabidopsis. Plant J. **45**: 1–16.

DeYoung, B.J. and Clark, S.E. (2008). BAM receptors regulate stem cell specification and organ development through complex interactions with CLAVATA signaling. Genetics **180**: 895–904.

Diévart, A., Dalal, M., Tax, F.E., Lacey, A.D., Huttly, A., Li, J., and Clark, S.E. (2003). CLAVATA1 Dominant-Negative Alleles Reveal Functional Overlap Between Multiple Receptor Kinases that Regulate Meristem and Organ Development. Plant Cell **15**: 1198–1211.

Dobrenel, T., Caldana, C., Hanson, J., Robaglia, C., Vincentz, M., Veit, B., and Meyer, C. (2016). TOR Signaling and Nutrient Sensing. Annu. Rev. Plant Biol. **67**: 261–285.

Doebley, J.F., Gaut, B.S., and Smith, B.D. (2006). The Molecular Genetics of Crop Domestication. Cell **127**: 1309–1321.

Dolzblasz, A., Nardmann, J., Clerici, E., Causier, B., van der Graaff, E., Chen, J., Davies, B., Werr, W., and Laux, T. (2016). Stem Cell Regulation by Arabidopsis WOX Genes. Mol. Plant **9**: 1028–1039.

Durbak, A.R. and Tax, F.E. (2011). CLAVATA Signaling Pathway Receptors of Arabidopsis Regulate Cell Proliferation in Fruit Organ Formation as well as in Meristems. Genetics **189**: 177–194.

Elliott, R.C., Betzner, A.S., Huttner, E., Oakes, M.P., Tucker, W.Q.J., Gerentes, D., Perez, P., and Smyth, D.R. (1996). AINTEGUMENTA, an APETALA2-like gene of arabidopsis with pleiotropic roles in ovule development and floral organ growth. Plant Cell **8**: 155–168.

Endo, S., Shinohara, H., Matsubayashi, Y., and Fukuda, H. (2013). A novel pollen-pistil interaction conferring high-temperature tolerance during reproduction via CLE45 signaling. Curr. Biol. **23**: 1670–1676.

Endrizzi, K., Moussian, B., Haecker, A., Levin, J.Z., and Laux, T. (1996). The SHOOT MERISTEMLESS gene is required for maintenance of undifferentiated cells in Arabidopsis shoot and floral meristems and acts at a different regulatory level than the meristem genes WUSCHEL and ZWILLE. Plant J. **10**: 967–979.

Engelhorn, J., Moreau, F., Fletcher, J.C., and Carles, C.C. (2014). ULTRAPETALA1 and LEAFY pathways function independently in specifying identity and determinacy at the Arabidopsis floral meristem. Ann. Bot. **114**: 1497–1505.

Engstrom, E.M. (2011). Phylogenetic analysis of GRAS proteins from moss, lycophyte and vascular plant lineages reveals that GRAS genes arose and underwent substantial diversification in the ancestral lineage common to bryophytes and vascular plants. Plant Signal. Behav. **6**: 850–854.

Engstrom, E.M., Andersen, C.M., Gumulak-smith, J., Hu, J., Orlova, E., Sozzani, R., Bowman, J.L., William, C., and Virginia, E.M.E. (2011). Arabidopsis Homologs of the Petunia HAIRY MERISTEM Gene Are Required for Maintenance of Shoot and. Plant Physiol. **155**: 735–750.

Etchells, J.P., Mishra, L.S., Kumar, M., Campbell, L., and Turner, S.R. (2015). Wood formation in trees is increased by manipulating PXY-regulated cell division. Curr. Biol. **25**: 1050–1055.

Etchells, J.P., Provost, C.M., Mishra, L., and Turner, S.R. (2013). WOX4 and WOX14 act downstream of the PXY receptor kinase to regulate plant vascular proliferation independently of any role in vascular organisation. Development **140**: 2224–34.

Etchells, J.P. and Turner, S.R. (2010). The PXY-CLE41 receptor ligand pair defines a multifunctional pathway that controls the rate and orientation of vascular cell division. Development **137**: 767–774.

Fan, C., Wu, Y., Yang, Q., Yang, Y., Meng, Q., Zhang, K., Li, J., Wang, J., and Zhou, Y. (2014). A novel single-nucleotide mutation in a CLAVATA3 gene homolog controls a multilocular silique trait in brassica rapa L. Mol. Plant **7**: 1788–1792.

Feng, Z., Zhang, B., Ding, W., Liu, X., Yang, D.L., Wei, P., Cao, F., Zhu, S., Zhang, F., Mao, Y., and Zhu, J.K. (2013). Efficient genome editing in plants using a CRISPR/Cas system. Cell Res. **23**: 1229–1232.

Fiers, M., Golemiec, E., Xu, J., Geest, L. Van Der, Heidstra, R., Stiekema, W., and Liu, C. (2005). The 14 – Amino Acid CLV3 , CLE19 , and CLE40 Peptides Trigger Consumption of the Root Meristem in Arabidopsis through a CLAVATA2 -Dependent Pathway. Plant Cell **17**: 2542–2553.

Fiers, M., Hause, G., Boutilier, K., Casamitjana-Martinez, E., Weijers, D., Offringa, R., Van Der Geest, L., Van Lookeren Campagne, M., and Liu, C.M. (2004). Mis-expression of the CLV3/ESR-like gene CLE19 in Arabidopsis leads to a consumption of root meristem. Gene **327**: 37–49.

Fiume, E., Monfared, M., Jun, J., Fletcher, J.C., and To (2011). CLE polypeptide signaling gene expression in Arabidopsis embryos. Plant Signal. Behav. **6**: 443–444.

Fiume E, Pires HR, Kim JS, Fletcher JC. (2010) Analyzing floral meristem development. In: Hennig L, Kohler C, editors. Methods in Molecular Biology. 655. Totowa, NJ: Humana Press. 130–52.

Fiume, E. and Fletcher, J.C. (2012). Regulation of Arabidopsis Embryo and Endosperm Development by the Polypeptide Signaling Molecule CLE8. Plant Cell **24**: 1000–1012.

Fisher, K. and Turner, S. (2007). PXY, a Receptor-like Kinase Essential for Maintaining Polarity during Plant Vascular-Tissue Development. Curr. Biol. **17**: 1061–1066.

Fletcher, J.C. (2018). The CLV-WUS Stem Cell Signaling Pathway : A Roadmap to Crop Yield Optimization. Plants **7**: 87.

Fletcher, J.C., Brand, U., Running, M.P., Simon, R., and Meyerowitz, E.M. (1999). Signaling of cell fate decisions by CLAVATA3 in Arabidopsis shoot meristems. Science **283**: 1911–1914.

Forner, J., Pfeiffer, A., Langenecker, T., Manavella, P., and Lohmann, J.U. (2015). Germline-Transmitted Genome Editing in Arabidopsis thaliana Using TAL-Effector-Nucleases. PLoS One **10**: e0121056.

Friml, J., Vieten, A., Sauer, M., Weijers, D., Schwarz, H., Hamann, T., Offringa, R., and Jürgens, G. (2003). Efflux-dependent auxin gradients establish the apical-basal axis of Arabidopsis. Nature **426**: 147–153.

Fu, Y., Xu, L., Xu, B., Yang, L., Ling, Q., Wang, H., and Huang, H. (2007). Genetic interactions between leaf polarity-controlling genes and ASYMMETRIC LEAVES1 and 2 in Arabidopsis leaf patterning. Plant Cell Physiol. **48**: 724–735.

Furner, I.J. and Pumfrey, J.E. (1992). Cell fate in the shoot apical meristem of Arabidopsis thaliana. Development **115**: 755–764.

Galli, M. and Gallavotti, A. (2016). Expanding the Regulatory Network for Meristem Size in Plants. Trends Genet. **32**: 372–383.

Gaillochet, C. and Lohmann, J.U. (2015). The never-ending story: from pluripotency to plant developmental plasticity. Development **142**: 2237–2249.

Gallois, J., Woodward, C., Reddy, G.V., and Sablowski, R. (2002). Combined SHOOT MERISTEMLESS and WUSCHEL trigger ectopic organogenesis in Arabidopsis. Development **129**: 3207–3217.

Galvan-Ampudia, C.S., Chaumeret, A.M., Godin, C., and Vernoux, T. (2016). Phyllotaxis: from patterns of organogenesis at the meristem to shoot architecture. Wiley Interdiscip. Rev. Dev. Biol. **5**: 460–473.

Gifford, E.M. (1954). The botanical. Bot. Rev. **20**: 429–447.

Goad, D.M., Zhu, C., and Kellogg, E.A. (2016). Comprehensive identification and clustering of CLV3/ESR-related (CLE) genes in plants finds groups with potentially shared function. New Phytol.: doi: 10.1111/nph.14348.

Gordon, S.P., Chickarmane, V.S., Ohno, C., and Meyerowitz, E.M. (2009). Multiple feedback loops through cytokinin signaling control stem cell number within the Arabidopsis shoot meristem. Proc. Natl. Acad. Sci. U. S. A. **106**: 16529–16534.

Greb, T., Clarenz, O., Scha, E., and Schmitz, G. (2003). Molecular analysis of the LATERAL SUPPRESSOR gene in Arabidopsis reveals a conserved control mechanism for axillary meristem formation. Genes Dev. **17**: 1175–1187.

Grienenberger, E. and Fletcher, J.C. (2015). Polypeptide signaling molecules in plant development. Curr. Opin. Plant Biol. **23**: 8–14.

Grooteclaes, M.L. and Frisch, S.M. (2000). Evidence for a function of CtBP in epithelial gene regulation and anoikis. Oncogene **19**: 3823–3828.

Guan, C., Wu, B., Yu, T., Wang, Q., Krogan, N.T., Guan, C., Wu, B., Yu, T., Wang, Q., Krogan, N.T., Liu, X., and Jiao, Y. (2017). Spatial Auxin Signaling Controls Leaf Flattening in Article Spatial Auxin Signaling Controls Leaf Flattening in Arabidopsis. Curr. Biol. **27**: 2940-2950.e4.

Guo, M., Thomas, J., Collins, G., and Timmermans, M.C.P. (2008). Direct repression of KNOX loci by the ASYMMETRIC LEAVES1 complex of Arabidopsis. Plant Cell **20**: 48–58.

Guo, Y., Han, L., Hymes, M., Denver, R., and Clark, S.E. (2010). CLAVATA2 forms a distinct CLE-binding receptor complex regulating Arabidopsis stem cell specification. Plant J. **63**: 889–900.

Gustafson-Brown, C., Savidge, B., and Yanofsky, M.F. (1994). Regulation of the arabidopsis floral homeotic gene APETALA1. Cell **76**: 131–143.

Gutiérrez-Alanís, D., Yong-Villalobos, L., Jiménez-Sandoval, P., Alatorre-Cobos, F., Oropeza-Aburto, A., Mora-Macías, J., Sánchez-Rodríguez, F., Cruz-Ramírez, A., and Herrera-Estrella, L. (2017). Phosphate Starvation-Dependent Iron Mobilization Induces CLE14 Expression to Trigger Root Meristem Differentiation through CLV2/PEPR2 Signaling. Dev. Cell **41**: 555-570.e3.

Ha, C.M., Jun, J.H., Nam, H.G., and Fletcher, J.C. (2004). BLADE-ON-PETIOLE1 encodes a BTB/POZ domain protein required for leaf morphogenesis in Arabidopsis thaliana. Plant Cell Physiol. **45**: 1361–1370.

Ha, C.M., Jun, J.H., Nam, H.G., and Fletcher, J.C. (2007). BLADE-ON-PETIOLE1 and 2 Control Arabidopsis Lateral Organ Fate through Regulation of LOB Domain and Adaxial-Abaxial Polarity Genes. Plant Cell **19**: 1809–1825.

Ha, C.M., Kim, G.-T., Kim, B.C., Jun, J.H., Soh, M.S., Ueno, Y., Machida, Y., Tsukaya, H., and Nam, H.G. (2003). The BLADE-ON-PETIOLE 1 gene controls leaf pattern formation through the modulation of meristematic activity in Arabidopsis. Development **130**: 161–172.

Haecker, A., Groß-Hardt, R., Geiges, B., Sarkar, A., Breuninger, H., Herrmann, M., and Laux, T. (2004). Expression dynamics of WOX genes mark cell fate decisions during early embryonic patterning in Arabidopsis thaliana. Development **131**: 657–668.

Han, H., Zhang, G., Wu, M., and Wang, G. (2016). Identification and characterization of the Populus trichocarpa CLE family. BMC Genomics **17**: 174.

Han, H., Yan, A., Li, L., Zhu, Y., Feng, B., Liu, X., and Zhou, Y. (2020). A signal cascade originated from epidermis defines apical-basal patterning of Arabidopsis shoot apical meristems. Nat. Commun. **11**: 1214.

Hastwell, A.H., Gresshoff, P.M., and Ferguson, B.J. (2015). Genome-wide annotation and characterization of CLAVATA / ESR (CLE) peptide hormones of soybean (Glycine max) and common bean (Phaseolus vulgaris), and their orthologues of Arabidopsis thaliana. J. Exp. Bot. **66**: 5271–5287.

Hayashi, N., Tetsumura, T., Sawa, S., Wada, T., and Tominaga-Wada, R. (2018). CLE14 peptide signaling in arabidopsis root hair cell fate determination. Plant Biotechnol. **35**: 17–22.

Hazak, O., Brandt, B., Cattaneo, P., Santiago, J., Rodriguez-Villalon, A., Hothorn, M., and Hardtke, C.S. (2017). Perception of root-active CLE peptides requires CORYNE function in the phloem vasculature . EMBO Rep. **18**: 1367–1381.

He, P., Zhang, Y., Liu, H., Yuan, Y., Wang, C., Yu, J., and Xiao, G. (2019). Comprehensive analysis of WOX genes uncovers that WOX13 is involved in phytohormone-mediated fiber development in cotton. BMC Plant Biol. **19**: 312.

Heidstra, R. and Sabatini, S. (2014). Plant and animal stem cells: similar yet different. Nat. Rev. Mol. Cell Biol. **15**: 301–12.

Hempel, F.D., Weigel, D., Alejandra Mandel, M., Ditta, G., Zambryski, P.C., Feldman, L.J., and Yanofsky, M.F. (1997). Floral determination and expression of floral regulatory genes in Arabidopsis. Development **124**: 3845–3853.

Hempel, F.D. and Feldman, L.J. (1994). Bi-directional inflorescence development in Arabidopsis thaliana : Acropetal initiation of flowers and basipetal initiation of paraclades. Planta **192**: 276–286.

Hepworth, S.R., Zhang, Y., Mckim, S., Li, X., and Haughn, G.W. (2005). BLADE-ON-PETIOLE–Dependent Signaling Controls Leaf and Floral Patterning in Arabidopsis Shelley. Plant Cell **17**: 1434–1448.

Hibara, K., Takada, S., Taoka, K., Furutani, M., Aida, M., and Tasaka, M. (2006). Arabidopsis CUP-SHAPED COTYLEDON3 Regulates Postembryonic Shoot Meristem and Organ Boundary Formation. Plant Cell **18**: 2946–2957.

Hirakawa, Y., Kondo, Y., and Fukuda, H. (2010). TDIF peptide signaling regulates vascular stem cell proliferation via the WOX4 homeobox gene in Arabidopsis. Plant Cell **22**: 2618–2629.

Hirakawa, Y., Shinohara, H., Kondo, Y., Inoue, A., Nakanomyo, I., Ogawa, M., Sawa, S., Ohashi-Ito, K., Matsubayashi, Y., and Fukuda, H. (2008). Non-cell-autonomous control

of vascular stem cell fate by a CLE peptide/receptor system. Proc. Natl. Acad. Sci. U. S. A. **105**: 15208–13.

Hirakawa, Y., Shinohara, H., Welke, K., Irle, S., Matsubayashi, Y., Torii, K.U., and Uchida, N. (2017). Cryptic bioactivity capacitated by synthetic hybrid plant peptides. Nat. Commun. **8**: 14318.

Hirakawa, Y., Uchida, N., Yamaguchi, Y.L., Tabata, R., Ishida, S., Ishizaki, K., Nishihama, R., Kohchi, T., Sawa, S., and Id, J.L.B. (2019). Control of proliferation in the haploid meristem by CLE peptide signaling in Marchantia polymorpha. PLOS Genet. **15**: e1007997.

Huang, T., Harrar, Y., Lin, C., Reinhart, B., Newell, N.R., Talavera-Rauh, F., Hokin, S.A., Barton, M.K., and Kerstetter, R.A. (2014). Arabidopsis KANADI1 Acts as a Transcriptional Repressor by Interacting with a Specific cis -Element and Regulates Auxin Biosynthesis, Transport, and Signaling in Opposition to HD-ZIPIII Factors. Plant Cell **26**: 246–262.

Husbands, A.Y., Benkovics, A.H., Nogueira, F.T.S., Lodha, M., and Timmermans, M.C.P. (2015). The ASYMMETRIC LEAVES complex employs multiple modes of regulation to affect adaxial-abaxial patterning and leaf complexityopen. Plant Cell **27**: 3321–3335.

Ikeda, M., Mitsuda, N., and Ohme-Takagi, M. (2009). Arabidopsis wuschel is a bifunctional transcription factor that acts as a repressor in stem cell regulation and as an activator in floral patterning. Plant Cell **21**: 3493–3505.

Irish, V.F. and Sussex, I.A.N.M. (1992). A fate map of the Arabidopsis embryonic shoot apical meristem. Development **753**: 745–753.

Ishida, T. et al. (2014). Heterotrimeric G proteins control stem cell proliferation through CLAVATA signaling in Arabidopsis. EMBO Rep. **15**: 1202–9.

Ishiwata, A., Ozawa, M., Nagasaki, H., Kato, M., Noda, Y., Yamaguchi, T., Nosaka, M., Shimizu-Sato, S., Nagasaki, A., Maekawa, M., Hirano, H.Y., and Sato, Y. (2013). Two WUSCHEL-related homeobox genes, narrow leaf2 and narrow leaf3, control leaf width in rice. Plant Cell Physiol. **54**: 779–792.

Ito, Y., Nakanomyo, I., Motose, H., Iwamoto, K., Sawa, S., Dohmae, N., and Fukuda, H. (2006). Dodeca-CLE Peptides as Suppressors. Science (80-.). **313**: 842–845.

Iwakawa, H., Ueno, Y., Semiarti, E., Onouchi, H., Kojima, S., Tsukaya, H., Hasebe, M., Soma, T., Ikezaki, M., Machida, C., and Machida, Y. (2002). The ASYMMETRIC LEAVES2 gene of Arabidopsis thaliana, required for formation of a symmetric flat leaf lamina, encodes a member of a novel family of proteins characterized by cysteine repeats and a leucine zipper. Plant Cell Physiol. **43**: 467–478.

Je, B. Il et al. (2016). Signaling from maize organ primordia via FASCIATED EAR3 regulates stem cell proliferation and yield traits. Nat Genet **48**: 785–791.

Jeong, S., Trotochaud, A.E., and Clark, S.E. (1999). The Arabidopsis CLAVATA2 gene encodes a receptor-like protein required for the stability of the CLAVATA1 receptor-like kinase. Plant Cell **11**: 1925–34.

Ji, J., Strable, J., Shimizu, R., Koenig, D., Sinha, N., and Scanlon, M.J. (2010). Wox4 promotes procambial development. Plant Physiol. **152**: 1346–1356.

Jun, J.H., Fiume, E., and Fletcher, J.C. (2008). The CLE family of plant polypeptide signaling molecules. Cell. Mol. Life Sci. **65**: 743–755.

Jun, J.H., Ha, C.M., and Fletcher, J.C. (2010). BLADE-ON-PETIOLE1 coordinates organ determinacy and axial polarity in arabidopsis by directly activating ASYMMETRIC LEAVES2. Plant Cell **22**: 62–76.

Jun, J., Fiume, E., Roeder, A.H.K., Meng, L., Sharma, V.K., Osmont, K.S., Baker, C., Ha, C.M., Meyerowitz, E.M., Feldman, L.J., and Fletcher, J.C. (2010). Comprehensive analysis of CLE polypeptide signaling gene expression and overexpression activity in Arabidopsis. Plant Physiol. **154**: 1721–1736.

Kalve, S., De Vos, D., and Beemster, G.T.S. (2014). Leaf development: a cellular perspective. Front. Plant Sci. **5**: 362.

Kang, H.G., Fang, Y., and Singh, K.B. (1999). A glucocorticoid-inducible transcription system causes severe growth defects in Arabidopsis and induces defense-related genes. Plant J. **20**: 127–133.

Kaufmann, K., Wellmer, F., Muiñ, J.M., Ferner, T., Wuest, S.E., Kumar, V., Serrano-Mislata, A., Madueño, F., Kraiewski, P., Meyerowitz, E.M., Angenent, G.C., and Riechmann, J.L. (2010). Orchestration of floral initiation by APETALA1. Science (80-.). **328**: 85–89.

Kayes, J.M. and Clark, S.E. (1998). CLAVATA2, a regulator of meristem and organ development in Arabidopsis. **3851**: 3843–3851.

Kerstetter, R.A., Bollman, K., Taylor, R.A., Bomblies, K., and Poethig, R.S. (2001). KANADI regulates organ polarity in Arabidopsis. Nature **411**: 706–709.

Kieffer, M., Stern, Y., Cook, H., Clerici, E., Maulbetsch, C., Laux, T., and Davies, B. (2006). Analysis of the transcription factor WUSCHEL and its functional homologue in Antirrhinum reveals a potential mechanism for their roles in meristem maintenance. Plant Cell **18**: 560–573.

Kinoshita, A., Betsuyaku, S., Osakabe, Y., Mizuno, S., Nagawa, S., Stahl, Y., Simon, R., Yamaguchi-Shinozaki, K., Fukuda, H., and Sawa, S. (2010). RPK2 is an essential receptor-like kinase that transmits the CLV3 signal in Arabidopsis. Development **137**: 3911–3920.

Kinoshita, a. et al. (2015). A plant U-box protein, PUB4, regulates asymmetric cell division and cell proliferation in the root meristem. Development **40**: 444–453.

Kondo, Y., Ito, T., Nakagami, H., Hirakawa, Y., Saito, M., Tamaki, T., Shirasu, K., and Fukuda, H. (2014). Plant GSK3 proteins regulate xylem cell differentiation downstream of TDIF-TDR signalling. Nat. Commun. **5**: 3504.

Kondo, T., Nakamura, T., Yokomine, K., and Sakagami, Y. (2008). Dual assay for MCLV3 activity reveals structure-activity relationship of CLE peptides. Biochem. Biophys. Res. Commun. **377**: 312–316.

Kondo, T., Sawa, S., Kinoshita, A., Mizuno, S., Kakimoto, T., Fukuda, H., and Sakagami, Y. (2006). A Plant Peptide Encoded by CLV4 Identified by in Situ MALDI-TOF MS Analysis. Science (80-.). **313**: 845–848.

Koornneef, M., Hanhart, C.J., and van der Veen, J.H. (1991). A genetic and physiological analysis of late flowering mutants in Arabidopsis thaliana. MGG Mol. Gen. Genet. **229**: 57–66.

Kuittinen, H. and Aguadé, M. (2000). Nucleotide variation at the CHALCONE ISOMERASE locus in Arabidopsis thaliana. Genetics **155**: 863–872.

Irish, V.F. and Sussex, I.A.N.M. (1992). A fate map of the Arabidopsis embryonic shoot apical meristem. Development **753**: 745–753.

Laux, T., Mayer, K.F.X., Berger, J., Jürgens, G., Genetik, L., and München, L. (1996). The WUSCHEL gene is required for shoot and floral meristem integrity in Arabidopsis. **96**: 87–96.

Lease, K.A. and Walker, J.C. (2006). The Arabidopsis unannotated secreted peptide database, a resource for plant peptidomics. Plant Physiol. **142**: 831–838.

Lee, J., Oh, M., Park, H., and Lee, I. (2008). SOC1 translocated to the nucleus by interaction with AGL24 directly regulates LEAFY. Plant J. **55**: 832–843.

Lei, Y., Lu, L., Liu, H.Y., Li, S., Xing, F., and Chen, L.L. (2014). CRISPR-P: A web tool for synthetic single-guide RNA design of CRISPR-system in plants. Mol. Plant **7**: 1494–1496.

Leibfried, A., To, J.P.C., Busch, W., Stehling, S., Kehle, A., Demar, M., Kieber, J.J., and Lohmann, J.U. (2005). WUSCHEL controls meristem function by direct regulation of cytokinin-inducible response regulators. Nature **438**: 1172–1175.

Lenhard, M., Jürgens, G., and Laux, T. (2002). The WUSCHEL and SHOOTMERISTEMLESS genes fulfil complementary roles in Arabidopsis shoot meristem regulation. Development **129**: 3195–3206.

Li, Z., Chakraborty, S., and Xu, G. (2017). Differential CLE peptide perception by plant receptors implicated from structural and functional analyses of TDIF-TDR interactions. PLoS One **12**: e0175317.

Lin, H., Niu, L., McHale, N.A., Ohme-Takagi, M., Mysore, K.S., and Tadege, M. (2013). Evolutionarily conserved repressive activity of WOX proteins mediates leaf blade outgrowth and floral organ development in plants. Proc. Natl. Acad. Sci. U. S. A. **110**: 366–371.

Lin, W.C., Shuai, B., and Springer, P.S. (2003). The Arabidopsis LATERAL ORGAN BOUNDARIES-Domain Gene ASYMMETRIC LEAVES2 Functions in the Repression of KNOX Gene Expression and in Adaxial-Abaxial Patterning. Plant Cell **15**: 2241–2252.

Livak, K.J. and Schmittgen, T.D. (2001). Analysis of relative gene expression data using real-time quantitative PCR and the 2-ΔΔCT method. Methods **25**: 402–408.

Long, J. and Barton, M.K. (2000). Initiation of Axillary and Floral Meristems in Arabidopsis. Dev. Biol. **218**: 341–353.

Long, J. a, Moan, E.I., Medford, J.I., and Barton, M.K. (1996). A member of the KNOTTED class of homeodomain proteins encoded by the STM gene of Arabidopsis. Nature **379**: 66–69.

Long, J.A., Ohno, C., Smith, Z.R., and Meyerowitz, E.M. (2006). TOPLESS regulates apical embryonic fate in Arabidopsis. Science (80-.). **312**: 1520–1523.

Lukowitz, W., Roeder, A., Parmenter, D., and Somerville, C. (2004). A MAPKK Kinase Gene Regulates Extra-Embryonic Cell Fate in Arabidopsis. Cell **116**: 109–119.

Machida, C., Nakagawa, A., Kojima, S., Takahashi, H., and Machida, Y. (2015). The complex of ASYMMETRIC LEAVES (AS) proteins plays a central role in antagonistic interactions of genes for leaf polarity specification in *Arabidopsis*. Wiley Interdiscip. Rev. Dev. Biol. **9**: n/a-n/a.

Mandel, T., Candela, H., Landau, U., Asis, L., Zelinger, E., and Carles, C.C. (2016). Differential regulation of meristem size , morphology and organization by the ERECTA , CLAVATA and class III HD-ZIP pathways.: 1612–1622.

Mandel, T., Moreau, F., Kutsher, Y., Fletcher, J.C., Carles, C.C., and Williams, L.E. (2014). The ERECTA receptor kinase regulates Arabidopsis shoot apical meristem size, phyllotaxy and floral meristem identity. Dev. **141**: 830–841.

Mansfield, S.G. and Briarty, L.G. (1991). Early embryogenesis in Arabidopsis thaliana . II. The developing embryo. Can. J. Bot. **69**: 461–476.

Mantegazza, O., Gregis, V., Chiara, M., Selva, C., Leo, G., Horner, D.S., and Kater, M.M. (2014). Gene coexpression patterns during early development of the native Arabidopsis reproductive meristem: Novel candidate developmental regulators and patterns of functional redundancy. Plant J. **79**: 861–877.

Matsubayashi, Y. (2014). Posttranslationally Modified Small-Peptide Signals in Plants. Annu. Rev. Plant Biol. **65**: 385–413.

Mayer, K.F.X., Schoof, H., Haecker, A., Lenhard, M., Ju, G., Laux, T., Morgenstelle, A. Der, and Tu, D.- (1998). Role of WUSCHEL in Regulating Stem Cell Fate in the Arabidopsis Shoot Meristem. Cell **95**: 805–815.

McCallum, C.M., Comai, L., Greene, E.A., and Henikoff, S. (2000). Targeting induced local lesions IN genomes (TILLING) for plant functional genomics. Plant Physiol. **123**: 439–442.

McConnell, J.R. and Barton, M.K. (1998). Leaf polarity and meristem formation in Arabidopsis. **2942**: 2935–2942.

McConnell, J.R., Emery, J., Eshed, Y., Bao, N., Bowman, J., and Barton, M.K. (2001). Role of PHABULOSA and PHAVOLUTA in determining radial patterning in shoots. Nature **411**: 709–713.

Meng, L., Ruth, K.C., Fletcher, J.C., and Feldman, L. (2010). The roles of different CLE domains in arabidopsis CLE polypeptide activity and functional specificity. Mol. Plant **3**: 760–772.

Michaels, S.D., Himelblau, E., Sang, Y.K., Schomburg, F.M., and Amasino, R.M. (2005). Integration of flowering signals in Winter-annual Arabidopsis. Plant Physiol. **137**: 149–156.

Miyashima, S., Honda, M., Hashimoto, K., Tatematsu, K., Hashimoto, T., Sato-Nara, K., Okada, K., and Nakajima, K. (2013). A comprehensive expression analysis of the arabidopsis MICRORNA165/6 gene family during embryogenesis reveals a conserved role in meristem specification and a non-cell-autonomous function. Plant Cell Physiol. **54**: 375–384.

Miyawaki, K., Tabata, R., and Sawa, S. (2013). Evolutionarily conserved CLE peptide signaling in plant development, symbiosis, and parasitism. Curr. Opin. Plant Biol. **16**: 598–606.

Mizukami, Y. and Fischer, R.L. (2000). Plant organ size control: AINTEGUMENTA regulates growth and cell numbers during organogenesis. Proc. Natl. Acad. Sci. U. S. A. **97**: 942–947.

Monfared, M.M., Carles, C.C., Rossignol, P., Pires, H.R., and Fletcher, J.C. (2013). The ULT1 and ULT2 trxG genes play overlapping roles in arabidopsis development and gene regulation. Mol. Plant **6**: 1564–1579.

Morita, J., Kato, K., Nakane, T., Kondo, Y., Fukuda, H., Nishimasu, H., Ishitani, R., and Nureki, O. (2016). Crystal structure of the plant receptor-like kinase TDR in complex with the TDIF peptide. Nat. Commun. **7**: 12383.

Müller, R., Bleckmann, A., and Simon, R. (2008). The receptor kinase CORYNE of Arabidopsis transmits the stem cell-limiting signal CLAVATA3 independently of CLAVATA1. Plant Cell **20**: 934–46.

Nakata, M., Matsumoto, N., Tsugeki, R., Rikirsch, E., Laux, T., and Okada, K. (2012). Roles of the middle domain-specific WUSCHEL-RELATED HOMEOBOX genes in early development of leaves in Arabidopsis. Plant Cell **24**: 519–535.

Nardmann, J., Ji, J., Werr, W., and Scanlon, M.J. (2004). The maize duplicate genes narrow sheath1 and narrow sheath2 encode a conserved homeobox gene function in a lateral domain of shoot apical meristems. Development **131**: 2827–2839.

Nardmann, J., Reisewitz, P., and Werr, W. (2009). Discrete shoot and root stem cell-promoting WUS/WOX5 functions are an evolutionary innovation of angiosperms. Mol. Biol. Evol. **26**: 1745–1755.

Nekrasov, V., Staskawicz, B., Weigel, D., Jones, J.D.G., and Kamoun, S. (2013). Targeted mutagenesis in the model plant Nicotiana benthamiana using Cas9 RNA-guided endonuclease. Nat. Biotechnol. **31**: 691–693.

Ni, J. and Clark, S.E. (2006). Evidence for Functional Conservation , Sufficiency , and Proteolytic Processing of the CLAVATA3. Plant Physiol. **140**: 726–733.

Ni, J., Guo, Y., Jin, H., Hartsell, J., and Clark, S.E. (2011). Characterization of a CLE processing activity. Plant Mol. Biol. **75**: 67–75.

Nimchuk, Z.L. (2017). CLAVATA1 controls distinct signaling outputs that buffer shoot stem cell proliferation through a two-step transcriptional compensation loop. PLOS Genet. **13**: e1006681.

Nimchuk, Z.L., Tarr, P.T., and Meyerowitz, E.M. (2011a). An evolutionarily conserved pseudokinase mediates stem cell production in plants. Plant Cell **23**: 851–854.

Nimchuk, Z.L., Tarr, P.T., Ohno, C., Qu, X., and Meyerowitz, E.M. (2011b). Plant stem cell signaling involves ligand-dependent trafficking of the CLAVATA1 receptor kinase. Curr. Biol. **21**: 345–352.

Nimchuk, Z.L., Zhou, Y., Tarr, P.T., Peterson, B. a, and Meyerowitz, E.M. (2015). Plant stem cell maintenance by transcriptional cross-regulation of related receptor kinases. Development **142**: 1043–9.

Norberg, M., Holmlund, M., and Nilsson, O. (2005). The BLADE ON PETIOLE genes act redundantly to control the growth and development of lateral organs. Dev. **132**: 2203–2213.

Oelkers, K., Goffard, N., Weiller, G.F., Gresshoff, P.M., Mathesius, U., and Frickey, T. (2008). Bioinformatic analysis of the CLE signaling peptide family. BMC Plant Biol. **8**: https://doi.org/10.1186/1471-2229-8-1.

Ogawa, M., Shinohara, H., Sakagami, Y., and Matsubayashi, Y. (2008). Arabidopsis CLV3 Peptide Directly Binds CLV1 Ectodomain. Science (80-.). **319**: 294–294.

Ohta, M., Matsui, K., Hiratsu, K., Shinshi, H., and Ohme-takagi, M. (2001). Repression domains of class II ERF transcriptional repressors share an essential motif for active repression. Plant Cell **13**: 1959–1968.

Ohyama, K., Shinohara, H., Ogawa-Ohnishi, M., and Matsubayashi, Y. (2009). A glycopeptide regulating stem cell fate in Arabidopsis thaliana. Nat. Chem. Biol. **5**: 578–80.

Otsuga, D., Deguzman, B., Prigge, M.J., Drews, G.N., and Clark, S.E. (2001). REVOLUTA regulates meristem initiation at lateral positions. Plant J. **25**: 223–236.

Pallakies, H. and Simon, R. (2014). The CLE40 and CRN/CLV2 signaling pathways antagonistically control root meristem growth in arabidopsis. Mol. Plant **7**: 1619–1636.

Palovaara, J., de Zeeuw, T., and Weijers, D. (2016). Tissue and Organ Initiation in the Plant Embryo: A First Time for Everything. Annu. Rev. Cell Dev. Biol. **32**: 47–75.

Perales, M., Rodriguez, K., Snipes, S., Yadav, R.K., Diaz-Mendoza, M., and Reddy, G.V. (2016). Threshold-dependent transcriptional discrimination underlies stem cell homeostasis. Proc. Natl. Acad. Sci. **113**: E6298–E6306.

Péret, B., De Rybel, B., Casimiro, I., Benková, E., Swarup, R., Laplaze, L., Beeckman, T., and Bennett, M.J. (2009). Arabidopsis lateral root development: an emerging story. Trends Plant Sci. **14**: 399–408.

Pfeiffer, A. et al. (2016). Integration of light and metabolic signals for stem cell activation at the shoot apical meristem. Elife **5**: e17023.

Plackett, A.R.G., Conway, S.J., Hazelton, K.D.H., Stilio, S. Di, Rabbinowitsch, E.H., and Langdale, J.A. (2018). LEAFY maintains apical stem cell activity during shoot development in the fern Ceratopteris richardii. Elife **7**: e39625.

Poethig, R.S. (1987). Clonal Analysis of Cell Lineage Patterns in Plant Development. Am. J. Bot. **74**: 581–594.

Poethig, R.S., Coe, E.H., and Johri, M.M. (1986). Cell lineage patterns in maize embryogenesis: A clonal analysis. Dev. Biol. **117**: 392–404.

Poethig, R.S. and Sussex, I.M. (1985). The cellular parameters of leaf development in tobacco: a clonal analysis. Planta **165**: 170–184.

Poethig, R.S. and Sussex, I.M. (1985). The developmental morphology and growth dynamics of the tobacco leaf. Planta **165**: 158–169.

Prigge, M.J. and Otsuga, D. (2005). Class III Homeodomain-Leucine Zipper Gene Family Members Have Overlapping , Antagonistic , and Distinct Roles in Arabidopsis Development. Plant Cell **17**: 61–76.

Qian, P., Song, W., Yokoo, T., Minobe, A., Wang, G., Ishida, T., Sawa, S., Chai, J., and Kakimoto, T. (2018). and vascular development through distinct receptors. Nat. Plants **4**: 1071–1081.

Reddy, G.V. and Meyerowitz, E.M. (2005). Stem-cell homeostasis and growth dynamics can be uncoupled in the Arbidopsis shoot apex. Science (80-.). **310**: 663–667.

Reinhardt, D., Mandel, T., and Kuhlemeier, C. (2000). Auxin regulates the initiation and radial position of plant lateral organs. Plant Cell **12**: 507–518.

Reinhardt, D., Pesce, E.R., Stieger, P., Mandel, T., Baltensperger, K., Bennett, M., Traas, J., Friml, J., and Kuhlemeier, C. (2003). Regulation of phyllotaxis by polar auxin transport. Nature **426**: 255–260.

Ren, S.C., Song, X.F., Chen, W.Q., Lu, R., Lucas, W.J., and Liu, C.M. (2019). CLE25 peptide regulates phloem initiation in Arabidopsis through a CLERK-CLV2 receptor complex. J. Integr. Plant Biol. **61**: 1043–1061.

Rensing, S.A. et al. (2008). The Physcomitrella Genome Reveals Evolutionary Insights into the Conquest of Land by Plants. Science (80-.). **319**: 64–69.

Rice, P., Longden, L., and Bleasby, A. (2000). EMBOSS: The European Molecular Biology Open Software Suite. Trends Genet. **16**: 276–277.

Robert, H.S., Grones, P., Stepanova, A.N., Robles, L.M., Lokerse, A.S., Alonso, J.M., Weijers, D., and Friml, J. (2013). Local auxin sources orient the apical-basal axis in arabidopsis embryos. Curr. Biol. **23**: 2506–2512.

Rodrıguez-Leal, D., Lemmon, Z.H., Man, J., Bartlett, M.E., Lippman, Z.B., Lemmon, Z.H., Man, J., Bartlett, M.E., and Lippman, Z.B. (2017). Engineering Quantitative Trait

Variation for Crop Improvement by Genome Editing Engineering Quantitative Trait Variation. Cell **171**: 1–11.

Rodriguez-leal, D. et al. (2019). Evolution of buffering in a genetic circuit controlling plant stem cell proliferation. Nat. Genet. **51**: 786–792.

Rodriguez, K., Perales, M., Snipes, S., Kishor, R., and Diaz-mendoza, M. (2016). DNA-dependent homodimerization, sub-cellular partitioning , and protein destabilization control WUSCHEL levels and spatial patterning. Proc. Natl. Acad. Sci. **113**: E6307–E6315.

Rojo, E., Sharma, V.K., Kovaleva, V., Raikhel, N. V., and Fletcher, J.C. (2002). CLV3 Is Localized to the Extracellular Space, Where It Activates the Arabidopsis CLAVATA Stem Cell Signaling Pathway. Plant Cell Online **14**: 969–977.

Sakakibara, K. et al. (2014). WOX13-like genes are required for reprogramming of leaf and protoplast cells into stem cells in the moss Physcomitrella patens. Dev. **141**: 1660–1670.

Sarkar, A.K., Luijten, M., Miyashima, S., Lenhard, M., Hashimoto, T., Nakajima, K., Scheres, B., Heidstra, R., and Laux, T. (2007). Conserved factors regulate signalling in Arabidopsis thaliana shoot and root stem cell organizers. Nature **446**: 811–814.

Satina, S., Blakeslee, A.F., and Avery, A.G. (1940). Demonstration of the Three Germ Layers in the Shoot Apex of Datura By Means of Induced Polyploidy in Periclinal Chimeras. Am. J. Bot. **27**: 895–905.

Scheres, B., Wolkenfelt, H., Willemsen, V., Terlouw, M., Lawson, E., Dean, C., and Weisbeek, P. (1994). Embryonic origin of the Arabidopsis primary root and root meristem initials. Development **120**: 2475–2487.

Schoof, H., Lenhard, M., Haecker, a, Mayer, K.F., Jürgens, G., and Laux, T. (2000). The stem cell population of Arabidopsis shoot meristems in maintained by a regulatory loop between the CLAVATA and WUSCHEL genes. Cell **100**: 635–644.

Schuster, C., Gaillochet, C., Medzihradszky, A., Busch, W., Daum, G., Krebs, M., Kehle, A., and Lohmann, J.U. (2014). A Regulatory Framework for Shoot Stem Cell Control Integrating Metabolic , Transcriptional , and Phytohormone Signals. Dev. Cell **28**: 438–449.

Scofield, S., Dewitte, W., and Murray, J.A.H. (2014). STM sustains stem cell function in the Arabidopsis shoot apical meristem and controls KNOX gene expression independently of the transcriptional repressor AS1. Plant Signal. Behav. **9**: e28934.

Scofield, S., Dewitte, W., Nieuwland, J., and Murray, J.A.H. (2013). The Arabidopsis homeobox gene SHOOT MERISTEMLESS has cellular and meristem-organisational roles with differential requirements for cytokinin and CYCD3 activity. Plant J. **75**: 53–66.

Segatto, A.L.A., Thompson, C.E., and Freitas, L.B. (2016). Molecular evolution analysis of WUSCHEL-related homeobox transcription factor family reveals functional divergence among clades in the homeobox region. Dev. Genes Evol. **226**: 259–268.

Sharma, V.K., Ramirez, J., and Fletcher, J.C. (2003). The Arabidopsis CLV3-like (CLE) genes are expressed in diverse tissues and encode secreted proteins. Plant Mol. Biol. **51**: 415–425.

Shi, B., Zhang, C., Tian, C., Wang, J., Wang, Q., and Xu, T. (2016). Two-Step Regulation of a Meristematic Cell Population Acting in Shoot Branching in Arabidopsis. PLoS Genet. **12**: e1006168.

Shimizu, N., Ishida, T., Yamada, M., Shigenobu, S., Tabata, R., Kinoshita, A., Yamaguchi, K., Hasebe, M., Mitsumasu, K., and Sawa, S. (2015). BAM 1 and RECEPTOR-LIKE PROTEIN KINASE 2 constitute a signaling pathway and modulate CLE peptide-triggered growth inhibition in Arabidopsis root. New Phytol. **208**: 1104–1113.

Shimotohno, A., Heidstra, R., Blilou, I., and Scheres, B. (2018). Root stem cell niche organizer specification by molecular convergence of PLETHORA and SCARECROW transcription factor modules. Genes Dev. **32**: 1085–1100.

Shinohara, H. and Matsubayashi, Y. (2013). Chemical synthesis of arabidopsis CLV3 glycopeptide reveals the impact of hydroxyproline arabinosylation on peptide conformation and activity. Plant Cell Physiol. **54**: 369–374.

Shinohara, H. and Matsubayashi, Y. (2015). Reevaluation of the CLV3-receptor interaction in the shoot apical meristem : dissection of the CLV3 signaling pathway from a direct ligand-binding point of view. Plant J. **82**: 328–336.

Shiu, S.H. and Bleecker, A.B. (2001). Receptor-like kinases from Arabidopsis form a monophyletic gene family related to animal receptor kinases. Proc. Natl. Acad. Sci. U. S. A. **98**: 10763–10768.

Siegfried, K.R., Eshed, Y., Baum, S.F., Otsuga, D., Drews, G.N., and Bowman, J.L. (1999). Members of the YABBY gene family specify abaxial cell fate in Arabidopsis. Development **126**: 4117–4128.

Simon, R., Coupland, G., Centre, J.I., Lane, C., and Nr, N. (1996). Activation of floral meristem identity genes in Arabidopsis. Nature **384**: 59–62.

Skopelitis, D.S., Benkovics, A.H., Husbands, A.Y., and Timmermans, M.C.P. (2017). Boundary Formation through a Direct Threshold-Based Readout of Mobile Small RNA Gradients. Dev. Cell **43**: 265-273.e6.

Smith, Z.R. and Long, J.A. (2010). Control of Arabidopsis apical-basal embryo polarity by antagonistic transcription factors. Nature **464**: 423–426.

Somssich, M., Je, B. Il, Simon, R., and Jackson, D. (2016). CLAVATA-WUSCHEL signaling in the shoot meristem. Development **143**: 3238–3248.

Somssich, M., Ma, Q., Weidtkamp-Peters, S., Stahl, Y., Felekyan, S., Bleckmann, A., Seidel, C.A.M., and Simon, R. (2015). Real-time dynamics of peptide ligand-dependent receptor complex formation in planta. Sci. Signal. **8**: 1–10.

Song, S.-K., Lee, M.M., and Clark, S.E. (2006). POL and PLL1 phosphatases are CLAVATA1 signaling intermediates required for Arabidopsis shoot and floral stem cells. Development **133**: 4691–8.

Song, X., Xu, T., Ren, S., and Liu, C. (2013). Individual amino acid residues in CLV3 peptide contribute to its stability in vitro. Plant Signal. Behav. **8**: e25344.

Song, X., Yu, D., Xu, T., Ren, S., Guo, P., and Liu, C. (2012). Contributions of Individual Amino Acid Residues to the Endogenous CLV3 Function in Shoot Apical Meristem Maintenance in Arabidopsis. Mol. Plant **5**: 515–523.

Soyars, C.L., James, S.R., and Nimchuk, Z.L. (2016). Ready, aim, shoot : stem cell regulation of the shoot apical meristem. Curr. Opin. Plant Biol. **29**: 163–168.

Stahl, Y., Wink, R.H., Ingram, G.C., and Simon, R. (2009). A Signaling Module Controlling the Stem Cell Niche in Arabidopsis Root Meristems. Curr. Biol. **19**: 909–914.

Stahle, M.I., Kuehlich, J., Staron, L., Von Arnim, A.G., and Golz, J.F. (2009). YABBYs and the transcriptional corepressors LEUNIG and LEUNIG-HOMOLOG maintain leaf polarity and meristem activity in Arabidopsis. Plant Cell **21**: 3105–3118.

Steeves, T.A. and Sussex, I.M. (1989). Patterns in Plant Development (Cambridge University Press: New York, NY).

Strabala, T.J., O'Donnell, P.J., Smit, A.M., Ampomah-Dwamena, C., Martin, E.J., Netzler, N., Nieuwenhuizen, N.J., Quinn, B.D., Foote, H.C.C., and Hudson, K.R. (2006). Gain-of-function phenotypes of many CLAVATA3/ESR genes, including four new family members, correlate with tandem variations in the conserved CLAVATA3/ESR domain. Plant Physiol. **140**: 1331–1344.

Strabala, T.J., Phillips, L., West, M., and Stanbra, L. (2014). Bioinformatic and phylogenetic analysis of the CLAVATA3 / EMBRYO-SURROUNDING REGION (CLE) and the CLE-LIKE signal peptide genes in the Pinophyta. BMC Plant Biol. **14**: 1–16.

Stuurman, J., Jäggi, F., and Kuhlemeier, C. (2002). Shoot meristem maintenance is controlled by a GRAS -gene mediated signal from differentiating cells. Genes Dev. **16**: 2213–2218.

Suer, S., Agusti, J., Sanchez, P., Schwarz, M., and Greb, T. (2011). WOX4 imparts auxin responsiveness to cambium cells in Arabidopsis. Plant Cell **23**: 3247–59.

Sun, B., Xu, Y., Ng, K.H., and Ito, T. (2009). A timing mechanism for stem cell maintenance and differentiation in the Arabidopsis floral meristem. Genes Dev. **23**: 1791–1804.

Sussex, I.M. (1954). Dorsiven Trality in Leaves. Nature **174**: 351–352.

Suzaki, T., Ohneda, M., Toriba, T., Yoshida, A., and Hirano, H.Y. (2009). FON2 SPARE1 redundantly regulates floral meristem maintenance with FLORAL ORGAN NUMBER2 in rice. PLOS Genet. **5**: e1000693.

Suzaki, T., Toriba, T., Fujimoto, M., Tsutsumi, N., Kitano, H., and Hirano, H.Y. (2006). Conservation and diversification of meristem maintenance mechanism in Oryza sativa: Function of the FLORAL ORGAN NUMBER2 gene. Plant Cell Physiol. **47**: 1591–1602.

Szemenyei, H., Hannon, M., and Long, J.A. (2008). TOPLESS mediates auxin-dependent transcriptional repression during Arabidopsis embryogenesis. Science (80-.). **319**: 1384–1386.

Tadege, M. et al. (2011). STENOFOLIA regulates blade outgrowth and leaf vascular patterning in medicago truncatula and nicotiana sylvestris. Plant Cell **23**: 2125–2142.

Takahashi, F., Suzuki, T., Osakabe, Y., Betsuyaku, S., Kondo, Y., Dohmae, N., Fukuda, H., Yamaguchi-Shinozaki, K., and Shinozaki, K. (2018). A small peptide modulates stomatal control via abscisic acid in long-distance signaling. Nature **556**: 235–238.

Tanahashi, T., Sumikawa, N., Kato, M., and Hasebe, M. (2005). Diversification of gene function: Homologs of the floral regulator FLO/LFY control the first zygotic cell division in the moss Physcomitrella patens. Development **132**: 1727–1736.

Tavormina, P., De Coninck, B., Nikonorova, N., De Smet, I., and Cammuea, B.P.A. (2015). The plant peptidome: An expanding repertoire of structural features and biological functions. Plant Cell **27**: 2095–2118.

Tian, C. et al. (2014). An organ boundary-enriched gene regulatory network uncovers regulatory hierarchies underlying axillary meristem initiation. Mol. Syst. Biol. **10**: 755.

To, J.P.C., Haberer, G., Ferreira, F.J., Deruère, J., Mason, M.G., Schaller, G.E., Alonso, J.M., Ecker, J.R., and Kieber, J.J. (2004). Type-A Arabidopsis response regulators are partially redundant negative regulators of cytokinin signaling. Plant Cell **16**: 658–671.

Trotochaud, A.E., Hao, T., Wu, G., Yang, Z., and Clark, S.E. (1999). The CLAVATA1 Receptor-like Kinase Requires CLAVATA3 for Its Assembly into a Signaling Complex That Includes KAPP and a Rho-Related Protein. Plant Cell **11**: 393–406.

Tsukaya, H. (2013). Leaf development. Arab. B. **1**: e0072.

Tyler, L., Miller, M.J., and Fletcher, J.C. (2019). The Trithorax group factor ULTRAPETALA1 regulates developmental as well as biotic and abiotic stress response genes in Arabidopsis. G3 Genes, Genomes, Genet. **9**: 4029–4043.

Uchida, N., Shimada, M., and Tasaka, M. (2013). ERECTA -Family Receptor Kinases Regulate Stem Cell Homeostasis via Buffering its Cytokinin Responsiveness in the Shoot Apical Meristem. Plant Cell Physiol. **54**: 343–351.

Ueda, M., Zhang, Z., and Laux, T. (2011). Transcriptional Activation of Arabidopsis Axis Patterning Genes WOX8/9 Links Zygote Polarity to Embryo Development. Dev. Cell **20**: 264–270.

Urano, D. and Jones, A.M. (2014). Heterotrimeric G Protein–Coupled Signaling in Plants. Annu. Rev. Plant Biol. **65**: 365–384.

van den Berg, C., Willemsen, V., Hendriks, G., Weisbeek, P., and Scheres, B. (1997). Short-range control of cell differentiation in the Arabidopsis root meristem. Nature **390**: 287–289.

Vatén, A., Soyars, C.L., Tarr, P.T., Nimchuk, Z.L., and Dominique, C. (2018). Modulation of Asymmetric Division Diversity Through Cytokinin and SPEECHLESS Regulatory Interactions in the Arabidopsis Stomatal Lineage. Dev. Cell **47**: 53–66.

Vernoux, T. et al. (2011). The auxin signalling network translates dynamic input into robust patterning at the shoot apex. Mol. Syst. Biol. **7**: 508.

Waites, R. and Hudson, A. (2001). The Handlebars gene is required with Phantastica for dorsoventral asymmetry of organs and for stem cell activity in Antirrhinum. Development **128**: 1923–1931.

Wang, J., Tian, C., Zhang, C., Shi, B., Cao, X., Zhang, T., Zhao, Z., Wang, J., and Jiao, Y. (2017). Cytokinin Signaling Activates WUSCHEL Expression during Axillary Meristem Initiation. **29**: 1373–1387.

Wang, Q., Kohlen, W., Rossmann, S., Vernoux, T., and Theres, K. (2014). Auxin Depletion from the Leaf Axil Conditions Competence for Axillary Meristem Formation in Arabidopsis and Tomato. Plant Cell **26**: 2068–2079.

Wang, W., Xu, B., Wang, H., Li, J., Huang, H., and Xu, L. (2011). YUCCA Genes Are Expressed in Response to Leaf Adaxial-Abaxial Juxtaposition and Are Required for Leaf Margin Development. Plant Physiol. **157**: 1805–1819.

Wang, X., Mitchum, M.G., Gao, B., Li, C., Diab, H., Baum, T.J., Hussey, R.S., and Davis, E.L. (2005). A parasitism gene from a plant-parasitic nematode with function similar to CLAVATA3/ESR (CLE) of Arabidopsis thaliana. Mol. Plant Pathol. **6**: 187–191.

Wang, Y., Wang, J., Shi, B., Yu, T., Qi, J., Meyerowitz, E.M., and Jiao, Y. (2014). The Stem Cell Niche in Leaf Axils Is Established by Auxin and Cytokinin in Arabidopsis. Plant Cell **26**: 2055–2067.

Wang, G., Zhang, G., and Wu, M. (2016). CLE Peptide Signaling and Crosstalk with Phytohormones and Environmental Stimuli. Front. Plant Sci. **6**: 1211.

Weigel, D., Alvarez, J., Smyth, D.R., Yanofsky, M.F., and Meyerowitz, E.M. (1992). LEAFY controls floral meristem identity in Arabidopsis. Cell **69**: 843–859.

Weight, C., Parnham, D., and Waites, R. (2008). LeafAnalyser: A computational method for rapid and large-scale analyses of leaf shape variation. Plant J. **53**: 578–586.

Whitewoods, C.D. et al. (2018). CLAVATA Was a Genetic Novelty for the Morphological Innovation of 3D Growth in Land Plants. Curr. Biol. **28**: 1–12.

Whitford, R., Fernandez, A., De Groodt, R., Ortega, E., and Hilson, P. (2008). Plant CLE peptides from two distinct functional classes synergistically induce division of vascular cells. Proc. Natl. Acad. Sci. U. S. A. **105**: 18625–30.

Wigge, P.A., Kim, M.C., Jaeger, K.E., Busch, W., Schmid, M., Lohmann, J.U., and Weigel, D. (2005). Integration of spatial and temporal information during floral induction in Arabidopsis. Science (80-.). **309**: 1056–1059.

Williams, R.W., Wilson, J.M., and Meyerowitz, E.M. (1997). A possible role for kinase-associated protein phosphatase in the Arabidopsis CLAVATA1 signaling pathway. Proc. Natl. Acad. Sci. U. S. A. **94**: 10467–10472.

Winter, C.M. et al. (2011). LEAFY Target Genes Reveal Floral Regulatory Logic, cis Motifs, and a Link to Biotic Stimulus Response. Dev. Cell **20**: 430–443.

Wu, C.C., Li, F.W., and Kramer, E.M. (2019). Large-scale phylogenomic analysis suggests three ancient superclades of the WUSCHELRELATED HOMEOBOX transcription factor family in plants. PLoS One **14**: e0223521.

Xu, C. et al. (2015). A cascade of arabinosyltransferases controls shoot meristem size in tomato. Nat. Genet. **47**: 784–792.

Xu, L., Xu, Y., Dong, A., Sun, Y., Pi, L., Xu, Y., and Huang, H. (2003). Novel as1 and as2 defects in leaf adaxial-abaxial polarity reveal the requirement for ASYMMETRIC LEAVES1 and 2 and ERECTA functions in specifying leaf adaxial identity. Development **130**: 4097–4107.

Xu, T.-T., Song, X.-F., Ren, S.-C., and Liu, C.-M. (2013). The sequence flanking the N-terminus of the CLV3 peptide is critical for its cleavage and activity in stem cell regulation in Arabidopsis. BMC Plant Biol. **13**: 225.

Yadav, R.K., Perales, M., Girke, T., and Jo, H. (2011). WUSCHEL protein movement mediates stem cell homeostasis in the Arabidopsis shoot apex. Genes Dev. **25**: 2025–2030.

Yadav, R.K., Perales, M., Gruel, J., Ohno, C., Heisler, M., Girke, T., Jonsson, H., and Reddy, G.V. (2013). Plant stem cell maintenance involves direct transcriptional repression of differentiation program. Mol. Syst. Biol. **9**: 654.

Yaginuma, H., Hirakawa, Y., Kondo, Y., Ohashi-Ito, K., and Fukuda, H. (2011). A novel function of TDIF-related peptides: Promotion of axillary bud formation. Plant Cell Physiol. **52**: 1354–1364.

Yamaguchi, N., Winter, C.M., Wu, M.-F., Kwon, C.S., William, D.A., and Wagner, D. (2014). PROTOCOL: Chromatin Immunoprecipitation from Arabidopsis Tissues. Arab. B. **12**: e0170.

Yamaguchi, Y.L., Ishida, T., Yoshimura, M., Imamura, Y., Shimaoka, C., and Sawa, S. (2017). A Collection of Mutants for CLE-Peptide-Encoding Genes in Arabidopsis Generated by CRISPR / Cas9-Mediated Gene Targeting. **9**: 1848–1856.

Yamamoto, R., Fujioka, S., Iwamoto, K., Demura, T., Takatsuto, S., Yoshida, S., and Fukuda, H. (2007). Co-regulation of brassinosteroid biosynthesis-related genes during xylem cell differentiation. Plant Cell Physiol. **48**: 74–83.

Yanai, O., Shani, E., Dolezal, K., Tarkowski, P., Sablowski, R., Sandberg, G., Samach, A., and Ori, N. (2005). Arabidopsis KNOXI proteins activate cytokinin biosynthesis. Curr. Biol. **15**: 1566–1571.

Yoshida, S., BarbierdeReuille, P., Lane, B., Bassel, G.W., Prusinkiewicz, P., Smith, R.S., and Weijers, D. (2014). Genetic control of plant development by overriding a geometric division rule. Dev. Cell **29**: 75–87.

Yue, M., Li, Q., Zhang, Y., Zhao, Y., Zhang, Z., and Bao, S. (2013). Histone H4R3 methylation catalyzed by SKB1/PRMT5 is required for maintaining shoot apical meristem. PLoS One **8**: e83258.

Zhang, F., Wang, Y., Li, G., Tang, Y., Kramer, E.M., and Tadege, M. (2014). STENOFOLIA recruits TOPLESS to repress ASYMMETRIC LEAVES2 at the leaf margin and promote leaf blade outgrowth in Medicago truncatula. Plant Cell **26**: 650–664.

Zhang, H., Lin, X., Han, Z., Qu, L., and Chai, J. (2016). Crystal structure of PXY-TDIF complex reveals a conserved recognition mechanism among CLE peptide-receptor pairs. Cell Res. **26**: 543–555.

Zhang, L. et al. (2019). CLE9 peptide-induced stomatal closure is mediated by abscisic acid, hydrogen peroxide, and nitric oxide in Arabidopsis thaliana. Plant Cell Environ. **42**: 1033–1044.

Zhang, T.Q., Lian, H., Zhou, C.M., Xu, L., Jiao, Y., and Wang, J.W. (2017). A two-stepmodel for de novo activation of wuschel during plant shoot regeneration. Plant Cell **29**: 1073–1087.

Zhang, Z., Tucker, E., Hermann, M., and Laux, T. (2017). A Molecular Framework for the Embryonic Initiation of Shoot Meristem Stem Cells. Dev. Cell **40**: 264-277.e4.

Zhou, Y., Liu, X., Engstrom, E.M., Nimchuk, Z.L., Pruneda-paz, J.L., Tarr, P.T., Yan, A., Kay, S.A., and Meyerowitz, E.M. (2015). Control of plant stem cell function by conserved interacting transcriptional regulators. Nature **517**: 377–380.

Zhou, Y., Yan, A., Han, H., Li, T., Geng, Y., Liu, X., and Meyerowitz, E.M. (2018). HAIRY MERISTEM with WUSCHEL confines CLAVATA3 expression to the outer apical meristem layers. Science (80-.). **361**: 502–506.

Zhu, Y., Wang, Y., Li, R., Song, X., Wang, Q., Huang, S., Jin, J.B., Liu, C.M., and Lin, J. (2010). Analysis of interactions among the CLAVATA3 receptors reveals a direct interaction between CLAVATA2 and CORYNE in Arabidopsis. Plant J. **61**: 223–233.

APPENDIX

CLE signaling pathway in diverse model organisms

Figure A.1. CLE signaling in *Zea mays* SAM. ZmWUS is expressed in the organizing center of the SAM. The CLE peptide ZmFCP1 signals through ZmFEA3 and ZmFEA2 receptors, and ZmCLE7 signals through ZmFEA2 to control stem cell accumulation by suppressing *ZmWUS*. *ZmFCP1* is expressed in lateral organs, while *ZmCLE7* expression pattern in the SAM is unknown. The TD1 receptor also restricts meristem size via an unknown ligand. Part of this figure is featured in Fletcher et al., 2018.

Figure A.2. CLE signaling in *Solanum lycopersicum* SAM. SlCLV3 and SlCLE9 signal through SlCLV1 to control meristem size. SlCLV3 is expressed in the central zone of the SAM, while SlCLE9 expression pattern in the SAM is unknown. Part of this figure is featured in Fletcher et al., 2018.

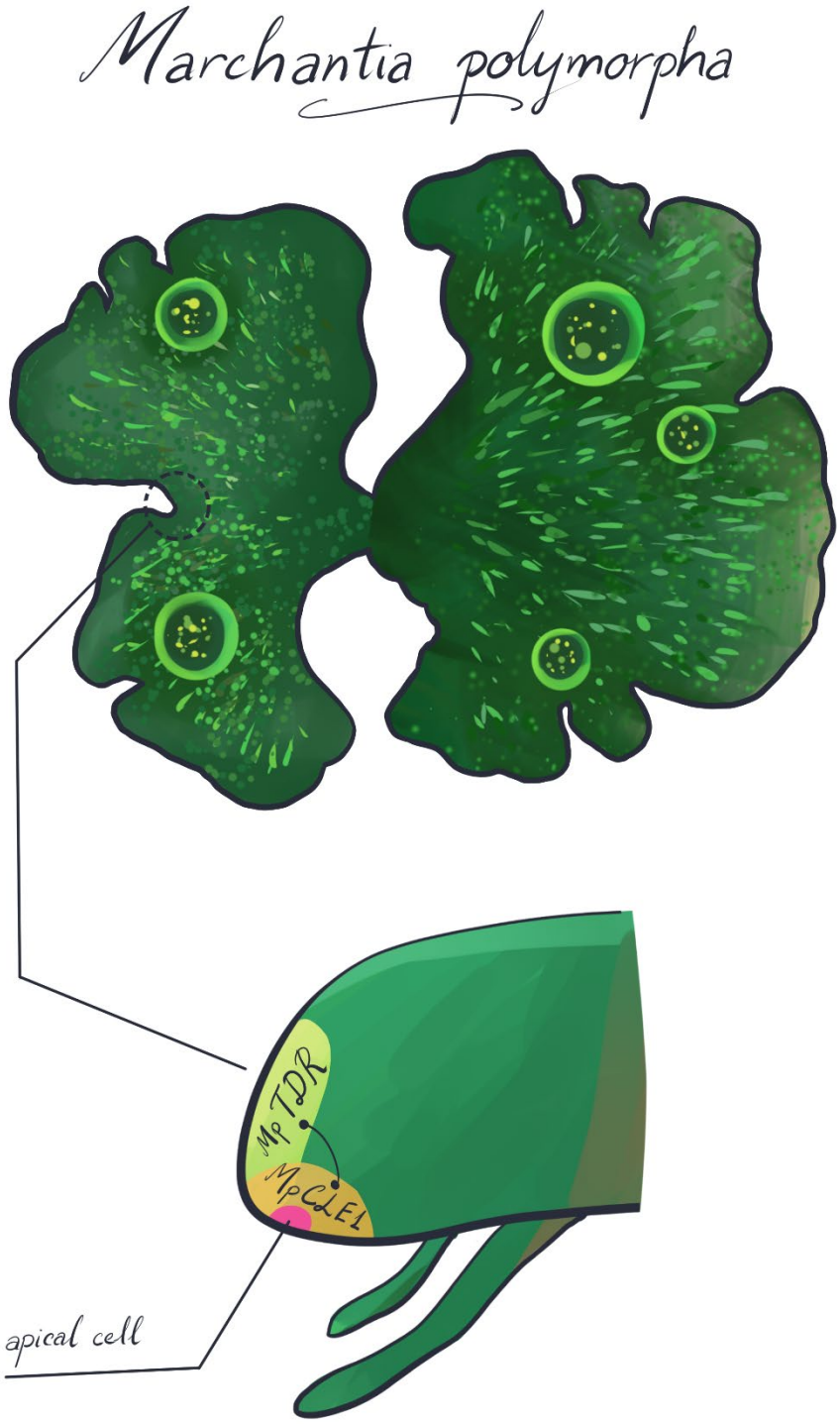

Figure A.3. CLE signaling in *Marchantia polymorpha* apical notch. MpCLE1 signals through MpTDR receptor to regulate stem cell proliferation at the apical notch. MpCLE1 is expressed in a small area around the apical cell, while MpTDR is expressed in the dorsal part of the meristem.

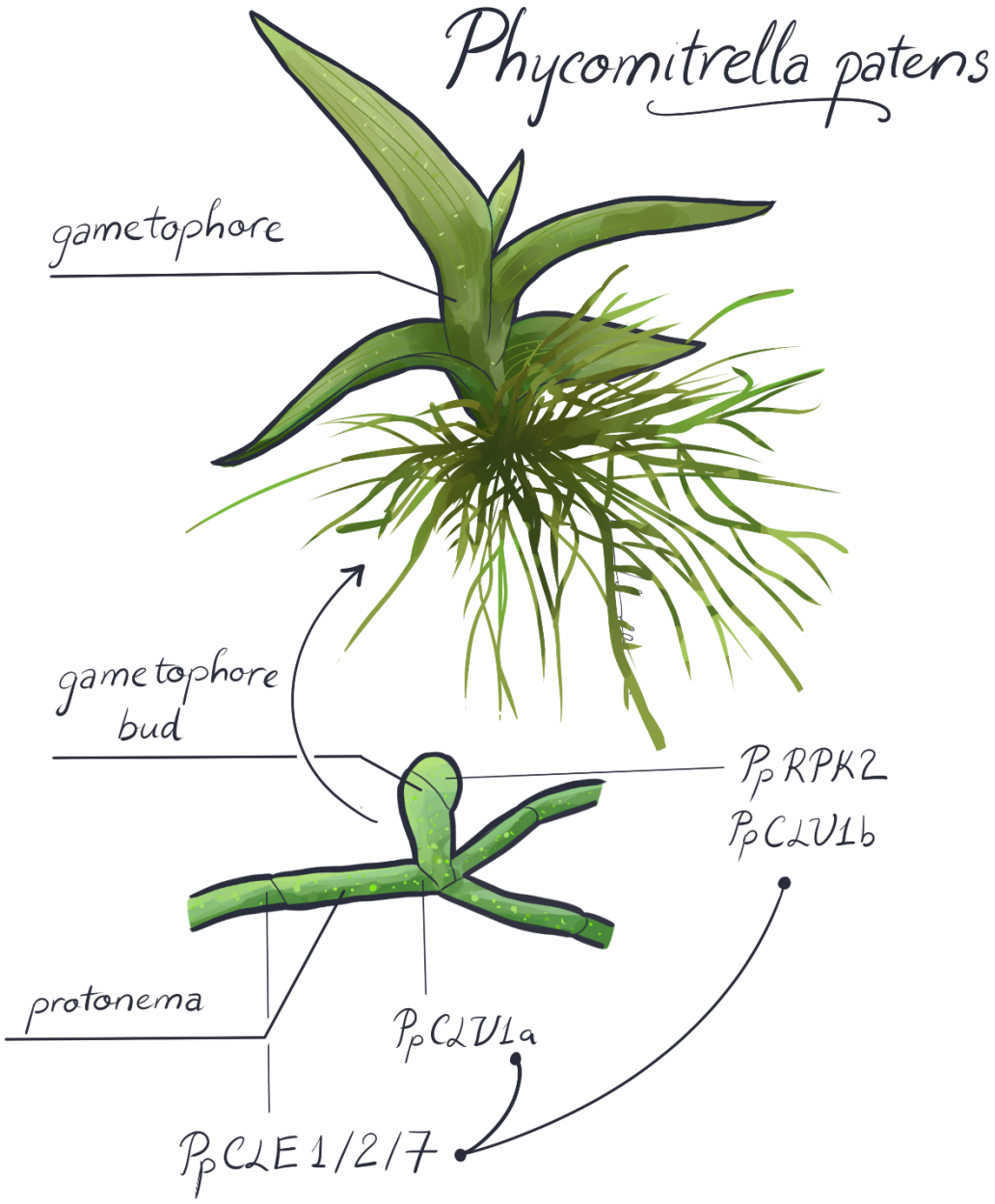

Figure A.4. CLE signaling in *Physcomitrella* gametophore development. PpCLEs signal through PpCLV1a/b and PpRPK2 receptors to regulate the initial cell divisions that form gametophore buds and apical cell activity. *PpCLE1/2/7* and *PpCLV1a* are expressed in protonemal cells around the developing bud, while *PpCLV1b* and *PpRPK2* are expressed in the gametophore towards the apex.